

Springer Tracts in Mechanical Engineering

Irene Fassi
David Shipley *Editors*

Micro- Manufacturing Technologies and Their Applications

A Theoretical and Practical Guide

 Springer

Springer Tracts in Mechanical Engineering

Board of editors

Seung-Bok Choi, Inha University, Incheon, South Korea

Haibin Duan, Beijing University of Aeronautics and Astronautics, Beijing,
P.R. China

Yili Fu, Harbin Institute of Technology, Harbin, P.R. China

Carlos Guardiola, Universitat Politècnica de València, València, Spain

Jian-Qiao Sun, University of California, Merced, USA

About this Series

Springer Tracts in Mechanical Engineering (STME) publishes the latest developments in Mechanical Engineering - quickly, informally and with high quality. The intent is to cover all the main branches of mechanical engineering, both theoretical and applied, including:

- Engineering Design
- Machinery and Machine Elements
- Mechanical structures and stress analysis
- Automotive Engineering
- Engine Technology
- Aerospace Technology and Astronautics
- Nanotechnology and Microengineering
- Control, Robotics, Mechatronics
- MEMS
- Theoretical and Applied Mechanics
- Dynamical Systems, Control
- Fluids mechanics
- Engineering Thermodynamics, Heat and Mass Transfer
- Manufacturing
- Precision engineering, Instrumentation, Measurement
- Materials Engineering
- Tribology and surface technology

Within the scopes of the series are monographs, professional books or graduate textbooks, edited volumes as well as outstanding PhD theses and books purposely devoted to support education in mechanical engineering at graduate and post-graduate levels.

More information about this series at <http://www.springer.com/series/11693>

Irene Fassi · David Shipley
Editors

Micro-Manufacturing Technologies and Their Applications

A Theoretical and Practical Guide

MIMAN-T
MICROMANUFACTURING
TRAINING SYSTEM for SMEs

 Springer

Editors

Irene Fassi
Institute of Industrial Technology
and Automation
Consiglio Nazionale delle Ricerche
Milan
Italy

David Shipley
Faculty of Engineering
University of Nottingham
Nottingham
UK



Lifelong Learning Programme
Education, Audiovisual and
Culture Executive Agency

“This project has been supported by the European Commission.
This publication reflects the views only of the authors, and the Commission cannot be held
responsible for any use which may be made of the information contained therein.”

ISSN 2195-9862 ISSN 2195-9870 (electronic)
Springer Tracts in Mechanical Engineering
ISBN 978-3-319-39650-7 ISBN 978-3-319-39651-4 (eBook)
DOI 10.1007/978-3-319-39651-4

Library of Congress Control Number: 2016958722

© Springer International Publishing Switzerland 2017

This work is subject to copyright. All rights are reserved by the Publisher, whether the whole or part of the material is concerned, specifically the rights of translation, reprinting, reuse of illustrations, recitation, broadcasting, reproduction on microfilms or in any other physical way, and transmission or information storage and retrieval, electronic adaptation, computer software, or by similar or dissimilar methodology now known or hereafter developed.

The use of general descriptive names, registered names, trademarks, service marks, etc. in this publication does not imply, even in the absence of a specific statement, that such names are exempt from the relevant protective laws and regulations and therefore free for general use.

The publisher, the authors and the editors are safe to assume that the advice and information in this book are believed to be true and accurate at the date of publication. Neither the publisher nor the authors or the editors give a warranty, express or implied, with respect to the material contained herein or for any errors or omissions that may have been made.

Printed on acid-free paper

This Springer imprint is published by Springer Nature
The registered company is Springer International Publishing AG
The registered company address is: Gewerbestrasse 11, 6330 Cham, Switzerland

Preface

This volume is a compilation of work undertaken in recent years by leading experts in the field of micro-manufacturing who are members of the consortium of the Leonardo da Vinci project MIMAN-T: Micro-Manufacturing Training System for SMEs (542424-LLP-1-2013-1-IT-LEONARDO-LMP). This includes Karlsruhe Institute of Technology (KIT), The University of Nottingham, ASERM, Eurecat, Institute of Industrial Technologies and Automation (CNR-ITIA).

This book collates contributions from within the fields of micro-manufacturing technologies and engineering, and complements the online training platform developed by the MIMAN-T consortium. This platform provides the reader with an in-depth exposure to the theoretical issues along with practical tips on some of the leading edge technologies for the manufacture and measurement of micro-components, devices, and products.

The introductory chapter reviews the main physical concepts behind the down-scaling of components and describes the impact of miniaturisation on materials, processes, and production systems. Subsequently, chapters present six technologies: micro-injection moulding, micro-additive manufacturing, micro-machining, micro-EDM, micro-waterjet, and micro-assembly, each addressing the physics of the process, materials, design and simulation, tools, machines, sectors, and applications.

A chapter is devoted to moulded interconnected devices, and another reviews the main issues and techniques for effectively measuring the surface topography and geometry of micro-components. Numerous examples are included to assist readers in learning and implementing the described technologies.

A further chapter is devoted to technological foresight, addressing challenges such as market analysis and business models for micro-manufacturing operations.

This book primarily targets technicians and prospective professionals operating within the sector and aims to serve as an effective tool to facilitate the translation of micro-manufacturing technologies into tangible industrial benefits.

We hope we have achieved this goal.

Milan, Italy
Nottingham, UK

Irene Fassi
David Shipley

Contents

1	Introduction to Miniaturisation	1
	Claudia Pagano and Irene Fassi	
2	Micro-injection Moulding	23
	Andreu Sancho, Laura Arribas and Daniel Teixidor	
3	Micro-additive Manufacturing Technology	67
	Felip Esteve, Djamila Olivier, Qin Hu and Martin Baumer	
4	Manufacturing Technology: Micro-machining	97
	Lorelei Gherman, Andrew Gleadall, Otto Bakker and Svetan Ratchev	
5	Micro-waterjet Technology	129
	Massimiliano Annoni, Francesco Arleo and Francesco Viganò	
6	Micro-electro-Discharge Machining (Micro-EDM)	149
	Francesco Modica, Valeria Marrocco and Irene Fassi	
7	Moulded Interconnect Devices	175
	Adrien Brunet, Ulrich Gengenbach, Tobias Müller, Steffen Scholz and Markus Dickerhof	
8	Micro-scale Geometry Measurement	197
	Samanta Piano, Rong Su and Richard Leach	
9	Micro-assembly	223
	Serena Ruggeri, Gianmauro Fontana and Irene Fassi	
10	Market Analysis, Technological Foresight, and Business Models for Micro-manufacturing	261
	Golboo Pourabdollahian and Giacomo Copani	
	Index	293

Acronyms

1D	One dimension
2D	Two dimensions
2PP	Two Photon Polymerisation
2,5D	Two and a half dimension
3D	Three dimensions
ABS (polymer)	Acrylonitrile Butadiene Styrene
ABS	Antiblock Braking System
ACC	Adaptive Cruise Control
AFEM	Atomic-scale Finite Element Method
AM	Additive Manufacturing
AMDA	Automated Micro Device Assembly
AR	Aspect Ratio
AU	Airy Unit
AWJ	Abrasive Water Jet
BIOMEMS	Biomedical Micro-Electro-Mechanical Systems
CAD	Computer Aided Design
CADD	Coupled Atomistic and Discrete Dislocation
CAM	Computer Aided Manufacturing
CBCT	Cone-Beam X-ray Computed Tomography
CCD	Charge-Coupled Device
CGMD	Coarse-Grained Molecular Dynamics
CM	Confocal Microscopy
CMM	Coordinate Measuring Machine
CNC	Computer Numerical Control
COC	Cyclic Olefin Copolymer
CPV	Concentrator PhotoVoltaics
CSI	Coherence Scanning Interferometry
CTE	Coefficient of Thermal Expansion
DC	Direct Current
DMD	Digital Micro-mirror Device
DoD	Drop on Demand

DoE	Design of Experiments
DoF	Degrees of Freedom
DRIE	Deep Reactive Ion Etching
EAP	ElectroActive Polymer
EDM	Electro Discharge Machining
ELID	Electrolytic In process Dressing
ELISA	Enzyme-Linked ImmunoSorbent Assay
ERM	Enhanced Resolution Module
ESP	Elektronisches Stabilitätsprogramm (Electronic stability control)
FDM	Fused Deposition Modeling
FD-OCT	Fourier-Domain Optical Coherence Tomography
FEA	Finite Element Analysis
FEAt	Finite Element-Atomistic
FF	Fill Factor
FIB	Focused Ion Beam
FOV	Field Of View
FP	Fringe Projection
FV	Focus Variation
GMR	Giant MagnetoResistance
GPS	Global Positioning System
HeCd	Helio-Cadmium
HMI	Human Machine Interface
HTN	High Temperature Nylon
ICT	Information and Communications Technology
IFF	Identification Friend or Foe
IT	Information Technology
LCP	Liquid Crystal Polymer
LDS	Laser Direct Structuring
LED	Light Emitting Diode
LIGA	Lithographie, Galvanoformung, Abformung (Lithography, Electroplating and Molding)
LOC	Lab-On-Chip
LT	Laser Triangulation
LTE	Long Term Evolution (telecommunication standard)
MAAD	Macroscopic Atomistic Ab initio Dynamics
MD	Molecular Dynamics
MDA	Micro Device Assembly
MEMS	Micro-Electro-Mechanical Systems
MID	Moulded Interconnect Device
MM	Micro-Machining
MNT	Micro and Nano-manufacturing Technologies
MRI	Magnetic Resonance Imaging
MRR	Material Removal Rate
MSL	Micro-StereoLithography
MST	Micro-System Technologies

NEMS	Nano-Electro-Mechanical Systems
NIR	Near InfraRed
OCT	Optical Coherence Tomography
OEM	Original Equipment Manufacturer
OPV	Organic PhotoVoltaics
PA	Polyamides
PAI	Polyamide-imide
PBT	Polybutylene terephthalate
PC	Polycarbonate
PCB	Printed Circuit Board
PCK	Printed Circuit Kollmorgen
PEEK	Polyetheretherketone
PEI	Polyetherimide
PES	Polysthersulfone
PET	Polyethylene terephthalate
PFA	Perfluoroalkoxy
PLA	Polylactic acid
PMMA	Polymethyl methacrylate
POM	Polyoxymethylene
PP	Polypropylene
PPA	Polyphthalamide
PPE	Polyphenyl ether
PPI	Pores Per Inch
PPS	Polyphenylene sulphide
PS	Polystyrene
PSU	Polysulfone
PWJ	Pure Water Jet
PZT	Piezoelectric
QC	QuasiContinuum
RFID	Radio-Frequency IDentification
RH	Relative Humidity
RPM	Revolutions Per Minute
SA	Self-Assembly
SCARA	Selective Compliance Assembly Robot Arm
SDA	Scratch Drive Actuator
SD-OCT	Spectral-Domain Optical Coherence Tomography
SEM	Scanning Electron Microscope
SKW	Sankyo Kasei Wiring board
SL	Stereolithography
SLM	Selective Laser Melting
SMA	Shape Memory Alloy
SMD	Surface Mount Device
SME	Small and Medium sized Enterprises
SMT	Surface Mount Technology
SPS	Syndiotactic Polystyrene

SS-OCT	Swept-Source Optical Coherence Tomography
SWOT	Strengths, Weaknesses, Opportunities, and Threats
TD-OCT	Time-Domain Optical Coherence Tomography
T _g	Glass transition temperature
TWR	Tool Wear Ratio
UHF	Ultra High Frequency
UMTS	Universal Mobile Telecommunications System (telecommunication standard)
USM	UltraSonic vibration Machine
UTS	Ultimate Tensile Strength
UV	Ultraviolet
UWM	Uniform Wear Method
WEDM	Wire Electro Discharge Machining
WJ	Water Jet
XCT	X-ray Computed Tomography

Chapter 1

Introduction to Miniaturisation

Claudia Pagano and Irene Fassi

1.1 Introduction

Miniaturisation of systems and devices is a trend that started a few decades ago, and which is becoming more and more relevant to our everyday lives. Miniaturised devices and components are present in an increasing number of applications; not only electronics devices, such as smart phones, laptops, sensors in vehicles and house goods, but also biological probes, medical systems and defence. Many objectives that originate from the futuristic vision of Feynman [1] in 1959 have already been realised, and significant knowledge gained. Indeed, from the outset, it was clear that miniaturisation from a straightforward downscaling of systems and technologies was not possible.

The concept of micro-manufacturing evolved as a direct result of non-conventional manufacturing technologies. Micro-electro mechanical systems (MEMS) evolved from electronics, with manufacturers mainly using integrated circuit (IC) fabrication technologies. This allowed batch processing of the parts, but limited the range of materials to semi-conductors, such as silicon. Moreover, high aspect ratio parts and 3D components were very difficult or impossible to produce using IC fabrication technologies. Therefore, in order to manufacture some more complex geometries, several technical areas started to evolve [2]. Material scientists studied innovative and high-performance materials suitable for mass production of miniaturised parts; engineers studied new technologies for the production of cheap and sophisticated devices, physicists studied the mechanics of miniaturised systems. Then, conventional manufacturing technologies were adapted and new technologies developed, so

C. Pagano · I. Fassi (✉)
Institute of Industrial Technology and Automation,
Consiglio Nazionale delle Ricerche, Milan, Italy
e-mail: irene.fassi@itia.cnr.it

C. Pagano
e-mail: claudia.pagano@itia.cnr.it

that micro-manufacturing can now be divided into two main categories, MEMS and non-MEMS manufacturing. The former is dedicated to the silicon-based technologies such as photolithography, chemical etching, plating, LIGA, laser ablation, etc. The latter refers to use with a much wider variety of materials and geometries, and includes micro-mechanical cutting, laser cutting/patterning/drilling, micro-electro-discharge machining, focused ion beam machining, micro-embossing, micro-injection moulding, micro-extrusion, micro-stamping, etc. Conventional technologies had to be revisited in order to overcome the issues due to the reduced dimensions of the components and tools. Fixturing issues can occur for some machining, the traditional tolerances might not fulfil the specifications; sticking issues occur during manipulation, both in manufacturing and assembly, residual stresses might also compromise the functionality of the parts.

The aim of this first chapter is to review the main physical phenomena related to miniaturisation, in terms of scaling laws, forces, materials, processes and production systems.

1.2 Scaling Laws

When approaching the micro-scale, some physical phenomena previously considered negligible at the macro-scale, become significant. The scaling laws help to explain these phenomena. The scaling laws relate the parameters of the systems (e.g. the surface area) with its length scale; the surface area is, indeed, proportional to the length squared. Therefore, when the length decreases of three orders of magnitude (from meters to millimetres) the surface area decreases of six orders of magnitude and its contribution can become less significant. Any engineer aiming at designing micro-systems should consider the scaling laws and predict whether the downscaling is possible and practical.

When a system is reduced isomorphically in size (i.e. all the dimensions of the system are scaled down uniformly), the ratio of the volume to the surface area is altered. Indeed, since the volume is proportional to the length cubed, and the surface area squared, the volume decreases faster than the surface (Fig. 1.1). For this reason, physical phenomena related to the volume (e.g. weight) become less significant at the micro-scale, whereas surface related phenomena strongly affect the physical behaviour of the system. This explains why the liquid in a water glass is easier to pour than from a capillary tube; indeed, it is due to the higher surface tension in a capillary tube than in a much larger water glass because of the reduced dimension of the tube. See Sect. 1.2.4 for more details.

The scaling laws allow the understanding and prediction of the effects negligible at the macroscopic level but which become important at the micrometre scale, and vice versa. The effects are related to the scaling of the size of a system, and of its phenomenological behaviour and they can be applied to each physical domain. In the following sections, some relevant scaling laws are explored, offering some practical examples [3].

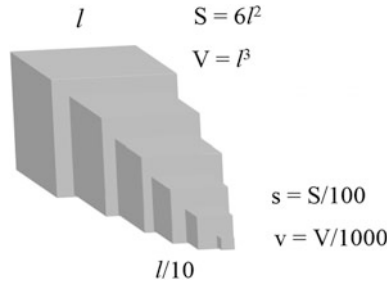


Fig. 1.1 Effect of miniaturisation on surface area and volume

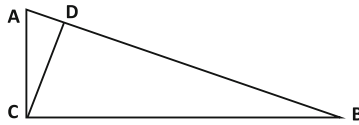


Fig. 1.2 Proof of Pythagoras theorem using the scaling law. ABC is a right-angled triangle and CD is the normal to the hypotenuse AB. The triangles ΔABC , ΔACD , and ΔBCD are similar, thus, their areas are proportional to the square of any characteristic length such as the hypotenuses. Thus, the area of $\Delta ABC = \lambda AB^2$, the area of $\Delta ACD = \lambda AC^2$ and the area of $\Delta BCD = \lambda CB^2$, where λ is a constant of proportionality, which, from simple trigonometric formulas, can be shown to be the same for all the triangles. Since Area of $\Delta ACD +$ Area of $\Delta BCD =$ Area of ΔABC , $\lambda AC^2 + \lambda BC^2 = \lambda AB^2$ that means $AC^2 + BC^2 = AB^2$ according to the Pythagoras theorem

1.2.1 Geometry

The scaling of a system can be:

- isometric, if all its elements scale in the same way, so that the geometry of the system is maintained.
- allometric, if different elements of the system scale in dissimilar way.

Geometric scaling is very simple and, given l the length scale, it follows the following laws:

$$\text{Perimeter} \propto l \qquad \text{Area} \propto l^2 \qquad \text{Volume} \propto l^3$$

In (Fig. 1.2) scaling laws are used to prove the Pythagoras theorem.

1.2.2 Mechanics

Let us consider a simple system, such as a suspended beam of length L , width w and thickness t . When a force F along the direction $-y$ is applied to the free end of the

beam, a deflection at the same end, δ , results along the same direction of F . The stiffness of the beam k is equal to the ratio of F to δ and δ is easily calculated as:

$$\delta = \frac{(FL^3)}{(3EI)}$$

in which:

E = Young's modulus

I = moment of inertia of the cross section of the beam about its neutral axis = $(1/12) wt^3$.

Therefore,

$$k = \frac{F}{\delta} = \frac{3EI}{L^3} = \frac{Ewt^3}{4L^3}.$$

Therefore, in case of an isometric scale of the system, the stiffness of a cantilever beam scales as the length scale (l) of the beam: $k \propto l$.

The stiffness of the beam under its own weight can be calculated given the force is proportional to its weight. So F scales as l^3 , k scales as l and, thus, the deflection δ is proportional to l^2 . Thus, the shrinkage of the beam leads to an increase of the stiffness.

Therefore, at the micro-scale, thinner and less bulky structures or weaker materials can be utilised.

1.2.3 Dynamics

The first resonance frequency of the beam (ω) in Fig. 1.3 can be written as:

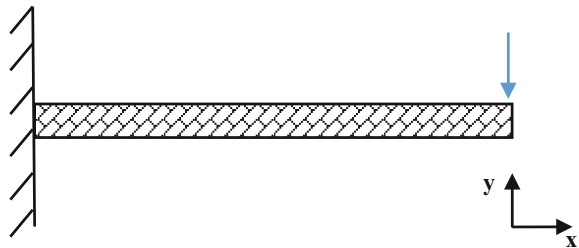
$$\omega = \frac{22.4}{2\pi L^2} \sqrt{\frac{EI}{\rho A}}$$

in which:

A = area of the cross section

ρ = density of the material.

Fig. 1.3 Suspended beam



Therefore, the natural frequency increases scaling down the system. Low interference and low response time are expected in the micro-range.

Mass moment of inertia scales as l^5 being the mass ($\propto l^3$) times dimension squared, so it becomes very small at micro-scale and allows almost instantaneous start and stop of micro-robots.

The inertial forces scale as l^3 , since they are the mass times the acceleration, so they can often be neglected at the micro-scale.

Energy and work scale as l^4 being the force times the displacement.

1.2.4 Micro-fluidics

The surface tension (F_γ) becomes predominant at the micro-scale because it scales as l , while, as already seen, the volume related forces scales as l^3 . This can be easily illustrated from the classic example shown in Fig. 1.4: the height, h , of the fluid in the circular tube of radius r can be calculated at the equilibrium between the competitive effects of the surface tension, F_γ , and gravitational force, F_g :

$$F_\gamma = F_g$$

$$F_\gamma = 2\pi r \gamma \cos\theta$$

$$F_g = \rho g \pi r^2 h$$

in which:

ρ = fluid density

γ = coefficient of the surface tension

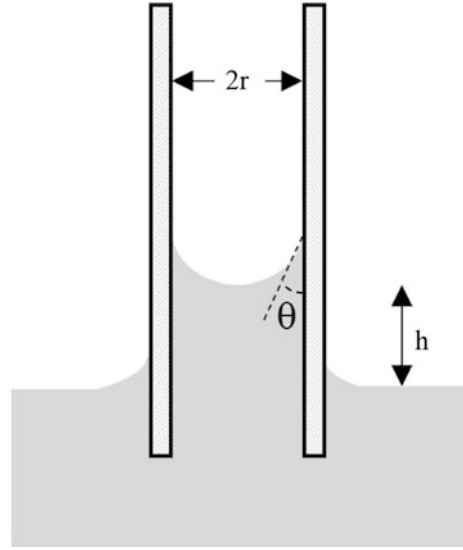
Therefore, reducing the dimension l of a factor of 10, the gravitational force (F_g) decreases by 10^3 , while F_γ only by 10, becoming much more influential.

Similar effects can be observed when a system is moving in a fluid (e.g. air). Unless we are in vacuum conditions, this is always the case. When a body moves in a fluid, it experiences the viscous drag offered by the fluid. This force limits its terminal velocity (v_{lim}), which for a spherical object of radius (r) can be written as:

$$v_{lim} \propto \frac{2gr^2\rho}{9\eta} \propto l^2$$

in which ρ and η are the density and viscosity of the fluid. Therefore, v_{lim} becomes very small for micro-objects and this explains why micro-robots cannot fly very fast. However, they have a greater chance of survival should they fall, when compared with a macro-sized robot.

Fig. 1.4 Capillary tube in a fluid



The miniaturisation of fluidic devices offers the advantage of using low sample quantity and occupying less space. However, the volumetric flow rate (Q) can be written according to Hagen–Poiseuille’s equation:

$$Q = \frac{(\pi r^4 \Delta p)}{(8 \eta L)}$$

where r and L are the radius and length of the channel, Δp is the pressure drop and η the viscosity of the fluid. Therefore for a given pressure drop, Q is proportional to r^4 and a drastic reduction of the volumetric flow is observed due to the miniaturisation; for a given volumetric flow rate the pressure drop $\Delta p \propto r^{-4}$, which, thus, dramatically increases.

Moreover, the fluid flow becomes less turbulent in micro-sized channels because the Reynolds number (Re) becomes very low:

$$Re \propto \frac{v d \rho}{\eta}$$

where ρ and η are as above the density and viscosity of the fluid, d the diameter of the channel and v is the velocity of the fluid. Thus, Re scales as l and decreases when the channel section decreases. The transaction between laminar and turbulent flow occurs when $Re \approx 10^3$. The almost laminar flow resulting in strait micro-channels causes difficulty in mixing fluids, and serpentine micro-channels are necessary in miniaturised fluidic systems such as lab on chip (LoC) [4].

1.2.5 Van der Waals Force

Figure 1.5 shows the well-known plot of the forces versus the system size. They are calculated assuming that a silicon sphere is picked up by a gripper with flat jaw surfaces [5]. As already mentioned, the gravity force becomes soon insignificant as the object size is reduced, whereas the predominant forces are the superficial ones, such as surface tension and also van der Waals forces, which are always present also at the macro-scale, but due to the presence of higher forces are normally neglected.

Van der Waals forces are due to three attractive contributions: the orientation or Keesom interaction, the induction or Debye interaction, and the dispersion or London interaction; moreover, a repulsive force exists when molecules approach closely.

The orientation effect (dipole-dipole) is the interaction between two permanent dipoles; in an isotropic material, where all the orientations are possible, it is expected to be zero, however, the molecules are usually not completely free to rotate, and some orientations are preferred over others, so there is a contribution different to zero. The induction effect (permanent dipole-induced dipole) is due to the interaction between a polar molecule and a non-polar one. Indeed, an induced polarisation occur for the non-polar molecule under the influence of an external electric field. In absence of a polar molecule, the above-mentioned interactions do not occur and only the dispersion effect (temporary dipole-induced dipole) is observable. This interaction arises from a temporary dipole inducing a complementary dipole in any adjacent molecule. Dispersion force is quantum mechanical in origin. Dispersion force generally exceeds the dipole-dependent induction and orientation forces except for small highly polar molecules, such as water. In the

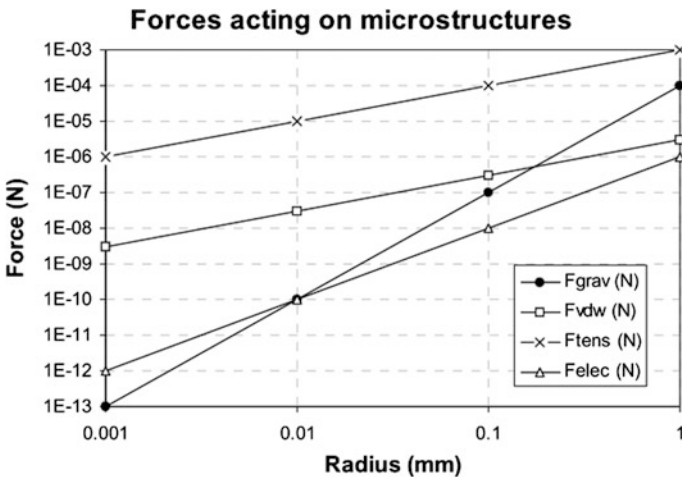


Fig. 1.5 Forces versus object radius

interaction between two dissimilar molecules of which one is non-polar, the van der Waals energy is almost completely dominated by the dispersion contribution. Since dispersion force is an interaction between two induced fluctuating dipoles, when dipoles are an appreciable distance apart it is enormously reduced (Fig. 1.7). Indeed, with increasing separation, the dispersion energy between two atoms can decay even faster than $1/r^6$, approaching a $1/r^7$ dependence. This is known as the *retardation effect* and the interaction London retarded force.

1.2.6 Electromagnetism

The resistance (R) scales as l^{-1} ; indeed, if the resistance (Fig. 1.6) has length equal to L , cross-sectional area A and specific resistivity ρ :

$$R = \frac{L\rho}{A} \propto l^{-1}$$

The capacitance C of a parallel plate capacitor (Fig. 1.6), with plates of area A , distance d , and insulator permittivity ε is:

$$C = \frac{\varepsilon A}{d} \propto l$$

The electrostatic force between the two plates can be obtained from the potential energy:

$$U = -\frac{1}{2}CV^2 = -\frac{\varepsilon A}{2d}V^2 \Rightarrow F_d = -\frac{\partial U}{\partial d} = -\frac{1}{2}\frac{\varepsilon A}{d^2}V^2 \propto l^2$$

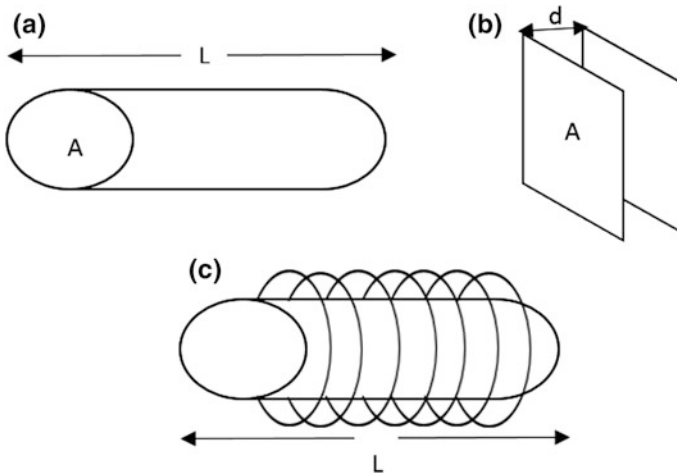


Fig. 1.6 a Resistance, b capacitor and c inductor

Therefore, when the plates shrink the force decreases less rapidly than the mass related forces.

For this reason at the micro-scale, the presence of residual charges can be catastrophic for the proper operation of a system. At the same time, together with the capillary forces (superficial tension) the electrical forces are extensively studied with the aim of being able to reduce or control them in order to conceive new actuation and manipulation methodologies (as discussed in Chap. 9).

Finally the inductance (λ) of an inductor (Fig. 1.6) made of N coils per unit length, each of whose has area A and length L , is:

$$\lambda = \frac{\mu N^2 A}{L} \propto l$$

in which μ is the permeability of the material between the coils.

The scaling laws for electromagnetic force are more complicate and the results depend on the assumptions made. The force between two magnetic coils (A and B) can be written as:

$$F = \mu_0 J_A J_B A_A A_B$$

where μ_0 is the permeability, J is the current density and A the cross-sectional area of the coil. The current density can reasonably assumed to be constant while the coil shrinks, even though this assumption has a limit due to the maximum power dissipation in form of heat that the coil can stand. With this assumption $F \propto A_A A_B \propto l^4$. Therefore, miniaturisation is unfavourable for electromagnetic force.

This is one of the reasons why electric actuation is much larger used at the micro-scale than magnetic actuation, enhanced by the difficulty in fabricating coils with micro-manufacturing technologies.

1.2.7 Thermodynamics

Thermal inertia is a measure on how fast the thermal equilibrium is achieved in a solid. It is an important parameter in the design of a thermally actuated device. It depends on the mass and, thus, scales as l^3 . The thermal conductivity of solids measures how fast heat is conducted in the solid. It scales as l or l^2 according to which principle dominates the heat transfer, conduction or convection respectively.

1.2.8 Scaling with Distances

In order to have smaller and more integrated devices, miniaturisation involves not only the downscaling of the dimensions of the objects, but also the fact that the

distances are between objects reduced. The components are closer and therefore short distance forces often become predominant.

In Fig. 1.7 a plot of different forces acting between a sphere and a plate versus their reciprocal distance is shown [6]. For smaller distance, short-range forces that are usually insignificant at conventional scales overcome the others: Van der Waal forces become significant and predominant together with the capillary force. Moreover, a force unknown at the macro-scale appears: the Casimir force [7]. It reminds us that at the smaller scales, the Newtonian mechanics do not govern the interaction and quantum mechanics is more appropriate.

The plot shows also that electric force (F_e) increases when the distance decreases. Indeed, according to the Coulomb law the electrostatic force between two charges is inversely proportional to the distance squared, therefore $F_e \propto l^{-2}$. This is the reason why the electrostatic forces are usually negligible, while they become highly significant at the micro-scale and, in particular, can provide a means of actuation. Indeed, one of the most widespread actuators for MEMS is based on the comb-drive principle [8]. However, the breakdown voltage also has to be taken into account during the design of miniaturised electric devices. According to the Paschen law, illustrated in Fig. 1.8 [9], the breakdown voltage strongly depends on the gap between electrodes. The Paschen law is based on the Townsend Avalanche mechanisms for gas ionization [10], while at small gap spacing other mechanisms for pre-breakdown current production can occur, such as electron field emission. Therefore, extreme caution has to be paid to gaps less than $5 \mu\text{m}$, and some corrections at the left part of Paschen curve have to be considered.

Figure 1.7 also shows that van der waals force can be comparable to electrostatic force at nano-metric distance and that the magnetic force is relatively small compared to the other interactions at short distances. However, it becomes more

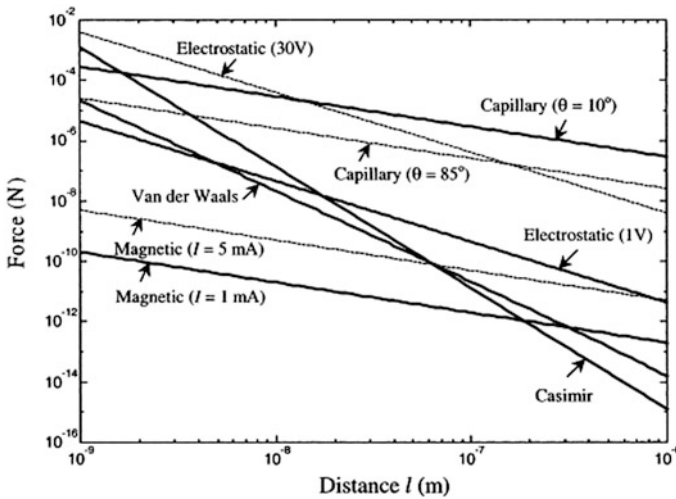
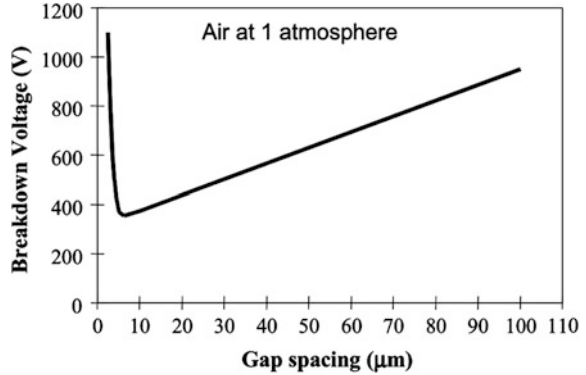


Fig. 1.7 Forces versus interaction distance [6]

Fig. 1.8 Paschen curve [9]

significant at larger distance when capillary and Van der Waals force are less effective. Depending on the type of application, the designer has to consider the effect of these forces and identify solutions either to exploit or to minimise their effects.

1.2.9 Scaling Exponent

Considering that in a miniaturised device the dimensions of the object and the distances are both scaled down, also the velocity ($v = lt^{-1}$) and acceleration ($a \propto lt^{-2}$) scale and also the main physical quantities scale according to Table 1.1.

1.3 Materials

Miniaturisation does not only affect the interaction between bodies, but its effects may be also observable on the material properties, due to the discrete internal structure. Indeed, even though materials can be approximated as homogeneous at the macro-scale, their heterogeneity on the micro-level is becomes evident and affects the manufacturing process. Grain boundaries are regions where the dislocations and high mobility occur during deformation tests, and their presence is easily detected from the observation of several material properties.

In micro-specimens either the grain size is reduced or they contain grains of the same size of macro-specimens. In both cases, the behaviour of the micro-specimens are likely to be different from the bulk. In the latter case the internal grain boundary fraction decreases, strengthening the material. When the specimens are so small that very few grains are contained the even distribution is not assured and inhomogeneous deformation occurs. The extreme case is a sample made of a single crystal where, due to the anisotropy, the properties depend on the direction of the

Table 1.1 Scaling exponent

$Q \propto l^n$	
Quantity name (Q)	n
Mass	3
Mass moment of inertia	5
Second moment of area	4
Inertia force	3
Tensile strength	2
Natural frequency	-1
Bending stiffness	1
Shear stiffness	1
Surface tension	1
Fluid force	2
Reynolds number	2
Heat capacity	3
Resistance power loss	1
Electrical resistance	-1
Electrical capacitance	1
Inductance	1
Electromagnetic force	3
Electrostatic force	2

deformation [11]. Furthermore, several studies have proved that, according to the Hall–Petch law, the polycrystalline materials strengthen when the grain size decreases [12, 13]. Therefore, a strengthening effect can be assumed for the former hypothesis, many smaller grains. In contrast with that result, however, at the nano-scale an opposite behaviour has been observed [14]. In conclusion, a combined effect of the grain size and the specimen dimension, not yet thoroughly understood, makes the mechanical behaviour difficult to predict [15]. For ceramics and other notch-sensitive materials, the volume reduction leads to a higher resistance to fracture.

Not only the mechanical properties, but also the magnetic properties are affected by the grain size. For example, in micro-specimens made of ferro-magnetic materials, multi-domains and easy magnetisation disappear leaving only single domain possible [16]. This occurs when the grain size is around 10–100 nm, while for smaller grains the coercivity decreases until a super-paramagnetic state is achieved [17].

The specimen dimension affect, thus, the properties of the material and, as a consequence, they influence material processing. Due to the grain dimension, material removal issues can occur, such as the limitation on the minimum uncut chip thickness. For thermal processes, such as micro-EDM, the different thermal properties between the grain and the grain boundary affect the machining performances [18]. Moreover, in case of anisotropy the process parameters may change and affect the results [19, 20].

The miniaturisation process impacts the choice of materials that are used. Indeed, micro-technology has its origin in electronics. Thus, semiconducting materials—first and foremost silicon, have been the most used materials. However, silicon structures fabrication is limited by the nature of the manufacturing processes to planar structures and by the material properties. Progresses in micro-manufacturing technologies (discussed in subsequent chapters) of more traditional materials, such as polymers, metals and ceramics make them suitable for micro-part fabrication in small to large batches. Moreover, these materials can offer a much larger variety of properties and part functionalities.

Also, more sophisticated materials, such as smart or functionalised metal or polymer alloys, play a role in micro-system production, due to the small amount of material required offering new development possibilities. Furthermore, the need of integration of several functions in few components requires the use of several types of smart materials, which can have applications in a very wide range of sectors [21].

1.3.1 Smart Materials

A smart material is defined as “a material which has built-in or intrinsic sensor(s), actuator(s) and control mechanism(s) whereby it is capable of sensing a stimulus, responding to it in a predetermined manner and extent, in a short/appropriate time, and reverting to its original state as soon as the stimulus is removed” [22].

They can be classified according to the stimuli to which they are sensitive: *piezoelectric* and *electrostrictive* materials undergo mechanical changes when subjected to a variation of voltage and vice versa, the mechanical change of electrostrictive materials is proportional to the square of the electric field; *magnetostrictive* materials are activated by a magnetic field and produce an induced mechanical strain; *shape memory alloys* subjected to a thermal field undergo a phase transformation that produce a shape change; *optical fibres* can measure strain, temperature, electromagnetic fields, pressure and other quantities using intensity, phase, frequency or polarisation of modulation [23].

1.3.1.1 Piezoelectric Materials

The piezoelectric effect consists of the ability of certain crystals to become electrically polarised when subjected to a mechanical strain, with the degree of polarisation proportional to the applied strain. Moreover, these materials deform when exposed to an electric field. Several natural materials exhibit the piezoelectric effect, such as quartz, tourmaline and sodium potassium tartrate, due to their crystals structure with no centre of symmetry. Beside these naturally-occurring crystals, there are several families of man-made ceramics, commonly known as PZT, exhibiting these piezoelectric properties. They are polycrystalline ferroelectric materials made of minute crystallites. The molecules of these materials have a

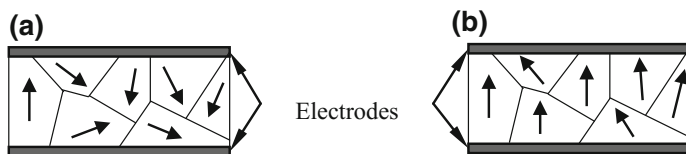


Fig. 1.9 **a** Randomly oriented Weiss domain dipoles, **b** aligned dipoles after polarisation using an electric field

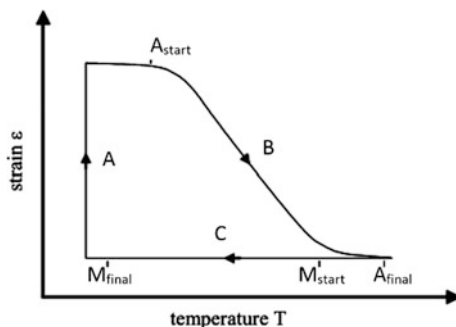
polarisation, which means that one end is more negatively charged and the other end is positively charged, so that a dipole occurs. This is a result of the arrangement of the atoms that form the molecule [24]. The dipoles are not randomly oriented throughout the material, since they affect each other and neighbouring dipoles align to form regions of local alignment known as Weiss domains. Therefore, within any Weiss domain there is a net dipole moment, and hence a net polarisation (dipole moment per unit volume) (Fig. 1.9). Different domains have randomly distributed direction of polarisation so that no overall polarisation or piezoelectric effect is exhibited. However, the piezoelectric effect in any chosen direction can be induced by a poling treatment, which involves exposing it to a strong electric field at a certain temperature.

Due to the electric field, the domains most nearly aligned with the field will grow at the expense of other domains. As a result, the material has a net polarisation and material is also lengthened in the direction of the field. This alignment persists even when the field is removed, giving the ceramic material a permanent polarisation and a permanent deformation (i.e. making it anisotropic) Due to this anisotropy, a compressive or tensile strain of the material changes the dipole moment causing a voltage difference between the electrodes, so that the material behaves as a generator converting the mechanical energy into electrical energy. On the other hand, if a voltage is applied to the electrodes, the material shortens or lengthens according to the direction of the voltage. In this case the ceramic behaves as a motor, converting the electrical energy into mechanical energy.

1.3.1.2 Shape Memory Alloy

Shape memory alloys (SMA) are functional materials that exhibit peculiar thermo-mechanical properties such as the Shape Memory Effect and the Super-elasticity. These properties are a consequence of a reversible thermo-elastic martensitic transformation occurring at the solid state. They have the ability to recover their original shape, upon heating after a deformation occurred at low temperature. From a microscopic point of view, they have two stable solid crystallographic phases, known as martensite and austenite, and they can transform reversibly from a crystal structure to the other [25]. The martensite is the crystallographic phase stable (M_{final}) at low temperature and has a low symmetric monoclinic structure. Austenite is stable at high temperature (A_{final}) and has a

Fig. 1.10 Shape memory effect



body-centered symmetric structure. Since the bond energy in the martensite is low, the material can be easily deformed (A) (Fig. 1.10), and after removal of the stress, the strain remains, but can be recovered by heating the material above the transition temperature, to achieve the austenite phase (A_{start}). This phase transformation causes the SMA to return to the original shape (B) (Fig. 1.10). The critical temperatures at which transition occurs depend not only on the composition of the alloy, but also its thermo-mechanical history and the applied load. When a SMA cools from the high temperature austenite (C) (Fig. 1.10), the material undergoes a martensitic transformation (from M_{start} to M_{final}). This cycle can be repeated millions of times; however, if the stress affects permanent, the shape memory alloy behaves different. They need to be subjected to some cycles as “training” in order to achieve high reproducibility when in function; their shape, thermos-mechanical treatment and applied load define the force and the displacement produced during operations.

Because the martensite phase shows a strong deformation-amplitude dependent internal friction, SMA have also a high damping capacity.

Due to their phase transformation above a certain temperature, SMA can be used as sensors too. However, they can be very good actuators, since during the phase transformation they generate mechanical work. Among the advantages over other actuation methods, there are the large displacement and actuation force within an extremely small envelope volume and a low operation voltage. Moreover, not having to rely on moving parts for actuation makes them highly attractive for applications where low or no noise levels are desired. Therefore, the combination of these advantages, together with the simplicity of mechanism, cleanliness, silent actuation, remote operability, and low driving voltage makes SMA ideal for the actuation of mini-micro devices in a variety of applications [26].

However, some problems, such as the low dynamic time response and the large hysteresis, limit their use [27].

1.3.1.3 Electroactive Polymers

Active polymers can convert another form of energy, such as electrical, electromagnetic or chemical or photonic, into mechanical energy. According to the

stimulus to which the polymers are responsive, they can be divided into two broad categories: non electrically deformable polymers (actuated by non-electric stimuli such as variation of pH, light, temperature, magnetic field etc.) and electroactive polymers (EAP), actuated by electric inputs. Polymers have the great advantage of being lightweight, inexpensive, fracture tolerant, pliable, and easily processed and manufactured. Therefore, they can be configured into complex shapes and their properties can be tailored according to demand [28]. Electrical stimulation is considered the most promising actuation, owing to its availability and advances in control systems. Electroactive polymers can be classified in electronic EAP, which are driven by electric field or coulomb forces and ionic EAP, which change shape by mobility or diffusion of ions and their conjugated substances [29]. Electronic EAP include electrostrictive, electrostatic, piezoelectric, and ferroelectric. They usually require high DC voltage ($>150 \text{ V}/\mu\text{m}$), very close to the breakdown level of the material, to hold the induced displacement and show rapid response time (in the order of milliseconds) Ionic EAP, such as gels, ionic polymer-metal composites and conducting polymers, require low driving voltages (1–5 V). However, they have to operate in a wet state or in solid electrolytes, which is a great constraint for several applications.

Electrostrictive polymers—also called dielectric elastomers—are among the most promising EAP. They exhibit low elastic stiffness and high dielectric constants so that they can achieve great deformations (10–400%) and support high voltage. Their operation principle is similar to the electro-mechanical transduction of a parallel plate capacitor: when an electric potential difference is applied across the polymeric film, coated with electrodes on both sides, a compressive stress, parallel to the electric field, is generated and, consequently, the material is compressed in thickness and expands in planar directions (Fig. 1.11). Therefore, mechanical energy is obtained from the electric energy.

As with many actuation principles, electronic EAP are reversible and they can be operated in generator mode. In this mode of operation, mechanical work is executed to produce an electric field and the EAP is acting as an electro-mechanical generator transducer. EAP exhibit deformations with orders of magnitude much higher than PZT, have higher response speed, lower density, and greater resilience than SMA. However, their applications are limited by low actuation forces, low mechanical energy density, and are inadequately robust.

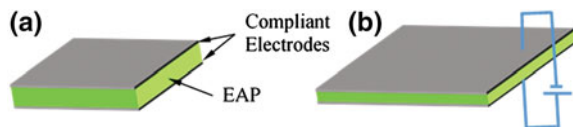


Fig. 1.11 Electrostrictive effect: **a** EAP at rest, **b** area expansion and thickness reduction due to the electric field

1.4 Micro-factories

Miniaturisation can have a positive impact also on production systems. Indeed, conventional factories are often an inefficient solution for the manufacturing of micro-products. Their large space and energy consumption are unfavourable considering the differing requirements for the production of miniaturised systems and micro-parts. The space required for the manufacture of micro-parts is usually very small, but often needs a controlled environment, such as clean rooms or vacuum chambers, which have a high maintenance cost. Therefore, the miniaturisation of the manufacturing machines allows not only space reduction, but also energy saving due to the reduced operational and maintenance cost. In addition with the lower amount of waste, this allows a more sustainable production in term of environmental impact.

Moreover, smaller machines, when correctly designed taking into account the scaling laws, are less affected by errors due to the heat deformation, vibration amplitudes. Furthermore, they require less material and, thus, the use of more expensive materials with better properties is affordable.

Since the concepts have been presented in the early 2000 [30], new requirements for the production of micro-products have been set based on two new paradigms; adaptive manufacturing and sustainable manufacturing. Adaptive and rapid responding production systems would allow the customisation of products at low price and, thus, hit the market where it is more responsive.

During the last two decades, the miniaturisation of traditional manufacturing machines and the study of innovative fabrication technologies suitable for micro-parts and systems have become key research areas in micro-manufacturing. Consequently, several highly miniaturised manufacturing systems, known as a micro-factory, have evolved, and been implemented into industrial applications. Below is a brief review of some of these micro-factories.

Initially, other names have been used, such as desktop factory, modular micro-factory, factory-in-a-suitcase, palm-top factory, portable factory, bench-top machines and others, which aimed to highlight not only the concept of miniaturisation of the production system, but also its flexibility and portability. Each system focusses on a few specific steps of the production of micro-devices whilst the ultimate goal is the development of a comprehensive miniaturised production system able to manufacture micro-components and transform them into a finished product. The micro-factory thus includes manufacturing, assembly and packaging facilities. This integration is an essential issue in micro-manufacturing in order to achieve the required positioning accuracy and to reduce manipulation steps. Indeed, the manipulation is a very critical step at the micro-scale due to the predominance of the superficial forces that complicate part grasping and holding, and make releasing extremely problematical and difficult to control [31]. These concepts are explored further, and in detail in Chap. 9. The first prototype ever of a micro-factory (Fig. 1.12) was developed in Japan in 1999 by the Mechanical Engineering Laboratory Tsukuba [32], following the development in 1996 of a micro-lathe

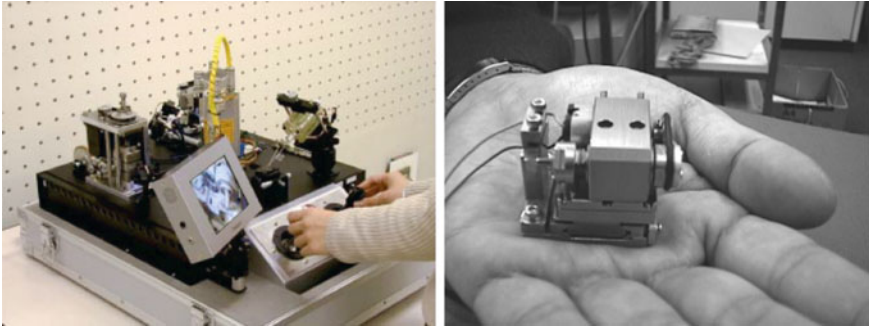


Fig. 1.12 Portable, tele-operated micro-factory [31] (left), micro-lathe developed by MMC Japan [31] (right)

smaller than a human hand (Fig. 1.12). It was 32 mm long, 25 mm wide, 30.5 mm high, with a weight of only 100 g. Parts with a minimum diameter of 60 microns were manufactured (Fig. 1.13). The linear stages were driven by piezoelectric actuators for fine and coarse positioning. The entire micro-factory includes the micro-lathe and other miniaturised machining machines; a milling machine and a press, installed together with a micro-transfer arm and a two-fingered micro-manipulator on a board. The whole micro-factory was installed inside a portable case 625 mm long, 490 mm wide and 380 mm high with a total weight of approximately 34 kg. The machines were tele-operated with two joysticks and visual aid. The power consumption was just 60 W.

After this first development, several other units followed. The Desktop Factory[®] (Fig. 1.14), developed by Niked Sankyo (ex Sankyo Seiki) in 2003, is the first commercial micro-factory, whose strengths are modularity, flexibility and portability. It is based on miniaturisation of conventional components and machines, such as motors, robots, pallets, vacuum pumps, developed in multi-purpose modules 170 mm wide able to clean, coat, camp, mate, screw, measure and heat [33].

Fig. 1.13 Examples of pieces produced [31]

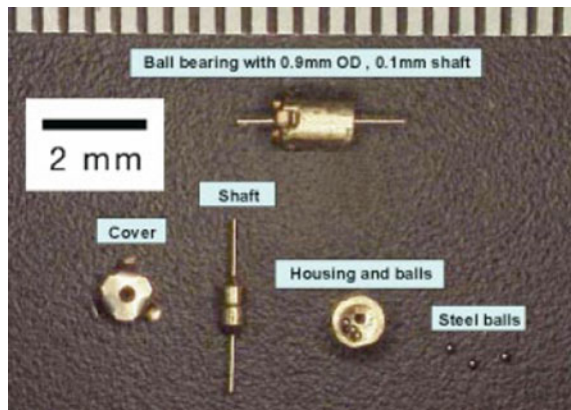




Fig. 1.14 DESKTOP FACTORY® by Niked Sanyo [33]

Olympus corporation developed two micro-factory prototypes since 1991 [34] (Fig. 1.15). One is a teleoperation system able to assemble small components with the aid of a microscope. It is suitable for operations at micro-scale that require manual assistance, such as micro-welding and inspection. It consists of a video microscope, a parallel-link micromanipulator, a parallel-link stage with 6 DoF for handling operations.

The other micro-factory has been conceived for the assembly of micro-optical parts of products, such as mobile phones and medical endoscopes; it was able to assemble lenses with 1 mm external diameter, a CCD and a lens frame with a footprint of 500×350 mm achieving a good space efficiency, high automation and great accuracy.

In Switzerland the Ecole Polytechnique Fédérale de Lausanne (EPFL) together with Centre Suisse d'Electronique et Microtechnique (CSEM) developed the Pocket Factory [35] in 2005. Its peculiarity with respect to other modular micro-factory concepts is the vertical piling of modules (Fig. 1.16). Each micro-box is a clean room (class 100 according to the Federal Standards 209E) of 50×50 mm containing several parts dedicated to assembly operations, namely an entry port, a

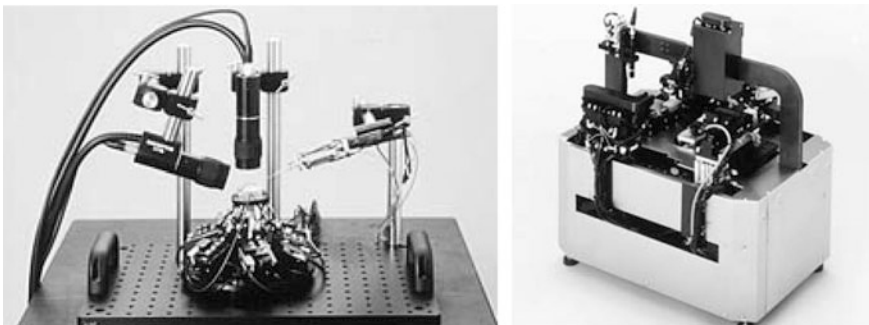


Fig. 1.15 Microparts Teleoperation System (*left*) Olympus assembly system (*right*) [34]

robot, sensors for process control. The miniaturised robot is $100 \times 100 \times 200$ mm, has 4 degree of freedom system and a cylinder of diameter and high of 130 and 20 mm as workspace [36].

On the base of Agile Assembly Architecture [37], Carnegie Mellon University developed an example of mini-factory (Fig. 1.17): a modular table-top precision

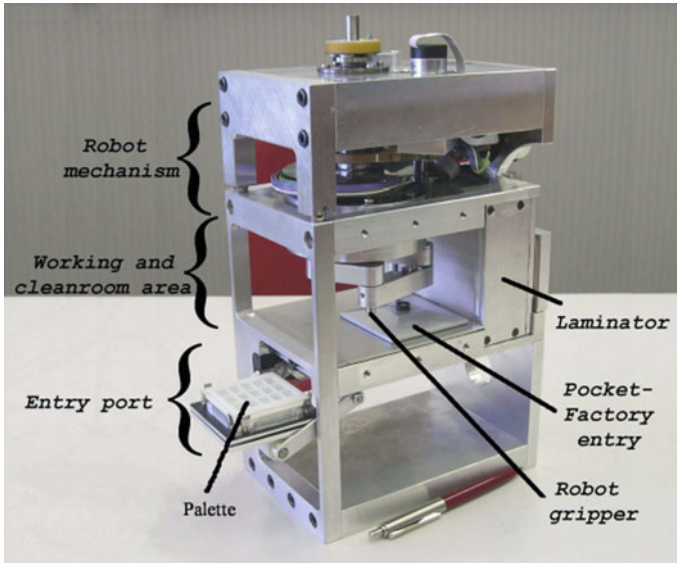


Fig. 1.16 Pocket Factory by EPFL [35]

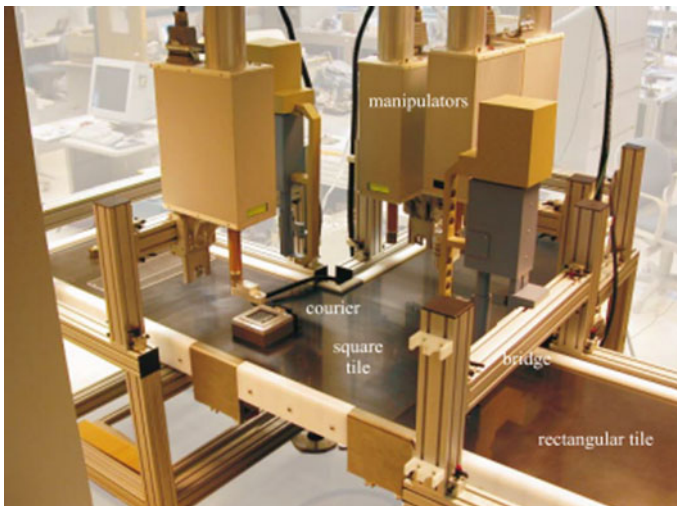


Fig. 1.17 Carnegie Mellon's Agile Assembly Architecture [37]

assembly system [38]. It integrates the product transport and positioning through multiple couriers with planar linear motors, which carries the sub-assemblies to multiple assembly systems with 4-dof, interchangeable modular end effectors and cameras and illumination device. An interface tool is used for a comprehensive centralized design, programming an operation monitoring.

Several other micro-factory concepts and equipment followed these pioneering works. Nowadays the concept is well established and may lead to the implementation of new business models (see also Chap. 10); however, a shift of manufacturing paradigms is required to ease its penetration in the market.

References

1. Feynman RP (1960) There's plenty of room at the bottom. *Eng Sci* 23(5):22–36
2. Madou MJ (2002) *Fundamentals of microfabrication: the science of miniaturization*. CRC Press, Cleveland
3. Ghosh A, Corves B (2015) *Introduction to micromechanisms and microactuators*. Springer, India
4. Squires TM, Quake SR (2005) Microfluidics: fluid physics at the nanoliter scale. *Rev of Mod Phys* 77(3):977–1026. ISSN 0034-6861
5. Van Brussel H, Peirs J, Reynaerts D, Delchambre A, Reinhart G, Roth N, Weck M, Zussman E (2000) Assembly of micro-systems. *Ann CIRP* 49(2):451–472
6. Zhou Shu-Ang (2003) On forces in microelectromechanical systems. *Intl J Eng Sci* 41:313–335
7. Milonni PW (1994) *The quantum vacuum: an introduction to quantum electrodynamics*. Academic Press, San Diego
8. Rob Legtenberg A, Groeneveld W, Elwenspoek M (1996) Comb-drive actuators for large displacements. *J Micromech Microeng* 6:320–329
9. Wallash AJ, Levit L (2003) Electrical breakdown and ESD phenomena for devices with nanometer-to-micron gaps. In: *Micromachining and microfabrication*. International society for optics and photonics, pp 87–96
10. Townsend JS (1915) *Electricity in gases*. Clarendon Press, Oxford
11. Nye JF (1985) *Physical properties of crystals*. Clarendon Press, Oxford
12. Hall EO (1951) Deformation and ageing of mild steel. *Phys Soc Proc* 64(B381):747–753
13. Petch NJ (1953) Cleavage strength of polycrystals. *J Iron Steel Inst* 174:25–28
14. Chang H, Altstetter CJ, Averbach RS (1995) Nanophase metals-processing and properties. In *Advanced materials and processing* 3
15. Fu MW, Chan WL (2014) *Micro-scaled products development via microforming*. Springer series in advanced manufacturing. Springer, London. doi:10.1007/978-1-4471-6326-8_2
16. Weissmüller J, Löffler J, Kleber M (1995) Atomic structure of nanocrystalline metals studied by diffraction techniques and EXAFS. *Nanostruct Mater* 6(1–4):105–114
17. Yoshizawa Y, Oguma S, Yamauchi K (1988) New Fe-based soft magnetic-alloys composed of ultrafine grain-structure. *J Appl Phys* 64:6044–6046
18. Liu QY, Zhang QH, Zhang JH, Zhang M (2014) Influence of grain size and grain boundary of workpiece on micro EDM. *Adv Mater Res* 941–944:2116–2120. doi:10.4028/www.scientific.net/AMR.941-944.2116
19. Vogler MP, DeVor RE, Kapoor SG (2004) On the modeling and analysis of machining performance in micro-endmilling. Part I: surface generation. *ASME J Manuf Sci Eng* 126:685–694

20. Vogler MP, DeVor RE, Kapoor SG (2004) On the modeling and analysis of machining performance in micro-endmilling. Part II: cutting force prediction. *ASME J Manuf Sci Eng* 126:695–705
21. Susmita K (2013) Introduction, classification and applications of smart materials: an overview. *Am J Appl Sci* 10(8):876–880
22. Ahmad I (1988) ‘Smart’ structures and materials. In: Rogers CA (ed) *Proceedings of army research office workshop on smart materials, structures and mathematical issues*. Virginia Polytechnic Institute and State University, Blacksburg, VA, pp 13–16, 15–16 Sept 1988
23. Akhras G (2000) Smart materials and smart systems for the future. *Can Military J* 1(3):24–31
24. Dineva P, Gross D, Müller R, Rangelov T (2014) *Piezoelectric materials in dynamic fracture of piezoelectric materials*. Springer International Publishing, Switzerland
25. Delaey L (1991) Phase transformations in materials. In: Cahn RW, Haasen P, Kramer EJ (eds) *Material science and technology*, vol 5. VCH, Weinheim
26. Nespoli A, Besseghini S, Pittaccio S, Villa E, Viscuso S (2010) The high potential of shape memory alloys in developing miniature mechanical devices: a review on shape memory alloy mini-actuators. *Sens Actuators A* 158:149–160
27. Hu M, Fu Y, Du H, Ling S (2004) Titanium nickel thin films for microactuation. In: *Proceedings of the 9th international conference on new actuators*, June. ISBN-3-933339-06-5: 79
28. Bar-Cohen Y (2001) *Electroactive polymer (EAP) actuators as artificial muscles (reality, potential, and challenges)*. SPIE Press, Bellingham
29. Samatham R, Kim KJ, Dogruer D, Choi HR, Konyo M, Madden JD, Nakabo Y, Nam JD, Su J, Tadokoro S, Yim W, Yamakita M (2007) *Active polymers: an overview in electroactive polymers for robotic applications: artificial muscles and sensors*. Springer, London
30. Kawahara N, Suto T, Hirano T, Ishikawa Y, Kitahara T, Ooyama N, Ataka T (1997) Microfactories; new applications of micromachine technology to the manufacture of small products. *Microsyst Technol* 3:37–41
31. Feddema JT, Xavier P, Brown R (1998) Assembly planning at the micro scale. In: *Proceeding of the workshop on precision manipulation at the micro and nano scales, proceedings of IEEE international conference on robotics and automation*, Leuven, Belgium, May 16–20
32. Tanaka M (2001) Development of desktop machining microfactory. *RIKEN Review* 34: focused on advances on micro-mechanical fabrication techniques
33. http://www.nidec-sankyo.co.jp/english/technology/core_technology.html
34. <http://www.olympus-global.com/en/news/1999b/nr991201mifae.jsp>
35. Verettas I, Clavel R, Codourey A (2005) “Pocket factory”: concept of miniaturized modular cleanrooms, not yet published (No. LSRO2-CONF-2005-017) available at <http://infoscience.epfl.ch/record/63609/files/TMMF05-pocketfactory.pdf>
36. Bacher JP, Bottinelli S, Breguet JM, Clavel R (2002) Delta3: a new ultra-high precision micro-robot. *Journal Européen des Systèmes Automatisés, Hermes* 36(9):1263–1275
37. Rizzi AA, Gowdy J, Hollis RL (1997) Agile assembly architecture: an agent based approach to modular precision assembly systems. In: *Proceedings of IEEE international conference on robotics and automation*, pp 1511–1516
38. Hollis RL, Cowdy J, Rizzi AA (2004) Design and development of a tabletop precision assembly system. *Mechatronics & robotics 2004, IEEE*, Aachen, Germany, pp 1624–1628, 13–15 Sept 2004

Chapter 2

Micro-injection Moulding

Andreu Sancho, Laura Arribas and Daniel Teixidor

2.1 Overview

The micro-injection of plastics is currently the technology with the greatest future potential development for the manufacture of plastics components weighing less than 1 g and with tolerances in the range of 10–100 microns, thus allowing complicated geometries and high surface quality (Fig. 2.1).

2.1.1 Technical Description

Manufacturing tiny plastic parts by injection process is developing as a specialised service. This is an emerging technology with immense potential for the development of mass produced components for many applications.

Micro-injection involves obtaining micro-moulded parts weighing less than a tenth of a gram and with high dimensional accuracy.

In general, the weight of a micro-component can range from a few thousandths of a gram to approaching one hundred hundredths of a gram with dimensional tolerances in the range of 0.0002–0.0005 mm (Figs. 2.2 and 2.3).

Mini-injection involves producing parts weighing between tenths of a gram to a few grams each, but with lower dimensional accuracy than micro-injection.

A. Sancho (✉) · L. Arribas · D. Teixidor
Technology Centre of Catalonia, Eurecat, Barcelona, Spain
e-mail: andreu.sancho@eurecat.org

L. Arribas
e-mail: laura.arribas@eurecat.org

D. Teixidor
e-mail: daniel.teixidor@eurecat.org

Fig. 2.1 Micro-toothed wheel. Weight 0.0022 g



Fig. 2.2 Micro-parts (*Source Fraunhofer IPT/WZL and Rwth Aachen*)



In summary, the main difference between mini and micro-injection, besides the volume of the part, is defined by the dimensional accuracy required.

In both cases, the mass transformation process resembles the conventional system. The differences are in the mechanisms of the nozzles, parameters, and the tooling used.

2.1.2 Definition of Technology

It is not just about the injection of small size parts; micro-injection is a very high precision injection process. The injection of tiny pieces which do not require great precision is not considered micro-injection, but conventional injection of small parts, or just mini-injection moulding.

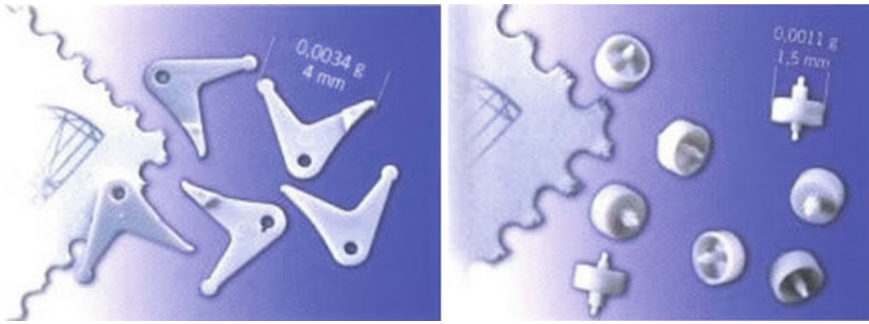


Fig. 2.3 Details of micro-parts (Reproduced from Wittmann-Battenfeld)

According to the “Institute of Design and Production in Precision Engineering (IKFF)” micro-injection comprises three different areas:

- Micro-injection parts: Components with very low weight (in the order of milligrams), small dimensions (few millimetres) and micro-metric details.
- Micro-structural parts: Components with standard dimensions, weighing several grams, but with areas with micro-structural details.
- Micro-precision parts: Parts of any size, but with tolerances in the order of a micro-metre (Fig. 2.4).



Fig. 2.4 Micro-parts (Reproduced from Sumitomo-Demag)

2.2 Materials

Although it is possible to inject any thermoplastic material into a mould, in micro-injection is necessary to take into account:

- Injection speeds are higher
- Shear rate is higher
- Cooling speeds are fast due to the high surface/volume ratio.

Materials behave differently at the micro-scale and hence compromises are sometimes required, depending on the component, mould geometry, and scale. For instance, the material with the best mechanical properties for an application may not be suitable for the micro-injection process, and an appropriate alternative should be used.

LCP, COC, PC, PS, PPE, PMMA, PEEK, PSU, PAI, PEI, PBT, PA and POM are plastic materials commonly used in micro-injection.

LCP or COC are good material choices for high reproduction. PC, PA, POM, PBT, PEI, PSU and PPE are materials with high fluidity. The following table presents the main thermoplastic materials (Table 2.1).

Table 2.1 Thermoplastic materials

Acronym	Polymer	Temperature stability (C)	Properties	Structure
COC	Cyclic Olefin Copolymer	140	High transparency	Amorphous
PMMA	Polymethylmethacrylate	80	High transparency	Amorphous
PC	Polycarbonate	130	High transparency	Amorphous
PS	Polystyrene	80	Transparent	Amorphous
POM	Polyomexymethylene	90	Low friction	Semi crystalline
PFA	Perfluoroalkoxy	260	High chemical resistivity	Semi crystalline
PP	Polypropilene	110	Mechanical properties	Semi crystalline
PET	Polyethylene Terephthalate	110	Transparent, low friction	Amorphous/Semi crystalline
PEEK	Polyetheretherketone	250	High temperature resistivity	Semi crystalline
PA	Polyamide	80–120	Good mechanical properties	Semi crystalline
PSU	Polysulfone	150	Chemical and temperature resistivity	Amorphous
LCP	Liquid Crystal Polymer	230	Stability, low shnnkage	Liquid crystalline

2.3 Design and Simulation

2.3.1 Characterisation—Micro-rheology

One way to characterise the rheological response of polymers is by measuring the deformation of a small sample of material (in the order of millimetres) when a traction force of small amplitude at different frequencies is applied (in the order of tens of Hertz) using a mechanical rheometer.

Using equipment to establish if the resulting output is in-phase, or out of phase, helps characterise the deformation as elastic or plastic.

However these conventional rheometers give an “average” measure and do not allow time or position specific measurements. Hence, they do not take into account the “non-homogeneity of the system”.

Therefore, to characterise materials at the micro-scale, a specific micro-rheology technique has been developed.

There are basically two methods of micro-rheology: those that involve physical manipulation of the sample by external forces, also called active method; and those that measure the movement of the particles introduced into the material due to thermal or Brownian fluctuations (caused by collisions between particles), also called the passive method.

Active methods include:

- Magnetic manipulation method: Metal micro-particles are incorporated into the material and are excited by magnetic fields. The trajectories are subsequently analysed by optic microscopy.
- Optical tweezers method: Two laser beams capture and manipulate small dielectric particles. The application of this force is extremely localised and moves in the order of pN. Detection and measurement of movement is also performed by interferometer techniques.

The passive micro-rheological methods only use the micro-particle’s thermal energy embedded in the polymer. The studied materials must have a viscosity low enough to allow movement of these micro-particles.

This movement depends on the type of material. These methods always work in the linear region because external force is applied.

2.3.2 Rheological Simulation

The benefits of computer simulation for injection moulding are well identified. A user will know, without building a mould, if:

- The cavity may be filled
- A wall is too thin

- The material has been selected properly
- The cycle time is acceptable
- The number, type and location of the gates are optimised and predict potential defects as weld lines, air trapping or part warping.

Rheological simulation of micro parts using software processes developed for conventional injection moulding presents uncertainties.

A significant increase in the area-volume ratio in a micro-part significantly affects the behaviour of filling and cooling.

The wall thickness of a micron or less of these parts must be modelled by finite elements of considerable size and may affect the accuracy of the results.

The Institut für Mikrotechnik Mainz GmbH (IMM) Johannes Gutenberg University of Mainz has performed simulations of micro-components shaped as membranes of 150 and 250 μm thick and predicted shrinkage/distortion in a waveguide.

Subsequent comparison of the simulated results and the actual parts has successfully verified the modelling process.

Mathematical models have been developed and verified for production of high accuracy micro-cavities by using Focused Ion Beam (FIB). Using these models, it is possible to produce micro-cavities with nano-scale surface accuracy for micro-replication and submicron polymeric, ceramic and metallic micro-components.

Subsequent studies have worked on the correlation between simulation with 3D MoldFlow algorithm and an experimental mould replication of micro-gears (Figs. 2.5 and 2.6).

2.3.3 Conclusions

- There are limitations on the size of the geometries using 3D to simulate the process of micro-injection.
- A cavity can be produced by the FIB process. This maskless technique makes the process more economic and flexible.
- A system has been developed for micro-replication, integrating both the thermal control unit and the vacuum, able to replicate 3D micro-components.
- Micro-components such as a 100 μm gears can be moulded successfully. It is also possible to produce other forms such as micro-lenses, striated surfaces, etc., by this process.
- The mould temperature has a dramatic effect on the process of micro-moulding. A mould temperature near the non-flow has proven practical to facilitate filling, even at low injection pressures.

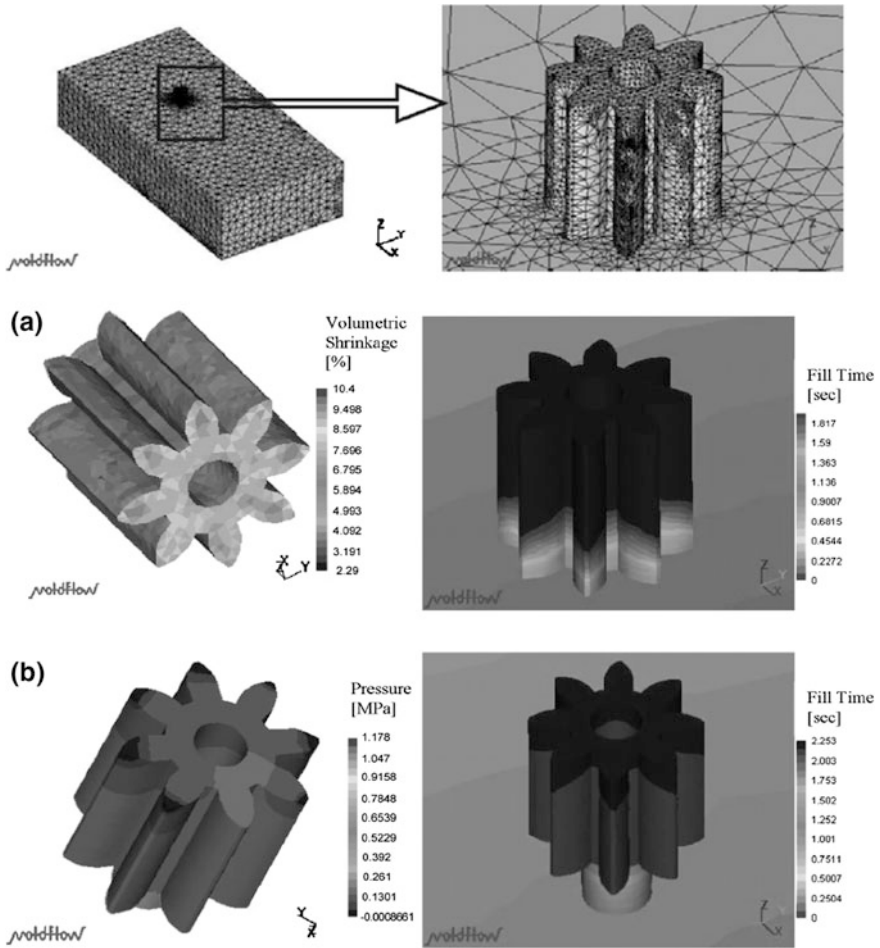


Fig. 2.5 3D MoldFlow Simulation of micro-gears

- To replicate a plastic micro-component with an optical finish, a cavity of Si can be used. For mass production, a cavity of a stronger material may be used (e.g. a Ni-Be).
- A qualitative comparison of the micro-cavity and the moulded component was made using a scanning electron microscope (SEM), which showed that this micro-replication process can duplicate accurately the micro-cavity geometry.

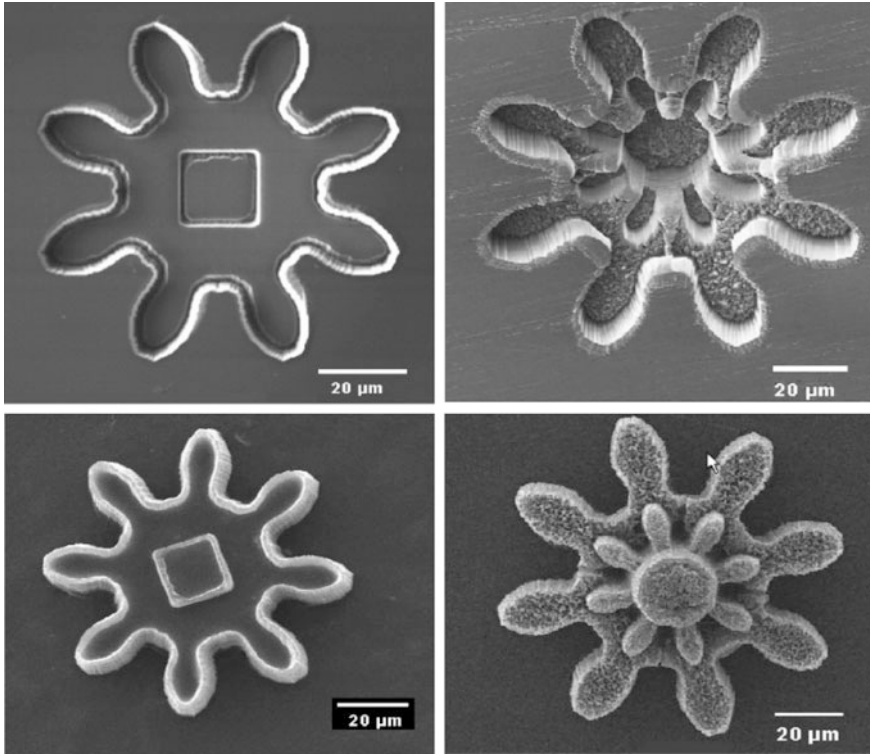


Fig. 2.6 3D MoldFlow Simulation of micro-gears

2.4 Process and Materials

The micro-injection process is a variation of the conventional injection process. The micro-injection technique is based on the characteristics imposed by the small size of the pieces.

2.4.1 Principles of the Injection Moulding Process

Thermoplastics injection moulding is a physical and reversible process. The heat supplied to the material by the plasticiser of an injection machine melts it and fills the hollow cavities of a mould, within pre-determined parameters of pressure, velocity and temperature (Fig. 2.7).

After a while, the molten plastic in the mould loses heat, solidifies and reproduces the shapes of the hollow parts of the mould. After opening the mould, the

Fig. 2.7 Injection parts

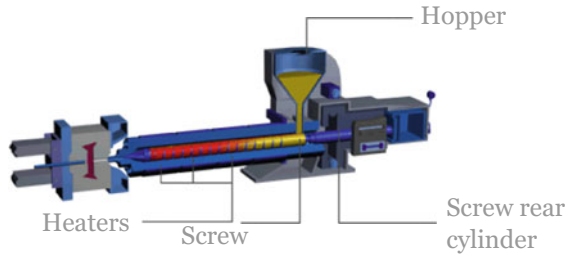
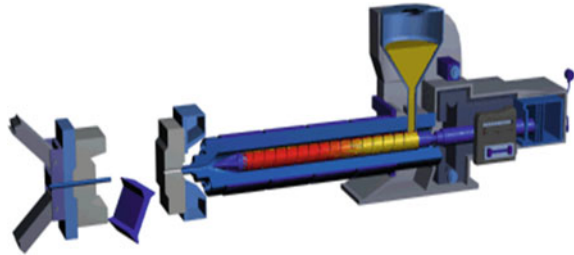


Fig. 2.8 Injection process



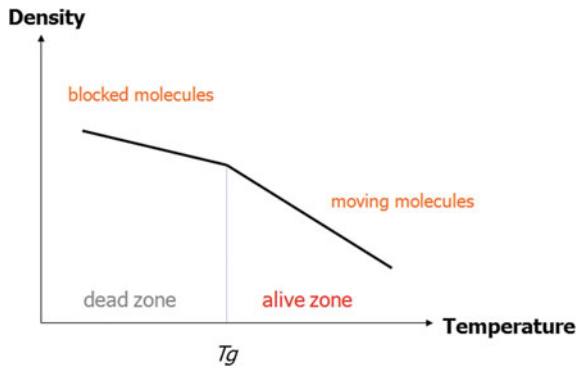
result is a solid piece with a texture and dimensions according to the areas and forms of mould cavities and to the natural contractions of the plastic (Fig. 2.8).

The amorphous and semi-crystalline polymers retain their three-dimensional shape when cooled below its T_g (glass transition temperature) and its melting temperature respectively.

Amorphous polymers are in a thermodynamic state of pseudo-balance when its temperature is below its T_g (glass transition temperature). In this state, the rotation and relaxation (unwinding of the chains) of the polymer are blocked. Thus, in the absence of applied forces, it retains its three-dimensional shape.

The semi-crystalline polymers also form crystals. These crystals provide dimensional stability to the molecule, which is thermodynamically stable in the crystalline region (Figs. 2.9 and 2.10).

Fig. 2.9 Amorphous polymer behaviour (Reproduced from Eurecat)



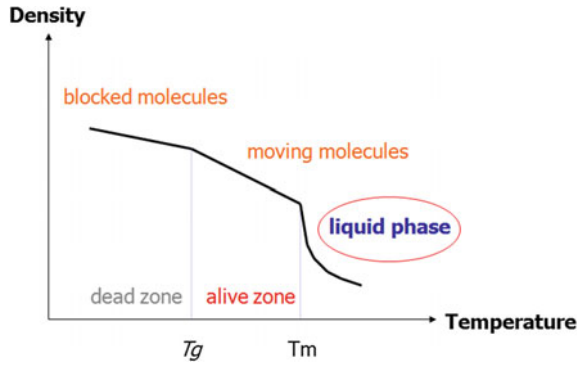


Fig. 2.10 Semi-crystalline polymer behaviour (Reproduced from Eurecat)

The injection steps are presented in the following diagram (Fig. 2.11):

1. Closing the mould
2. Moving forward the cylinder*
3. Injection: Filling phase. The screw acts as a piston forcing the material through the nozzle to the mould cavities.

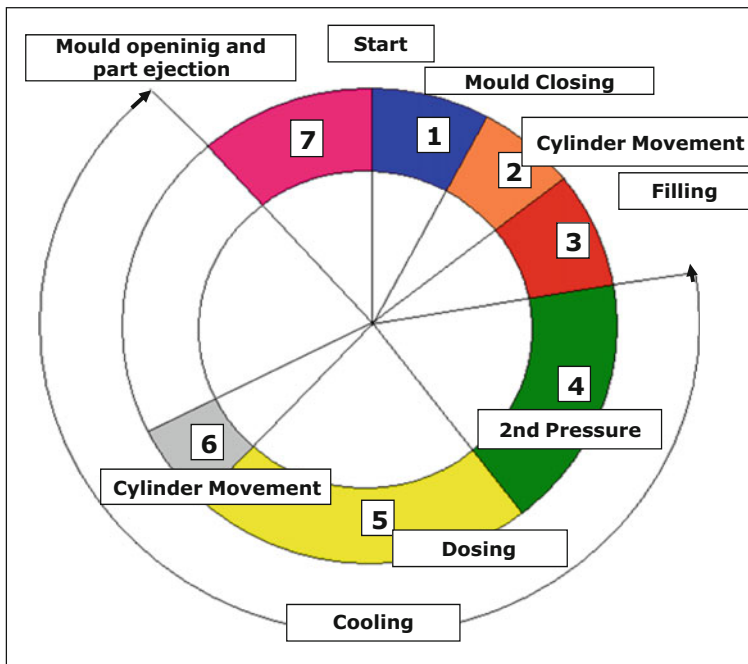


Fig. 2.11 Injection steps diagram (Reproduced from Eurecat)

4. Second pressure. It compensates the plastic volume reduction due to the solidification process.
5. Plasticisation. The screw rotates to dose material, including reversing.
6. Moving back the cylinder*
7. The part cools in the mould, the machine releases the clamping pressure and the mould opens. Then the ejection system acts removing the moulded parts
8. The clamping force closes the mould and the cycle starts again.

(*) In case of hot runner mould these movements are not necessary.

2.4.2 Key Features

The big challenge is the ability to produce suitable micro-parts with the precision and accuracy required in a long series.

Essential differences between micro-injection and conventional injection:

- Due to the small size of the parts, the process requires high injection rate and pressure. It should complete filling and compaction in a single stage.
- Generally, runner systems comprise 75% of the injected material volume.
- Broadly speaking, injection presses require spindles with small diameters (e.g. 10, 12, 14 mm) or extrusion and injection dosage mechanisms by a high precision small piston that pushes melted resin through the nozzle and flow channels. These systems provide high specific pressure injection on the material.
- The small amount of injected material requires cycle times as short as possible.
- It is necessary to use micro-granulated material (not standard) to feed the small diameter spindles.
- In heat sensitive polymers the injected volume should be adjusted in order to allow sufficient cooling.

From the point of view of the process, the main features to consider are:

- Need to keep accurate dosing.
- Have very controlled residence time of the material.
- Good control of the material temperature.
- Good control of the mould temperature.
- Need to use a high speed injection.
- Need to evacuate air from the mould to obtain a good reproduction.
- Always keep in mind the extremely rapid cooling of micro-parts.

2.4.3 Dosage (Charge)

The accuracy of the dosage, a homogenous melt, and establishing the correct dosage time are all extremely important.

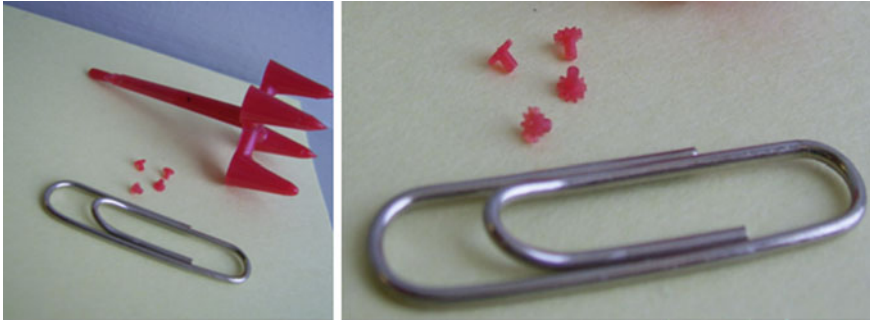


Fig. 2.12 Injected parts where 90% of the total shot volume corresponds to the runner system (Reproduced from Eurecat)

The limitations of the dosing systems of conventional injection moulding machines are also considered when developing miniature plastic parts weighing only a few hundredths of a gram. This raises a reasonable doubt about the capacity to obtain a rational and repeatable production using a standard injection machine.

The following table shows the accuracy of the stroke for a shot of 1 mg depending on the size of the screw (Fig. 2.12 and Table 2.2).

Generally, injection machines equipped with conventional screw systems are not able to use conventional raw material for micro-injection applications as the material grain size is too large.

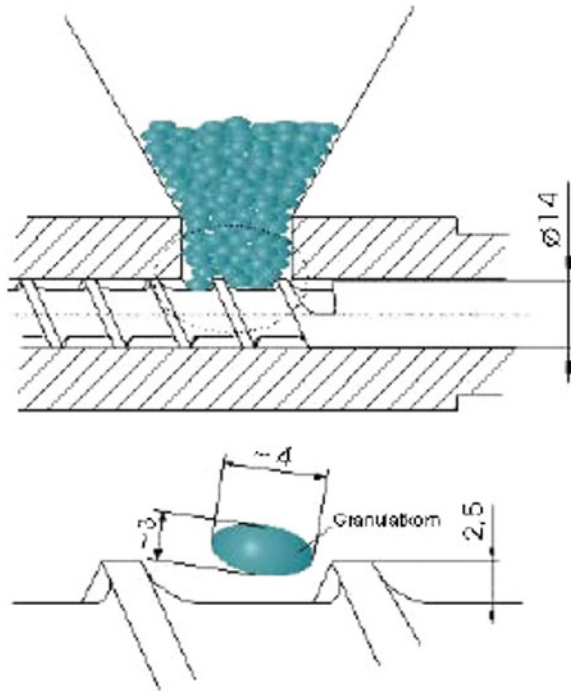
For this reason, in micro-injection machines it's necessary to use special pellets from 0.05 to 0.5 mm in diameter and thus prevent slipping and dosage problems in the feeding zone of the screw (Fig. 2.13).

Table 2.2 Accuracy of the stroke for a shot of 1 mg depending on the size of the screw

Screw piston-diameter (mm)	Stroke 4D (mm)	Stroke-volume 4D (cm ³)	Stroke-volume 5% 4D (cm ³)	Stroke for 1 mg shot weight (mm)	Resolution limit A/D for 4D stroke (mm)
22	88	33.45	1.673	0.0024	0.0430
20	80	25.13	1.257	0.0028	0.0391
18	72	18.32	0.916	0.0034	0.0352
14	56	8.62	0.431	0.0056	0.0273
12	40	3.14	0.157	0.0112	0.0195
9	36	2.29	0.115	0.0138	0.0176
7	28	1.08	0.054	0.0228	0.0137
5	20	0.39	0.020	0.0446	0.0098
4	16	0.20	0.010	0.0697	0.0078

Reproduced from Wittmann-Battenfeld

Fig. 2.13 Grain size required in a screw of 14 mm diameter or less (Reproduced from Wittmann-Battenfeld)



2.4.4 Injection Speed

In general, the micro-parts must be injected at the maximum speed provided by the machine to fill the micro-cavities in the shortest time possible and thus preventing material solidifying during the filling.

Furthermore, a high injection rate causes material shearing which raises the material temperature, improving flow within the cavity. However, it is important not to exceed the maximum shear value, which would degrade the material and thus the mechanical properties of micro-parts would be affected.

On the other hand, filling in the shortest possible time (maximum speed) implies using high pressure, which can be harmful, causing internal stresses in the component. Therefore, to reduce these high pressures is important that during the filling phase the mould is kept at an elevated temperature.

2.4.5 Injection Pressure

As with conventional injection moulding, it is necessary to maintain a high pressure in the first stage of micro-injection to maintain an injection rate as high as possible. In most cases, the same level of pressure may compact and define the final weight of the components.

2.4.6 Holding Pressure

Another important factor to take into account with micro-injection is the limited functionality of the second pressure or holding pressure due to the low thickness of the injected parts.

When the control system of the injection machine is hydraulic, it must be highly dynamic to allow extremely low injection volumes with injection times lower than 0.1 s.

2.4.7 Holding Pressure Time

Given the rapid solidification during the first stage, generally second stage pressure application is pointless as it will only act on the sprue—beyond which, material has usually solidified (Fig. 2.14).

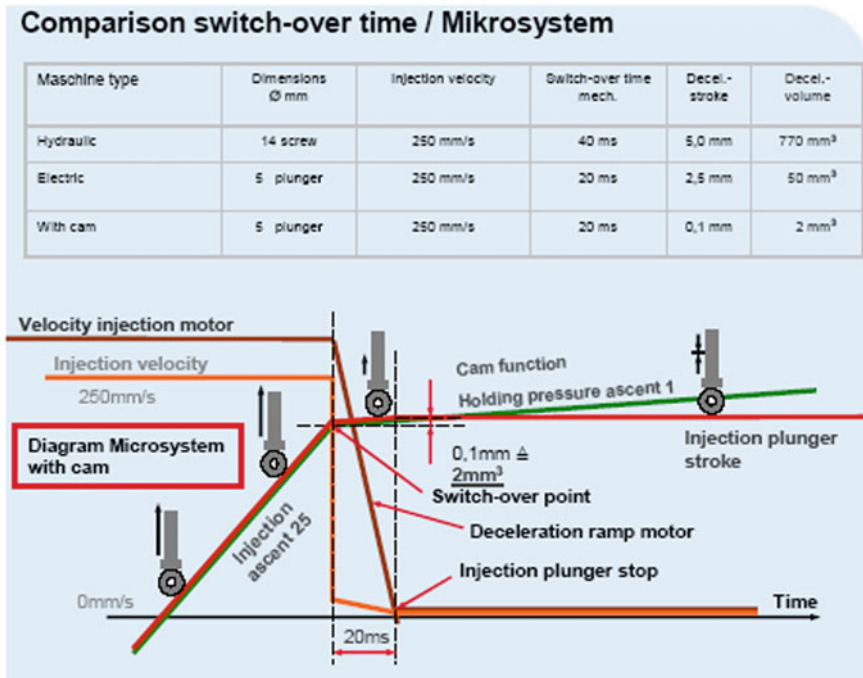


Fig. 2.14 Comparison of theoretical switchover time for different machine technologies (Reproduced from Wittmann-Battenfeld)

2.4.8 Cooling Time

After the holding pressure has been applied, the micro-parts can usually be demoulded since the melt will have cooled and solidified. However, it is still important to allow time for runners to cool sufficiently.

2.4.9 Process Temperatures in the Mould, Expansion and Balance

One of the biggest problems with micro-injection results from the high “aspect ratio” of the parts. The material solidifies instantly upon contact with the walls of the mould. This could be compensated by changing parameters such as injection speed. In this way, the material fills the cavity before cooling down and, at the same time, increases the temperature due to the shear rate, which would also help the process.

Depending on the geometry, this will not be sufficient to achieve a total reproduction (filling) of the cavity. In this case, it will be necessary to increase the temperature of the mould.

It is possible to see this influence in the following case which consists of micro-cavities placed radially with different aspect-ratios and details up to $300\ \mu\text{m}$ (Fig. 2.15).

This test illustrates what happens to the material away from the entry point. The mould construction system is as follows (Fig. 2.16).

The injection test results, with a nozzle temperature of $300\ ^\circ\text{C}$ and a filling time constant of 1.5 s, can be seen in the Fig. 2.17.

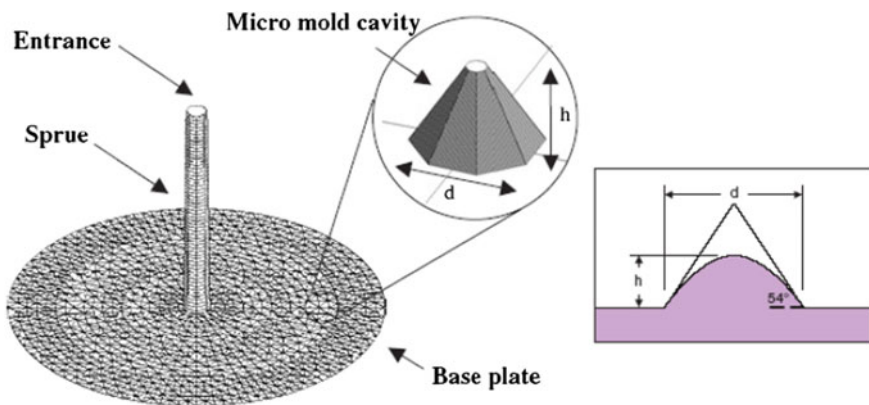


Fig. 2.15 Micro-cavities placed radially (Reproduced from Author SU et al. 2004)

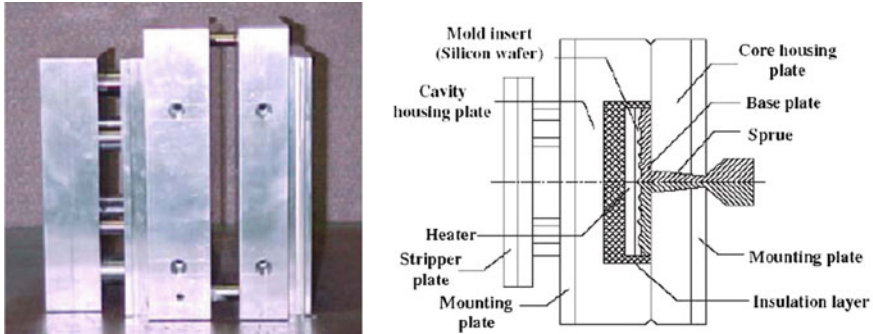


Fig. 2.16 Mould construction system for micro-cavities manufacturing (Reproduced from Author SU et al. 2004)

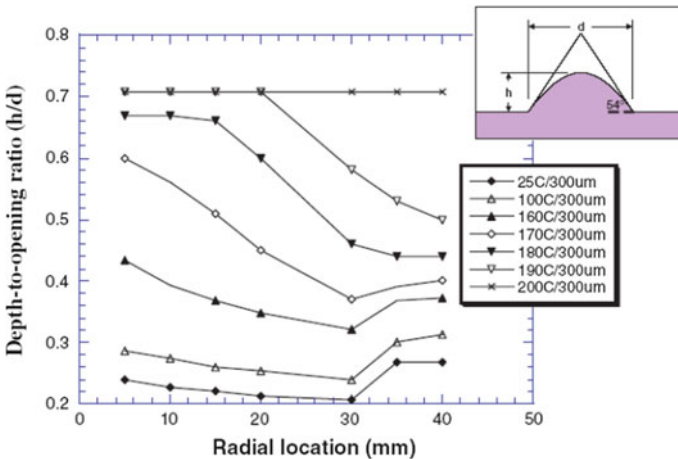


Fig. 2.17 Micro-cavities test results (Reproduced from Author SU et al. 2004)

The result is still not uniform until the mould temperature has reached 200 °C. This confirms the fact that micro-injection must be transformed with a mould temperature 40 or 50 °C above the T_g of the thermoplastic material (PC, T_g ≈ 145 °C).

It is important to remember that there is a risk of material degradation and cycle time increase. Besides, the dimensional variations are greater than in a conventional mould precisely because of this temperature increase. In some cases, there may be a temperature difference of 200 °C between ejection and expulsion. For this reason, some manufacturers of micro-injection machines propose using centring systems for micro-moulds, as shown in Fig. 2.18.

Optimal centring guides for micro-injection process are square or rectangular. In addition, it requires a floating cavities system.

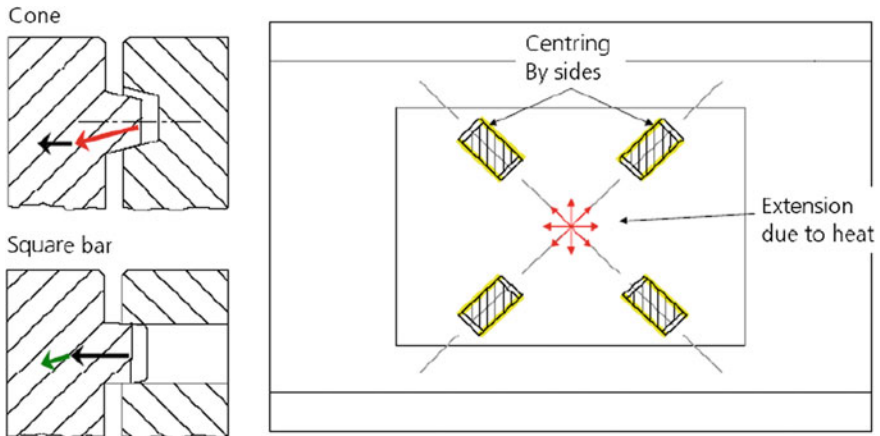


Fig. 2.18 Centring system for micro-moulds (Reproduced from Wittmann-Battenfeld)

With square or rectangular guides, a better focusing of the cavity is achieved because the adjustment is made between two parallel faces. Smaller closing forces are required to close the mould with square or rectangular guides (Figs. 2.19, 2.20 and 2.21).

2.4.10 Mould Venting

One of the typical problems of micro-injection moulding is the design of the venting system.

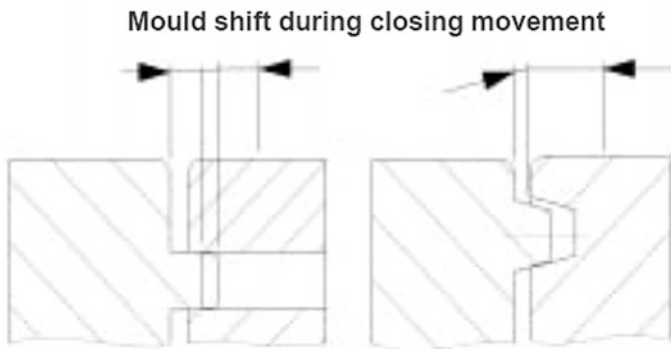


Fig. 2.19 Typical problems with conventional centring (Reproduced from Wittmann-Battenfeld)

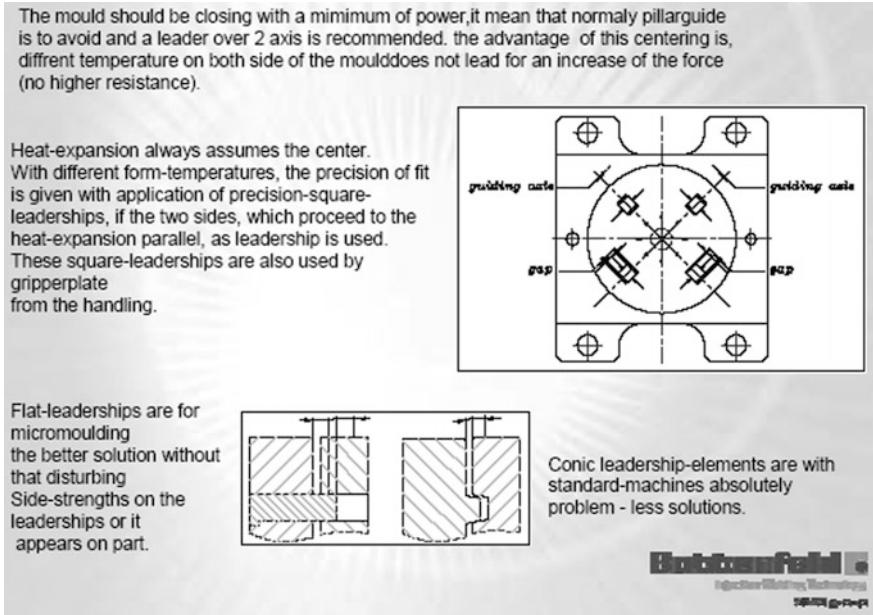


Fig. 2.20 Recommendations on the design for the mould centring system (Reproduced from Wittmann-Battenfeld)

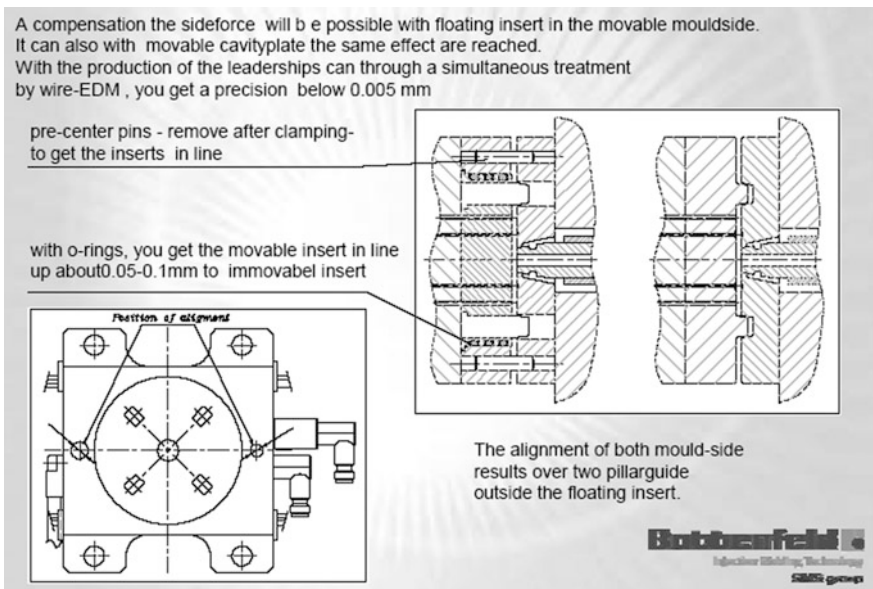


Fig. 2.21 Recommendations on the design for the mould centring system (Reproduced from Wittmann-Battenfeld)

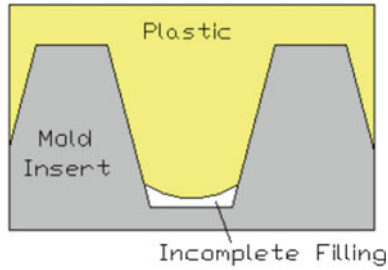


Fig. 2.22 Detail of an incomplete filling due to venting problems (unknown author)

The thickness of the part has the same order of magnitude as the thickness of the channels of conventional gas purging, so if conventional sizes are used, plastic material could potentially escape through the venting channels.

For this reason, and especially to get a faithful reproduction of the mould surface, in many cases, a vacuum pump is used to remove air from inside the mould. This requires installing a perimeter O-ring, usually on the fixed side of the mould, a valve in the nozzle of the machine and a small vacuum pump, which acts after the mould has been closed and sealed.

In some cases, the modification of the injection parameters or the mould temperature increase may not be sufficient to achieve an optimal filling, as seen illustrated in the following images (Figs. 2.22, 2.23 and 2.24).

Although we have no apparent filling problems, the vacuum generated into the mould avoid the “diesel effect” in the moulded parts (Fig. 2.25).

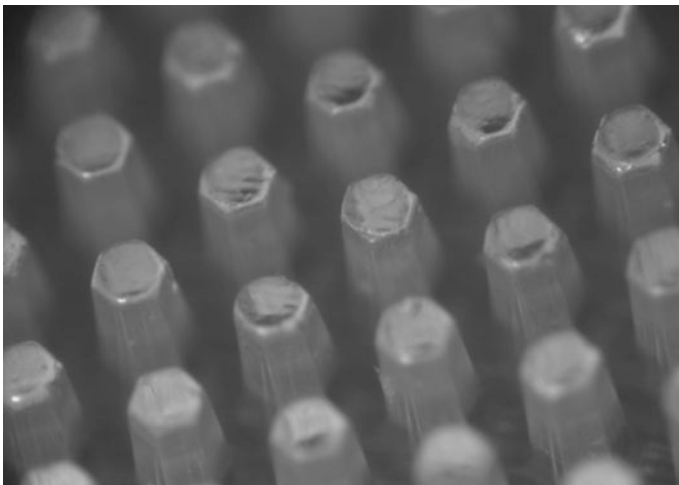


Fig. 2.23 Real image of the venting problem (unknown author)

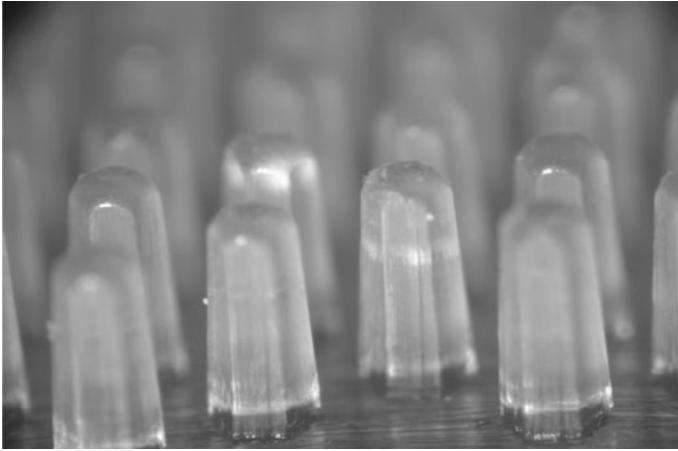


Fig. 2.24 Same parts using vacuum system (unknown author)

Fig. 2.25 Diesel effect
(Reproduced from Eurecat)



2.5 Tools and Machines

2.5.1 *The Injection Machine*

Injection machines have two different parts: The clamping unit and the plasticisation unit.

The clamping unit is responsible for opening and closing the mould and ejects the part using some form of ejector. This unit consists of the following elements:

- Fixed platen to support half of the mould
- Mobile platen to support the other mould half
- Reaction platen to support the clamping and retention forces

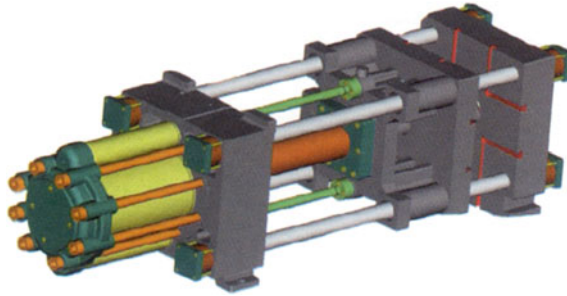


Fig. 2.26 Hydraulic drive (Reproduced from Eurecat)

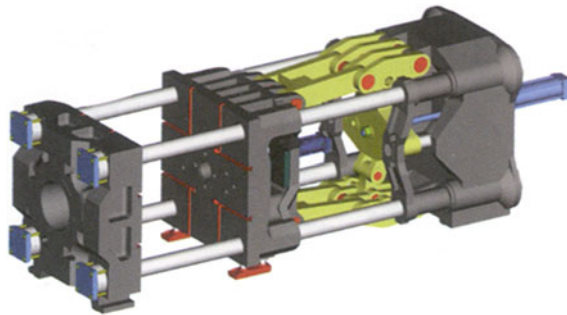


Fig. 2.27 Mechanical drive (Reproduced from Eurecat)

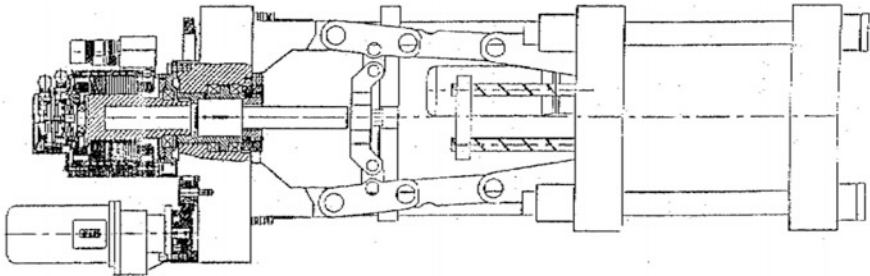


Fig. 2.28 Electrical drive (Reproduced from Eurecat)

- Four ties to resist the mobile platen forces
- Clamping system
- Ejection system.

There are three different clamping drives: Hydraulic, mechanical and electrical (Fig. 2.26, 2.27 and 2.28).

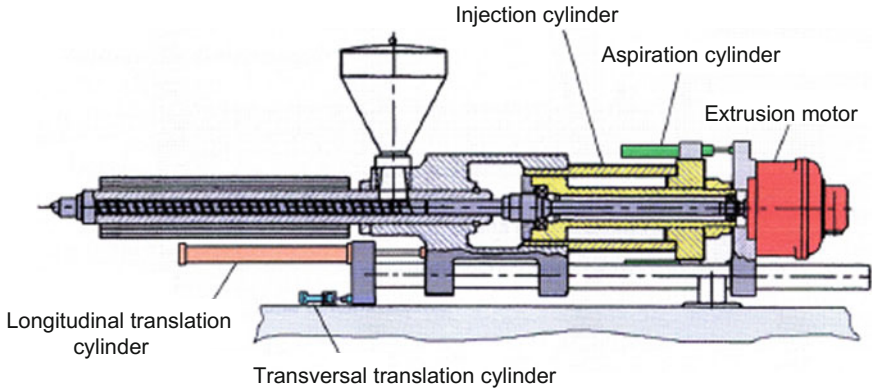


Fig. 2.29 Injection machine parts (Reproduced from Eurecat)

The plasticisation unit is a heated system, consisting of a rotating screw that introduces the melted polymer pressured into a closed mould. This unit consists of the following elements:

- Hopper
- Plasticisation chamber
- Electrical heaters
- Screw
- Nozzle
- Injection barrel
- Extruder engine (Fig. 2.29).

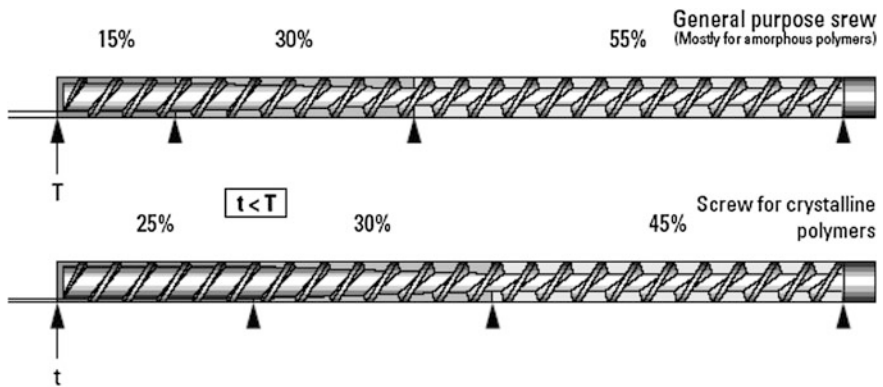


Fig. 2.30 Screw zones (Reproduced from Arburg)

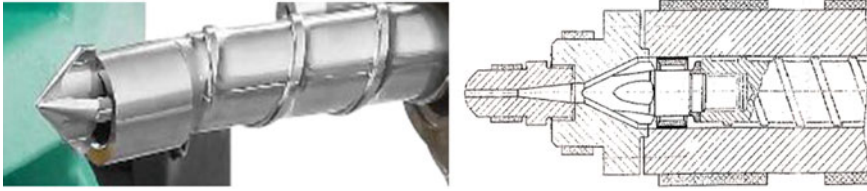


Fig. 2.31 Screw and non-return valve (Reproduced from Arburg)

The most important element for the injection moulding is the screw. There are three different screw zones:

- Feeding: Transport the material
- Compression: Heat the polymer by shear stress
- Dosing: Final homogenisation, the material is ready to be injected (Fig. 2.30).

The non-return valve in the nozzle allows injection of the plastic into the mould and prevents the material flowing back into the plasticisation cylinder (Fig. 2.31).

2.5.2 Plasticising Systems

For micro-injection, there are different plasticising systems. Two of the most widespread are presented here:

- The most commonly used plasticising system used is a direct injection unit using a screw. It consists of a scaled plasticiser with small-diameter conventional screw, ring and valve on the top. Other typical systems include ball valve seals, which are used for both dosing and injecting the plastic.
- Alternatively, injection units with two stages, extruder and injection plunger are sometimes used. This system consists of a set of mechanisms, where a small extruder makes the dosage, the material passes to the chamber and is pushed by a piston during the injection process (Figs. 2.32, 2.33 and 2.34).

When using machines with screw injection system it is necessary that moulds have a sufficiently sized runner, which does not need to be as precise delivering the minimum volume of material—it can be absorbed by the runner itself.

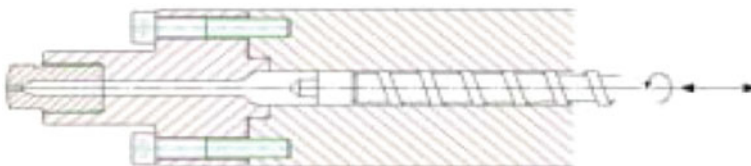


Fig. 2.32 Conventional scaled screw (Reproduced from Wittmann-Battenfeld)

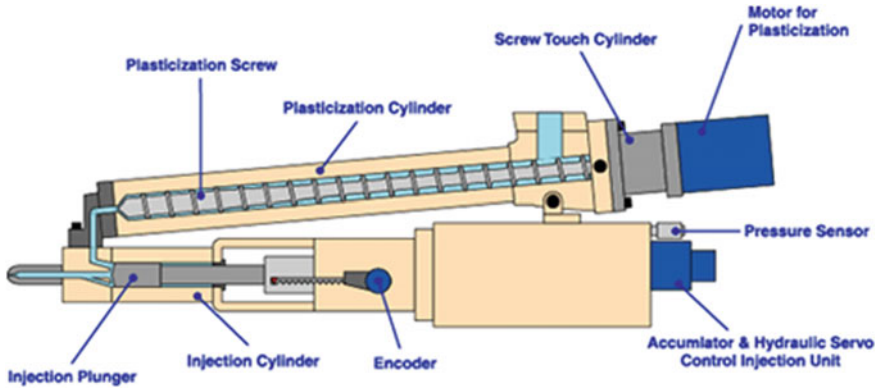


Fig. 2.33 Plasticiser with extruder and injection piston

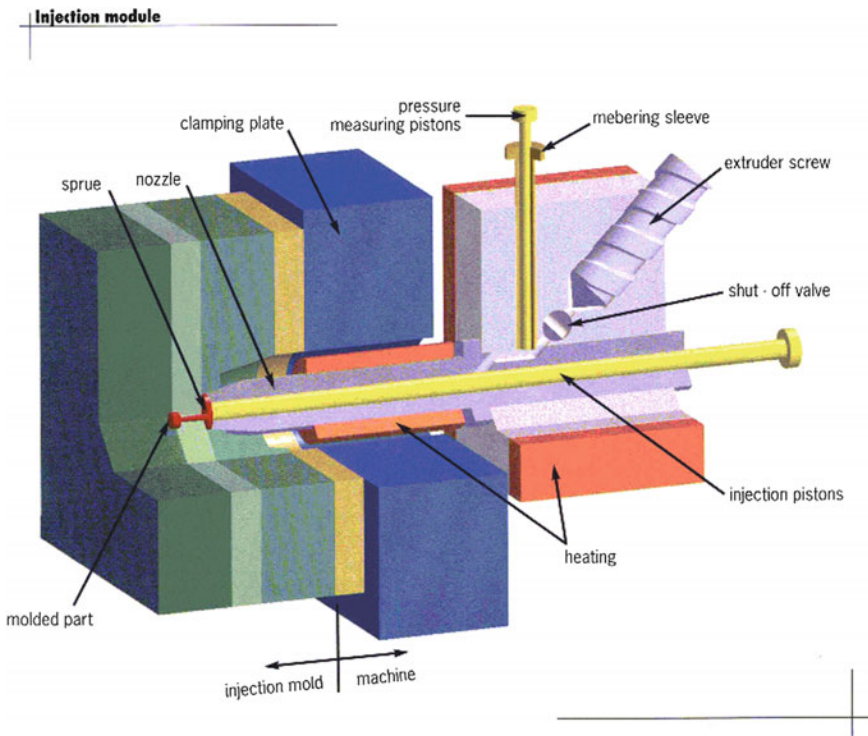


Fig. 2.34 Schematic representation of a plasticiser (Reproduced from Wittmann-Battenfeld)

The use of a larger runner, in addition to distributing the polymer from the entrance of the mould to the cavity or cavities, avoids the degradation of the material in the screw plasticiser due to an excessive residence time.

Therefore, the volume of the runner must be calculated to ensure a constant renewal of the polymer injected in each shot.

The main disadvantage of using an injection system with a high volume runner system is the increased total cycle time, as a result of increased cooling times.

2.5.3 Micro-injection System Without Plasticising

One of the main problems with conventional micro-injection is the amount of time the melted material is kept in the plasticiser of the injection unit, where it can easily degrade. Modern micro-injection systems often do not have a plasticiser. Instead, they apply ultrasonic waves to the material, melting it instantaneously (Fig. 2.35).

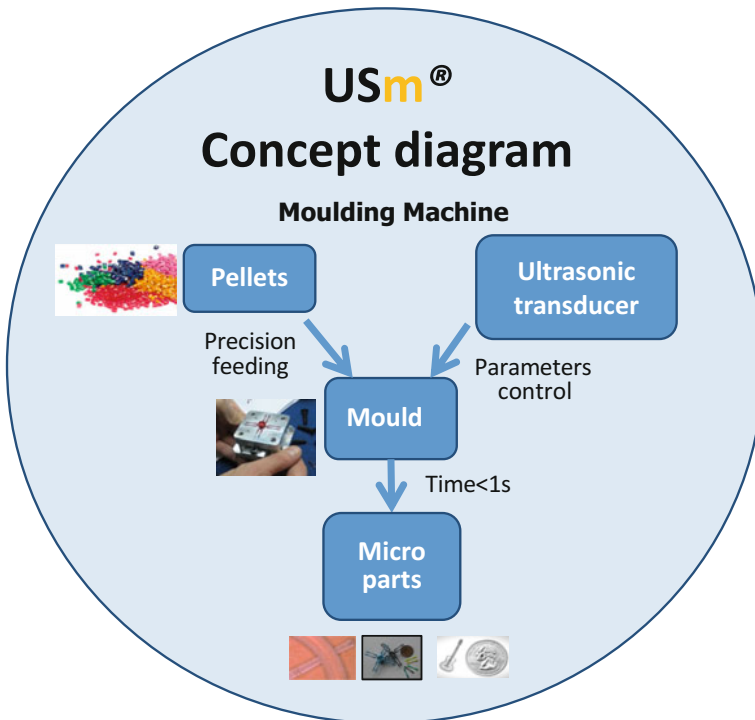


Fig. 2.35 Ultrasonic moulding concept diagram (Reproduced from Ultrason)

Table 2.3 Micro-injection moulding machines

Manufacturer and machine	Clamping force (kN)	Injection unit
Arburg—Microinjection module/Microinjection equipment	—	Screw diameter: 8/12/15 mm
Cronoplast/Rambaldi—Babyplast 610P	62.5	Piston diameter: 10–18 mm
Desma Tech—formicaPlast 1K and 2 K	10	Pre-plastification piston: 6 mm Plastification piston: 3 mm
Dr. Boy-Boy XS	100	Screw diameter: 12 mm
Juken Kogyo—JMW-017S-1.5t	15	Screw diameter: 14 mm
L.K. Technology Holdings—SP2 and SP5	20/50	Screw diameter: 12 mm/14 mm
Manner—Micro man 50 and Micro man 50 2C	50	Screw diameter: 14 mm
Milacron—Fanuc Roboshot S2000i 17B	150	Screw diameter: 14/16/18 mm
Mold Hotrunner Solutions—M3 and M3 mini	20	—
Nissei America—NEX15	150	Screw diameter: 16/19 mm
Sodick Plustech—LP10EH2, LP20EH3 and LP40A	100/200/400	Screw diameter: 14 or 18 mm
Sumitomo (SHI) Demag—Special plastification unit	Up to 500	Screw diameter: 12–35 mm
Toshiba Machine—EC5 and EC7	50	Screw diameter: 14 or 16 mm
Ultrasion—Sonus 1G	30	—
Wittmann Battenfeld—MicroPower 5—15t	50 to 150	Piston

2.5.4 Main Micro-injection Moulding Machines

The following table presents the main micro-injection moulding machines that can be found in the market (Table 2.3).

2.5.5 Micro-injection Moulds

In order to produce such small components, it is necessary to have moulds with features scaled to the required size. This is not possible to achieve using conventional machine tools. The usual techniques for the manufacture of prototype and production tools are not generally effective for producing moulds for micro-parts, which require other micro-machining techniques (Fig. 2.36).

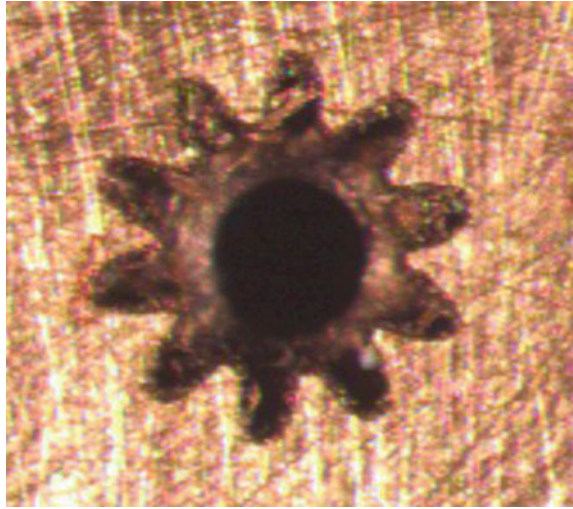
Different technologies are used to perform micro-machining, among the most prominent are:



Fig. 2.36 Micro-machining machines (Reproduced from Fraunhofer IPT, WZL Rwth Aachen)

- Mechanical systems:
 - Micro-milling. A typical micro-machining cutting tool can be 0.1–0.5 mm in diameter. For micro-machining the minimum spindle speed is 20,000 RPM, and in exceptional circumstances can be as high as 500,000 RPM. See the Micro-cutting chapter for more details.
 - Machining by monocrystalline diamond.
- Electrical systems:
 - Laser ablation involves the application of energy from a laser beam to produce a hot spot on the surface to be machined.
 - Micro-electro-erosion EDS. The micro-electro-erosion compared to traditional electro-erosion presents a better “aspect ratio”. It consists of an electro-machining process, which uses the erosive or eroding effect of the electrical discharges occurring due to the potential difference between the electrode (the part that gives form) and the material to be machined (Fig. 2.37).

Fig. 2.37 Detail cavity laser ablation on a micro-gear
(Reproduced from Eurecat)



- Chemical systems:
 - Selective Reactive Ion Etching.
 - DRIE.
- Combined systems:
 - Diamond and ultrasonic machining.
 - ELID-Grinding (Electrolytic In process Dressing). A combined technique for polishing and finishing.
 - LIGA (Lithographic Galvanic process). Sectored radiation from a photo-polymer with laser or X-ray.

It is recommended that for micro-injection moulds cavity cooling is achieved by Conformal Cooling Channels, which allow for more efficient monitoring of mould temperature, improves the quality of injected parts and can reduced the cycle time (Fig. 2.38).

It is also possible to use the Variotherm system or similar process, which involves mould cavity heating by induction, or other methods, and which equip the mould with a cooling circuit (with liquid). With this system, the mould is isolated (Fig. 2.39).

Small heating resistors controlled by thermocouples are used when it is necessary to get temperatures between 100° and 200 °C in the mould. In the big moulds it is possible to use the classic thermal channels by constantly circulating a previously tempered fluid (Fig. 2.40).

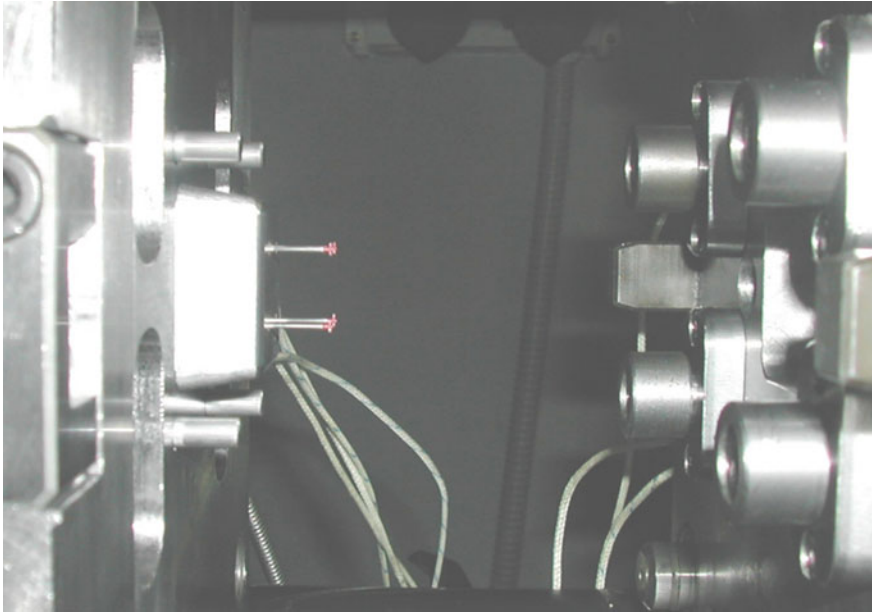
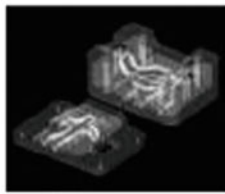
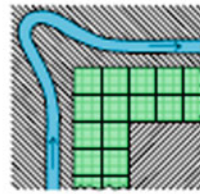
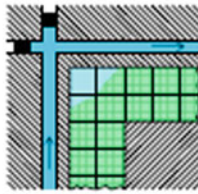


Fig. 2.38 Detail of a micro-injection mould (Reproduced from Eurecat)



Source: POM Inc.



Function principle

- More efficient mould temperature control by optimum positioning of cooling channels

State of the technology

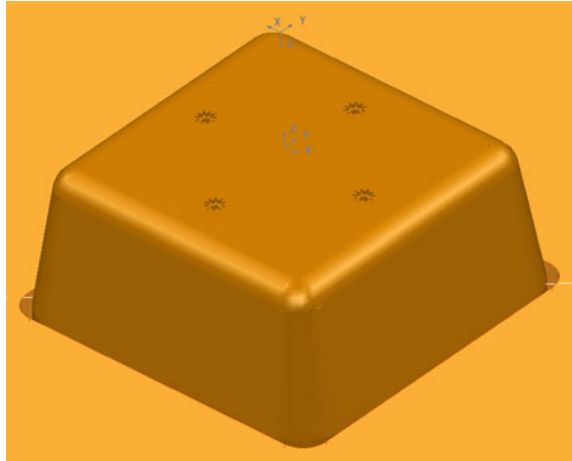
- Basic feasibility studies
- Further development of RT techniques towards series tool life necessary

Future potential

- Cycle time reduction in injection moulding
- Enhancement of the quality and complexity of injection moulded parts

Fig. 2.39 Variotherm system (Reproduced from Fraunhofer IPT, WZL Rwth Aachen)

Fig. 2.40 CAD3D, four micro-cavities in a mould (Reproduced from Eurecat)



2.6 Sectors of Application

Wide varieties of tiny plastic components that are manufactured by micro-injection are used in the following sectors:

- IT and communication: Printer heads and other writing heads, components for optical fibre, optical switches, waveguides, and beam splitter guides.
- Medical sector: Components for pacemakers, hearing aids, test of in vitro diagnostic, micro-vision sensor, components for measuring blood glucose, micro-fluidics chips.
- Biotechnology: Micro-plates for identification of micro-organisms.
- Home automation: All kinds of micro-sensors.
- Micro-mechanical: Watches, measuring instruments, micro-mechanisms, etc.
- Automotive: Pressure sensors, engine management, air and gas quality control, gearshifts, ABS, control of the dynamics of the vehicle. Adaptive navigation control (ACC), airbag, obstacle detection and improved visibility, etc.
- Electronics: Chips, sensors, accelerometers.
- Aeronautics: All kinds of micro-sensors.
- Aerospace and defence: Measuring air pressure, acceleration, sensors, humidity, pressure, gas, temperature, stabilisers, micro-seismometers, micro-hygrometers, micro-motors drive, and infrared photo detectors, micro-robots.
- Environment and agriculture: Micro-spectrometers, gas sensors, instrumentation control pollution (Figs. 2.41, 2.42, 2.43, 2.44, 2.45, 2.46 and 2.47).



Micro – clip
Part weight: 0,037 g



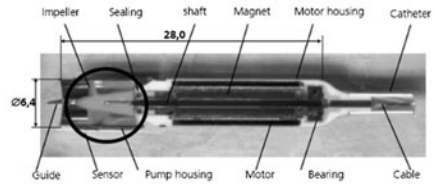
Micro – implant
Part weight: 0,022 g



Micro – bearing cap
Part weight: 0,01 g /
0,02 g

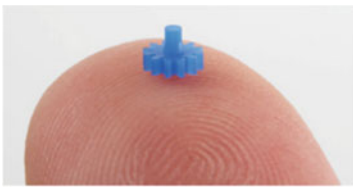


Disposable cartridge for in vitro
diagnostic tests [Philips, 2010]

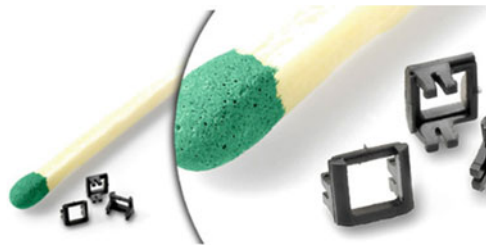


Intracardiac pumping system

Fig. 2.41 Products for the medical, pharmaceutical and bio-technological sectors



Micro-gear
[Mold Hotrunner Solutions]



Micro-clamping frames
[Arburg]



Micro-gears and micro-encoders
[Makuta]



Micro-mechanical components
[U moulding]

Fig. 2.42 Products for micro-mechanics



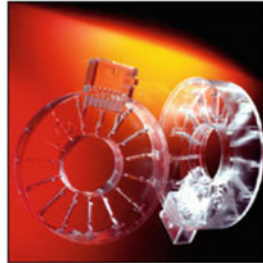
Micro-connectors [Accumold USA]



Umbrella valves [Accumold USA]



High temperature component [Makuta]



Micro-housings [Accumold USA]



Clip for car door [Makuta]

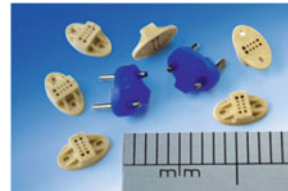
Fig. 2.43 Products for the automotive sector



Micro-electronic circuit board component [Mold Hotrunner Solutions]



Electrical bracket [Mold Hotrunner Solutions]



Micro-connectors [Accumold USA]



Electrical bracket [Mold Hotrunner Solutions]



Telecommunication - Socket [Mold Hotrunner Solutions]



Micro-connector [U moulding]

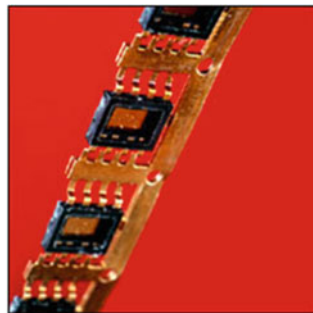
Fig. 2.44 Products for the automotive sector



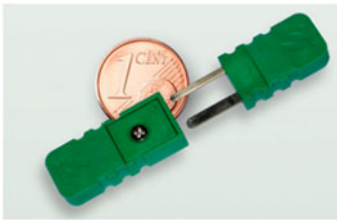
Fig. 2.45 Products for the optics sector



Insert Mould Lamp Capsule [Accumold USA]



Lead Frame SO8 [Accumold USA]



Micro-connector for temperature sensor [Thermo Sensor]



Micro-mould Rotor Pinion [Accumold USA]

Fig. 2.46 Products for the aeronautics, aerospace and defence sectors

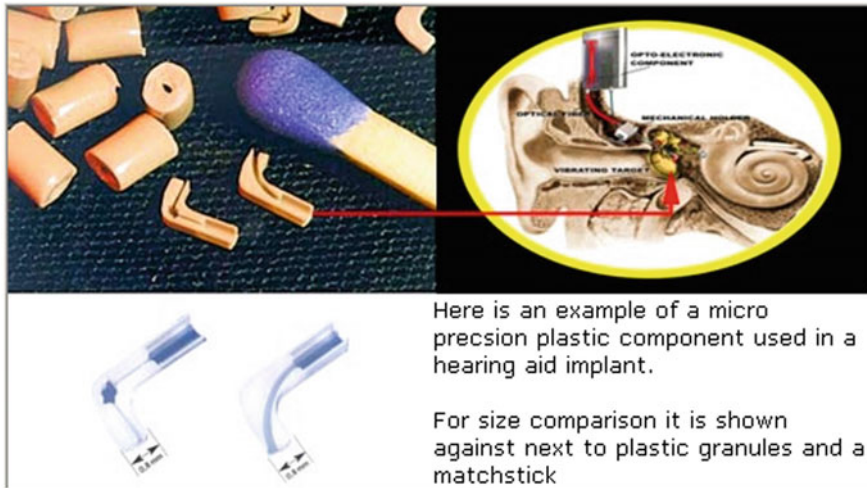


Fig. 2.47 Example application of a micro-parts (Reproduced from Battenfeld Microsystem 50)

2.7 Handling and Verification of Micro-parts

One of the main problems in the field of micro-injection is the handling and verification of the injected parts, not only dimensionally but also structurally.

2.7.1 Handling

Working to dimensions at the microns level creates a number of difficulties that do not occur in normal sizes, including cohesive forces, electrostatic forces, van der Waals and capillary action.

The working environment is paramount, and should be temperature, humidity, and particle (dust) controlled—effectively to a clean-room standard. It should also be insulated from external vibrations.

Basically, there are two handling systems: Contact and non-contact. Although non-contact systems solve the problem of the cohesive forces, it is limited by the order of magnitude of the forces that it can apply to the parts.

One way to decrease the cohesion forces is reducing the contact forces, as we see in the following figures (Fig. 2.48).

In a contact handling system, it is necessary to carefully control the forces applied to the parts. In this case, it is necessary to incorporate piezoelectric sensors (Fig. 2.49).

Specific micro-injection machines, such as Battenfeld Microsystem 50, can provide handling and inspection systems for micro-parts. With an overall working

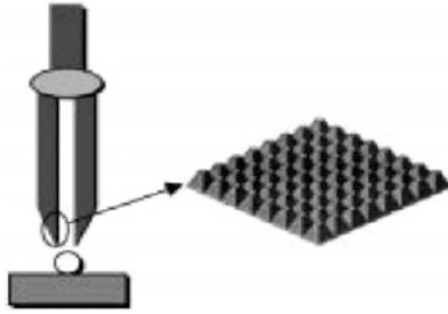


Fig. 2.48 Micro-parts handling (Reproduced from Fraunhofer IPT, WZL Rwth Aachen)

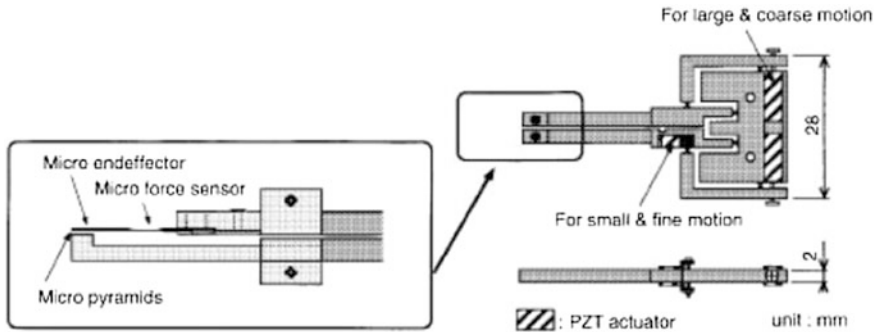


Fig. 2.49 Piezoelectric sensor (Reproduced from Fraunhofer IPT, WZL Rwth Aachen)

envelop of 1 cm³ and a positioning accuracy of 1 μm, it is able to incorporate different tools, depending on the application: Clamps, clips, cutting elements, tools for deburring, etc.

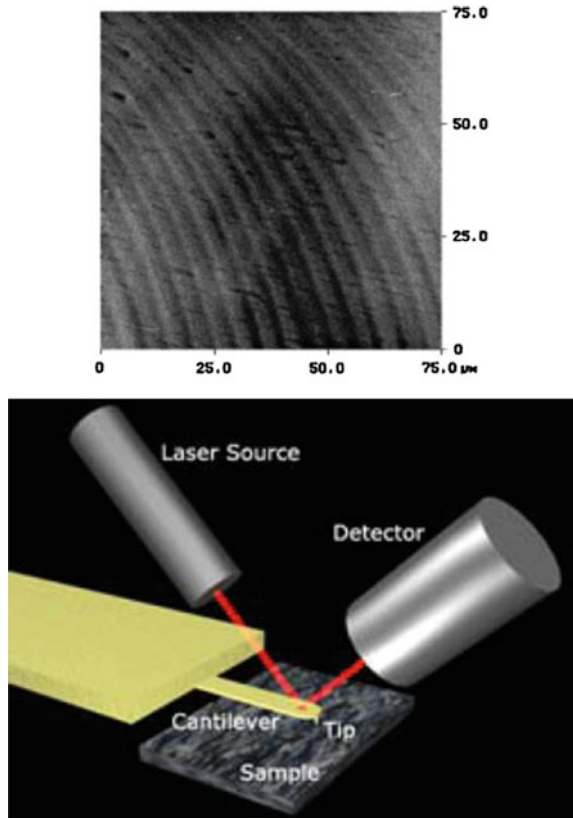
2.7.2 Inspection

Analysis of surface finish:

The AFM (Atomic Force Microscopy) produces images as shown below, where in the surface of a moulded part, POM material, we can see the machining marks of 5 microns caused by the cutting tool used to produce the mould (Fig. 2.50).

The operating principle consists of a silicon micro-cantilever with a micro-tip at its extreme. The microscope uses a laser source and a detector to monitor the deflection.

Fig. 2.50 Photographs obtained with the AFM and operating sketch



This system not only provides the “topographic” information, with the proper configuration, it can provide structural characteristics and material information.

The white light interferometer (an instrument in which wave interference is employed to make precise measurements of length of displacement in terms of the wavelength) is a technique used to obtain a map of the component profiles without contact, by optical reflection. It is used to determine both distances and wavelengths (Fig. 2.51).

All measurement techniques using optical systems have two basic limitations: The multi-reflection due to the surface roughness and the difficulty detecting the reflection in complex part geometries (Fig. 2.52).

2.7.3 Morphological Analysis

Dissolution techniques allow the selective removal of the amorphous part of a semi-crystalline material, and subsequently analyse its structure. A semi-crystalline

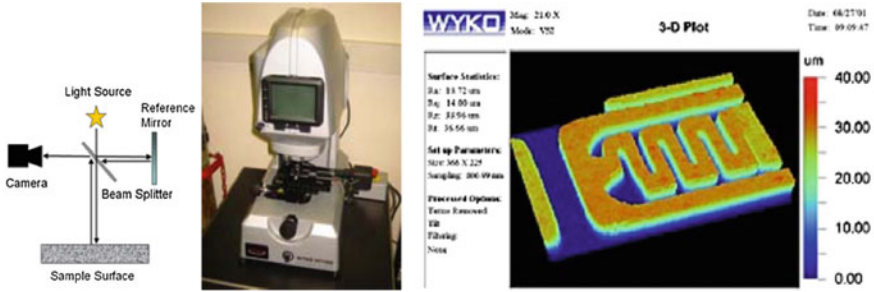


Fig. 2.51 White light interferometer

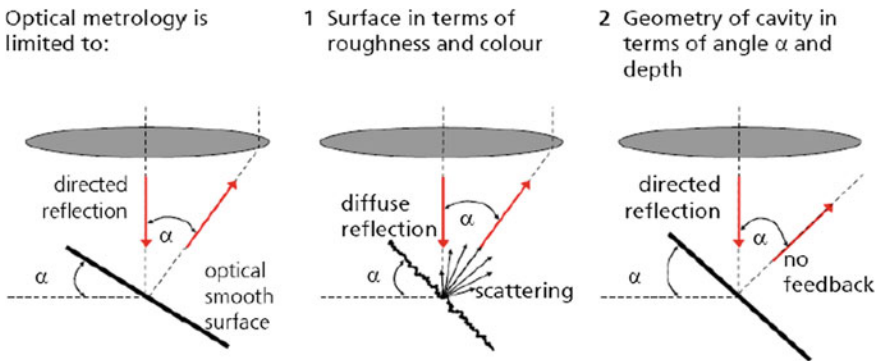


Fig. 2.52 Optical metrology (Reproduced from Fraunhofer IPT, WZL Rwth Aachen)

material that resists solvent chemical attack is necessary to perform this test (Fig. 2.53).

The test result (previous figure) shows how in the inside of the piece to 125 microns from the surface, spherulitic¹ crystalline formations occur, but crystal growth decreases as the surface is approached (the last image on the right) where the crystal growth is zero. This is due part being cooled too quickly. Thus, we can conclude that mechanically, the material structure will not be homogeneous.

2.7.4 Mechanical Analysis

The micro-durometer allows analysis of surface hardness in micro-parts and the viscoelasticity, (making cyclic loads) elastic modulus and creep (Fig. 2.54).

¹A spherulite is a cluster of radiating acicular or lath-like crystals.

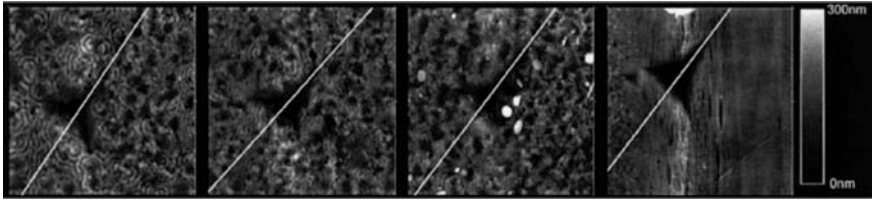


Fig. 2.53 Photographs of morphological analysis

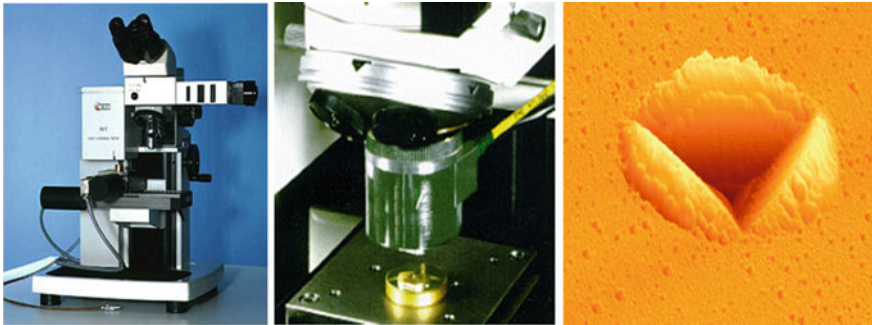


Fig. 2.54 Micro-photonic micro-durometer

MicroDAC (micro-deformation analysis by means of correlation) is a technique that allows viewing surface tension in micro-parts, scanning the part and comparing it with mathematical algorithms of the same areas at different stress levels.

2.8 Application Case: Micro-filter

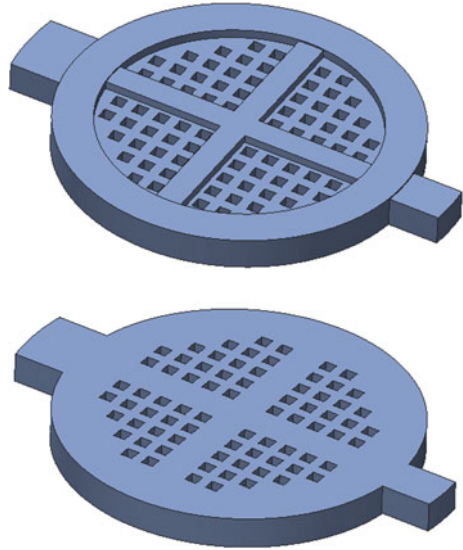
2.8.1 Description

This application case reports on design, fabrication and characterization of a micro-filter to be used for hearing aid, dialysis media and inhaler (Surace 2015) (Fig. 2.55).

Main features:

Technical specification	Unit	Value
External diameter	mm	2
Squared holes size	µm	70
Pitch between holes	µm	80
Material	-	POM
Flow pressure	bar	1

Fig. 2.55 CAD3D
Micro-filter (Courtesy of
CNR-ITIA)



Micro-filter manufacturing:

- Micro-injection moulding (μ IM) process
- DesmaTec FormicaPlast 1K machine.

Mould manufacturing:

- Micro-electrical discharge machining (μ EDM) process
- Sarix SX 200 machine.

Micro-filter characteristics investigated:

- Filter material
- Holes shape
- Squared holes size
- Spacing between holes (holes density)
- Overall number of pores
- Filter thickness
- Shape, number and position of reinforcing ribs
- Requirements and specification of the application
- Manufacturing constraints.

2.8.2 Micro-filter Design Analysis (FEM/CAE)

- Numerical simulation, using finite element method FEM, provided a guideline for optimising the geometry.
- Structural analysis was conducted using SW Inventor Pro 2013 in order to predict the resultant stress distribution on the filter applying a pressure of 1 bar on the whole front surface (Fig. 2.56).

2.8.3 Micro-injection Process Simulation

2.8.3.1 Filling and Parameters

μ IM process simulation program: Moldflow2013 SW

- 1st simulation: Front flow and filling phase (Fig. 2.57)
- Process parameters optimisation after capturing pressure values during the experimentation (Fig. 2.58).

2.8.3.2 Gate Positioning Optimisation

- Number of gates and their positioning. Simulations and size optimisation (Figs. 2.59 and 2.60)

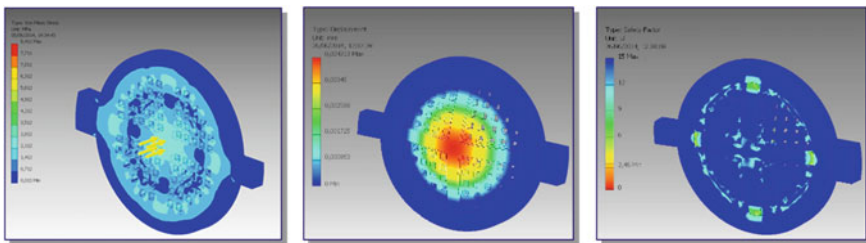


Fig. 2.56 Von Mises Stress, Displacement and Safety Factor simulations (Courtesy of CNR-ITIA)

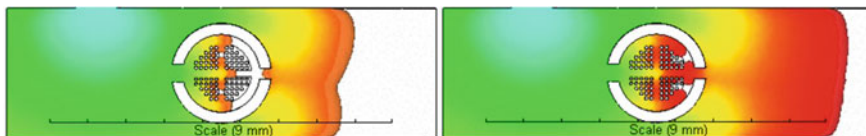


Fig. 2.57 MolFlow simulations (Courtesy of CNR-ITIA)

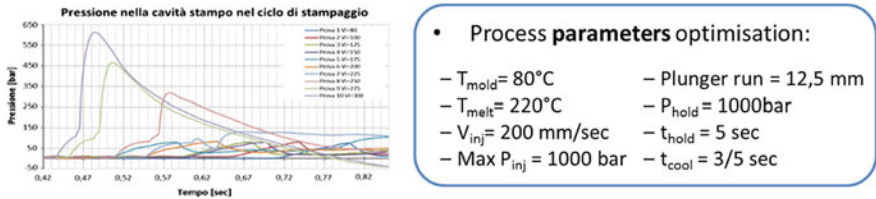


Fig. 2.58 Process parameters optimisation (Courtesy of CNR-ITIA)

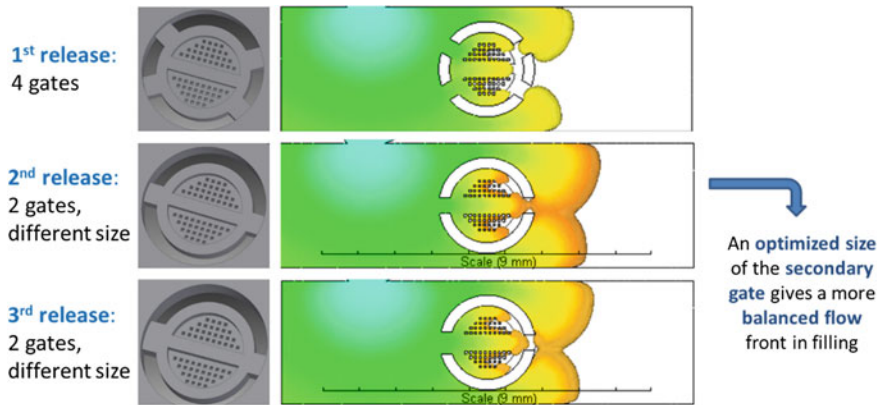


Fig. 2.59 Gate positioning optimisation (Courtesy of CNR-ITIA)

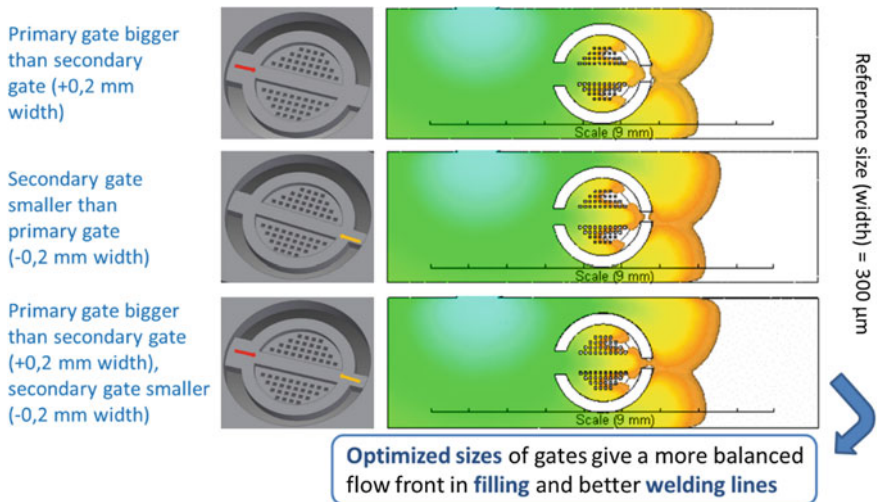


Fig. 2.60 Gate positioning optimisation (Courtesy of CNR-ITIA)

2.8.3.3 Welding Lines and Air Traps Analysis

Other important issues are welding lines and air traps:

- Weld lines are structural weaknesses in the part
- Air traps give us warnings on filling (Fig. 2.61).

2.8.4 Mould Design and Manufacturing

μ EDM process

The μ EDM process was applied in two different working approaches: Sinking and milling.

The tool used was a tungsten carbide (WC) cylindrical rod having nominal diameter equal to 0.4 mm (Figs. 2.62 and 2.63).

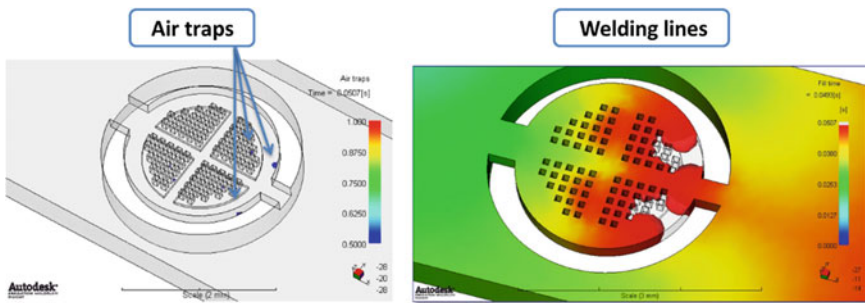
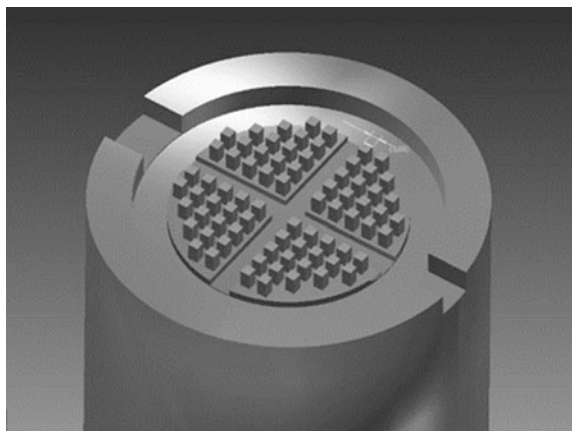


Fig. 2.61 Welding lines and air traps analysis (Courtesy of CNR-ITIA)

Fig. 2.62 μ EDM tool (Courtesy of CNR-ITIA)



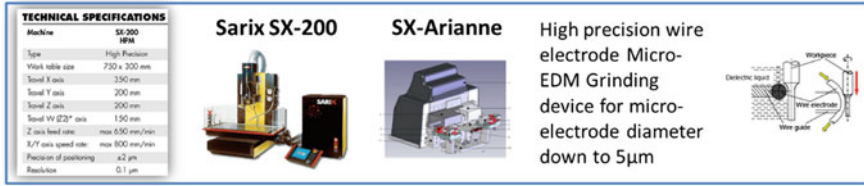


Fig. 2.63 μEDM machine (Courtesy of CNR-ITIA)

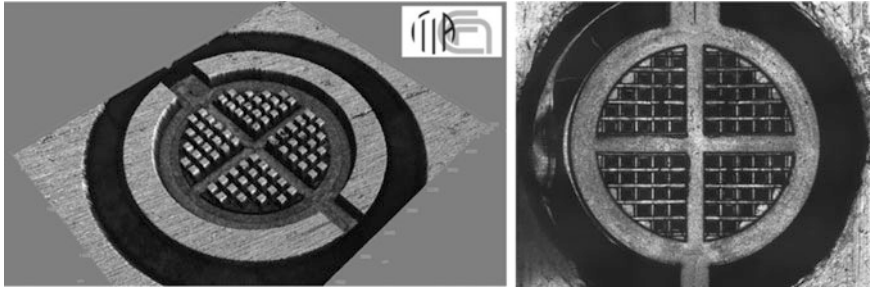


Fig. 2.64 Micro-filter (Courtesy of CNR-ITIA)

The μEDM sinking of the pins (80 μm square size), was produced by machining the electrode into the desired shape using the wire tool embedded on Sarix machine, including consideration of the tool wear compensation and by working the piece in vertical and horizontal directions (Fig. 2.64).

The μEDM milling of the channels (70 μm width), was done by adopting the layer by layer strategy. The total machining time was about six hours.

2.9 Process Optimisation and Part Production

- Part micro-injection moulding using the insert manufactured with EDM mounted on master mould in a screwless/two plungers micro-moulding machine.
- Parameters process configuration (melt and mould temperature, injection velocity, holding time and pressure, cooling time), starting from previous researches and simulation, was performed for obtaining the final part.
- Dimensional characterisation of the part by confocal microscope Zeiss CSM 700. Further step, still to be implemented, will be the micro-filter testing in medical device (Fig. 2.65).

Fig. 2.65 Micro-filter injected (Courtesy of CNR-ITIA)



Bibliography

DEMAG ERGOTECH

BATTENFELD SMS group

Fundación privada ASCAMM/EURECAT

IPT Fraunhofer

ULTRASION

WITTMANN-BATTENFELD

WZL RWTH AACHEN UNIVERSITY

Su Yu-C, Shah J, Lin L (2004) Implementation and analysis of polymeric microstructure replication by micro injection molding. *J Micromech Microeng* 14(2004):415–422

The Institut für Mikrotechnik Mainz (IMM) Johannes Gutenberg

Surace R, Bellantone V, Trotta G, Basile V, Modica F, Fassi I (2015) Design and fabrication of a polymeric microfilter for medical applications. *ASME J Micro Nano-Manufact* 4(1): 011006-011006-7, JNMN-15-1048. doi:[10.1115/1.4032035](https://doi.org/10.1115/1.4032035)

Chapter 3

Micro-additive Manufacturing Technology

Felip Esteve, Djamila Olivier, Qin Hu and Martin Baumers

3.1 Overview

Many fields, including medical, aerospace, military/defence, optics, automotive, consumer products, and communications, have been increasingly demanding miniature devices and components with complex micro-scale features made from a wide selection of materials. Current applications for miniature componentry—with dimensions ranging from a few micro-metres to tens of millimetres—include miniature motors and turbines, micro-satellites, implantable medical devices, minimally invasive surgery equipment, micro-robots, and miniature moulds and dies. It is expected that miniature parts will be increasingly demanded in the future [1].

Additive Manufacturing (AM) in particular offers capabilities for producing accurate features in a genuine three dimensional mode of manufacturing to a growing number of technological disciplines. Among these fields are, regenerative medicine, medical devices, new techniques of biological medicine based on the controlled release of drugs and organic principles, bionics, micro-electronics and opto-electronics as the most prominent disciplines. Biochips, MEMS, micro-fluidic devices, photonic crystals, scaffolds for tissue engineering and carriers for drug-delivery devices are some common applications of growing interest.

AM can be defined as a collection of technologies capable of joining materials to make objects from 3D model data, usually layer upon layer, as opposed to subtractive (or formative) manufacturing methodologies [2]. AM has originally evolved from a group of technologies developed for rapid prototyping. Two generic

F. Esteve (✉) · D. Olivier
Asociación Española de Rapid Manufacturing (ASERM), Barcelona, Spain
e-mail: festeve@aserm.net

Q. Hu · M. Baumers
Additive Manufacturing and 3D Printing Research Group (3DPRG),
The University of Nottingham, Nottingham, UK

advantages are associated with AM over other manufacturing techniques [3]: firstly, AM allows the manufacture of components without many of the geometric limitations that constrain subtractive and formative processes. Secondly, AM enables the production of small quantities of potentially customised products at a comparatively low average unit cost. However, besides these advantages, it has been suggested that AM is also associated with a number of process limitations [4], including the following aspects:

- Limited selection of materials and characteristics;
- Relatively low process productivity;
- Low accuracy of product dimensions;
- The requirement for post processing due to poor surface quality;
- Process variability and limited repeatability;
- Relatively high unit cost at medium and high volumes.

This chapter compiles five additive manufacturing methodologies that were developed initially for deployment in general manufacturing applications and that have demonstrated promise for manufacturing at the micro/nano scale. It is important to note, however, that there have been developments in other areas of deposition technology based upon the principle of direct writing. Even though the direct writing-based technologies are included in Fig. 3.1. Classification of 3D Micro-Additive Manufacturing Processes, 3D micro-structures are not developed currently to that extent. The available 3D direct writing techniques use a 2½ dimensional approach which allows for some additional freedom compared to silicon planar fabrication, but still fall short of spatially volumetric manufacturing [5]. Additionally, Fig. 3.1 includes hybrid processes, which refer to any combination of down-scaled Additive Manufacturing, 3D writing technology, and conventional manufacturing routes at the micro-scale.

Thus, the prerequisite for the successful adoption of 3D micro-additive manufacturing is to resolve the generic problems associated with AM. Additionally, it will be necessary to increase the resolution within these processes for the production of micro-sized parts. This will deliver sufficient surface quality to minimise post-processing.

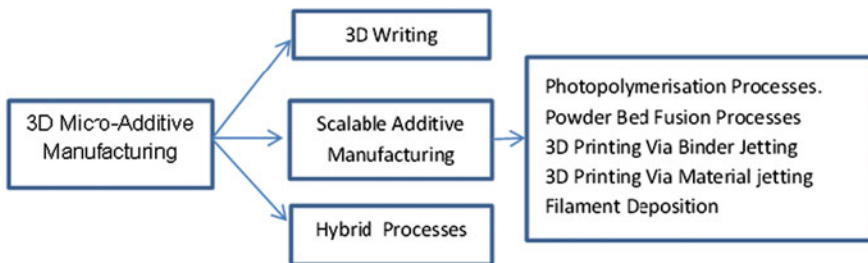


Fig. 3.1 Classification of 3D micro-additive manufacturing processes

3.2 Micro-stereolithography (MSL) and Two Photon Polymerisation (2PP)

Stereolithography was the first AM technique, being invented in 1984 by Charles Hull and commercialised by 3D Systems Inc. [6]. It has introduced several aspects regarding materials, machine sizes, laser sources and controlling software. Some years later this technology provided the foundation for the variety of mask projection resin systems involving the use of a micro-mirrors system for mask projection, essentially allowing the fabrication of one layer at once. Such mask projection platforms have been optimised for an appropriate resolution for micro-fabrication. Additionally, a powerful system based upon two photon absorption has been developed capable of achieving the nano-metric scale.

3.2.1 Operating Principles

Micro-stereolithography

Micro-Stereolithography (MSL) is a 3D micro-additive manufacturing process which was first introduced by Ikuta and Hirowatari [7]. MSL is based on conventional Stereolithography (SL), in which a light source radiates UV laser beam on a surface of a UV-curable liquid photopolymer, bringing about solidification of the photopolymer. MSL has micro-metric resolution for the x, y, z translational stages. For this technique, laser spot has small diameter of a few microns, leading photopolymer solidification to occur in a very small area of the resin, therefore enabling MSL to produce micro-parts with 1–10 μm layer thickness.

Two main MSL techniques, namely, scanning MSL and projection MSL have been developed depending on the different beam delivery system. Figure 3.2 shows the schematics of the scanning process found in scanning MSL.

Scanning MSL solidifies the photopolymer (including UV photo-initiator, monomer, and other additives) in a point-by-point and line-by-line style in each layer. In projection MSL, build time is saved significantly compared with the scanning MSL as whole layer of the photopolymer is cured once via exposure through the provided mask.

Bertsch's research group proposed that the Digital Micro Mirror Device (DMD) which is embedded in Digital Light Processing projectors can be applied as the dynamic mask within the MSL process. In this approach, a metal halide lamp is combined with optical filters to select a band of visible wavelength for the irradiation of the resin [9]. In 2004, Stampfl et al. proposed a variant of DMD-based MSL, in which visible light is projected from below the resin vat to produce high quality 3D micro-parts [10]. Furthermore, UV light was utilised by Hadipoespito et al. and Cheng et al. instead of visible light, to cure the resin.

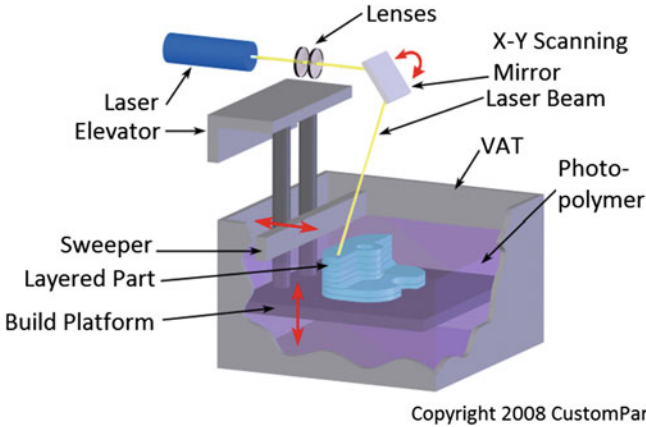


Fig. 3.2 Schematics of the scanning stereolithography (SL) process. Reproduced with permission from CustomPartNet [8]

The DMD device is a semiconductor chip that has been developed by Texas Instruments[®] for high-quality digital projection. It involves around 1.5 million micro-mirrors (each side at $\sim 13 \mu\text{m}$) which are positioned in a matrix and each mounted on tiny hinges that can be individually controlled. Each micro-mirror stands for 1 pixel in the projected pattern and can be inclined autonomously at a small angle ($\pm 10\text{--}12^\circ$) via an electrostatic force to reflect the light and can be repositioned quickly for turning the light on and off. As the resolution of the projected image is related to the size and number of the mirrors, high resolution DMDs featuring 2800×2100 mirrors have been utilised in MSL to produce finer 3D micro-parts. To improve achievable resolution, DMD based MSL systems are augmented with an enhanced resolution module (ERM), whereby for each pixel built there are two exposure modes. These produce a shift by half a pixel, which halves the native resolution of the system [11]. A micro-fluidic device made with this technique is shown in Fig. 3.3.

Two-Photon Polymerisation

This technique is also known as direct laser lithography, multi-photon lithography or direct laser writing and it can create geometrically complex 3D nano/micro structures.

The two-photon polymerisation (2PP) process was developed by Maruo and Kawata with the aim of overcoming the resolution limitations of the MSL technique. To accomplish that, an ultra-fast laser is used, instead of conventional UV laser. The peak energy of ultra-fast laser is very high and the irradiance projected is high enough to provide the photon density required. In the 2PP process, the photo-initiator requires two photons to release a free radical that can initiate polymerisation. We can tune the laser power to make the energy (only at the central point of the focused laser spot) to exceed the threshold for polymerisation. In this

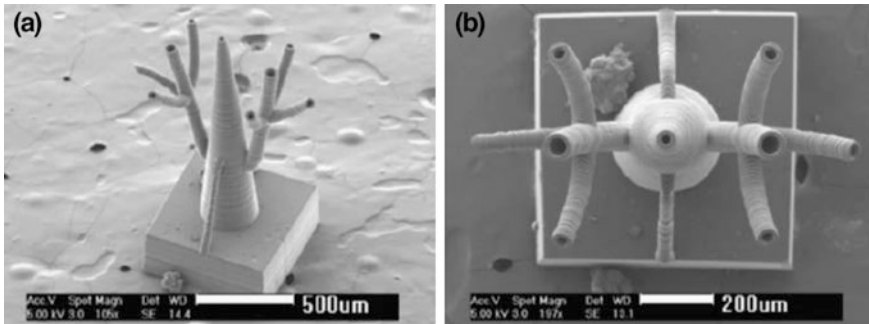


Fig. 3.3 a, b SEM images showing highly branched capillary network structure (inner radius of capillaries vary 10–30 μm) fabricated by Projection Micro-Stereolithography. *Source* Biomed Micro-devices Journal [12]

way, although the exposure area by focused laser beam may be in micro-meter range, the polymerised area can be much smaller, thus improving the resolution [5].

Different micro/nano-3D structures can be manufactured accurately using the 2PP process. By accurately focusing a femtosecond laser beam in the 2PP process, it has been shown to be capable of delivering a high spatial resolution around 100–200 nm. This process has successfully adopted the 2PP principle in the 3D micro-fabrication for micro-rotors, micro-oscillators, optical memories, and photonic crystals. Currently the technology is commercially available through some providers, such as the Nanoscribe Company.

3.2.2 Technology Overview and Systems

Two important methods of fabrication are compared in Fig. 3.4 (MSL versus 2PP comparison). The most significant difference is in terms of resolution, with the 2PP system capable of achieving the nano-scale.

Another relevant difference is the material's solidification strategy. In MSL, the exposure activity takes place at the surface of the liquid photopolymer. Hence any solid geometry is necessarily built up in a layer-by-layer approach. In the case of the 2PP process, the NIR femtosecond pulsed laser beam can be focused to any desired location in the volumetric space covered by the liquid photopolymer. This effectively enables a truly three-dimensional approach to the deposition of physical structures.

Both techniques are available in the marketplace as commercial platforms for micro-manufacturing, each with interesting capabilities. For example, UNIRAPID Inc. in Japan has developed a μSL system: "UNIRAPID III". It is capable of printing very detailed designs, with a maximum build envelope of $150 \times 150 \times 150 \text{ mm}^3$. The machine prints with a minimum layer thickness of

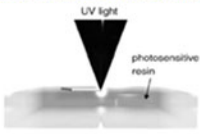
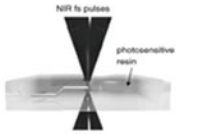

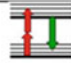


	Microstereolithography	Two-Photon Polymerization
		
Essential elements	CAD design, 2D layer preparation function, laser scanning & controlling system with monitoring devices	
Mechanism for polymerisation	One-photon absorption (Linear absorption) 	Multi-photon absorption (Non-linear absorption) 
Laser type	UV laser	NIR femtosecond laser
Resolution	~ 1 μm 	~ 100 nm 
Strategy for 3D fabrication	Polymerisation at the surface → layer-by-layer approach	Polymerisation at any desired location → Built 3D structure 'recording' the beam path

Fig. 3.4 MSL versus 2PP comparison. *Source* University of Nottingham

0.05 mm. The UNIRAPID III is suitable for making micro-metric resolution parts for research and development, but it is not recommended to make large models because the speed of construction is slow.

In addition, the company has also developed an MSL device for laboratory the URM-HP301, a starter kit for micro-modelling. It employs a HeCd laser to cure colourless acrylic resin. The HeCd Laser beam diameter is about 7 μm , and build envelope is maximum 30 mm XYZ (Fig. 3.5).

On the other hand, the company Nanoscribe GmbH, has developed a 3D Laser Lithography system based upon two-photon polymerisation process. It is called Photonic Professional GT and stands for setting new standards in 3D micro-printing and maskless lithography with around 100–200 nm resolution. It combines two

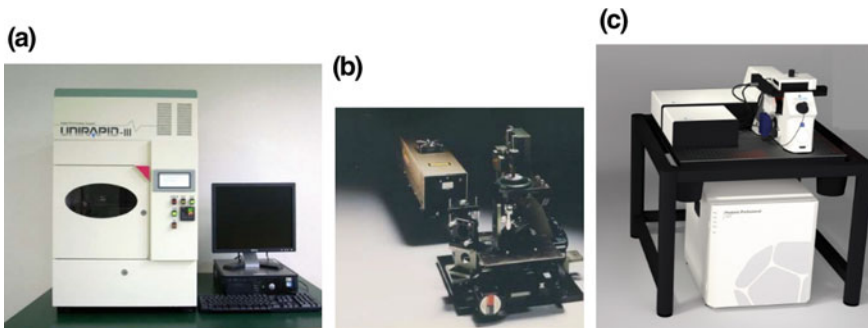


Fig. 3.5 Commercial MSL and 2PP Systems. *Sources* UNIRAPID [13], Nanoscribe [14]. **a** MSL UNIRAPID III System. **b** MSL URM-HP301Lab System. **c** 2PP Photonic Professional GT

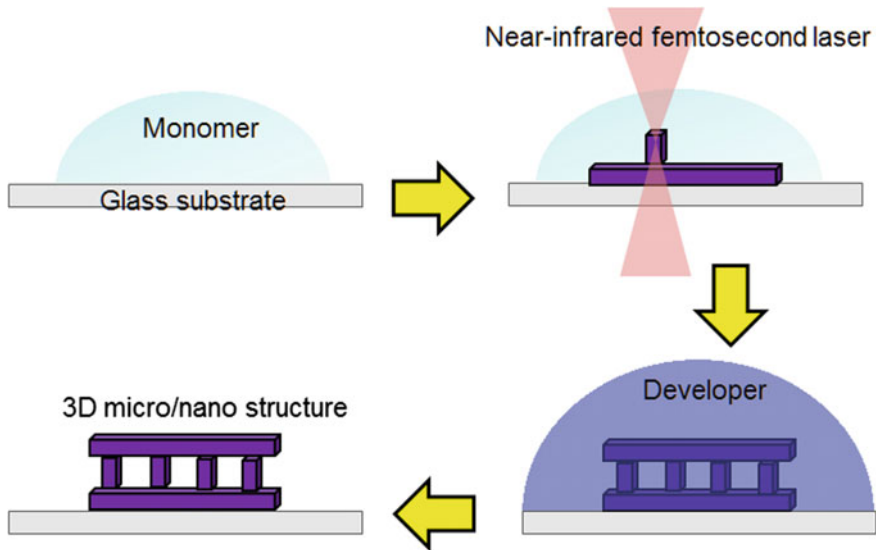


Fig. 3.6 Schematic illustration of the workflow for two-photon lithography. *Source* Dr. Qin Hu, University of Nottingham

writing modes in one device: an ultra-precise piezo mode for arbitrary 3D trajectories and the high-speed galvo mode for fastest structuring in a layer-by-layer fashion. All mentioned systems are shown in (a) MSL UNIRAPID III System. (b) MSL URM-HP301Lab System. (c) 2PP Photonic Professional GT.

The workflow of two-photon lithography is shown in Fig. 3.6. The femtosecond laser focused the beam within the liquid monomer placed over the cover glass. Point to point, the photoresist are cured giving place to the solid structure. The structure is washed with the developer liquid to remove the unsolidified resin. Finally a 3D polymeric structure is obtained.

3.2.3 Materials

For the selection of the appropriate photopolymer formulation, it is necessary to consider several factors that will affect directly the properties of the photopolymer. It is necessary to set up tuned compositions of monomers and reactants. The photo initiators should be selected according to the chemistry of the reaction, their influence over the solidification parameters and the final properties desired for the micro-part to be built. The monomers are the main raw material that will determine the final structure of the cured resin obtained, so they must be carefully designed as well as any additional material, e.g. metallic nano-particles or metallic salt nano-particles, according to the intended functionalities of the material in the design.

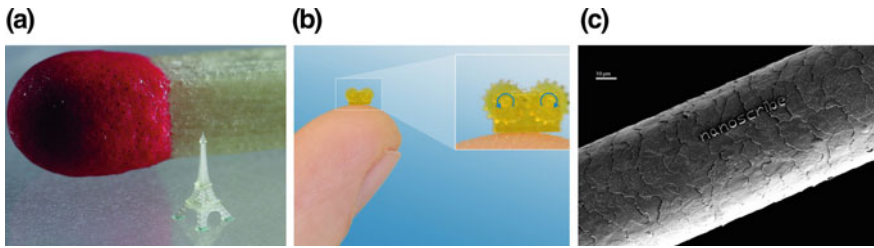


Fig. 3.7 Examples of micro-structures created with two-photon polymerisation. *Source* Nanoscribe [15]

For the 2PP process, there are a number of requirements that the monomer and initiator must satisfy. As the femtosecond laser operates in the near infrared regions, the monomer has to be transparent in the visible and near infrared regions. It should also show a fast curing speed so that only the resin in the focal point of the laser beam is polymerised instantaneously. Considering the subsequent washout process that the part will suffer, it is mandatory that the monomer exhibits chemical resistance to the solvent used. Finally, in regards of the application requirements, the resultant material should provide suitable mechanical properties and thermal stability to maintain shape and properties in service. There is a wide group of materials that can be blended within the photopolymer matrix either physically or chemically, resulting in new functional composites or hybrid materials. For those materials there is a window of opportunity taking advantage of the customisable functional capabilities. Some families of materials already being used are [5]:

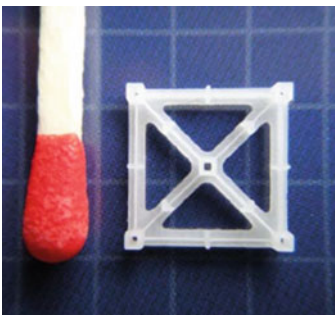
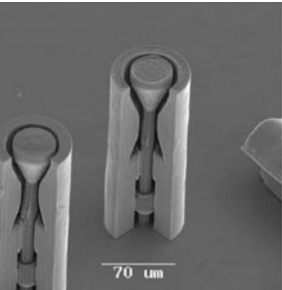
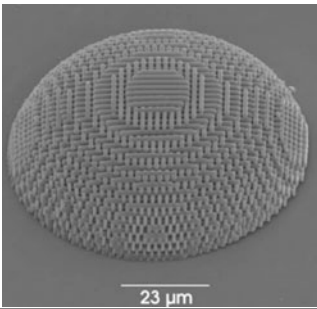
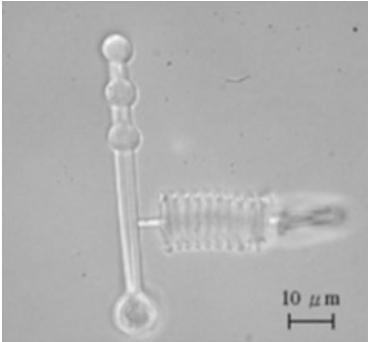
- Polymer material
- Metallic material
- Hybrid materials
- Nanomaterials
- Biomaterials.

Some examples of hybrid materials and their applications are shown in Fig. 3.7. The polymers suitable for resin vat type technology are commercially available from providers like Huntsman Advanced Materials, DSM Somos, 3D Systems, JSR, American Dye Source, Asahi Denka, Teijin Seiki, and Allied Photochemical [16].

3.2.4 Applications

These micro-additive processes are used in various areas such as micro-machines, micro-sensors, micro-fluidic systems, optical waveguides, 3D photonic band gap structures, fluid chips for protein synthesis and bio-analysis. Some examples are shown in Table 3.1.

Table 3.1 Examples of applications of micro-stereolithography and two-photon polymerization (2PP)

Micro-connector		Unirapid III MSL equipment. Material: nano-tool; model: height 0.6 mm; thickness 0.1 mm fabrication time: 39 min. Reproduced with permission from [13]
Ready assembled micro-valve		Optical image of a complex shape, readily assembled micro check valve using the 2PP technique. Reproduced with permission from [17]
Micro-channels with built-in micro turbines		SEM images of micro-optical elements fabricated by two-photon polymerization. Reproduced with permission from [18]
Optical tweezers		Optical image of an optically driven micro-lever that can increase the applied optical force by ~9 times. Fabricated using 2PP technique. Reproduced with permission from [19]

3.3 Powder Bed Fusion Technologies

In 1992, Carl Deckard patented the selective laser sintering method. By 1994, DTM developed the first rapid prototyping system to build metal prototypes with this method [20]. The operating principle of such powder bed fusion systems is simple: powder particles are selectively joined together through the melting of the granules by a laser beam source. Starting from the early developments, the equipment, materials and the systems have evolved; currently it is possible to reliably obtain parts with almost 100% density and acceptable mechanical properties [21].

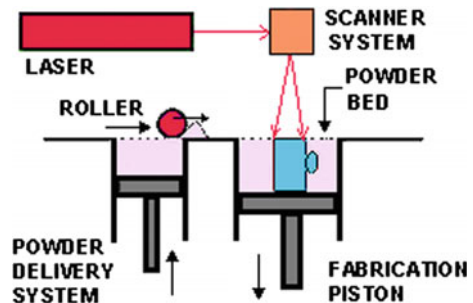
3.3.1 Operating Principles

In polymeric Laser Sintering, a high-temperature laser is utilised to expose layers of fine powders selectively. The drawing of each layer is scanned by the laser spot over the build platform. As shown in Fig. 3.8, when a layer is built over the fabrication powder bed, a powder deposition mechanism spreads a fresh layer of powder from the powder delivery system and the process repeats until the part is completed [22]. Selective Laser Melting (SLM) uses a very similar concept for the deposition of metallic components, with the main difference being an adapted thermal management during the build process.

To successfully produce metal parts by SLM, additional support structures are needed to support overhanging surfaces in order to dissipate process heat and to minimise geometrical distortions induced by internal stresses. These structures are often massive and require additional post-processing time for their removal. Experimental results have shown that the supporting effort can generally be reduced through adapting part design or orientation [24].

In metallic powder bed fusion processes, it is necessary to protect the atmosphere during the sintering or melting process as the presence of air or oxygen can induce undesired oxidation and impurities. A further consideration for the case of fabrication of micro-components is that melting the powder bed may benefit from

Fig. 3.8 Schematics of the laser sintering and selective laser melting processes.
Source Additive3D [23]



the use of finer powder particles, with particle sizes ranging from nanometres to tens of microns [25].

3.3.2 *Technology Overview and Systems*



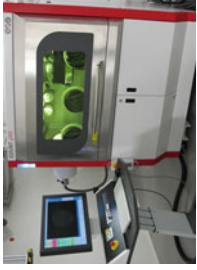
The forming process in powder bed fusion systems proceeds along the scanning direction of the laser beam. Each cross-section (layer) of the part is sequentially filled with tracks of molten powder material, implying that such processes form a superposition of tracks and layers. Therefore, the layer morphology substantially determines the final product properties. A number of factors (including direct and indirect parameters) have an effect on such processes. Principal process parameters are laser power, wavelength, spot size diameter, scanning speed, hatch distance, powder layer thickness. Material-based input parameters are powder granulomorphometry, chemical composition, thermal, optical, metallurgical, mechanical and rheological characteristics.

Physical behaviour of “laser radiation–powder–substrate” system includes absorption, reflection, radiation and heat transfer, phase transformations, a moving interface between solid phase and liquid phase, fluid flow caused by surface tension gradient and mass transportation within the molten pool, and chemical reactions. This system has non-linear response when the process parameters are modified: changing laser power or scanning speed can lead to various undesirable effects as irregularity and balling effect. Therefore, it is important to establish links between the principal deposition parameters and surface morphology. Studies have investigated the influence of the hatch distance and thickness of powder layer on morphology of the first layer and the surface structure of thin walls produced by SLM from metal powders. Obtained data can be used in surface structuring and micro-part manufacturing characterised by a small number of layers within a part and, thus, are sensitive to the geometric dimensions and the shape of surface [21].

3.3.3 *Machines and Materials*

Commercial Laser Sintering systems are unable to produce micro-components smaller than 500 μm because the laser focus diameter is limited (50–300 μm). Thinner layers and powders with smaller particles sizes are required to achieve finer details. Taking a deeper look into the differences at processing, some intrinsic features of the different processes can be understood. In SLM processes, the laser beam projector may be located closer to the point of application and the intensity of laser shows a higher order of magnitude. Forming a special variant of metallic powder bed fusion systems, Laser Cusing[®], allows an x/y translation of the beam projector of the solid state laser beam over the build plate, allowing a tighter control of beam accuracy.

Table 3.2 Equipment description for micro-selective laser melting



Concept laser Mlab cusing [26]	Realizer GmbH [27]	EOS machine—EOSINT μ 60 [28]
 <p>Build envelope:</p> <ul style="list-style-type: none"> • 50 × 50 mm (x, y) • 70 × 70 mm (x, y) • 90 × 90 mm (x, y) • z = 80 mm <p>Layer thickness: 15 μm</p> <p>Materials</p> <ul style="list-style-type: none"> • Stainless steel (1.4404) • Cobalt-chromium alloy • Titanium alloy (TiAl6V4 ELI) • Pure titanium Grade 2 • Bronze • (930%₀₀ Silver powder) 	 <p>Build envelope:</p> <ul style="list-style-type: none"> • Platform diameter 70 mm • Construction height 40 mm • Thickness of Layers: 20–50 μm <p>Layer thickness: 20–50 μm</p> <p>Materials</p> <ul style="list-style-type: none"> • Cobalt Chrome • Stainless Steel • Gold alloys • Titanium 	 <p>Build envelope:</p> <ul style="list-style-type: none"> • \varnothing 57 mm × 30 mm height <p>Layer thickness: 15–50 μm</p> <p>Materials</p> <ul style="list-style-type: none"> • Tungsten • Cu • Ag • Tungsten/Cu mixtures • Stainless Steel 316L • Molybdenum <p>Also applied for process of ceramics and composite materials</p>

Depending on material processed, most powder bed fusion systems work under inert atmosphere typically with nitrogen and argon. In some cases, such systems also operate in a vacuum. Some build environments are more compatible with particular metals, for example argon used to process stainless steel induces a significant increase over elongation at break compared to a nitrogen atmosphere [26]. The commercially available system SLM 50 of Realizer GmbH, Germany has the capability to produce fine features in the range of 40 μm, as it uses fine powders (smaller than 30 μm) and minimum layer thickness of 20 μm [27]. A wide range of metals, including: Super alloys, gold (Au), silver (Ag), aluminium (Al), stainless steel, tool steel, cobalt (CoCr) chromium, and titanium (Ti) have been processed successfully by Realizer’s SLM system [5]. New SLM machines provide feature resolutions of less than 30 μm. With this system it is possible to build multi-material micro-components. As outlined in the previous section, three different systems capable of achieving microscale are currently commercially available. Table 3.2 summarises their features for reference.

In 2006, the equipment manufacturer EOS GmbH has entered a venture with MicroMac AG, taking advantage of both experiences in the field of micro-manufacturing. A new powder bed fusion system called EOSINT μ60 for micro-manufacturing has been developed and it was launched to the market in 2014.

3.3.4 Applications (Table 3.3)

Table 3.3 Some applications of powder bed fusion techniques at the small scale

	<p>Situation: Increasing costs for precious metals motivate material savings for jewellery without compromising its appearance Solution: Hollow structures save material; Plasma polishing enhances surface finish Advantages: Jewellery can be personalised without extra cost; Structures are a unique design feature [28]</p>
	<p>EOS Challenge: Mixing solution required for 3 liquid components; applied mechanical load has to be minimised Solution: Spiral shaped pipes with 200 μm wall thickness and 150 μm inner diameter. Advantages: Applied load is minimised, no moving parts required for mixing; Mixing ratio can be easily modified by pipe diameter, flow ratio and design of the mixing chamber [28]</p>

(continued)

Table 3.3 (continued)

	<p>SLM 50 Realizer: An important application for the SLM 50 is the manufacturing of crown frameworks, bridge frameworks or brackets made of cobalt-chrome and gold alloys for the Dental Industry. Following moulding by the dentist, initially a conventional dental die is prepared. The dental technician scans the model and prepares the data for the individual components using special CAD software. Based on this 3D data, the SLM 50 produces exactly fitting dental components [27]</p>
	<p>SLM 50 Realizer: The fabrication possibility of hollow parts for the jewellery industry is especially attractive. An important advantage of the SLM 50 is the small amount of material needed for the manufacturing of jewellery made of expensive precious metals [27]</p>
	<p>Concept Laser MLab Cusing With the support of the Jewellery Industry Innovation Centre (JIIC), students from Birmingham City University (BCU) had the opportunity to design items of jewellery in 3D CAD software and have them built on the Concept Laser Mlab machine [26]</p>

3.4 Three Dimensional Printing via Binder Jetting

The process was developed in the early 90 s by Emanuel Sachs at the Massachusetts Institute of Technology [29]. The patent for this technique has been licensed to several companies and it has been possible to use the same process for manufacturing all kind of materials: polymers, ceramics and metals. Regarding the micro-metric scale, it has been developed into an efficient 3D printing process for the manufacture of metal components. Currently, it is commercially available through the company Hogānas, AB.

3.4.1 Operating Principles

The binder jetting variant of the 3D Printing technique is based in the controlled agglomeration of powdered material through the controlled jetting of a liquid ink that promotes the binding of the powder granules. The ink is deposited on each layer and the part grows successively in a layer by layer fashion. Such systems often utilise two powder chambers, one for storage and feeding of the powder represented at Fig. 3.9 at the left side. The other chamber, represented at the right side, is the building chamber, where the deposition process takes place.

The sequence of 3D Printing of the binder jetting type is as follows: The multi-channel jetting head (A) deposits a liquid adhesive compound onto the top layer of a bed of powder object material (B). The particles of the powder become bonded in the areas where the adhesive is deposited. Once a layer is completed the piston (C) moves down by the thickness of a layer. The piston moves upward incrementally to supply powder for the process and the roller (D) spreads and compresses the powder on the top of the build cylinder. In order to achieve an operational finished part, the printed component may be infiltrated with another agent to improve the mechanical strength for handling.

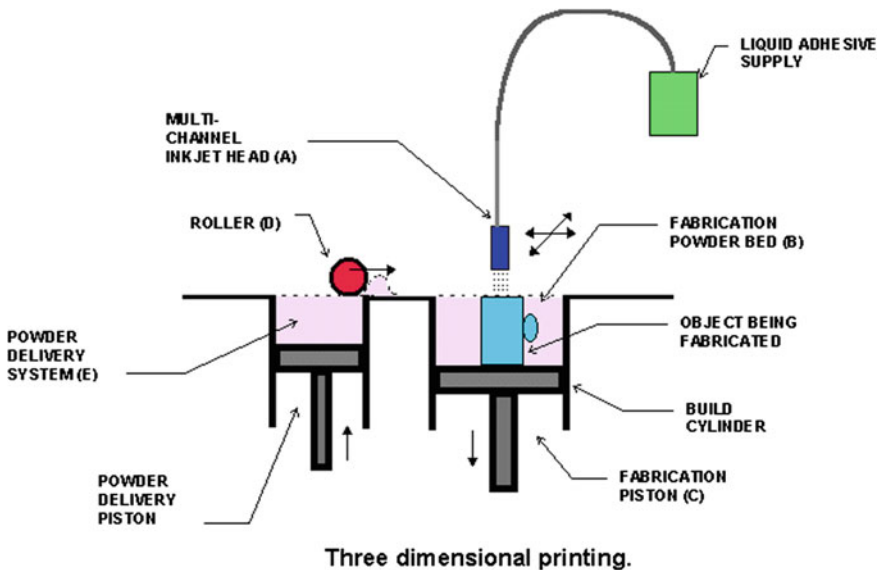


Fig. 3.9 Schematics of the fabrication system for three dimensional printing. *Source* Additive3D [30]

3.4.2 Technology Overview and Systems

Digital Metal is the equipment commercialised by Höganäs AB, the world's leading producer of iron and metal powders. Formed in 2003, a small company, Fcubic developed the precision inkjet technology Digital Metal. In 2012, Höganäs AB acquired the Fcubic for the development of 3D Printing of metallic components at the micro-scale. For this technology, thinner layers and correspondingly smaller powder particles are required. Additional benefits from using finer powders include the potential of lower surface roughness.

To achieve the required high-resolution for 3D Printing at the micro-scale, such platforms utilise piezoelectric printing heads instead of thermal printing heads. Höganäs states that the Digital Metal process offers enhanced component precision, tolerances, surface finish and cost efficiency, whilst maintaining fast time to market. Figure 3.10 shows a build platform after the deposition of an 11×8 array of fasteners, ready for post-processing steps.

The workflow of the technique is outlined in Fig. 3.11. In a preliminary step, the part is designed within a CAD application and when the file is prepared, it can be sent to the printer for the slicing procedure. Following this pre-requisite step, the layer-by-layer fabrication process is performed. The 3D printed parts obtained, shown in Fig. 3.10, are “green parts” that have to be finished through the application of a thermic treatment and finishing procedures. If complicated small features are present, a rectification/polishing is applied to obtain the finished parts.

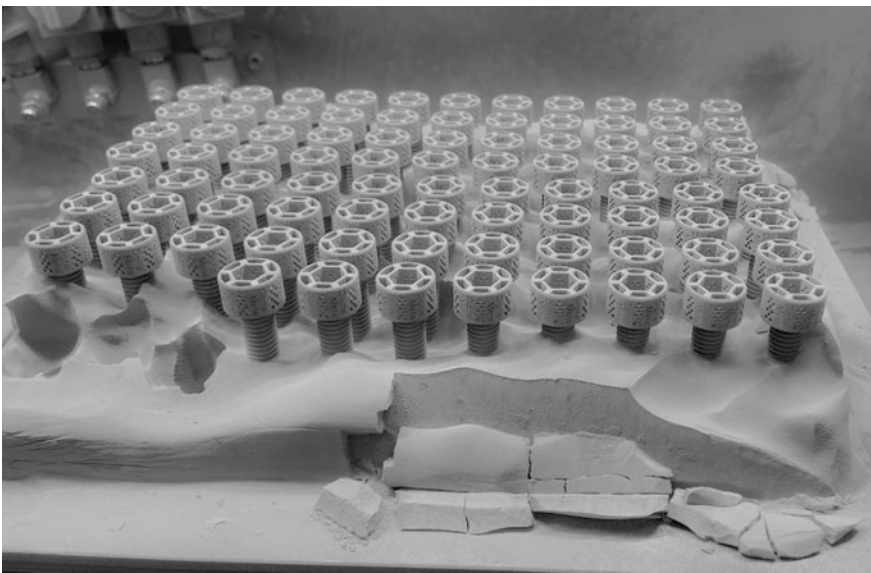


Fig. 3.10 11×8 array of hollowed screws after printing at the Höganäs direct metal fabrication. Source Höganäs

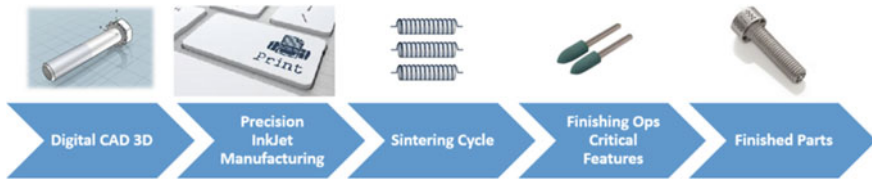


Fig. 3.11 Workflow for metal 3D printing. *Source* Voxeled Materials

3.4.3 Machines and Materials

The Digital Metal Equipment has capabilities that allow the fabrication of parts with a minimum feature size of 20 μm and a tolerance of 100 μm . The parts can be finished in a post-processing polishing to a radius of 1 μm . The minimum thickness for the powder layer is 45 μm . In terms of achievable surface quality, the high resolution is noteworthy. Hogänäs offers several surface quality enhancing techniques, including:

- Peening/Blasting/Tumbling (yielding an average of Ra 3.0 μm)
- Superfinished (yielding an average of Ra 1.0 μm)
- Superfinished + (yielding an average of Ra < 1.0 μm).

Considering the manufacturing capacity, the Hogänäs Digital Metal system is claimed to be capable of producing thousands of parts per day. Figure 3.12a shows a build envelope holding a large number of components for production in a single process. As the binder jetting process is performed at room temperature, the whole volume of the build envelope can be exploited and the components can be packed tightly because no account of thermal conductivity needs to be taken.

The Digital Metal technology is currently limited to working with stainless steel. Other materials under development include gold, silver and titanium. Comparable

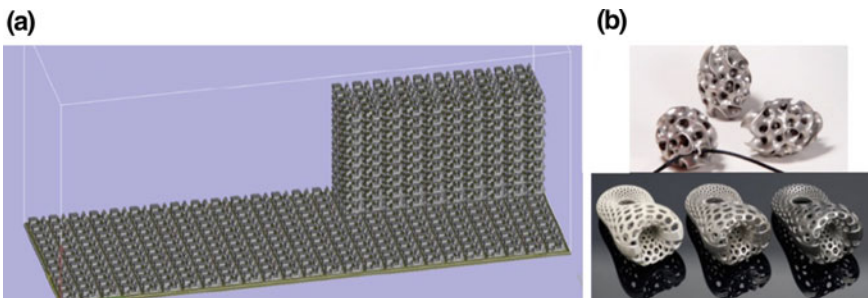


Fig. 3.12 **a** Schematic representation of the build box for Digital Metal System. **b** Samples of Jewellery [31]

binder jetting technology at the macro-scale has already been tuned for several different materials including: Ceramics, metals (titanium, silver, copper), shape-memory alloys (SMA) and polymers.

3.4.4 Applications

Because of the ability to deposit hollowed and lightweight components, binder jetting approaches can help to significantly reduce the weight of small non-critical parts. This benefit is specially valued in the aerospace industry. Additionally, the comparatively high resolution and the fact it can be polished have opened new possibilities for customisation of dental and medical devices. Further, the freeform hollow structures enabled make the technique very useful for fashion design as shown in Fig. 3.12b, where it is applied for the manufacture of cutting-edge designs in jewellery, furniture, accessories and much more. For industrial applications, this micro-additive technology variant enables the rapid and cost effectively realisation of special features like hollowed and meshed metal components with undercuts, ducts, cavities and internal structures [5, 31].

3.5 Three Dimensional Printing via Material Jetting

Processes based on the direct jetting of build materials have been commercially introduced to the AM industry in 2001 by Objet Geometries Ltd. branded as Polyjet technology. Almost simultaneously, in 2002, 3D Systems released a competing proprietary technology based upon the same operating principle, branded as MultiJet Technology.

3.5.1 Operating Principles

Material jetting processes operate via layer-by-layer deposition and solidification of a liquid material in the form of a digitally controlled matrix of droplets. The additive deposition of each layer onto the previous one is repeated until the process is complete. It is noteworthy that the liquid build material distributed as droplets is often referred to as 'ink'. The ink is usually solidified by a combination of chemical changes promoted by the light-initiated crosslinking of a photosensitive polymer or solvent evaporation.

Figure 3.13 shows a schematic of such a material jetting platform. As in other additive processes, the part is deposited over a build platform, often referred to as a build substrate. Two cartridges for build material and support material provide the liquid droplets to the jetting head for layer generation. Simultaneously, a light

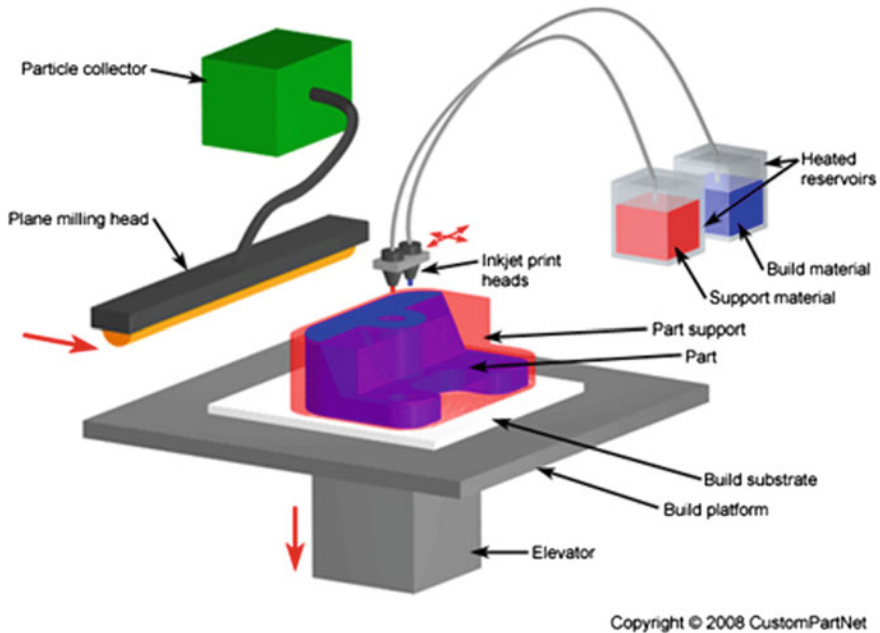


Fig. 3.13 Schematics of the material jetting technology. *Source* CustomPartNet [32]

source provides energy to the droplets, promoting the immediate solidification of the layer [5].

In some processes roller or a milling device planish the deposited material in order to correct any shrinkage or elevations that could be generated during the curing of the layer. In this way, each layer forms a suitable substrate for the next layer to be built on. In case of loose particles generating impurities, they are vacuumed by a particle collector device placed besides the roller for this purpose. The support material can be removed easily because it has an alternative chemistry, allowing for the creation of very complex geometries [5]. In the next section, the details of the technology will be reviewed and the different systems will be described.

3.5.2 *Technology Overview and Systems*

Filled with inks of suitable properties, a stream of droplets can be expelled from tiny nozzles on demand when the print head is driven by electric pulses. Based on different Drop-on-Demand (DoD) operating principles, such as thermal, piezo-electric, electrostatic, and acoustic, the ejected droplets generally undergo morphological transition due to interplay of viscous force and surface tension, from initial to necking stages as demonstrated in Fig. 3.14.

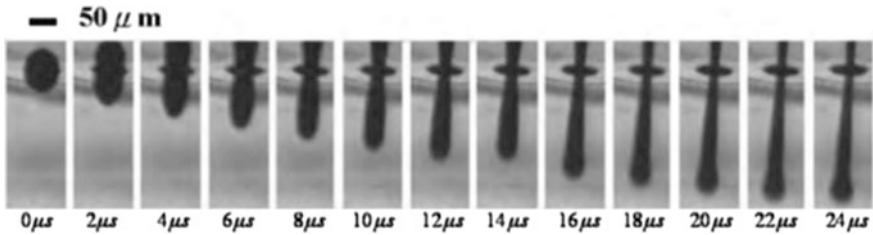


Fig. 3.14 Dynamic evolution of droplet formation in tens of micro-seconds. *Source* National Kaohsiung University of Applied Sciences [33]

In this case the droplets ejection is activated by a pressure pulse generated by an actuator. The actuators are mainly of two kinds; thermal or piezoelectric. The piezoelectric element is the most common industrial system which makes a change in the internal volume of the ink reservoir using an electric field to create pressure waves. The pressure waves results in ink ejection from the print head nozzle and afterward correspondingly filling again the reservoir. Vaporisation of small volume of the ink results in consequential limitations on the usable materials in the thermal DOD process [33].

For additive processes at the micro-scale, DOD technology preferred over continuous jetting principles as there is no need for unused liquid recycling since ink droplets are solely delivered when they are needed. Usually print heads include several separate nozzles which are fed via a single-ink manifold in a participatory manner but each separately controllable. The droplet over substrate surface dynamically evolves into three distinct stages in succession: impacting, spreading (and wetting), and drying, as shown in Fig. 3.15. As a result, the droplet deposition process, of interest for practical applications can be characterised to be controlled as process parameter.

3.5.3 Machines and Materials

Two inkjet printing systems have been commercialised under the same principle: Eden printer by Objet Geometries and ProJet printer by 3D Systems. Objet's

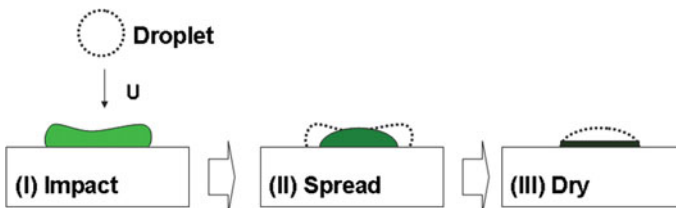


Fig. 3.15 Hydro-dynamic evolution of a droplet on substrate surface through three distinct stages in succession: (I) impacting (II) spreading, and (III) drying

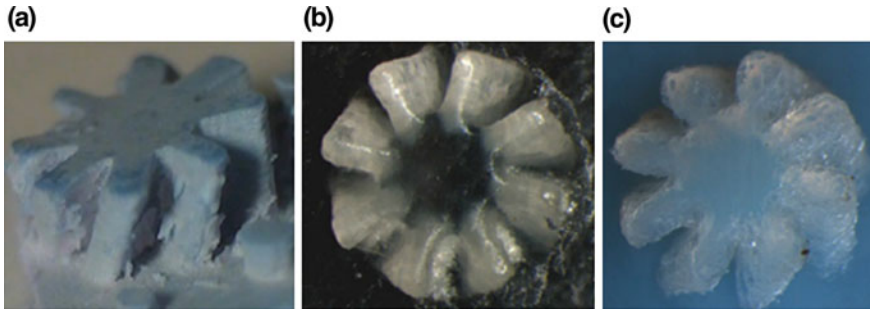


Fig. 3.16 Blade with 400 μm thickness produced using different inkjet printing systems [5]. **a** Solidscape's T76, the part was made with ~ 5 μm resolution and in 12.7 μm layers. **b** 3D System's ProJet HD 3000plus, the part was made in the extreme high definition mode (34 μm resolution and 16 μm layers). **c** Objet's Eden 260 V 3D printer, the part was made with (42 μm resolution and in 16 μm layers)

printers use special print heads with many individual nozzles to deposit a number of different acrylic-based photopolymer materials with 42- μm resolution and in 16- μm layers. Each photopolymer layer is cured by UV light immediately as it is printed, producing fully cured models. Support structures are built in a gel-like material, which is removed by hand and water jetting.

The ProJet printer uses the same technique varying that support structure used with this machine is a wax which has a much lower melting temperature than the part printed and is easily melted out. This method of "hands-free" support removal allows for highly complex 3D micro components/assemblies and delicate applications. Figure 3.16 shows sample micro-parts with 400- μm blade thicknesses which have been fabricated via different commercially available inkjet-based systems, including Eden 260 V, ProJet HD 3000plus, as well as Solidscape's T76 3D printer which is a commercial piezoelectric DOD micro-AM system for printing of polymer inks [5].

3.5.4 Materials

- Optical polymers
- Solders
- Thermoplastics
- Light emitting polymers
- Organic transistor
- Biologically active fluids.

It is believed that the most important limitation of inkjet printing systems is currently support removal for complex 3D micro-structures. In the meantime, resolution of the process should be improved to expand the range of applications.

3.5.5 Applications

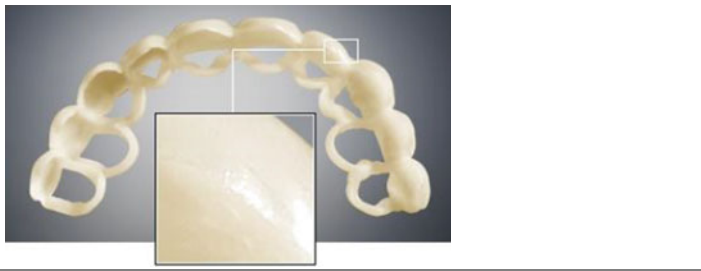
A range of common applications of material jetting are shown in Table 3.4. Mainly prototypes used for form and fit testing are built. Other applications include jewellery, medical devices, and high-precisions products.

Table 3.4 Most common applications of materials jetting

	<p>Hearing aids. They are customised according to the anatomy of the patient. The externally customised boxes internally host the micro-electronic devices to amplify and transmit sounds. <i>Source</i> [34, 35]</p>
	<p>The application of new robotic technologies in flexible endoscopy and laparoscopy to natural orifice surgery promises significant benefits to the patient in terms of comfort and recovery time. <i>Source</i> [36]</p>

(continued)

Table 3.4 (continued)

	Dental: VeroGlaze for Objet EdenV and OrthoDesk; 3D Printers delivers teeth color match with accuracy and good appearance [37]
---	--

3.6 Filament Deposition

Initially developed by Stratasys Inc., the filament deposition technique was one of the early generation of processes commercialised for rapid prototyping applications in 1992. For micro-fabrication applications, filament deposition processes are mainly being selected to take advantage of the intrinsic porous properties of the parts made by this technique. Since it is possible to control the extruded filament diameter, the distance between filaments and the building pattern that the filament follows, it is possible to engineer the porosity pattern of the final part. Using bio-compatible polymers has opened the window to the fabrication of a growing number of applications at scaffolds for tissue engineering as well for innovative drug delivery mechanisms as for regenerative medicine [38].

3.6.1 Operating Principles

Due to the simplicity of the operating principles of this technique, filament deposition is one of the most widespread processes currently within the additive manufacturing field. This level of diffusion is also promoted by the expiry of key initial patents. This has opened a wide window of opportunity for the development of new applications with this manufacturing technique.

The process operates by depositing a thread of polymeric material extruded through a micro-metric nozzle that traces the cross sectional geometry of the part while stacking layer over layer until the solid body is completed. As shown in Fig. 3.17, the build and the support materials are supplied as filament spools. The filaments are fed to the extrusion system by driving wheels, with the purpose of pulling and driving the filaments in a controlled speed and tension to feed the heated nozzle.

The extrusion nozzles contain resistive heaters that keep the polymer at a temperature just above its melting point so that it flows easily through them forming the layer. Immediately after flowing from the nozzle, the melted plastic bonds to the

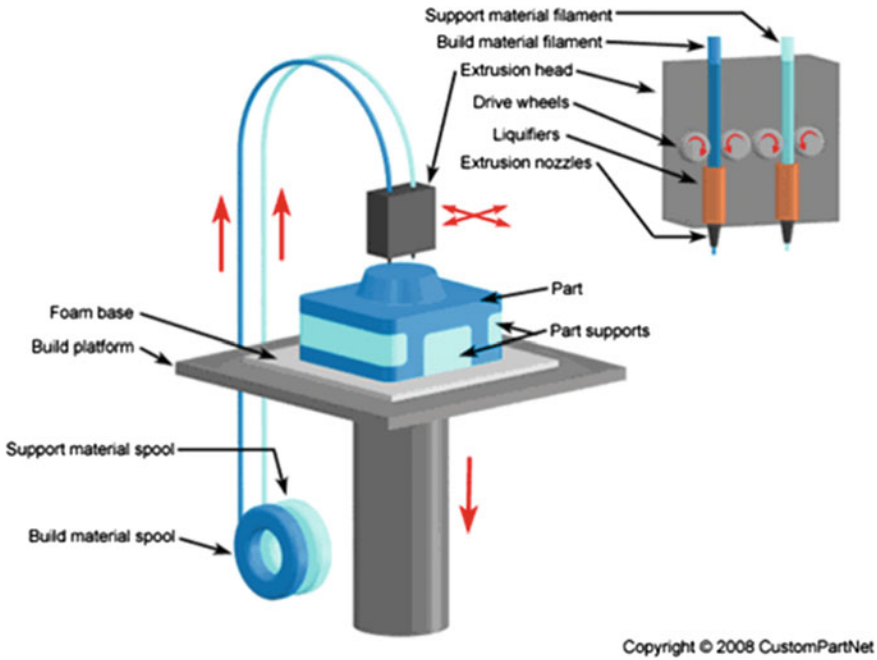


Fig. 3.17 Schematic representation of the Fused Deposition Modelling Process. Image courtesy of CustomPartNet

layer below and hardens. Once a layer is built, the platform lowers, and the extrusion nozzles are repositioned at the zero point to initiate the deposition of a subsequent layer [39].

3.6.2 Technology Overview and Systems

Within filament deposition processes, the dimensional accuracy, surface roughness, mechanical strength and above all, functionality of built parts are dependent on many process variables and their settings. Examples of relevant process parameters for this technique are the layer thickness, orientation of the part, raster angle, raster width and air gap, which have shown in several studies to have an influence over the meso-structural configuration of the build part. The identified parameters have been observed to have an effect over the bonding and distortion within the part in a complex manner, resulting in the anisotropic and brittle characteristics of parts created via filament deposition processes [38].

The parts generated using filament deposition processes effectively resemble a laminate composite with vertically stacked layers consisting of contiguous material fibres (raster) with interstitial voids (air gaps) as it presented in the example of Fig. 3.18.

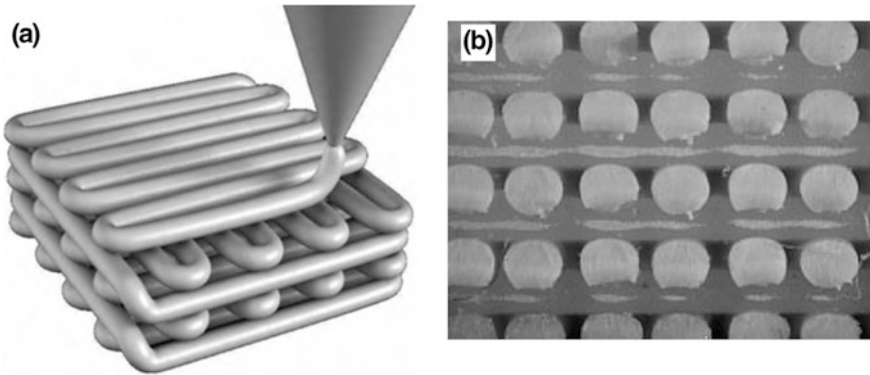


Fig. 3.18 **a** Schematics of the fused deposition modelling [40]. **b** Micro-structure of a FDM part. Rapid Prototyping Journal [41]

The bonding between neighbouring fibres takes place via thermally driven diffusion welding. Diffusion phenomenon is more prominent for adjacent filaments in bottom layers as compared to upper layers and bond quality depends on envelope temperature and variations in the convective conditions within the building part [38].

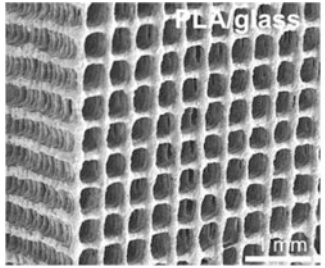
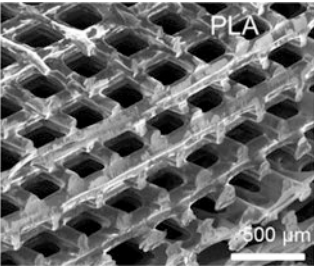
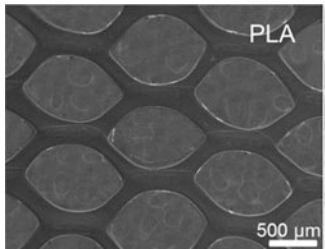
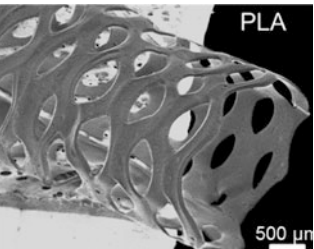
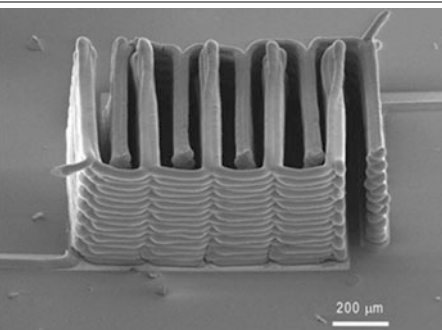
As described in the above, the dimensions of the interstitial voids are of considerable magnitude and they can be engineered at convenience. This quality makes the resulting material interesting for its intrinsic discrete conformation. At micro-manufacturing, in fact this feature is being used as an engineered porosity or spatially controlled deposition of material to be applied for specific applications mainly medicine for tissue engineering scaffolds and drug delivery devices or for electronics as it is shown at Table 3.5.

3.6.3 *Machines and Materials*

Tissue engineering is an interdisciplinary field which applies the principles of engineering to life science to generate living tissue and organ replacement. It is considered to be a highly promising approach for tissue reconstruction. This approach has tremendous potential to overcome the shortage of living tissues and organs needed for transplantation, and great efforts have been made in this field in the past two decades, especially in bone tissue engineering. 3D porous scaffold made of various bio-materials by progressive methods for bone graft in orthopaedics have the potential to achieve the required morphology, structure and function of bone tissues and thereby can optimise the integration with surrounding tissues. Thus, candidate materials and scaffold fabrication technologies and strategies for developing scaffolds are meticulously analysed and selected.

An example of a filament deposition micro-additive manufacturing system of this type is the 3D-300 series (nScript Inc.). It is a digital manufacturing system

Table 3.5 Examples of applications for different geometries of scaffolds

		<p>With two levels of visualisation scales it is shown a square mesh of Poly-lactic Acid (PLA) scaffold structure. <i>Source</i> IBEC</p>
		<p>It is also possible to design and fabricate tubular hollowed scaffold structures made from Poly-lactic Acid. <i>Source</i> IBEC</p>
		<p>Layered micro-battery made by FDM. <i>Source</i> [44]</p>

based on an automated dispensing mechanism that produces 3D structures by the layer-by-layer deposition of different materials. It allows the fabrication of well-defined, computer designed 3D structures with pre-determined geometry in a reliable and highly reproducible manner with a high control of the structure's porosity, pore distribution and morphology. It enables the fabrication of 3D structures using polymers and ceramics with a wide range of viscosities. There are existing predefined protocols for the production of polymer scaffolds based on polylactic acid (PLA), chitosan and also PLA/calcium phosphate glass composite scaffolds. Additionally the dispensing of proteins and cell suspensions is also available. The main application of this system is the fabrication of 3D porous scaffolds of defined geometry and porosity for tissue engineering applications. Dispensing and locating cells in specific positions on defined substrates is also possible due to the high precision levels of this tool (Fig. 3.19).



Fig. 3.19 Scaffolds fabrication equipment 3D-300 series from nScript Inc. *Source* nScript [42]

In terms of build materials, this kind of systems uses three heads for simultaneous injection of different materials including types of polymers, ceramics and living cells. The literature reports the fabrication of scaffolds with materials including [43]:

- Poly(ϵ -caprolactone) PCL
- Polypropylene/tricalcium phosphate (PP/TCP)
- Polycaprolactone/hydroxylapatite (PCL/HA)
- Poly(ϵ -caprolactone)/tricalcium phosphate PCL/TCP
- Poly(lactide-coglycolide) (PLGA).

Controlled by the proprietary software, the system facilitates the creation of a micro-environment appropriate for each mixture of materials and proteins and to achieve high rates of cell viability. The allowed viscosities vary from 1 to 106 centipoise enabled by a high-precision dispensing pump for dynamic control of the flow rate. Some additional features include visual monitoring system based on a digital camera, FireWire cameras and high magnification lenses, with detection and measurement of colorimetric–monochromatic variations.

3.6.4 Applications

As mentioned before, the applications for electronics and regenerative medicine are the most common at FDM micro-manufacturing. Some examples are shown at Table 3.5.

References

1. MINDS@UW-Madison, International conference on micromanufacturing (ICOMM). Available: <http://minds.wisconsin.edu/handle/1793/64713>. Accessed 12 May 2015
2. ASTM F2792—12a, Standard terminology for additive manufacturing technologies. Available: <http://www.astm.org/Standards/F2792.htm>. Accessed 2 Oct 2015
3. Tuck CJ, Hague RJM, Ruffo M, Ransley M, Adams P (2008) Rapid manufacturing facilitated customization. *Int J Comput Integr Manuf* 21(3):245–258
4. Ruffo M, Hague R (2007) Cost estimation for rapid manufacturing—simultaneous production of mixed components using laser sintering. *Proc Inst Mech Eng Part B J Eng Manuf* 221(11):1585–1591
5. Vaezi M, Seitz H, Yang S (2013) A review on 3D micro-additive manufacturing technologies. *Int J Adv Manuf Technol* 67:1721–1754
6. Hull CW, Apparatus for production of three-dimensional objects by stereolithography. US 4575330 A, 11 Mar 1986
7. Ikuta K, Hirowatari K (1993) Real three dimensional micro fabrication using stereo lithography and metal molding. In: *Proceedings IEEE micro electro mechanical systems, 1993*, pp 42–47
8. Rapid Prototyping—Stereolithography (SLA). Available: <http://www.custompartnet.com/wu/stereolithography>. Accessed 2 Oct 2015
9. Yang H, Ratchev S, Turitto M, Segal J (2009) Rapid manufacturing of non-assembly complex micro-devices by microstereolithography. *Tsinghua Sci Technol* 14(suppl 1):164–167
10. Stampfl J, Baudis S, Heller C, Liska R, Neumeister A, Kling R, Ostendorf A, Spitzbart M (2008) Photopolymers with tunable mechanical properties processed by laser-based high-resolution stereolithography. *J Micromechan Microeng* 18(12):125014
11. Limaye AS, Rosen DW (2007) Process planning method for mask projection micro-stereolithography. *Rapid Prototyp J* 13(2):76–84
12. Xia C, Fang NX (2009) 3D microfabricated bioreactor with capillaries. *Biomed Microdevices* 11(6):1309–1315
13. Small 3D Printer, Unirapid III. Available: http://www.unirapid.com/eng_ur3.html. Accessed 2 July 2015
14. Photonic Professional GT—Nanoscribe GmbH. Available: <http://www.nanoscribe.de/en/products/photonic-professional-gt/>. Accessed 1 July 2015
15. Zhang YL, Chen QD, Xia H, Sun HB (2010) Designable 3D nanofabrication by femtosecond laser direct writing. *Nano Today* 5(5):435–448
16. Savla Associates, Photopolymers for additive manufacturing, 2008. Available: <http://www.photopolymer.com/stereolithography.htm>. Accessed 5 May 2015
17. Schizas C, Melissinaki V, Gaidukeviciute A, Reinhardt C, Ohrt C, Dedoussis V, Chichkov BN, Fotakis C, Farsari M, Karalekas D (2009) On the design and fabrication by two-photon polymerization of a readily assembled micro-valve. *Int J Adv Manuf Technol* 48(5–8):435–441
18. Chichkov BN, Ostendorf A (2006) Two-photon polymerization: a new approach to micromachining. *Photonics Spectra* 40:72–79

19. Lin C-L, Lee Y-H, Lin C-T, Liu Y-J, Hwang J-L, Chung T-T, Baldeck PL (2011) Multiplying optical tweezers force using a micro-lever. *Opt Express* 19(21):20604–20609
20. Deckard CR. Method and apparatus for producing parts by selective sintering, US4863538 A, 5 Sept 1989
21. Yadroitsev I, Smurov I (2011) Surface morphology in selective laser melting of metal powders. *Phys Procedia* 12:264–270
22. Kruth J, Levy G, Schindel R, Craeghs T, Yasa E (2008) Consolidation of polymer powders by selective laser sintering. In: International conference on polymers and moulds innovations, 2008
23. Selective Laser Sintering. Available: http://www.additive3d.com/sls_int.htm. Accessed 2 Oct 2015
24. Cloots M, Spierings B, Wegener K (2013) Assessing new support minimizing strategies for the additive manufacturing technology SLM. In: International solid freeform fabrication symposium. 12–14 Aug 2013
25. Spierings AB, Schneider M, Eggenberger R (2011) Comparison of density measurement techniques for additive manufactured metallic parts. *Rapid Prototyp J* 17(5):380–386
26. Laser C, MLab laser cusing. Available: <http://www.concept-laser.de/en/industry/jewellery/machines.html>. Accessed 6 July 2015
27. GmbH, Available: <http://www.realizer.com/en/startseite/products>. Accessed 6 July 2015
28. Goebner J (2014) A peek into the EOS Lab : micro laser sintering
29. Sachs EM, Haggerty JS, Cima MJ, Williams PA (1993) Three-dimensional printing techniques
30. Three Dimensional Printing. Available: <http://www.additive3d.com/3dp.htm>. Accessed 8 July 2015
31. Höganäs 3D Printing Minutiae Precision—TCT—3D Printing. Additive manufacturing and product development technology. Available: <http://www.tctmagazine.com/euromold-news/hoganas-minutiae/>. Accessed 8 July 2015
32. Custom_part_net, Ink-jet-printing. Available: <http://www.custompartnet.com/wu/ink-jet-printing>
33. Chen C (1998) Inkjet printing of microcomponents : theory, design, characteristics and applications
34. Stratasys Hearing Aids. Available: http://usglobalimages.stratasys.com/Main/Secure/MaterialSpecsMS/PolyJet-Material-Specs/HAids_3Dmodeling_Letterlow.pdf?v=635011192407864638. Accessed 2 Oct 2015
35. Rapid Prototyping Laboratory, India. Available: <http://ed.iitm.ac.in/~gsaravana/rplab.htm>. Accessed 2 Oct 2015
36. Project Case Study: ProJetTM HD 3000 Success at Sant’Anna. Available: <http://www.senztech.cc/showsuccessfulstories.aspx?caseid=88>. Accessed 10 July 2015
37. Additive3d (2014) New Veroglaze Dental Material for Stratasys 3D Printers. Available: <http://www.additive3d.com/news/inr2312.htm>
38. Ahn S-H, Montero M, Odell D, Roundy S, Wright PK (2002) Anisotropic material properties of fused deposition modeling ABS. *Rapid Prototyp J* 8(4):248–257
39. Turner BN, Strong R, Gold SA (2014) A review of melt extrusion additive manufacturing processes: I. Process design and modeling. *Rapid Prototyp J* 20(3):192–204
40. Duty C (2012) Carbon fiber reinforced polymer additive manufacturing
41. Ahn S-H, Lee CS, Jeong W (2004) Development of translucent FDM parts by post-processing. *Rapid Prototyp J* 10(4):218–224
42. nScript, Micro Dispense Pump 3Dn Series. Available: <http://www.nscript.com/micro-dispensing-systems-equipment/direct-print-3dn-machines/index.php>. Accessed 1 July 2015
43. Arafat MT, Gibson I, Li X (2013) State of the art and future direction of additive manufactured scaffolds-based bone tissue engineering. *Rapid Prototyp J* 20(1):13–26
44. Cloud Color Media, Layered micro-battery created using FDM 3D printing technology, 2014. Available: <http://tobuya3dprinter.com/3d-printer-extrusion-made-easy/>

Chapter 4

Manufacturing Technology: Micro-machining

Lorelei Gherman, Andrew Gleadall, Otto Bakker and Svetan Ratchev

4.1 Overview

4.1.1 Why Micro-machining?

The ever-increasing demand for smaller and more precise products has fuelled continuous developments in micro-machining technologies.

Global competition has driven improvements in the accuracy of manufactured parts as well as the requirement for high productivity and reduced costs.

Micro-machining technologies have been the subject of many studies and developments over recent decades due to their importance in the production of micro-moulds, micro-valves, medical components, micro-electrical-mechanical-systems, sub-miniature actuators, motors and micro-products generally. Developments in micro-machining have facilitated the use of micro-sensors in the medical, aviation or wearable devices industries.

Contributions from: David Shipley, Mark Strickland and Matthew Hutchinson.

L. Gherman (✉) · A. Gleadall · O. Bakker · S. Ratchev
Institute for Advanced Manufacturing, The University of Nottingham, Nottingham, UK
e-mail: Lorelei.Gherman@nottingham.ac.uk

A. Gleadall
e-mail: Andrew.Gleadall@nottingham.ac.uk

O. Bakker
e-mail: Otto.Bakker@nottingham.ac.uk

S. Ratchev
e-mail: Svetan.Ratchev@nottingham.ac.uk

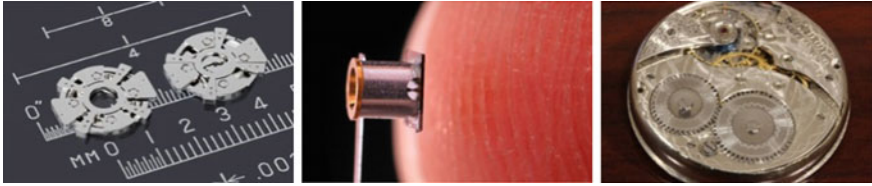


Fig. 4.1 Micro-parts in automotive, medicine and watch manufacture [1 – 2]

Different product types can present unique challenges, but the general requirements that accompany micro-scale production are precision, accuracy and repeatability. Two key challenges for those undertaking micro-machining are machining precision and the cost of manufacture (Fig. 4.1).

Machining precision reflects the quality of the micro-products, while the cost of manufacture reflects how marketable or profitable the process is for the manufacturer.

Achieving machining precision at the micro-level involves the following technical considerations.

- Size effects—including tool miniaturisation issues, the minimum chip thickness effect, or material grain size considerations, and
- Rigidity of the micro-machining system—with specific consideration being given to the overall process accuracy, including vibration and chatter in micro-cutting.

This chapter will define some key terms (in the context of micro-machining) and will then outline:

- Material considerations
- Challenges in obtaining the desired surface finish
- Simulation techniques and considerations
- The process and machine aspects of micro-machining, and finally
- Examples of micro-manufacturing sectors and applications.

4.1.2 Definitions

4.1.2.1 Micro-cutting

Definitions of micro-machining vary greatly, even within the academic community. There is not one accepted definition that can be applied to adequately cover all aspects of micro-cutting.

When we attempt to define micro-machining, several factors have to be taken into account, including, but not limited to:

- The size of the feature that is to be manufactured
- Tool size
- The specific machine-tool (e.g. machining centre) and the fixtures.

Micro-cutting (including milling and drilling) is generally considered to occur when features are produced within the 1–100 μm range.

Macro-cutting is generally considered to occur when machined features are larger than 100 μm .

Features produced less than 1 μm are generally referred to as resulting from nano-machining.

Of the above factors, the most important consideration is the size of the feature *being manufactured, which has a direct relationship to the depth of cut.*

Alternative definitions have been proposed, such as those defining micro-cutting in relation to tool dimensions, predominantly referring to the cutting tool diameter. Tools having a diameter of 0.5 mm are certainly capable of micro-machining. For example, Özel et al. [3] used 0.6 mm tools for their micro-milling experiments. Morcom [4] however, proposes that micro-milling tools have a diameter of 3.2 mm or smaller, half the size described by other authors.

Contrary to this, Özel et al. [3] suggest the cutting edge radius is more relevant when defining micro-cutting. Some tools with 0.5 mm diameters can perform very small depths of cut, at sub-micron level. This establishes a relationship between certain geometrical features of the tool and the minimum chip thickness that can be obtained with each tool.

The material micro-structure has also been used to define micro-machining [5]. In this case, the structure of the uncut chip thickness was correlated with the average grain size of the workpiece material.

4.1.2.2 Size Effect

Metals have a crystalline structure—this is not usually visible to the naked eye, but it can be seen on galvanised lamp posts for example. When a metal solidifies from the molten state, millions of tiny crystals start to grow. The size of the grains depends mainly on the cooling rate; the longer the metal takes to cool the larger the crystals grow. These crystals form the grains making up the solid metal. Each grain is a distinct crystal with its own orientation. The areas between the grains are known as grain boundaries.

Size effects is a term applied to the fact that in micro-machining, the layer of material to be removed is frequently in the same order of size as the material grain size which is dictated by the material grain structure. For example, in order to achieve the required form and surface finish, material has to be removed by cutting through individual grains rather than removing complete grains, which is the case on larger-scale machining.

For further information on material grain structure and failure of materials see Sect. 4.2.2. For further information on size effects, see Sect. 4.4.1.3.

4.1.2.3 Uncut Chip Thickness

The uncut chip thickness is the thickness of the un-deformed chip, prior to deformation occurring during the metal removing process. Due to the small scale of micro-machining, the uncut chip thickness is similar in scale to the cutting edge radius. Below a certain value, chips will not form, resulting in poor accuracy and surface finish.

4.1.2.4 Rake Angle

Rake angle describes the angle of the cutting face relative to the work. There are three types of rake angles: positive, negative, and zero. Positive rake angles reduce cutting forces and encourage chip removal.

4.1.2.5 Shearing, Ploughing, and Rubbing

In machining we encounter three phenomena. The desired condition is shearing which is material fracture. However there are always components of the other two less desirable phenomena. Ploughing involves plastic deformation of the workpiece material, whilst rubbing or slipping involves elastic recovery of the workpiece material. These phenomena are explained in more detail in the next section.

4.2 Engineering Materials and Material Properties

This section gives an overview of the important mechanical properties of materials that affect micro-cutting including elastic behaviour, plastic behaviour and material failure. Most of the discussion relates to metals, although many of the topics apply also to other materials.

4.2.1 *Elastic and Plastic Material Behaviour*

Elasticity describes the ability of a material to sustain temporary deformation in response to an applied force. For elastic deformation, the material returns to its original size and shape once the applied forces are removed. For metals, the deformation is predominantly accommodated by the atoms moving slightly closer together for compression or slightly separating for tension. Upon removing the applied force, the atoms return to their initial, preferred positions. Elastic behaviour is described by the elastic modulus, also referred to as **Young's modulus** or stiffness. This describes how resistant the material is to deformation. For stiffer

materials, with a higher modulus, more force must be applied to achieve a given deformation.

Plasticity refers to the manner in which a material undergoes permanent deformation. For plastic deformation, the material does not return to its original size and shape after an applied load is removed. The permanent deformation results from large-scale reorganisation of the atomic structure. The ability of a material to deform plastically is an important attribute for manufacturing; in particular, for processes in which a material is formed into a new shape, but also for mechanical cutting.

A useful method used to characterise the mechanical properties of a material is to perform a tension or compression test, in which a specimen is gradually deformed while the applied force is measured. Figure 4.2a shows a schematic of a dog bone-shaped tensile test sample. The larger sections at either end of the sample are clamped in a tensile testing machine and the specimen is elongated. The values of stress and strain in the central test section are calculated throughout the test. If the sample is strained beyond its elastic limit, some elongation of the test section remains after removing the forces as indicated in the bottom-left image in Fig. 4.2.

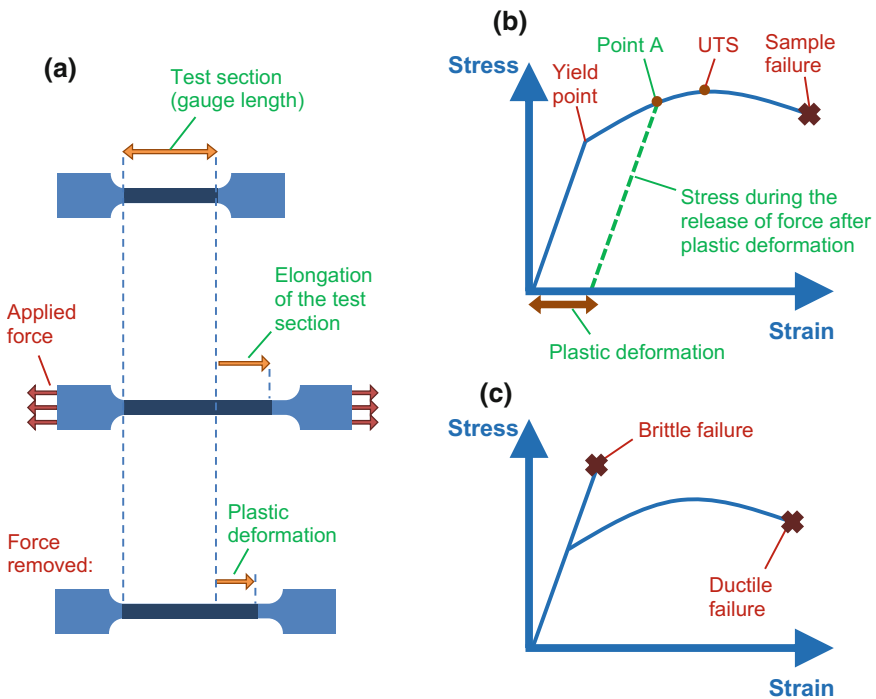


Fig. 4.2 a Test specimen subject to tensile testing. From *top to bottom*: before, during, and after applying a tensile force. b Typical stress versus strain curve for a ductile metal. The *dashed line* shows the relationship if the applied forces are removed at point A. c Typical stress versus strain curves for brittle and ductile metals

The results of the test can be plotted as stress versus strain. An example of such a plot is shown in Fig. 4.2b. Metals display a linear region at the beginning of the stress versus strain curve. The elastic modulus is equal to the slope of this linear region. The point at which the curve becomes non-linear is defined as the yield point and indicates that the elastic limit has been reached; any further elongation results in permanent plastic deformation. If the applied forces were gradually reduced at the value of strain indicated by point A in the figure, the strain would reduce according to the dashed line. Once all the force is removed, the remaining strain is permanent plastic deformation. The maximum level of stress achieved at any point during a test to failure is the ultimate tensile strength (UTS). Beyond this point, the sample quickly fails and breaks into multiple parts.

The material properties of the workpiece and the cutting tool are of critical importance for effective machining. The elastic modulus, yield point, UTS, and strain at which failure occurs all impact the process.

4.2.2 Failure of Materials

Metals typically fail due to fracture, whereby an applied stress causes a crack to propagate through the sample and separate it into two parts. There are two fundamental types of fracture; either brittle or ductile, with the difference being attributed to the level of plastic deformation sustained. Figure 4.2c shows how the stress versus strain curves differ for the two types of fracture. For brittle materials, a sample undergoes elastic strain until such high stresses are achieved that a crack forms and rapidly propagates across the entire specimen with very little plastic deformation. In many cases the crack initiates and propagates so rapidly that there is no visual indication of the imminent fracture. Cracks are initiated at flaws within or on the surface of a specimen. By contrast, in ductile fracture a crack propagates more slowly and significant plastic deformation occurs. Plastic deformation may lead to a narrowing of a section of the specimen as it is stretched, referred to as necking. Since this section has a reduced cross-sectional area it has an increased stress, and hence, cracks will typically form there.

Figure 4.3a shows how brittle cracks may propagate through metal grains, referred to as transgranular fracture, and (b) shows how a crack may follow grain boundaries, referred to as intergranular. Many factors affect which type of fracture occurs: the size of the grains and the strength of grain boundaries are particularly important. For micro-cutting, the grain boundaries may be larger than the required precision in which case, intergranular fracture is detrimental to the performance of the process.

Figure 4.3c shows a schematic of crack propagation during ductile fracture. High stresses result in localised plastic deformation and the formation of micro-voids. As these micro-voids increase in size, they gradually coalesce to form a crack. Higher stresses near to the crack tip result in the formation of micro-voids

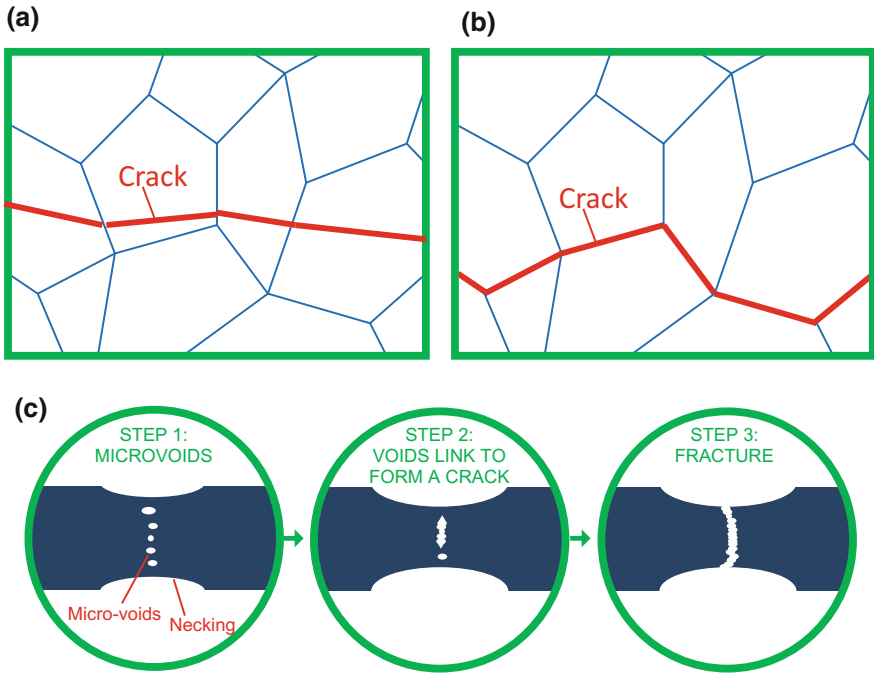


Fig. 4.3 **a** A brittle fracture crack propagating through microstructure grains. **b** A brittle fracture crack propagating along grain boundaries. **c** A ductile fracture crack propagation by coalescence of micro-voids

nearby which again grow and are eventually encompassed into the crack until it has propagated through the entire specimen.

4.2.2.1 Crack Propagation

The stress required for material failure due to the sudden propagation of a crack in brittle materials can be predicted according to:

$$\sigma_c = \left(\frac{2E\gamma_s}{\pi a} \right)^{0.5}$$

in which:

σ_c critical stress for crack propagation

E Young's modulus

γ_s specific surface energy

a crack length

For ductile fracture, plastic deformation also occurs near the crack tip and must also be considered in addition to surface energy considerations. Hence a higher stress or longer crack (than is the case for brittle failure) is required for ductile crack propagation. The above equation can be used to identify fracture strength for brittle materials based on the size of natural flaws that are present.

For micro-cutting, crack propagation is important for the formation of chips.

4.3 Design and Simulation

4.3.1 Introduction

Micro-cutting simulation is a complex and highly technical area that requires significant and specialised training and experience. Micro-cutting simulation may give the impression that it is similar to conventional machining process simulation, but as this section aims to explain, it is very different and subject to many complex interacting phenomena.

Additionally, micro-cutting simulation requires expensive, complicated software packages that are still evolving.

This section aims to put this into context and help the reader understand and appreciate the complexities of simulating micro-cutting. In a competitive global market, commercial organisations may well find it makes financial sense to seek the support of experienced consultants as and when required.

4.3.2 Why Simulate Micro-cutting?

As previously stated, the specific cutting energy, minimum chip thickness, surface roughness, burr formation, micro-structural effect, and tool wear combine to make micro-cutting operations very distinct from conventional machining.

Also, micro-tools are relatively expensive and therefore tool breakage is highly undesirable. Compared to conventional machining, the relatively high cutting forces, the sensitivity of micro-tools to vibrations, along with rubbing and ploughing phenomena, result in different chip formations, and add to the complexities.

By definition, the high level of accuracy needed requires stable, high precision machines.

As a result of these sensitivities, a wide range of issues need to be considered and managed effectively.

For instance:

- Environmental changes that impact the process (usually temperature)
- Vibration (sources internal and external to the machining centre)
- Small size of the parts resulting in issues with

- Part management (fixturing and workpiece location)
 - Low stiffness of the workpiece
 - Cutting fluids and its interaction with the cutting tool and workpiece
 - Accuracy; tolerances down to 0.1 μm
- Deflection and cutting forces, which can be up to 20 times higher than expected, causing high tool and part deflections
 - Chip-loads and feedrates; high spindle speeds (RPMs) allow reasonable feedrates, but have a negative impact on tool life and can easily contribute to tool breakage.

Furthermore, unlike conventional machining, machinists cannot rely on machining noise to monitor micro-cutting and detect tool loading issues and wear. As a result, small changes in the cutting conditions, such as tool wear, or tool deflection can result in instantaneous tool breakage.

This all combines to make it imperative that the feeds, speeds, and tool path are right first time. As there is little margin for error, simulation becomes invaluable.

4.3.2.1 Micro-machining Simulation

Dedicated simulation software for micro-machining is commercially available, such as Cimatron E Micro-Milling [6] and G-Wizard [7]. However, the cost of these software packages is often prohibitive and there can be system compatibility issues, IT infrastructure challenges, etc. Significant research has been undertaken in the “Micro Milling” Project [8] to establish simulation software, but this still requires significant further development in order that micro-cutting simulation software becomes as accessible as that for conventional machining.

It is therefore not always practical for SMEs to use dedicated simulation software for micro-machining. However, by utilising shop floor experience and in some cases mechanistic modelling, see Sect. 4.3.5, it is possible to develop machining strategies appropriate for micro-machining. For instance, similarities between high-speed machining and micro-machining exist, such as the need to avoid abrupt tool motion.

When using simulation software intended for use under conventional machining simulation conditions, it is important to be aware of potential CAD/CAM translation problems due to the small dimensions involved. In order to minimise these problems, when importing CAD parts, surfaces must accurately connect. Secondly, the simulation software should be able to process with high numerical precision in order to avoid problems with small features, especially on larger surfaces where the ratio between the overall part dimensions and the feature dimensions can be in order of 10^3 – 10^4 .

4.3.2.2 Machining Strategies

Simulation is often used to develop machining strategies.

It is vital to utilise operator and shop-floor experience when it is available. Machine operators often have a lot of experience, transferable skills and experience.

It is highly recommended that organisations develop and effectively implement machining strategies appropriate for micro-machining. There are similarities between high-speed machining and micro-machining, which can be extremely helpful. Many of the fundamentals of metal cutting apply to both regimes, and it is important to build on such prior knowledge, despite the differences.

Strategies should include considerations such as:

- Avoiding abrupt tool motion.
- For corner features, tool paths should be rounded where possible—which is influenced by the up-stream product design, and may or may not be feasible.
- Feed rates should be reduced as the features requiring a change of direction are approached. This reduces the loading on small and relatively fragile micro-tools.
- Conventional milling is generally more effective than climb-milling.
- It may also be advisable, or even necessary, to combine roughing and finishing operations for high aspect ratio parts. Positioning and setting up micro-components for machining is difficult and time consuming, and the number of setups should therefore be minimised.

Simulation software is of great value when planning micro-machining operations. There are some important considerations for the design/generation of tool-paths and process parameters:

- Spindle speeds (rpm) and feedrate are inherently connected due to the chip formation dynamics.
- Powerful coolant flow may deflect some micro-tools, introducing inaccuracies.
- Careful consideration must be given to tool deflection; relatively small tool loads can impact here—depending on the overall cutting environment.
- It is important that the cutting regime results in the use of appropriate tool loads as insufficient load will result in rubbing and no chip formation, but excess loading will cause deflections or worse still, breakage.
- Attempts should be made to maintain constant tool loads to maximise accuracy and avoid tool breakage.

Consequently, any simulation software used must be able to accurately maintain a constant chip load throughout the cutting process.

4.3.3 *Micro Versus Conventional Machining*

The features of a typical micro-machined part are in the order of 1–25 μm , and required accuracies can be less than 2.5 μm in size. Often, tools have to operate

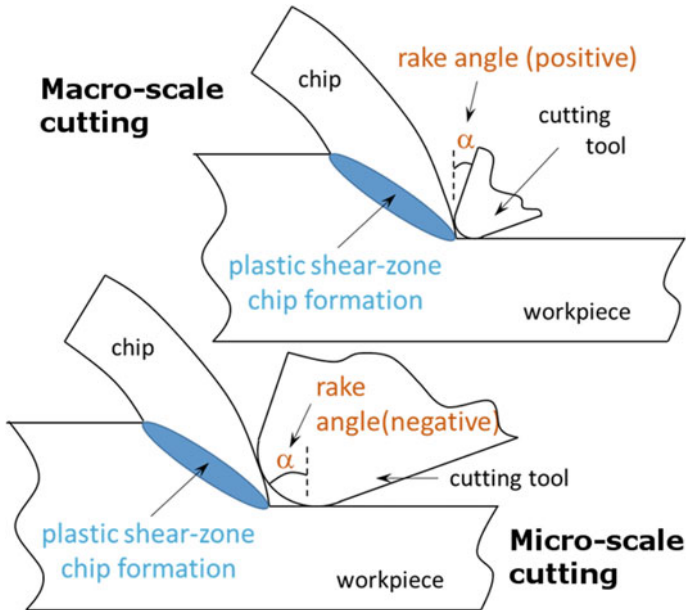


Fig. 4.4 Rake angle in micro and macro-cutting

with negative rake angles, hence rubbing and ploughing dominate over shearing [9]. This cutting regime is a result of the small scale in which micro-cutting takes place. Quality tools with sharp cutting edges, along with a feed-rate per tooth in the order of the cutter radius are required, as shown in Fig. 4.4.

Predominant factors that combine to make this a very different process include: the aforementioned *size effect* (cutting tool edge radius being of comparable size to the undeformed chip thickness and material grains); negative rake angles, resulting in rubbing, ploughing and poor/intermittent chip formation (not every revolution); and the resulting chip loads [10, 11].

As a result of these *size effects*, the required micro-cutting forces can be 10–20 times higher than predicted with conventional macro-scale models, whilst at the same time, using smaller, relatively fragile cutting tools [9].

4.3.4 Issues Covered by Modelling of Micro-machining

As already discussed, simulation is used to generate toolpaths and predict forces. It makes use of some simple relationships derived experimentally or from establishing a model of the physics of the cutting process. The phrase “modelling of the micro-machining process” in this context means the building of a model that describes the physics of the cutting process that can eventually be used (within

certain limitations) to estimate the value of a number of parameters required to define tool paths. Micro-cutting is a process that involves many variables and is, therefore, relatively complex to understand and to model. For example, the micro-tool plays a crucial role in the process. And furthermore, the size-effect should be taken into account. To establish working models, a number of assumptions are made about the process variables in order to reduce the level of model complexity. Numerical models of the micro-cutting process use the same underlying assumptions as the analytical models [12, 13].

It should be noted here that numerical modelling of micro-cutting has seen increased popularity over the recent years. However, it requires specialised knowledge to build and assess the model quality, not only to identify errors and potential issues inherent to the discretisation into finite elements itself, but also to assess whether the underlying assumptions about the cutting process to reduce the model complexity are valid.

Most research on micro-cutting processes, including the numerical modelling of the process, focuses on a number of characteristic problems associated with the micro-cutting process: the minimum achievable chip thickness, tool edge radius—with the latter strongly influencing the former, the microstructure of the workpiece material, and the specific cutting force. All of these influence chatter, the dynamic instability phenomenon, which is another topic studied in the modelling of the micro-cutting process. Surface finish is another field of study in the modelling of the cutting-process [12]. However, an observation made in a recent literature review by Anand and Patra [12] indicates that there are not many publications on this issue and the effect of ploughing.

4.3.5 Mechanistic Modelling of the Micro-cutting Process

Mechanistic modelling techniques deserve separate consideration as they are not based on building a model from first principles [12]. Mechanistic modelling proves very useful in establishing the cutting coefficient.¹ However, cutting coefficients are generally established empirically by considering the relation between chip loads and cutting forces and a number of other process parameters. The parameters obtained can subsequently be used in simulation software. The application of this methodology requires less specialist knowledge and is therefore more practical for use in small and medium sized enterprises in industry.

¹The cutting coefficient (also known as the specific cutting force) is the force, in the cutting direction, required to make a cut with a cross sectional area of 1 mm^2 and a chip thickness of 1 mm, for a specific cutter and material combination.

4.3.6 *Finite Element Analysis (FEA)*

The cutting tool plays a crucial role in the micro-cutting process, with specialist knowledge required to build and assess simulation models.

It is worth noting that there is a significant increase in computational power required modelling 3D as opposed to 2D.

Finite Element Analysis (FEA) is a computational technique to simulate real-world physical effects including forces, temperatures, vibrations and material flow. FEA can be used to simulate a range of scales—from the sub-micron level to construction bridges. For micro-cutting, FEA can be used to model the interaction between the tool and workpiece in 3D.

The atomic-scale finite element method (AFEM) has recently been developed [14]. In this method, the interatomic cohesive forces between the individual atoms in the (workpiece) material are modelled with forces exerted by non-linear spring elements² making it distinct from the molecular dynamics approach discussed in Sect. 4.3.7. The AFEM can be seen as the bridge between the molecular dynamics (MD) method and the conventional FEA for the modelling of continuum mechanics. We are not aware of any reported work, applying AFEM to model the micro-cutting process.

4.3.6.1 **Established Predictive FEA Models**

The FEA technique has been successfully utilised to predict the following [9]:

- Micro-burr formation (burrs can be problematic and difficult to remove from micro-components).
- Cutting forces (as already discussed, these differ significantly from macro-cutting models).
- Stress distribution on the cutting tool.
- Tool breakage.
- Thermal analysis (prediction of heat stress concentrations, thermo-mechanical material properties).

Figure 4.5 below shows two images from simulation software generated as part of the study “Modelling and simulation of micro-milling cutting forces” [15].

²A non-linear spring element is a special structural element that only has a specified spring stiffness, and can be placed between two nodes or between one node and the “ground” to exert a force on the node(s) based on the relative displacement.

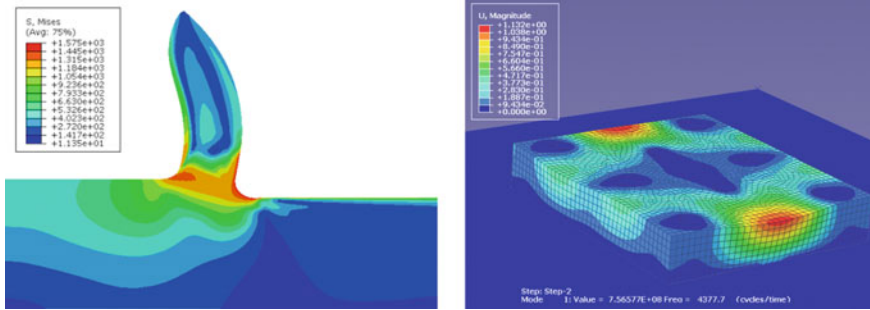


Fig. 4.5 *Left* Von Mises stresses and chip formation at 4 μm uncut chip thickness, cutting velocity of 1571 mm/s and edge radius of 3.5 μm . *Right* Workpiece natural frequency at the first shape model

4.3.7 Molecular Dynamics Modelling Approach

The Molecular Dynamics (MD) modelling approach performs analysis at the atomic level, based on the atomic interaction potentials (mathematical functions for calculating the potential energy of atoms based on their positions relative to one another) [9, 12]. MD simulations have very high computational demands, and specialised knowledge is required to build, test and interpret the results. For machining, it is predominantly, but not exclusively, used for nano-scale cutting. Simulations at larger scales quickly become unfeasible due to the number of atoms involved.

4.3.7.1 Established MD Models

Models are established for the following:

- Understanding the mechanism of chip formation and surface generation.
- Creating models for cutting.
- Investigation of the effect of material atomic structure on chip formation and cutting forces.
- Understanding mechanisms for friction, wear and scratching.

4.3.8 Multi-scale Simulation Methods

Simulations that consider greatly varying size scales are particularly challenging for computer simulations. For example, a tool may require analysis at the nano-scale

for the tool tip and macro-scale for the tool body. Simulation methods that are able to consider the tool body may not capture the fine details of the tool tip, whereas methods that are applicable to the tool tip would require unfeasible computational resources to consider the full tool body. Therefore multi-scale simulation techniques have been developed that combine different numerical methods into a single model [9, 12]. For a multi-scale model FEA,³ the tool tip may be analysed in an MD simulation which transfers forces and temperatures to a larger FEA model of the tool body. Thus the model captures atomic-scale interactions at the tip and also macro-scale temperature and force distribution in the overall tool. Many alternative combinations of simulation techniques exist. However, such models require highly specialised knowledge, and are included here mainly for information and awareness. It is beyond the scope of this book to discuss them in any detail.

- Quasicontinuum (QC) method
- Coupled Atomistic and Discrete Dislocation (CADD) method
- Bridging method
- Finite Element-Atomistic (FEAt) method
- Macroscopic, Atomistic, Ab initio Dynamics (MAAD) method, and,
- Coarse-Grained Molecular Dynamics (CGMD) method

Of these, QC, CADD and FEAt are the most popular methods being applied to study material removal mechanisms, and property evaluation of micro-structures.

4.3.9 Indicative Costs

At the time of writing (2015) indicative costs for FEA software are in the order of £10–20,000 per license, although there may be cheaper cloud-based solutions emerging.

Expertise can be sourced from specialist engineering consultancies or universities across the EU.

4.4 Process, Tools and Machines

4.4.1 Process

This section provides an overview of process considerations for micro-machining.

³The atomic-scale finite element method [14] is not a multi-scale method.

4.4.1.1 Machining Scale

As we have previously outlined, although they have similar kinematics, micro-cutting has distinct requirements and different parameters to regular cutting. For example, micro-cutting is only possible at spindle speeds higher than 20,000 rpm, whereas for regular cutting these are generally much lower. The mechanics of micro-cutting are also different. Usually the material micro-structure is an important factor in generating the workpiece surface, given the material grains often have to be split (as opposed to separated) to achieve the required feature size and surface finish. However, the main difference between machining and micro-machining processes, beside the size, is the uncut chip thickness [9].

The following section outlines some of the key differences between macro and micro-cutting scale operations, with respect to different considerations; namely the tool, the machine-tool and the uncut chip thickness.

This distinction will not only help set the boundaries for micro-scale cutting, but it will also help those intending to undertake micro-cutting prepare appropriately.

Tool implications for the micro-cutting process

Special tooling is necessary to achieve the accuracy required for micro-cutting (e.g. depths of cut are often in the order of a few microns). However, the differences between regular cutters and micro-cutting tools are not limited to size. Micro-tools are usually designed with one or two flutes and have a distinct geometry. Since the uncut chip thickness and the cutting edge are of comparable dimensions, the cutting edge must have improved mechanical properties. It must be able to endure high levels of thermal and mechanical stress, induced by the high rotational speed.

Some regular tools, such as a 1 mm diameter end-mill, are capable of performing micro-level depths of cut in the order of 10 μm . In such cases, micro-cutting is enabled by the **cutting edge radius**, and not the tool diameter. However, there are limitations to what can be achieved with a non-specialised tool.

Machine-tool implications for the micro-cutting process

Specialised machining centres are also required for micro-cutting. There are two types of equipment that perform micro-cutting: ultra-precision machining centres and micro-machines, such as micro-factories and miniature machines.

Unlike a regular machine-tool, micro-machining centres require greater stability, and the machines themselves must act as dampers, to absorb the inherent process-induced vibrations. Specialist micro-machine tools have high rigidity, are ultra-precise and should operate within controlled environments, e.g. temperature, humidity, etc. [16].

Micro-cutting machining equipment must also have better stability, precision at sub-micron level, stiffness and must be more precisely aligned. They should also have a high degree of static and dynamic stiffness, thermal stability, and compensation of positioning errors [17].

By way of example, high speed machines such as the KERN Triton (20,000–50,000 RPM) are capable of damping any inherent and resulting vibrations; essential to achieve the required tolerances and surface finish.

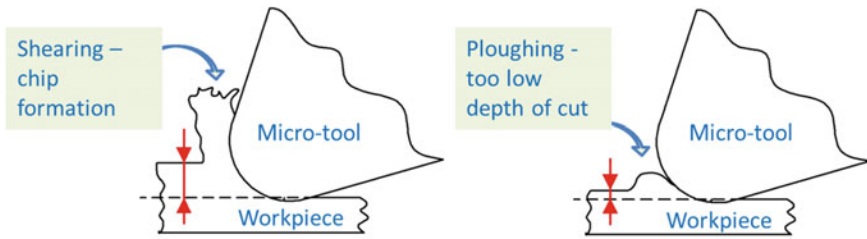


Fig. 4.6 Size effects resulting from a small ratio of the uncut chip thickness to tool edge radius

Uncut chip thickness implications for the micro-cutting process

The ratio of the cutting tool edge radius and the uncut chip thickness is also a distinguishing factor between regular and micro-scale machining. At small cutting depths, ploughing and slipping are more prone to occur. Some researchers have observed that a reduction in depth of cut values indicated a non-linear specific cutting energy increase [18]. These so-called *size effects* represent the most important difference when comparing regular and micro-scale cutting.

Figure 4.6 illustrates the effects of the small ratio of the uncut chip thickness to tool edge radius. These images indicate the difference between regular scale and micro-scale cutting. The main difference derives from the size of the radius compared to that of the uncut chip thickness. With regular cutting, the radius is significantly smaller, and thus the tool has a high degree of sharpness. However, with micro-cutting, the radius can be considered to be of a similar size to the average grain size of the workpiece material. This affects the sharpness and the shear zone formation.

Figure 4.6 (left) shows desirable cutting conditions, resulting in shearing, whilst Fig. 4.6 (right) shows a small depth of cut, resulting in ploughing. The micro-tool has a different geometry than the one used in conventional milling.

4.4.1.2 Cutting Forces

The energy (and hence the cutting force) necessary to shear along a grain boundary is less than the energy required to shear through a grain (intergranular fracture) for a given material.

The net cutting forces in micro-machining are often less than those experienced in conventional machining. However, they are usually being exerted by smaller and more fragile cutting tools. Rapid and significant changes to the cutting dynamics, although small in magnitude, are more significant and can result in tool failure at the micro-scale. Hence, all factors have to be taken into account.

One factor is the shear zone formation and how the cutting force is developed.

Another factor affecting cutting forces is tool wear. Tool wear leads to increased cutting tool edge radius, and subsequently an increased minimum chip thickness, which cannot always be accurately predicted during machining. This has greater impact at the micro-machining level resulting in ploughing. Ploughing is considered in more detail in the next section, but in summary, when ploughing occurs the tool does not effectively facilitate shearing and the stress on the tool increases significantly.

An off-centred cutting process can increase wear in one or more of the tool flutes, which in turn changes the cutting force distribution. This results in uneven surface roughness on the part, gradual tool wear and, subsequently, tool breakage.

There are various cutting models that describe cutting force evolution during processing. Among the first were those offered by Merchant, by Ernst and by Piispanen [19]. Other models are derived from these, but they have the limitation of simplifying hypotheses. Some researchers, such as Astakhov [20], debate whether they provide appropriate modelling for the micro-cutting process, due to the fact that experimental work does not reliably support the models.

Further studies include those undertaken by Altintas and Lee [21] who worked on cutting force models for helical end mills. They took into consideration shear and friction angles, along with shear stress, in order to predict machining forces, forced and chatter vibration, and errors. The chip formation was analysed by means of true trochoidal⁴ motion of milling models, considering static displacements. Their studies extended to mechanics and dynamics of ball end-milling [21, 22]. The models proved accurate for ball end-milling using helical cutters, but could be further extended to end-milling models.

Most mechanistic models assume that the tool edge is sharp, and the radius has minimum values [23]. However, given that the radius of the micro-cutting tool edge (0.5–3 μm) is of comparable size to the workpiece material's grain structure, mechanistic models still need to be improved. Specialist micro-cutting modelling software could potentially be utilised to take into account the tip radius and grain structure, such as CimatronE [6]. This was developed for high surface accuracy solutions at the Fraunhofer Institute for Production Technology (IPT) in Aachen, Germany, for tool makers and for micro-milling operations [6, 8]. However, commercially available software has yet to take into consideration atomic-scale effects, and ploughing in particular.

In order to better analyse the micro-cutting process, work undertaken by Câmara et al. [17] investigating micro-milling, identified input parameters for micro-milling specifically. These aspects are synthesised in three subsections, namely workpiece material, tool characteristics and machine-tool concerns. This consideration of the input factors to a micro-milling process can be used as a model to define the process and to highlight the properties that can affect the results.

⁴A trochoid (derived from the Greek word for wheel, “trochos”) is the curve described by a fixed point on a circle as it rolls along a straight line.

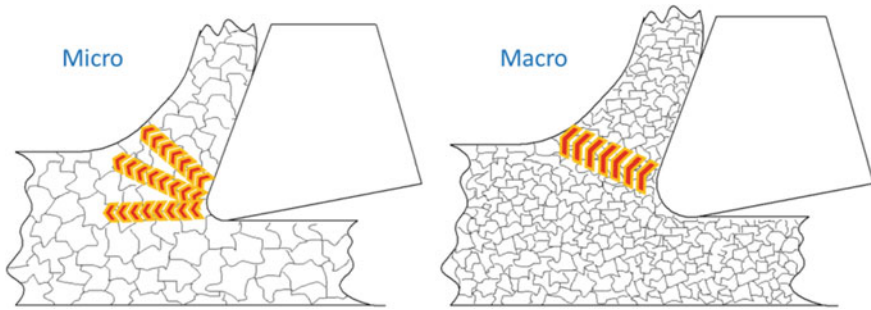


Fig. 4.7 Difference between micro and macro-cutting phenomena

4.4.1.3 Size Effect

As discussed, **size effects** play an important role in micro-chip formation, which affects machinability and in turn the quality of the micro-machined surface. The fact that the layer of material removed is at the same order of size as the material grain affects the shearing phenomenon and, thus, the chip formation.

The difference can be explained by surface free energy effects, as illustrated in Fig. 4.7, by material impurities or defects at crystallographic level [24].

The minimum chip thickness is dependent on the ratio between the uncut chip thickness and the cutting tool edge radius. The precise value of the minimum chip thickness depends on the workpiece material. Values for the minimum chip thickness can vary from 5 to 40% of the tool edge radius, and they can be empirically determined.

The mechanical properties of the micro-tool, e.g. rigidity, will play an important part in determining the minimum depth of cut achievable under specific conditions.

4.4.1.4 Burr Formation

A priority when micro-cutting is achieving the required surface finish in a single operation. Using a new tool or one in good condition, under optimal operating parameters is the best way to achieve this and it will also help minimise burr formation.

Specialised software such as DEFORM-2D is useful when considering the minimum chip thickness and consequently the chip formation process. Alternatively, cutting models such as Merchant's slip-line model can be used. These shear plane models are robust, having been verified by experimental investigation.

The chip formation process is dependent on the cumulative effect of several factors including workpiece material, tool material, cutting feeds and speeds, and even depth of cut. Poor chip formation will result in burr formation as illustrated in Fig. 4.8.

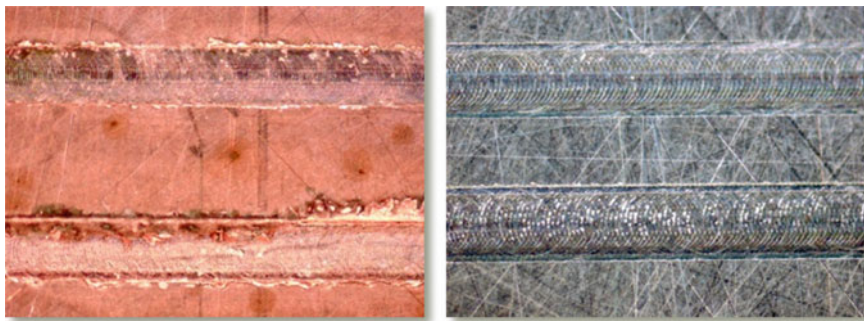


Fig. 4.8 Burr formation in copper and steel under analogous cutting conditions

4.4.2 *Micro-tools*

This section provides an overview of tool considerations for micro-machining, including size, wear, breakage and material coatings.

4.4.2.1 Tool Size

Drills, end-mills, ball-nose mills or engraving tools are frequently used for micro-cutting applications. They are generally made out of tungsten carbide, or diamond, in order to prevent stress-related breakage.

Due to the small nature of such tooling, micro-tooling is an entire industry in itself. Not only does the size of the tool decrease significantly, 8 μm for the smallest drills or 20 μm for mills, but their geometry has to change accordingly. They usually have only one or two flutes in order to allow the chip to flow. The tool shank is shorter (a few millimetres) to maximise stiffness, to suppress vibrations and to maintain positional accuracy of the tool. Since the uncut chip thickness and the cutting edge are of comparable dimensions, the cutting edge must have improved mechanical properties. It must be able to endure high levels of thermal and mechanical stress, induced by the high rotational speed.

Micro-tooling is expensive due to the specialist knowledge required and the challenges of producing complicated tooling geometry at sizes lower than 0.1 mm, as illustrated in Fig. 4.9. Since tool failure is a major consideration for micro-cutting, everything possible must be done to minimise the risk of tool breakage given the subsequent cost to production.

One of the significant challenges in the manufacture of micro-tools is how to produce a small cutting tool edge radius. The smaller the radius, the smaller the achievable depth of cut can be. Focused Ion Beam (FIB) is sometimes used to

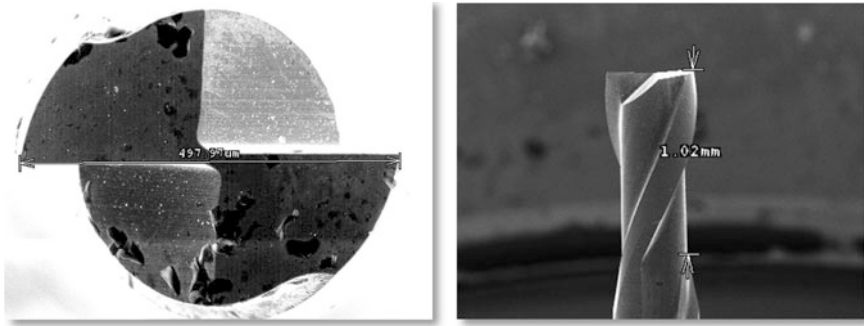


Fig. 4.9 Tool size

machine sharp edges. Electrical Discharge Machining (EDM) and Wire Electrical Discharge Machining (WEDM) are employed to cut smaller features on micro-tools. However, these technologies have long process times, and limitations on geometries, and thus, cost invariably influences process selection [9].

4.4.2.2 Tool Wear and Breakage

Tool wear is not as gradual in micro-machining as macro-machining. Very soon after wear causes an increase in the cutting edge radius, tool breakage occurs with little or no warning.

An uncontrolled process can result in rapid and unpredictable tool wear which affects surface accuracy, quality and ultimately cost. The main challenge for a manufacturer is the optimisation of the operating parameters (feed, speed, rotation, depth of cut) in order to obtain both the desired surface, but also to control wear and prevent tool breakage. The inspection of tooling prior to use and in-process tool monitoring can help ensure the optimum performance of micro-tools. Effective simulation and modelling, although complex, challenging and expensive, can help enormously.

Furthermore, tool wear can be more difficult to monitor during micro-machining, which makes it more challenging to account for during the cutting process. This results in a reliance on manufacturer specifications and recommendations and, just as importantly, on the technician's experience selecting and actively adjusting the right set of cutting parameters.

Tool failure has been explained as a consequence of different mechanisms:

1. Fatigue induced failure—there is a risk that fatigue cracks may develop and lead to breakages as a result of the high cutting speeds, and therefore high number of stress cycles.



Fig. 4.10 Example of a broken and a worn out tool

2. Stress induced failure—when a tool is subject to cutting forces above its normal operating limits, the tool can quickly break. This is due to chips forming on the cutting edge; cutting edge wear. When this occurs, the tool will no longer cut, but it will push against the work material and this will increase the stress in the tool.
3. The increase in specific energy, as the depth of cut decreases.

These mechanisms can result in either tool wear or breakage, as shown in Fig. 4.10.

A number of other factors contribute to tool wear, such as the size effect, negative rake angles, multi-phase workpiece materials or material elastic recovery. These detrimental effects can be diminished by appropriate tool inspection, process monitoring and effective cutting strategies. Tool inspection prior to machining can minimise the risk of in-process tool failure. An example of tool damage is shown in Fig. 4.11.

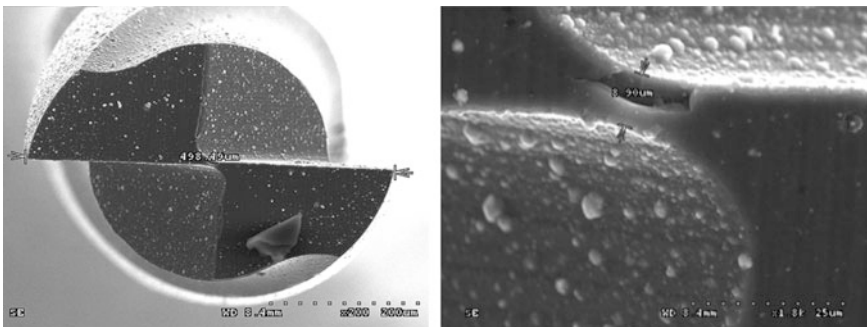


Fig. 4.11 Importance of tool inspection prior to processing. The above illustrates a defect in the tool web

4.4.2.3 Micro-tool Coatings

Macro-tool coatings are used to increase the hardness at the cutting interface, along with providing better resistance against chemical and mechanical wear. Given the small scale, micro-cutting tool coatings need to be more compact—they need a finer grain structure. They need to be more crystallographically consistent and have a thinner and smoother top surface, so that friction forces are further reduced at the tool-workpiece interface.

Coatings used for commercially available micro-tools include:

- TiN—titanium nitride
- TiAlN—titanium aluminium nitride
- CrTiAlN—chromium titanium aluminium nitride

4.4.3 Machine-Tools

This section provides an overview of machine considerations for micro-machining operations.

4.4.3.1 Micro-machining Platform Characteristics

Whilst it is true that an experienced machinist on standard workshop equipment can produce exceptional detail and accuracy (think early watchmakers), with this alone, it is not possible to survive in a highly competitive environment where repeatability, response times and high volume manufacturing is required.

So, what are the main machine attributes required?

Spindle speed

There is no way round the need for surface speed for milling (though this is not always the case for drilling). Ideally circa 50,000 + rpm is desirable. 20,000 + rpm may suffice, but with no guarantees. Speed increasers can be useful but may lack sensitivity for <0.5 mm tooling.

Machine construction

Polymer concrete bases and hydrostatic slideways help deliver very good rigidity, insulation from heat, and vibration. This enhances the sensitivity of the machine and isolates forces that can interfere with the very small cutting forces required for micro-machining.

A heavy duty cast machine construction with linear drives or high precision, alloy ball screw and digital drives may suffice in most cases. Standard machine shop construction, cast iron ball screw and analogue drives will be inadequate.

Repeatability

It is crucial that the machine can exhibit high levels of repeatability. Again, this brings a new level of sensitivity into the machining process along with the knowledge that the equipment can make parts consistently without constant intervention. The higher specification machines available should be capable of sub-micron positional repeatability, whilst the mid-range should be under 10 μm and the standard under 25 μm .

Control

The machine control needs to be able to process large amounts of information as programs produced on Computer Aided Manufacturing (CAM) platforms are often very large. Individual movements of the cutting tools may be very small, so maintaining a constant feed rate requires a powerful processor and a “look-ahead” program buffer is essential. For example, the Heidenhain TNC530 (or newer) would be considered suitable. Any control with a look-ahead facility may prove adequate, but some early controls, and any without the look-ahead functionality, simply will not cope.

Number of axes

The decision to employ 4 or 5 axes over the traditional 3 axes layout may be driven by specific job requirements or building in platform flexibility. There is a trade off in rigidity and repeatability. This will have less of an impact on the highest specification machines, but is worth being aware of, if considering mid-specification machines.

Every extra axis introduces more positional error. By way of an example, a high specification machine that is sub-micron accurate point to point on a jig boring operation, may be $>5 \mu\text{m}$ on a 5 axis simultaneous tool path. This error can also be made worse by the adoption of a poor tool strategy and limited control functionality.

Hence, when selecting machine-tools for micro-cutting applications, all of these factors need to be considered holistically and not in isolation.

4.4.3.2 Machine-Tools Suppliers

There are many micro-machining centre manufacturers, and the capabilities of the machines vary within different price bands.

A typical Kern machining centre (Fig. 4.12) offers the advantage of having a polymer concrete bed, which damps vibrations during processing. Tolerances are usually within $\pm 0.5 \mu\text{m}$ for micro-cut features [25].

At the time of writing (2015), the Kern Evo costs in the region of £250,000–£300,000.

Röders Tec on the other hand, offers high stiffness, optimum layout of the mass inertia and geometric compensation for increased precision during machining. These machines are priced up to £250,000. A typical machine, such as the RXP400DS—5-axis machine, offers spindle speeds up to 50,000 rpm.



Fig. 4.12 KERN machining centres

The Hermle Machine Company, builds ultra-compact machining centres designed for larger parts. Some of them, such as the C12 5-axis machining centre, can process parts as heavy as 100 kg and have prices up to £250,000. They have the advantage of built-in functions such as automatic vibration measurement and control, which is a critical consideration in micro-cutting applications (Fig. 4.13).

Sodick machining centres have spindle speeds of up to 40,000 rpm and cost up to £300,000. The HS430L high speed mill offers the advantage of a BLUM laser



Fig. 4.13 A Hermle machining centre which is constantly in high demand in the University of Nottingham Manufacturing Labs

tool length measuring device, which is critical in acquiring tool wear estimates, without the need to remove it from the tool holder.

Other companies, such as Fanuc and Kugler, have a range of machining centres specialising in micro-cutting. The demand for micro-products has brought with it the development of many micro-machining centres, competing on a balance of price and capabilities. There is a balance to be achieved within the cost of machine procurement and the products and features to be produced.

It should be emphasised that machine-tool manufacturers are constantly evolving their products, underpinning technologies, packages, and price positions, and all information provided is only intended to be indicative.

4.4.4 Measurement Systems

It is logical to assert that in order to ensure the highest product quality, the ability to accurately and reliably measure components is absolutely critical.

The two main areas requiring measurement are geometric and process parameter measurement. Micro-geometric measurement is discussed in more detail in the subsequent chapter “Micro-scale Geometry Measurement”.

Typically, measurements taken during the micro-cutting process are:

- The tool (before, during and after machining)
- The workpiece
- Various process parameters that could affect the micro-cutting process (vibrations, tool position etc.).

Geometric measurement can be considered at three stages:

- Pre-processing
- In-process
- Post-processing.

4.4.4.1 Geometric Measurement: Pre-processing

Prior to beginning the cutting process, the tool dimensions and position must be clearly established. The second step is determining the workpiece surface position. These two sets of coordinates help ensure the accuracy of the micro-cutting process. Laser equipment and infra-red touch probes are the preferred equipment for the job.

4.4.4.2 Geometric Measurement: During Processing

Linear variable displacement transducer devices can be very effective in determining tool height and radius with the aid of a vertical and horizontal contacting

type tool set station. (AMETEK Precitech Ultracomp equipment can establish this to an accuracy of $0.4\ \mu\text{m}$). Cutting tools can be measured in different positions attaining this data with the controller. Whilst these measurements are known, the machine will accurately and reliably know the tool dimension and position.

4.4.4.3 Geometric Measurement: Post-processing

A number of high accuracy measurement technologies can be used to determine the form, geometry, dimensions and surface roughness of a micro-machined part.

These include non-contact systems such as: laboratory microscopes, scanning electron microscopes, and interferometers. Contact systems (stylus/probe based systems) include: surface profilometers and co-ordinate measuring machines. In addition to measuring surface roughness, a stylus profilometer such as the AMETEK Taylor Hobson TalySurf, see Fig. 4.14, can also measure form. This allows the system to be used to check the machine set-up for turning applications (i.e. tool centring) in addition to measuring component accuracy in 2D. A white

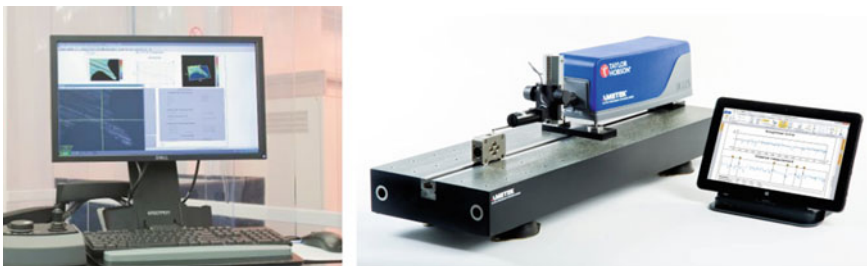


Fig. 4.14 NP FLEX interferometer and AMETEK Taylor Hobson TalySurf Intra

An example of in-process parameter measurement is equipment mounted on the spindle that determines position of the surfaces with regards to the spindle orientation.

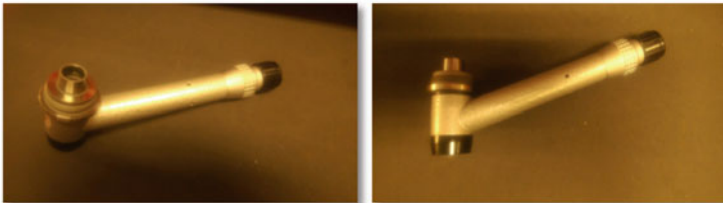


Fig. 4.15 Equipment for spindle position measurement

light interferometer such as the Bruker NP Flex, see Fig. 4.14, can measure 3D surface topography at the micro and nano scale.

4.4.4.4 Process Parameters Measurement

Although not commonly used in industry, in-process cutting force measurement can be useful for large batches or mass production. Cutting force evolution can negatively impact tool life and, as such, can prove invaluable in process monitoring,

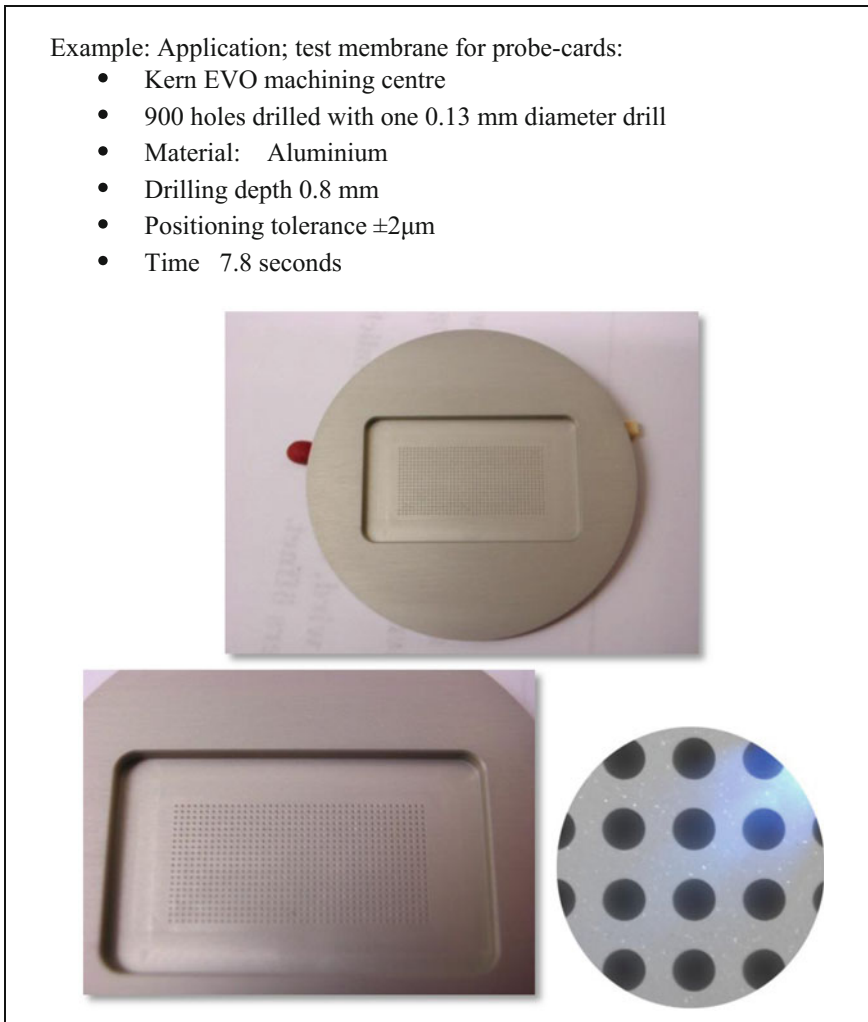


Fig. 4.16 Probe-card and 60 times magnification of drilled holes

helping to minimise costs. Despite its usefulness, this kind of measurement is usually the remit of research institutions. Cutting forces can be measured using a dynamometer (e.g. those manufactured by Kistler). This can provide accurate information regarding the cutting force and its variation, about the periodicity of the process, and even about tool wear. As the tool becomes worn, the cutting force required for the same depth and type of cut increases. At high cutting forces, the micro-tool is at high risk of breakage. Thus, an in-process monitoring system such as a dynamometer can be very helpful in preventing tool breakage (Figs. 4.15 and 4.16).

4.5 Sectors and Applications

Micro-cutting, and especially micro-milling, has the benefit of machining parts with high aspect ratios and high geometric complexity.

Some micro-manufacturing technologies are less capable of mass or batch production. Micro-milling is perfectly suitable if appropriate processes and tools are adopted—for example, in the production of masks for X-ray lithography.

Micro-cutting is used in a large variety of applications. As previously explained, micro-cutting can be used in isolation to produce finished parts. However, it is often linked with various other technologies: e.g. with other processing types, measurement devices, etc.

4.5.1 *Industry Sectors and Application Areas*

Industry sectors and application areas were identified by Desarollo [26] as:

- Watch and jewellery making; manufacturing of tools for watch making, engraving of base plates, moulds for rings and pendants, detailed micro-machining of all watch parts.
- Automotive: electrodes for cutting inserts, fuel injection nozzles, diesel injection nozzles, parts with tight tolerances for micro-drilling.
- Aerospace: instrumentation and electronic connectors and hydraulics, miniature devices for rockets, moulds for miniature planetary gear wheels attached to a turbine.
- Mould fabrication: plastic optics for micro-moulds based on micro-replication techniques.
- Biomedical: cochlear implants, micro-tools for surgery, moulds in micro-dosage application, lab-on-a-chip, in orthodontics (such as dental brackets), replication moulds for cells, moulds in biotechnology applications (microchip electrophoresis devices, polymeric BIOMEMS (biomedical micro-electromechanical systems) devices, accelerating polymerase chain reaction for modular lab-on-a-chip systems), cataract lenses, retinal micro-tacks, etc.

- IT: test membrane for PC chip manufacturing.
- Others: direct machining of optics either ceramic lenses or metallic mirrors, scientific instrumentation, components for measuring devices, electrodes for toy industry, electrodes for manufacturing shaving head of electric razors, crack detection (creating a micro-crack on a helix for turbines/drive shafts), gas leak detection (micro-feature with a special shape—different shapes for different gases).

As an aside, micro-machining specific benefits translate into improved meso⁵- and macro-scale machining outputs when performed on micro-capable equipment. Better results can be achieved in terms of tool life, productivity, and enhanced product quality.

References

1. Waurzyniak, P (2013) Micro Manufacturing Keeps Shrinking the Envelope. Available: <http://www.sme.org/MEMagazine/Article.aspx?id=69873>, 28 May 2015
2. RAL Space website. Available: <http://www.stfc.ac.uk/ralspace/11291.aspx>, 28 May 2015
3. Özel T, Liu X, Dhanorker A (2007) “Modelling and simulation of micro-milling process”, 4th international conference and exhibition on design and production of machines and dies/molds, Cesme, Turkey, pp 21–23
4. MORCOM (2013) Micro-machining involves a lot more than using scaled-down tools. Available: <http://www.micromanufacturing.com/content/micro-machining-involves-lot-more-using-scaled-down-tools>, 25 Feb 2014
5. Simoneau A, Elbestawi MA (2006) The effect of microstructure on chip formation and surface defects in micro-scale, mesoscale and macroscale cutting of steel. *Ann CIRP* 55:97–102
6. CIMATRONE, CimatronE micro milling simulation software by Cimatron. Available: <http://www.cimatron.com/NA/general.aspx?FolderID=5320>, 5 Oct 2015
7. G-WIZARD, G-Wizard Software by CNC Cookbook. Available: <http://www.cnccookbook.com/CCNCSoftware.html>, 5 Oct 2015
8. PROMOLDING BV (PRO) (2005) Final technical report and progress report (combined). Available: http://promolding.nl/contentdownloads/Final_Report_MicroMilling_18.pdf
9. Cheng K, Huo D (2013) *Micro-cutting. Fundamentals and applications*, 1st edn. The Wiley Microsystem and Nanotechnology Series. Wiley, Oxford
10. Elkaseer AA (2011) “Modelling, simulation and experimental investigation of the effects of material microstructure on the micro-endmilling process. Ph.D. thesis, Cardiff University, Institute of Mechanical, and Manufacturing Engineering, Cardiff
11. Mian AJ (2011) *Size effect in micromachining*, Ph.D. thesis. Cardiff University, School of Mechanical, Aerospace and Civil Engineering, Manchester
12. Anand RS, Patra K (2014) Modelling and simulation of mechanical micro-machining—a review. *Mach Sci Technol: Intl J* 18(3):323–347
13. Leopold J (2014) Approaches for modelling and simulation of metal machining—a critical review. *Manuf Rev* 1(7):1–16
14. Liu B, Huang Y, Jiang H, Qu S, Hwang KC (2004) The atomic-scale finite element method. *Comput Methods Appl Mech Eng* 193:1849–1864

⁵In machining terms, meso-scale generally refers to the scale spanning micro and macro-machining.

15. Afazov SM, Ratchev SM, Segal J (2010) Modelling and simulation of micro-milling cutting forces. *J Mater Process Technol* 210:2154–2162
16. Chae J, Park SS, Freiheit T (2006) Investigation of the dynamics of micro end milling—Part I: model development. *J Manuf Sci Eng* 128(4):893–900
17. Câmara MA, Campos Rubio JC, Abrão AM, Davim JP (2012) State of the art on micro-milling of materials, a review. *J Mater Sci Technol* 28:673–685
18. Filiz S, Conley C, Wasserman M, Ozdoganlar O (2007) An experimental investigation of micro-machinability of copper 101 using tungsten carbide micro-end mills. *Intl J Mach Tools Manuf* 47:1088–1100
19. Atkins AG (2003) Modelling metal cutting using modern ductile fracture mechanics: quantitative explanations for some longstanding problems. *Intl J Mech Sci* 45:373–396
20. Astakhov VP (2005) On the inadequacy of the single-shear plane model of chip formation. *Intl J Mech Sci* 47(11):1649–1672
21. Altıntaş Y, Lee P (1996) A general mechanics and dynamics model for helical end mills. *CIRP Ann—Manuf Technol* 45(1):59–64
22. Altıntaş Y, Jin X (2011) Mechanics of micro-milling with round edge tools. *CIRP Ann—Manuf Technol* 60:77–80
23. Dornfeld D, Lee D-E (2008) *Precision manufacturing*. Springer, New York
24. Pham DT, Dimov SS, Popov KB, Elkaseer AMA (2008) Effects of microstructure on surface roughness and burr formation in micro-milling: a review. In: *Proceedings of the 3rd virtual international conference on innovative production machines and systems (IPROMS)*, pp 270–275
25. Rainford Precision, Kern Ultra and Nano Precision Machining Centres. Available: <http://rainfordprecision.com/kern/>, 26 Feb 2016
26. Desarollo, Micromilling (2009) Available: <http://www.micromanufacturing.net/didactico/Desarollo/micromilling/1-6-micromilling-applications>, 27 Sept 2015

Chapter 5

Micro-waterjet Technology

Massimiliano Annoni, Francesco Arleo and Francesco Viganò

5.1 Introduction to Waterjet Technology

The intuition to use a high velocity water stream to clean surfaces or cut various materials was developed in the middle of the XX Century. The inspiring natural phenomenon of water erosion is artificially accelerated and concentrated for industrial applications.

In the 1950s, forestry engineer Norman Franz experimented to cut lumber with an early form of pure waterjet cutter (PWJ). In the 1970s Mohamed Hashish created a technique to add abrasives to the main water jet, thus creating the Abrasive waterjet technology (AWJ).

Many types of water jets have been developed during these years, including pure water jets, abrasive water jets, percussive water jets, cavitation jets and cryogenic jets. The reason why waterjet technology (WJ) has encountered an always growing success is the fact that it is a simple, versatile and flexible machining tool.

A general overview on WJ technology is given in this Chapter. Then the focus is moved on the actual technology development trend, called micro-AWJ, enhancing WJ towards fine features machining on small size parts.

M. Annoni · F. Viganò (✉)
Manufacturing and Production Systems, Mechanical Engineering Department,
Politecnico di Milano, Milano, Italy
e-mail: francesco.vigano@polimi.it

F. Arleo
WatAJet S.r.l., Legnano, Milano, Italy

5.2 High Energy Fluid Jet Generation

Waterjet is one of the most powerful and versatile machining technologies if compared to all the high energy fluid jet ones, as reported by Axinte et al. [1].

The physical phenomenon underlying WJ technology is the conversion of a water flow pressure energy into a high-velocity water beam kinetic energy. This conversion is performed by the capillary restriction of a tiny orifice, through which the water flow passes. Once the jet is formed, downstream the orifice, it is driven directly towards the workpiece (PWJ) or it is mixed with fine abrasive particles (AWJ) to enhance its cutting power in case of tough materials machining.

The equipment needed to generate the jet is described in this Section by following the water flow, from the supplying network to the machining zone, as shown in Fig. 5.1.

5.2.1 High Pressure Pump

In the pumping system the water pressure is raised from network supply pressure up to the working pressure (p_{water}). The system is composed by the following components:

- Low-pressure circuit, which is powered by an oil volumetric pump. The typical working oil pressure (p_{oil}) is set at 20 MPa.
- High-pressure circuit, which is powered by the water pump, fed by the oil coming from the low-pressure circuit (3).

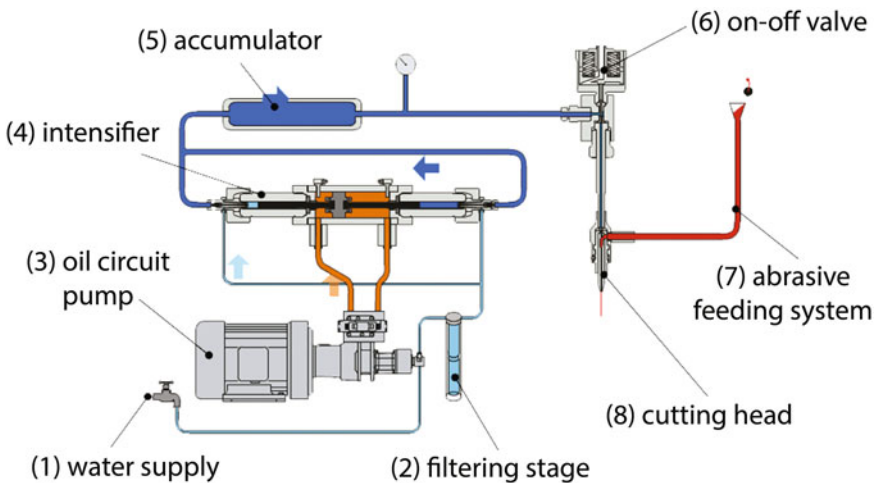


Fig. 5.1 Waterjet machining system general layout (courtesy of Ingersoll-Rand)

The oil acts on the primary piston surface (A_{oil}), pushing it forward and backward. A secondary piston with smaller section (A_{water}) is connected to the primary one. The water pressure is increased proportionally to the ratio between the areas of the primary and secondary piston.

For instance, a ratio of 20:1 with an oil circuit at 19 MPa allows to reach 380 MPa in the high pressure circuit, according to the relationship shown in Eq. (5.1)

$$p_{water} = p_{oil} \cdot \frac{A_{oil}}{A_{water}} \quad (5.1)$$

Two types of water pressure intensifiers (4) exist: single effect and double effect intensifiers. In the double effect ones, the primary piston has two active strokes, pressurising water alternatively with the left and with the right motions. In the single effect intensifiers, each piston has just one active stroke. Therefore, three or more pistons operate in parallel in order to maintain p_{water} as constant as possible.

When a double effect pump is used, its alternative motion produces fluctuations in p_{water} . An accumulator (5), like a tank with a capacity around 2 l, is needed in order to damp the pressure oscillations and maintain the downstream circuit pressure quite constant. In case of single effect pumps, an adequate phasing of the single piston strokes allows obtaining less pressure fluctuations. The accumulator is not needed in this case.

Standard pumps are usually applied also in the case of micro-AWJ. Moreover, the pump is not stressed in micro applications due to the low flow rate required by the small orifices employed (Sect. 5.2.4).

5.2.2 High Pressure Circuit

The pressurised water flow is carried from the high pressure pump to the machining area by means of a specific pipeline. All the pipes and the junctions are made of solid stainless steel, strengthened by the *autofrettage* treatment before the use at ultra-high pressure.

Filters and sensors are located along the pipeline in order to respectively avoid pump and cutting head components damage due to particles and to monitor the actual pressure along the line. Additional water treatment plants are usually employed especially when water hardness is over a limit declared by the pump builder. Small orifices used in micro-AWJ require such water treatments in order to avoid orifice clogging.

An on-off valve (6) is placed immediately upstream the cutting head (8), to hold or release the pressurised water flow. This device is constituted by a metal pin that closes or opens the water discharge orifice when moved by a pneumatic actuator.

5.2.3 Handling System and Fixturing

The piping end side near the cutting head has usually a small diameter to be more flexible and allow the head to freely move in the machining area. The handling system where the cutting head is mounted can have from 2 to 5 axes and can be based on a cartesian or an anthropomorphic arm structure, depending on the specific customer needs. The precision of these handling systems, measured as positioning repeatability, can range from 0.1 to 0.004 mm. This increasing precision is inversely proportional to the machining area dimensions and the handling system axis number. Nevertheless, it is directly proportional to the volumetric compensation effectiveness and to the overall machining centre price.

Handling systems for micro-AWJ machines usually apply linear motors or high precision recirculating-ball screws and are equipped with glass scales on the linear axes.

Large workpieces are usually simply placed on the working table without any fixtures because their own weight is enough to keep them in position during machining operations. Nevertheless, when the workpiece is particularly little or lightweight, like in micro applications, it is necessary to fix it to the main pool frame by means of clamps and side references in order to prevent any drift or vibration. However, the fixturing procedure is flexible for all the specific needs (Fig. 5.2).

5.2.4 Energy Conversion

The energy conversion is performed by the capillary orifice housed in the component usually called “primary orifice” or “primary nozzle”, shown in Fig. 5.3. The core of this component is a small and hard stone (usually sapphire or synthetic

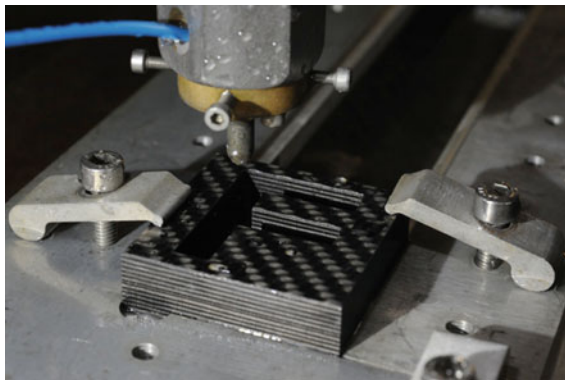


Fig. 5.2 Fixturing equipment for small parts at WJ_Lab of Politecnico di Milano. A main frame and a sliding bar sustain the part over the pool and locate it according to the machine reference system. The part is fixed to the frame by means of a suitable clamp positioning, which does not occupy the machining trajectory

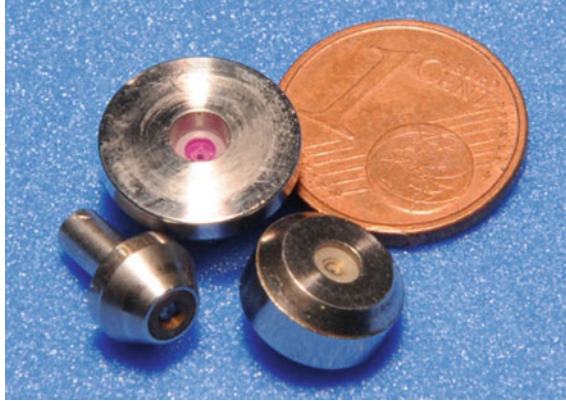


Fig. 5.3 Primary orifices for WJ applications

diamond) pierced by laser and finished by ultrasonic technologies. The capillary characteristic diameter ranges from \varnothing 0.33 to \varnothing 0.05 mm, but it is usually equal to \varnothing 0.10 or \varnothing 0.05 mm in case of micro-waterjet.

The highly pressurised water flow passes through the capillary and is accelerated according to the following Eq. (5.2):

$$v_j = c_v \cdot \psi \cdot \sqrt{\frac{2 \cdot p_{\text{water}}}{\rho_0}} \quad (5.2)$$

where v_j is the resulting jet speed, c_v is the velocity coefficient ($c_v = 0.75\text{--}0.85$), ψ is water compressibility coefficient ($\psi = 0.97$ for $p_{\text{water}} = 300$ MPa), p_{water} is the water flow pressure and ρ_0 is water density.

The hydraulic power P , required to generate a high-speed water jet through an orifice, must be maximum (related to the pump system) to improve productivity. Equation (5.3) shows the link between the jet hydraulic power P and the primary orifice diameter d_o :

$$P = \frac{c_d \cdot \pi \cdot d_o^2 \cdot \sqrt{2} \cdot p_{\text{water}}^{3/2}}{4 \cdot \sqrt{\rho_0}} \quad (5.3)$$

The adimensional discharge coefficient c_d is related to the localized energy loss in the primary orifice, therefore it often ranges between 0.65 for thin and sharp-edged capillaries and 0.75 or more for large and round-edged capillaries.

5.2.5 Machining Mechanism and Cutting Heads

In PWJ (Fig. 5.4, left), the jet generated by the primary orifice directly hits the workpiece surface. The jet core and its surrounding part made of droplets are able to

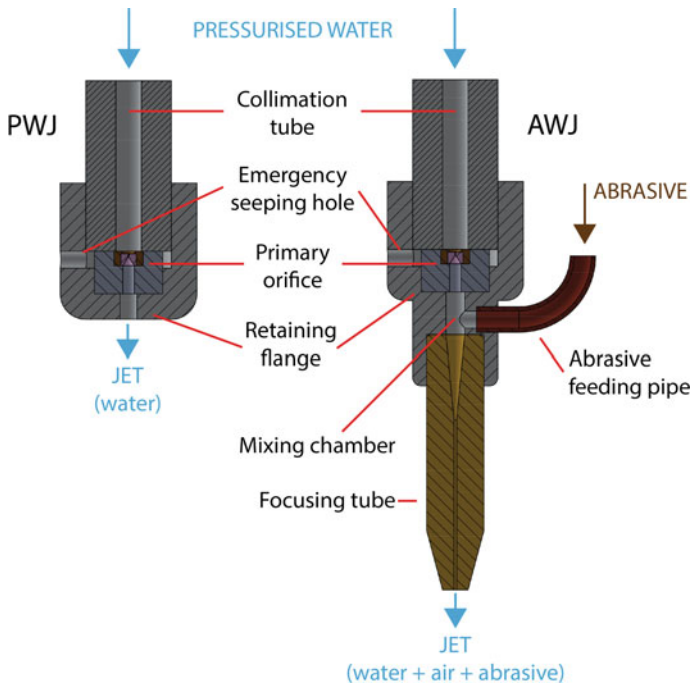


Fig. 5.4 PWJ and AWJ cutting head comparison

locally remove the target material, thanks to their high momentum. Since the jet is a high energy beam, the macroscopic effect is similar to the action of a cutting wire, cutting the workpiece and moving along complex trajectories.

The just described PWJ solution is suitable for soft materials machining, e.g. rubber, polymeric foils and foams, thin plywood or food. When tough materials machining is needed, abrasive sands are added to the main water stream to enhance the jet cutting power. In AWJ (Fig. 5.4, right), the water momentum is transferred to the abrasive particles, which become microscopic cutting tools. Therefore, the material removal process is dominated by erosion and abrasion mechanisms.

5.2.6 Abrasive Feeding System

Disposable abrasive particles are the machining tools of AWJ machining. This is an advantage in comparison with other technologies because tool wear issues make no sense in this case. After machining, particles are just collected in a catcher under the cutting head. The main particles properties are:

- homogeneous size,
- no hygroscopicity,

- high density,
- high hardness,
- no dust, in order to avoid clogging.

Typical *mesh* number used in standard applications are #80 and #120. The latter is used when a better roughness is required. Micro-AWJ needs fine grains, thus typical *mesh* numbers in this case range from #200 to #350. Fine abrasives like these ones imply serious problems of transportation to the cutting head because of their tendency to clog when not perfectly dry. In addition, the small abrasive mass flow rates used in micro-AWJ applications require specific feeding systems and piping.

The common types of used abrasive are garnet, olivine and aluminium oxide. Garnet is used for its good cutting properties and low price. It has also a very low hygroscopicity, which allows it to be used in wet applications. Olivine is required for applications where very smooth surfaces are required, but it is also characterized by high powder content. Aluminium oxide is instead characterized by higher hardness compared to the other types of abrasive, but it is not widely used, due to its high price.

5.2.7 *Catcher*

After the jet performs its material removal action, some residual energy must be managed downline of the workpiece together with the produced chip and the worn abrasive. A water tank is located under the entire machining area to damp the residual energy and to catch the solid particles. Since this water is significantly polluted by slurry and chip powder, it is not possible to re-use it for processing. Therefore, dirty water and slurry are separately collected and dumped according to the local standards about industrial wastes. Sometimes it is convenient to recycle abrasives. Nevertheless, in micro-AWJ the waste management is a less relevant problem because of the very low abrasive mass flow rates required, as pointed out in Table 5.2.

5.3 AWJ Quality Assessment

Several parameters have to be managed in WJ technology to achieve the desired quality and productivity performances. Since AWJ technology is the most complex, an Ishikawa diagram drawn on this configuration by Annoni and Monno [2] (Fig. 5.5) is exhaustive for the whole WJ panorama, even for micro applications.

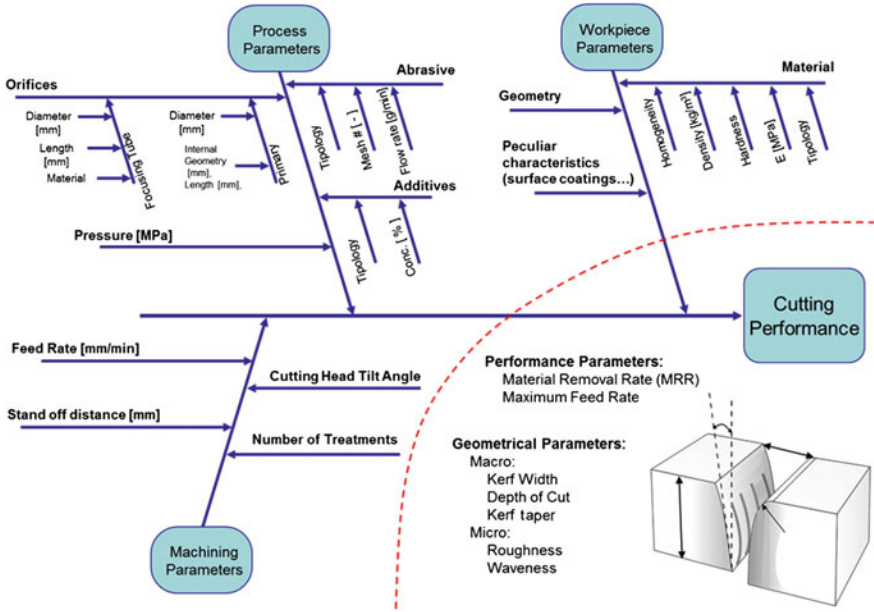


Fig. 5.5 AWJ Ishikawa diagram

The diagram highlights three parameter families (i.e. process, workpiece and machining parameters) to assess the cutting performance. Table 5.1 shows indicative values for a conventional AWJ machining centre. The machining parameter on which manufacturers often act is the *feed rate* (v_f). For this reason, next to the possible process parameters, Table 5.1 shows an ordinary v_f choice for a given configuration.

Table 5.1 AWJ indicative process parameters and v_f levels

Conventional AWJ process parameters		Indicative v_f levels
p_{water} (MPa)	80–600	AWJ configuration: p_{water} : 380 MPa d_0 : 0.33 mm d_f : 1.02 mm
Q_{water} water flow rate (l/min)	1.0–2.5 Depending on primary orifice diameter	
d_0 primary orifice diameter (mm)	0.10–0.25 (PWJ) 0.25–0.33 (AWJ)	Abrasive size: #80 mesh Q_{abr} : 350 g/min Workpiece thickness: 1 mm
d_f focusing tube \varnothing (mm)	0.76–1.20	
l_f focusing tube length (mm)	76–120 ($100 \cdot d_f$)	Fe alloys: 800 mm/min Al alloys: 2400 mm/min Ti alloys: 1200 mm/min Carbon fibre: 3000 mm/min
Abrasive type	Garnet, Olivine, Alumina	
Abrasive size [mesh (μ m)]	#80 (250)–#120 (74)	
Q_{abr} abrasive mass flow rate (g/min)	100–400	
Machining area	Usually 2000 by 4000 mm	

Some of these parameters are discussed in the following Sections. In general, it is possible to monitor most of those parameters before or during the cutting operation. It is also possible to control some of them in order to compensate the WJ typical defects or several unpredicted events.

5.3.1 Machining Defects Description

Typical AWJ defects can be identified by some macro-scale and micro-scale geometrical parameters.

The cutting depth strictly depends on p_{water} , v_f and Q_{abr} . A cutting depth at least equal to the workpiece thickness is needed. The component wall roughness at microscopic level depends on the abrasive characteristics (i.e. type, mesh) and it is usually set before the working campaign and never changed during machining operations.

Instead, other three defects (*kerf waviness*, *kerf taper* and *jet lag*) deserve a deeper analysis because they can be managed and varied even during the single machining operation.

AWJ machined parts show some irregularities in the kerf surface lower zone. This first type of defect is usually called “*waviness*” (Fig. 5.6, bottom view) because it is a macroscopic low-frequency deviation from the nominal part wall. The imperfect jet behaviour is caused by its progressive energy loss when cutting deep in the workpiece and it is highlighted by a v_f increase or an inhomogeneous material structure.

The second typical AWJ defect is the formation of an undesired workpiece wall slope, called “*kerf taper*” (Fig. 5.6, front view). This defect is measurable for example by observing a test-cut and comparing the top (W_{top}) and the bottom (W_{bot}) kerf width.

The jet energy loss along the workpiece thickness causes also the cutting front backward bending respect to the cutting direction (Fig. 5.6, side wall). This third kind of defect is called “*jet lag*” and it is measurable for example by comparing the average striation inclination respect to the jet vertical direction.

5.3.2 Defect Reduction Methods

All the defect reduction methods share a common approach: after performing some preliminary tests on the target material, thus understanding the specific material behaviour, the machining parameters are adapted for the working task.

The simplest way to reduce the typical AWJ defects is to globally lower the imposed v_f , especially at the corners or where fine features have to be machined. This strategy is commonly applied on 3 axes machines by the CAM software. Therefore, the jet has enough time to machine the part in its whole thickness,

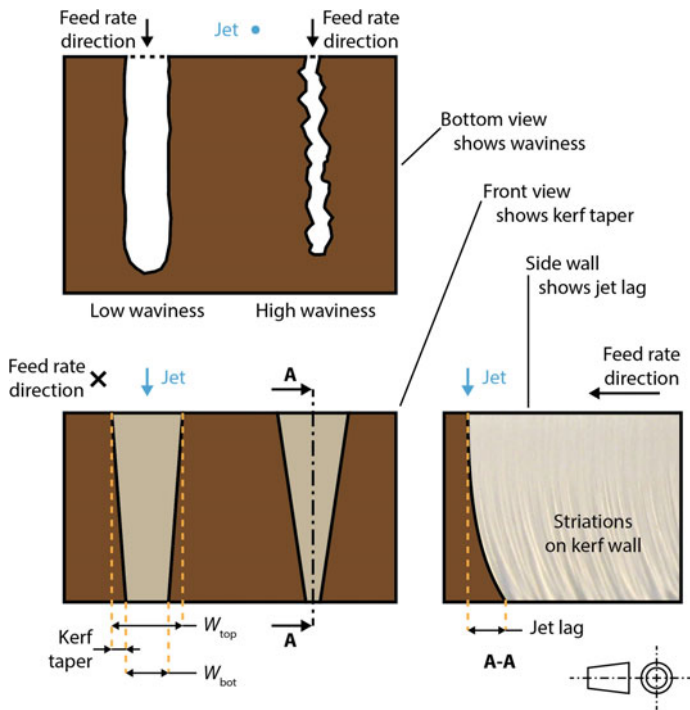


Fig. 5.6 Typical AWJ defects (defects are amplified for clarity). W_{top} and W_{bot} are the top and bottom kerf width

according to the required wall quality. Nevertheless, this approach significantly affects the overall process productivity and can not effectively work on high thickness workpieces (e.g. more than 15 mm).

Several scientific and industrial studies propose suitable defect compensation solutions by exploiting more advanced handling systems and correction algorithms.

Hoogstrate [3] applied the defect compensation strategy by managing simple geometrical parameters as the 5 axes cutting head tilt angles. The cutting head is tilted to compensate the unwanted wall slope deriving from the *kerf taper* (Fig. 5.6, front view). The cutting head is also tilted forward along the feed direction to compensate the *jet lag* (Fig. 5.6, side wall). The use of the CAD-CAM tools enables the new machines to use geometrical models that take into account the jet behaviour and apply compensation strategies even in case of curved geometries, as reported by Westkämper et al. [4].

Several studies concerning circular parts compensation have been published, like the ones by Matsui [5] and Hlaváč [6], obtaining valuable results in terms of *kerf taper* and *jet lag* defect reduction through cutting head tilting.

On the basis of this scientific and industrial background, the Waterjet Laboratory of Politecnico di Milano (WJ_Lab) has implemented this kind of geometric compensation strategies to reduce the defects occurrence on the target components, as shown in Fig. 5.7.

The industrial validity of these strategies, actually offering valuable performances, is confirmed by some patents (e.g. FLOW[®] Dymanic Waterjet[®] [7] and OMAX[®] Tilt-A-Jet[®] [8]) and by the increasing diffusion of 5 axes systems with integrated compensation.

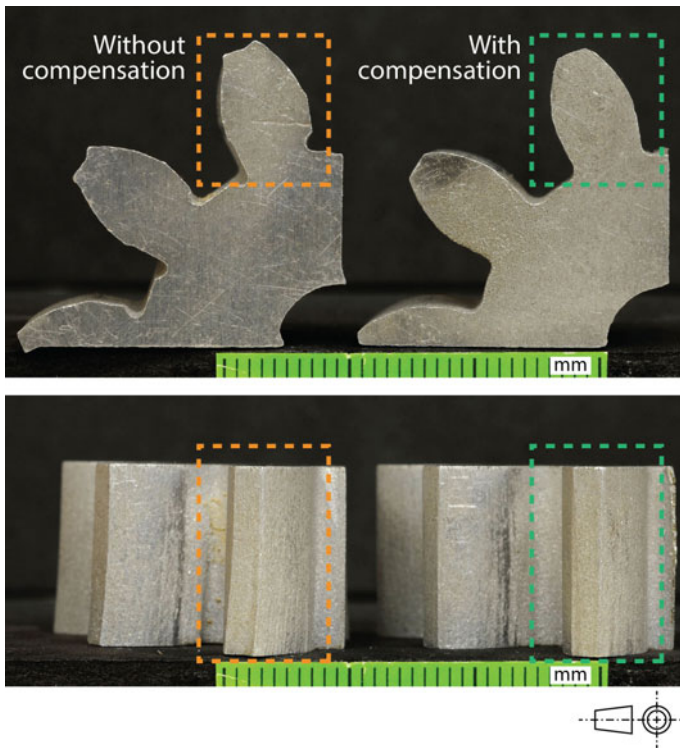


Fig. 5.7 Defect compensation on a complex shape obtained at WJ_Lab of Politecnico di Milano. Different approaches are compared: the first one simply uses the X-Y-Z linear axes (without compensation) whilst the second exploits the two additional rotary axes to tilt the cutting head, thus reducing the defect (with compensation)

5.4 Micro-AWJ Technology

Although quality, flexibility and performance characteristics of conventional AWJ are valuable, a lower limit to the achievable feature dimensions and surface finish depends on its typical jet and abrasive dimensions. An additional limit in terms of machined part precision is introduced by the huge conventional machining centre dimensions. Therefore, a progressive jet downsizing has been performed towards a tool able to machine fine features, still preserving the Waterjet process distinctive advantages. Enhanced precision can be obtained first of all by designing smaller machining areas and using more accurate handling systems, thus going down to 0.004 mm positioning repeatability and lower, as mentioned before and therefore approaching near-net-shape machining.

To distinguish this configuration from conventional ones, the downsized AWJ solution is usually called micro-AWJ. Its key features do not depend only on working area dimensions and handling system accuracy. The micro-AWJ most relevant features are discussed in the following Paragraphs.

5.5 Micro-AWJ Key Features

Since the micro-AWJ plant general layout is pretty similar to the conventional one, this technology is often identified as the downsized version of AWJ. Key components are similar, but several issues arise because of the significant downscaling and the need for enhanced machining precision. Table 5.2 shows the main micro-AWJ features. Some of them are discussed more in detail hereafter.

Table 5.2 Micro-AWJ indicative process parameters and v_f levels

Micro AWJ process parameters		Indicative v_f levels
p_{water} (MPa)	80–380	Micro-AWJ configuration: p_{water} : 380 MPa d_o : 0.10 mm d_f : 0.30 mm Abrasive size: #220 mesh Q_{abr} : 70 g/min Workpiece thickness: 1 mm Fe alloys: 200 mm/min Al alloys: 600 mm/min Ti alloys: 260 mm/min Carbon fibre: 800 mm/min
Q_{water} water flow rate (l/min)	0.3–0.8 Depending on primary orifice diameter	
d_o primary orifice diameter (mm)	0.05–0.10	
d_f focusing tube \varnothing (mm)	0.20–0.30	
l_f focusing tube length (mm)	20–30 ($100 \cdot d_f$)	
Abrasive type	Garnet, Olivine, Alumina	
Abrasive size [mesh (μm)]	#200 (74)–#350 (44)	
Q_{abr} abrasive mass flow rate (g/min)	10–80	
Machining area	Up to 800 by 800 mm	

The primary orifice and the focusing tube diameters are significantly smaller than the AWJ ones. The importance of the cutting head components alignment becomes a pressing need because even a little energy loss or an elliptical jet cross section may cause severe effects on the cutting power and to the part dimensional precision. Therefore, the cutting head component machining must be performed using standards and procedures deriving from high precision industrial fields like watchmaking. Precise component coupling guarantees a good alignment between the primary orifice, the mixing chamber and the focusing tube axes.

Another arising issue is linked to the abrasive feeding system. In conventional applications a hopper equipped with a discharging hole is sufficient. A dedicated feeding system is needed in micro-AWJ in order to manage low mass flow rates of fine abrasives. Discharging belt abrasive feeders, like the ones designed by Allfi and applied by Daetwyler on *microwaterjet*[®] machines, are often used in this applications. This solution avoids the abrasive clogging due to particle arching on small holes and allows managing the mass flow rate by tuning the belt speed. In addition, fine abrasives are exposed to clogging also in the feeding pipes and in the mixing chamber due to their hygroscopicity. Refined abrasives with low dust content are used and drying operations are performed before machining to avoid clogging and cutting operation failures.

The low water and abrasive flow rates cause a cutting power reduction. Therefore micro-AWJ machining cannot be effectively performed on thick parts. As an indicative value, 20 mm of steel can be machined using the Ø 0.3 mm focusing tube configuration described in Table 5.2. In any case, the suggested v_f levels are significantly lower than the ones currently used in conventional AWJ machining.

5.5.1 *Micro-AWJ Enabling Characteristics*

WJ technology, and in particular micro-AWJ, can compete on equal footing with both well-established and non-conventional technologies for near-net-shape parts machining. Some micro-AWJ enabling characteristics are summarized in Table 5.3 to give an overview on the technology and to allow making comparisons with the other ones available.

Since micro-AWJ is a fast evolving technology, the academic and industrial R&D continuously overcome the limits reported in Table 5.3. For instance, the arduous control in milling-like operations does not allow obtaining finished part by micro-AWJ, thus making a finishing operation by conventional milling necessary. This issue could be overcome in the very near future, when an advanced jet power and orientation control will be implemented.

Table 5.3 Micro-AWJ enabling characteristics

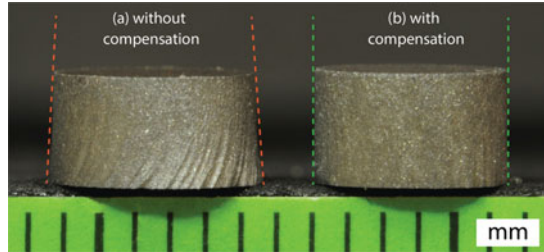
Micro-AWJ enabling characteristic	Value/description
Machinable materials	Almost everything, if an abrasive harder than the target material is selected. Garnet (8 Mohs) is suitable for most applications
Allowed operations	Cutting and piercing Surface cleaning and <i>decoating</i> , engraving, rough milling
Tool setup	Single tool (the jet) for all the allowed machining operations
Cutting thickness	Up to 20 mm on Fe alloys. Over this value, the cutting quality decreases and the machining time becomes prohibitive
Minimum feature size	Sharp edges and thin walls (down to 0.1 mm) can be achieved. The jet radius defines the lower concave feature dimension. Using a \varnothing 0.20 mm focusing tube, the resulting kerf width ranges from 0.23 to 0.28 mm
Workpiece setup	A simple fixturing is needed to face the small lateral forces generated by the jet (usually less than 1 N). Fixturing systems must prevent part damages produced by their uncontrolled detachment from the original sheet. Bridges are often programmed along the tool path to keep the small parts in position till the cut completion
Workpiece size	Depending on the machining area, up to 800 by 800 mm
Thermal/chemical affections	Negligible. Some metals like carbon steel can oxidise because of the wet environment
Mechanical affections	Negligible. The jet gently works on the material without inducing high mechanical stresses apart from a slight residual compression on the surface
Compliance with tolerances	Down to 0.004 mm, depending on the handling system precision and jet stability
Surface roughness	Down to 500 nm Ra, depending on the abrasive size and v_f

5.6 Micro-AWJ Case Studies

Some case-study parts are presented in this Section in order to discuss some interesting micro-AWJ characteristics through challenging materials and features. The described parts have been machined using the \varnothing 0.3 mm and the \varnothing 0.2 mm focusing tube configurations at WJ_Lab of Politecnico di Milano [9] and at WatAJet S.r.l. [10], a WJ_Lab spin-off.

5.6.1 Precision Through Defect Compensation

The typical AWJ defects discussed in Sect. 5.3.1 severely affect the machined part precision when operating at high v_f , even in micro-AWJ non compensated cutting (Fig. 5.8a). It is possible to compensate the main defects by tilting the cutting head angles according to the strategies reported in Sect. 5.3.2.



Material	p_{water}	Abrasive	Jet diameter	Tolerance
Ti 6Al 4V thickness = 3 mm	300 MPa	Garnet #200 mesh	Ø 0.3 mm	± 0.05 mm on diameter

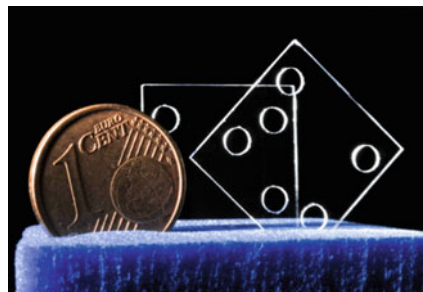
Fig. 5.8 Comparison between non compensated and compensated parts made with micro-AWJ (WJ_Lab)

In the specific case of Fig. 5.8, the difference between the top and the bottom diameters is 0.40 mm in the first cylinder (Fig. 5.8a) and it is reduced to 0.02 mm in the compensated one (Fig. 5.8b), working at the same v_f .

Through geometric compensation strategies it is therefore possible to obtain near-net-shape parts without reducing the v_f and thus preserving productivity.

5.6.2 Thin Layers Drilling

Brittle materials piercing is often a challenging operation, especially on very low thickness parts, because it is very easy to scratch or crack them. The squares shown



Material	p_{water}	Abrasive	Jet diameter	Tolerance
Quartz thickness = 0.7 mm	100 - 300 MPa	Garnet #200 mesh	Ø 0.3 mm	± 0.05 mm on diameter

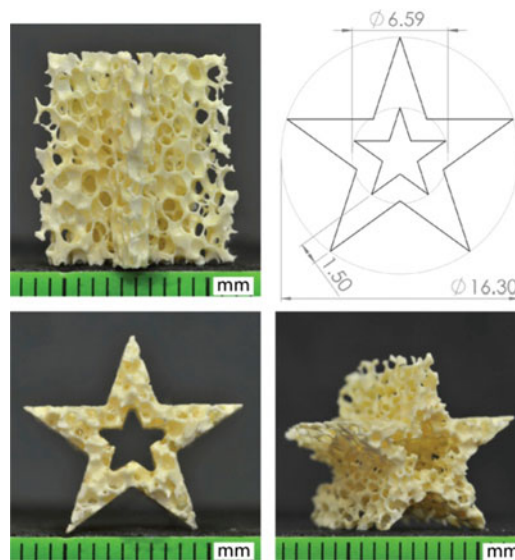
Fig. 5.9 Thin quartz piercing (WJ_Lab)

in Fig. 5.9 are made of 0.7 mm thick quartz, through which four holes are drilled. Before machining, the workpiece is covered with a polymeric adhesive foil to preserve the surface from accidental scratching and to limit unwanted vibrations. This protection also damps the jet impact at the initial impingement, thus allowing the actual part being machined by micro-AWJ.

5.6.3 Inhomogeneous Materials

Inhomogeneous materials are intrinsically hard-to-machine because of the quick alternation of regions characterized by significantly different mechanical properties. Ceramic sponges are an extreme example of this kind of materials.

A complex shape part is machined in order to demonstrate the micro-AWJ cutting valuable performances in terms of precision and delicacy on inhomogeneous materials. The presence of both convex and concave corners in the star shown in Fig. 5.10 makes it a challenging geometry to machine, even using diamond wires or ultrasonic machining.



Material	p_{water}	Abrasive	Jet diameter	Tolerance
Ceramic sponge thickness = 15 mm	300 MPa	Garnet #200 mesh	\varnothing 0.3 mm	\pm 0.05 mm on profile

Fig. 5.10 Illustrative geometry on 40 PPI (pores per inch) alumina-zirconia ceramic sponge (WJ_Lab)

A specifically developed pore filling procedure is needed in this case. After incorporating the base material in ethylene-vinyl-acetate, the part is cut and then unfilled. Micro-AWJ proved to be effective in machining both the sharp edges of the outer profile and the fine corners of the inner one, preserving a 1.5 mm thick wall on a 15 mm thick ceramic sponge. The *kerf taper* and *jet lag* defects are reduced by suitably selecting the machining parameters (especially v_f) as shown by the side-view picture. Since the five sharp edges are parallel, it is demonstrated that the *kerf taper* and *jet lag* defects are negligible.

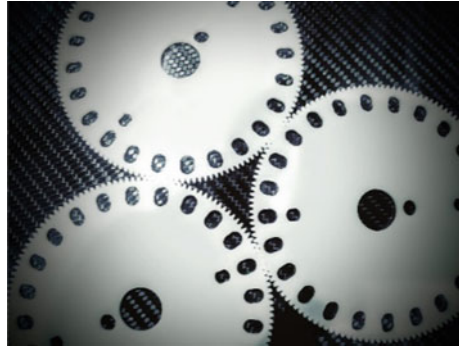
5.6.4 Advanced Alloys for Biomedical Applications

Special alloys for advanced applications in biomedical field need high erosive power from the micro-AWJ jet, provided along with an extreme dimensional precision (tight tolerances). Therefore the cutting head handling system precision must be enhanced as well as the reliability and the repeatability of the jet dimensional characteristics. For instance, the system available at WatAJet S.r.l. allows to meet the tight tolerances required by the component shown in Fig. 5.11, performing the entire drilling and cutting programme with a single jet in a time interval that is 20 times smaller than the one required by EDM technology, direct competitor of micro-AWJ in these applications.



Material	p_{water}	Abrasive	Jet diameter	Tolerance
Grade 5 Titanium alloy thickness = 3 mm	340 MPa	Garnet #230 mesh	Ø 0.3 mm	0 / +0.03 mm on hole diameter

Fig. 5.11 Prosthesis support made of Grade 5 Titanium alloy for BBG S.r.l. (WatAJet S.r.l.)



Material	p_{water}	Abrasive	Jet diameter	Tolerance
POM thickness = 3 mm	350 MPa	Garnet #230 mesh	Ø 0.2 mm	0 / +0.018 mm on hole diameter

Fig. 5.12 Gearwheels machined for ARCA S.r.l. (WatAJet S.r.l.)

5.6.5 Thin Details Cutting on POM

Gearwheels machining for banknote counters like the ones shown in Fig. 5.12 need to meet very tight tolerances also on polymeric base materials. Thin details must be machined using the finest jets available (in the specific case, a Ø 0.2 mm jet is used, since it is the finest achievable nowadays with micro-AWJ).

5.6.6 Stainless Steel Racks Small Batch

The reduced thickness of the component shown in Fig. 5.13 makes fine die cutting suitable for this task. Nevertheless, a small-batch prototyping phase may be useful to test the component, before spending a huge amount of money and resources to create the final die. Micro-AWJ can machine a small-batch series with the same characteristics expected from fine die.

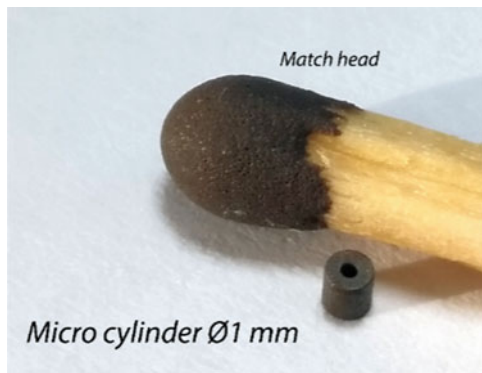
5.6.7 Deep Holes with Tight Tolerances

Micro-holes drilling on sintered metal brings state-of-the-art micro-AWJ technology to its limit. The subsequent external cylindrical profile cutting completes the machining sequence of the component shown in Fig. 5.14, which is a micro-magnet



Material	p_{water}	Abrasive	Jet diameter	Tolerance
Stainless steel thickness = 0.6 mm	320 MPa	Garnet #220 mesh	Ø 0.3 mm	± 0.02 mm on coupling features

Fig. 5.13 Racks for automotive applications (WatAJet S.r.l.)



Material	p_{water}	Abrasive	Jet diameter	Tolerance
Sintered metal (magnetic steel) thickness = 1 mm	340 MPa	Garnet #230 mesh	Ø 0.2 mm	± 0.006 mm on hole diameter

Fig. 5.14 Micro-magnet for step motors (WatAJet S.r.l.)

for step motors A machining strategy divided in two rounds, exploiting suitable adhesive tapes to sustain the components, makes possible to obtain the net-shaped part without any need of additional machining operations.

References

1. Axinte DA, Karpuschewski B, Kong MC, Beaucamp AT, Anwar S, Miller D, Petzel M (2014) High energy fluid jet machining (HEFJet-Mach): from scientific and technological advances to niche industrial applications. *CIRP Annals-Manufacturing Technol* 63(2):751–771
2. Annoni M, Monno M (2000) A lower limit for the feed rate in AWJ precision machining. International conference on water jetting, in BHR group conference series publication, vol 41. Professional Engineering Publishing, Bury St. Edmunds, pp 285–296
3. Hoogstrate AM (2000) Towards high-definition abrasive waterjet cutting—a model based approach to plan small-batch cutting operations of advanced materials by high-pressure abrasive waterjets. Delft University of Technology, TU Delft
4. Westkämper E, Henning A, Radons G, Friedrich R, Ditzinger T (2000) Cutting edge quality through process modeling of the abrasive waterjet. *CIRP, Proceedings of 2nd CIRP international seminar on intelligent computation in manufacturing engineering (ICME)*, Capri, Italy
5. Matsui S (1991) High precision cutting method for metallic materials by abrasive waterjet. *Jetting Technology*
6. Hlaváč LM (2009) Investigation of the abrasive water jet trajectory curvature inside the kerf. *J Mater Process Technol* 209:4154–4161
7. “Flow Dynamic-Waterjet”, patented technology by Flow International Corporation [Online]. Available at: <http://www.flowwaterjet.com/Cutting-Heads/Dynamic-Waterjet> 4 Dec 2015
8. “OMAX Tilt-a-jet” patented technology by OMAX Corporation [Online]. Available at: <https://www.omax.com/accessories/tilt-a-jet> 4 Dec 2015
9. WJ_Lab Laboratory web page on Department of Mechanical Engineering Department—Politecnico di Milano website, [Online]. Available at http://tecnologie.mecc.polimi.it/water_jet_lab_en.htm 4 Dec 2015
10. WataJet S.r.l. company website, showing applications, performances and services, [Online]. Available at: <http://www.watajet.com> 4 Dec 2015

Chapter 6

Micro-electro-Discharge Machining (Micro-EDM)

Francesco Modica, Valeria Marrocco and Irene Fassi

6.1 Principle of Electro-Discharge Machining (EDM)

Electro discharge machining (EDM) is one of the most widely used non-conventional technologies for the manufacturing of electro-conductive materials. The contactless nature of this technology avoids mechanical stresses, chatter and vibration problems: this characteristic makes it suitable to machine materials of high strength and hardness. The functioning principle is based on the concept of the electrical erosion. A series of discrete electrical discharges occurs in between two electrodes, the tool and the workpiece, both immersed in a dielectric fluid. During discharging, the electrical energy is turned into thermal energy [1]. The thermal energy generates a channel of plasma between the cathode and anode [2], at a temperature ranging between 8000 and 12,000 °C [3], or as high as 20,000 °C [4]. This mechanism initialises a substantial amount of heating and melting of materials at the surface of each electrode. When the pulsating direct current supply occurring at the rate of approximately 20–30 kHz is turned off, the plasma channel breaks down [5]. Part of the removed material evaporates, whilst another part forms the debris particles which are removed by the dielectric fluid usually kept in motion during machining [6].

Recently, a version of this process has been implemented for micro-scale [7]. The main differences between macro and micro-EDM are essentially due to the energy densities, the temperatures and the tool dimensions involved in the process. In macro-EDM process, the voltage generator responsible for the electrical

F. Modica (✉) · V. Marrocco · I. Fassi
Institute of Industrial Technology and Automation,
Consiglio Nazionale delle Ricerche, Milan, Italy
e-mail: francesco.modica@itia.cnr.it

V. Marrocco
e-mail: valeria.marrocco@itia.cnr.it

I. Fassi
e-mail: irene.fassi@itia.cnr.it

discharges is a switch-like one: the generator is connected to the electrodes by a switch. When the switch is closed, the generator supplies the potential difference to the electrodes; when the switch is open, the electrical discharge can take place. In this condition the achievable pulse energy value is around 1 μJ .

In micro-EDM, generally, a relaxation type (RC circuit) generator is used. In this case, the energy is stored in capacitors, which determine the maximum possible energy released in the sparking gap existing between the tool and the workpiece through the electrical discharge. In micro-EDM processes, the available energy can be of the order of few nJ, hence three order of magnitude smaller than the energy provided in macro-EDM. The capacitances of the RC pulse generator can be tuned in order to regulate the desired pulse energy in dependence on the type of machining: for instance, when small pulse energy featuring high local energy density is required, the capacitances must be reduced. Furthermore, the temperature in a micro-EDM process ranges between ~ 4000 and $\sim 50,000$ $^{\circ}\text{C}$. Finally, the tool electrode dimension and polarity are key factors to take into account in micro-EDM machining: generally, the tool diameter varies from 1 mm down to 0.005 mm and its polarity is usually set to negative, whilst for macro-EDM, the diameter is in the order of few mm and the polarity is set to positive.

The versatility of the micro-EDM is well represented by the possibility of implementing different approaches (Fig. 6.1): wire, sinking, milling and drilling. In dependence on the design of the part and feature to produce, their required accuracy and the materials, the user can choose the best approach or a combination of some of them. To this aim, Sect. 6.5 reports some examples of micro-EDM versatility of using and combining micro-EDM approaches.

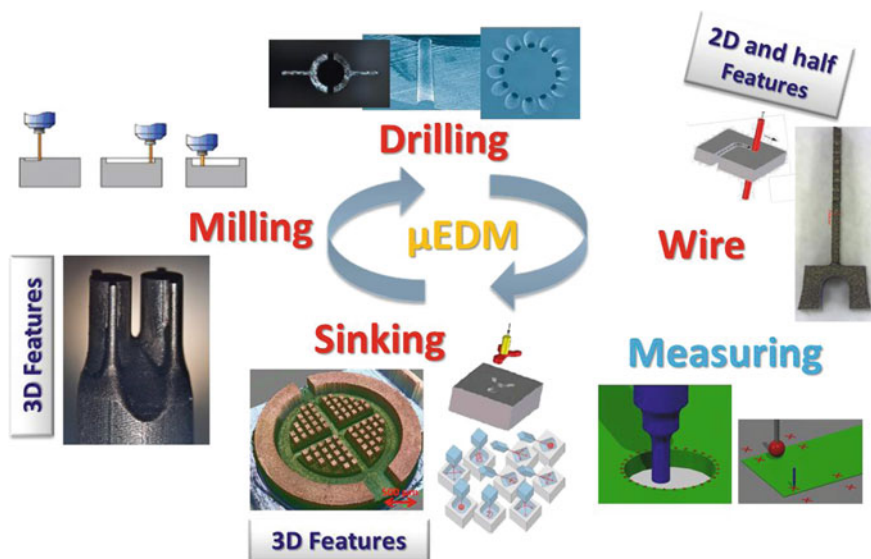


Fig. 6.1 Micro-EDM approaches and applications

In micro-wire EDM approach, the tool consists of a wire, usually made of brass, having a diameter ranging from 0.3 mm to 0.02 mm. The wire rolls between two rotating reels: one is in charge of the feeding and the other one is used for wrapping, so that, during a process, the tool is always renewed. The workpiece is mounted on the spindle and then located in proximity to the wire. This technique is typically employed to fabricate dies, mechanical parts or to re-shape tools. It is worth stressing that the main limitation of this approach is the limited geometries which can be fabricated (2D and half).

Die-sinking is characterised by reduced machining times compared to other EDM approaches and it is usually preferred when complex shapes have to be fabricated. Nonetheless, this approach requires a former operation before the die-sinking process can be performed. In fact, the tool electrode must be “dressed” or reshaped according to the mirror image of the final feature. After this step, the dressed electrode is “sunk” into the workpiece and the electrical discharges can proceed to remove material and imprint into it the shape of the feature.

Drilling EDM approach is generally preferred to the conventional drilling technique for producing holes when hard-to-machine materials are involved or to produce micro-holes with a high aspect ratio. The use of simple tubular or cylindrical micro-tools makes drilling capable of better controlling some dimensional characteristics during machining, such as the hole tapering. The tapering is the effect describing the reduction of the hole section along its depth occurring during machining. This effect is mainly due to tool wear (see Sect. 6.3.3 for details) and cannot be completely avoided. However, due to its ease of implementation and reasonable machining times, this technique is widely used in industry.

Micro-EDM milling is the most versatile approach, since it allows to manufacture features having complex and 3D geometries and to have a better control of dimensional and surface accuracy of the final components. These advantages are provided by the type of tool electrodes, which are simple tubular or cylindrical rods. The micro-EDM milling implementation is executed using a layer-by-layer strategy, i.e. the material is removed in various step, set by the layer thickness. This value is properly chosen taking into account the machining regime, i.e. the discharge energy involved in the erosion process. The tool electrode is forced to follow a path, defined within a CAD-CAM environment and conceived to limit tool wear and reduce dimensional errors. Although the complex geometries manufacturing performance provided by such approach is apparently superior than the others, micro-EDM milling industrial use is currently very limited: in fact, the main drawback of this approach is the exponential growth of machining times checked as the feature complexity and required accuracy increase.

6.2 Micro-EDM Process Parameters

Though very simple in principle, the way to obtain an optimised micro-EDM process is still a hot topic for the research community working in this field. The process is characterized by a random nature which adds some unpredictability to the manufacturing process. The first step to approach a micro-EDM manufacturing is the appropriate selection of process parameters: this choice is primarily imposed by the workpiece and tool electrodes materials. Once the feature and the final dimensional and surface accuracy have been decided, it is mandatory to set the energy value involved in the erosion process, which determines the machining regime. Distinct regimes are generally considered: roughing, semi-finishing, finishing and eventually, fine-finishing. The lower the energy value is, the slower the process: the latter condition usually ensures a high dimensional accuracy and good surface roughness.

The energy value involved in a micro-EDM process can be set in different ways, depending on the specific micro-EDM machine. Some of them allow direct setting of the capacitor values of the relaxation type generator. Others consider some index values which are indirectly linked to the capacitors values of the relaxation type generator. For instance, Sarix SX 200 HP allows the setting of an index E, energy, followed by a number (365, 110, 100, 15, 13). The highest number selects a switch-like generator, actually, and provides an energy density suitable for roughing machining. The smallest values indicate the selection of the relaxation type micro-EDM generator. The E index is in charge of limiting the maximum energy density available during the process, along with the maximum voltage and current values.

In micro-EDM, two types of voltage have to be distinguished: the first is the open voltage (often indicated as V_o , see Fig. 6.2), which refers to the voltage applied by the micro-EDM generator to the electrodes. The second is the discharge voltage (V_d , Fig. 6.2), which refers to the voltage recorded during the spark occurring between the electrodes. The current parameter I limits the maximum available current value occurring during a spark. More frequently, for micro-EDM this parameter can be regulated by acting on other process parameters and usually only after a measurement, the actual I value can be known. For SARIX SX 200 HP machine, the parameter I is an index, but other EDM machines report directly the ampere value. I index does not have direct correspondence to the discharge current (I_d , Fig. 6.2) measured during a micro-EDM process.

Another important process parameter is the pulse width W, often also called t_{on} or delay time, which is the time interval the micro-EDM generator is supplying the tool and the workpiece (see table in Fig. 6.2).

Frequency F is the parameter required to set the occurrence of micro-EDM generator pulses. The inverse value of frequency defines the total time interval in which a spark can take place ($1/F = t_{on} + t_{off}$).

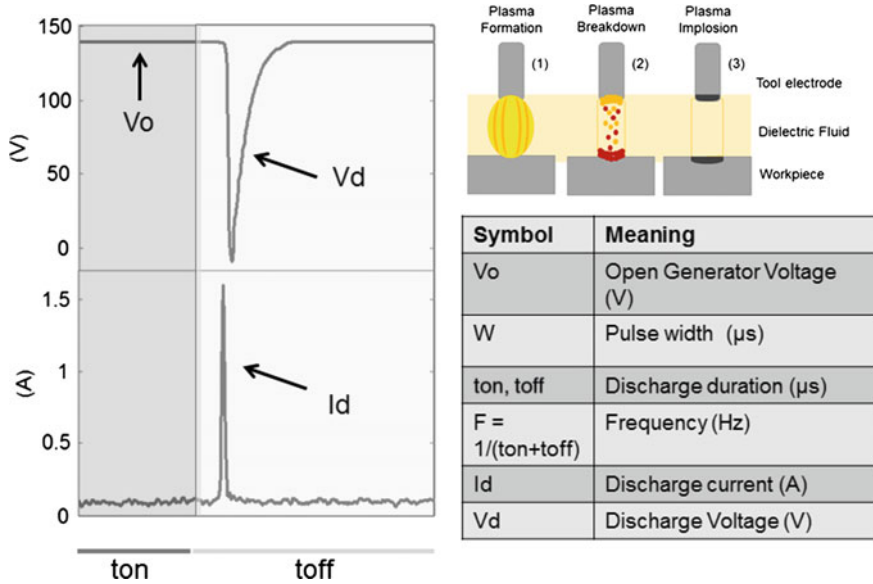


Fig. 6.2 Example of voltage and current waveforms during a micro-EDM milling process on hardened steel are reported. Micro-EDM process is summarised in the following steps: plasma formation 1, plasma breakdown 2, plasma implosion 3. The table shows the main process parameters common to all micro-EDM machines

The electrode polarity in micro-EDM is generally set in the following fashion: the tool is negative (-) and the workpiece is positive (+). This choice is due to the main issue linked to micro-EDM technology: tool wear. Several works underline that the material removal process is more massive onto the positive electrode rather than onto the negative one.

Other important parameters are generally taken into account through the servo control loop system which is specific to each micro-EDM machine, such as feed rate, and tool rotational speed.

Figure 6.2 reports also a sketch of the whole erosion process, along with the main process parameters and voltage and current waveforms.

In order to achieve process stability and obtain the desired feature accuracy, other settings and physical phenomena must be taken into account [8, 9]. To this aim, the choice of the dielectric fluid providing the flushing is a key factor. The dielectric fluid is fundamental to increase the energy density locally during the erosion process and to remove the molten material from the working zone. Generally, hydrocarbon oil is used. However, depending on the materials involved in the process or for safety and environmental considerations, deionized water or compressed air (such as in the case of dry-EDM) can be also considered as good alternatives to hydrocarbon oil, though the resulting surface quality of the machined parts is not as good as that obtained using hydrocarbon oil.

The tool rotation speed is a parameter which can be properly set to accomplish an uniform wearing of the tool during machining and assist the debris removal. Debris removal from the working zone is an important issue since, if this mechanism is non-effective, it may induce a local deposition of conductive particles, which can cause the occurrence of multiple harmful discharges, thus producing process instability and inaccuracy of the final features.

Finally, several physical phenomena and chemical reactions must be taken into account due to the temperature increase occurring during a micro-EDM process: among these, layer recast (caused by the re-deposition of particles onto the workpiece surface) and the heat affected zone (where the homogeneity and surface of the workpiece have been modified by increasing temperature) can affect the erosion process, and, in the worst case, impede the discharge occurrence.

6.3 Performance of the Micro-EDM Process: Quality Indices

The machining performance is usually estimated through the evaluation of specific quality indices:

- Material Removal Rate (MRR), defined as the ratio between volume of material removed from the workpiece and the erosion time
- Tool Wear Ratio (TWR), defined as the ratio between tool wear volume and volume of material removed from the workpiece
- Surface roughness (R_a)
- Dimensional accuracy: estimated as difference between nominal feature dimension and real machined feature.

In order to have a clear glance of how manufactured surfaces of different materials may look like, Scanning Electron Microscope (SEM) images of surface quality after different micro-EDM processes are illustrated as examples in the following figures.

Figure 6.3 shows the micro-EDM surface related to a nozzle machined in hardened steel. The overlap of the craters is visible, especially in Fig. 6.3b, where a magnification of the cavity wall is shown. In this case, the machined surface is considered relatively homogeneous.

Figure 6.4 reports an example of a pillar machined within a cavity using a ceramic composite, $\text{Si}_3\text{N}_4\text{-TiN}$ (the characteristics of this material will be provided in detail later on in Sect. 6.4). In this case, a very low energy is used during the process. Generally, lower energy ensures good surface quality when metals are machined in identical process conditions, but this image witnesses something different: surface quality is worse for the conductive ceramic composite. The reason is mainly due to the material composition, since this composite material is not electro-conductively homogenous and its grains have different sizes.

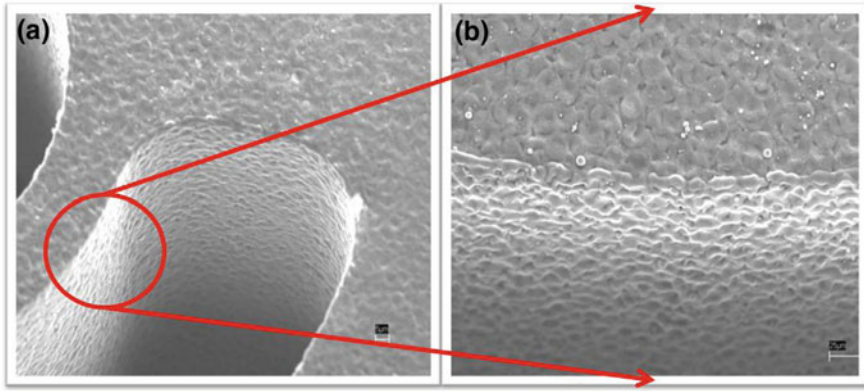


Fig. 6.3 SEM images of nozzle machined in hardened steel via micro-EDM milling. **a** Section of the nozzle; **b** magnification of the inner side of the nozzle cavity

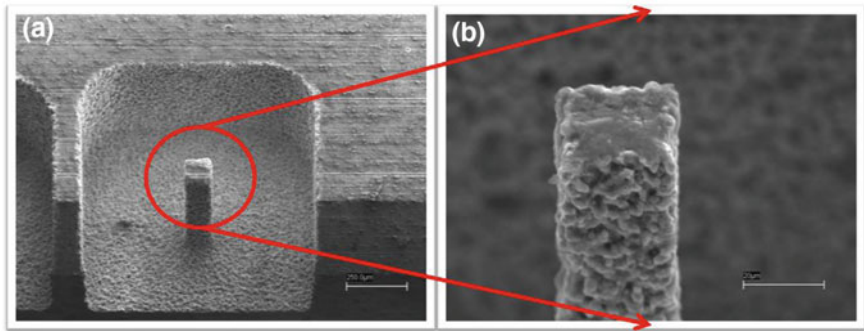


Fig. 6.4 SEM images of pillar machined in ceramic composite ($\text{Si}_3\text{N}_4\text{-TiN}$) via micro-EDM milling. **a** Pillar machined in a cavity; **b** magnification of the pillar

The reported examples shed the light on the variability of the micro-EDM process performance and surface quality, underlining that the assessment of the process parameters must be done by experimentations. Once the materials and features are set, trials are undertaken by varying process parameter values to proceed to the evaluation of the machining performance. Different approaches can be then used to analyse the data resulting from experiments.

Yu et al. [8] presented the results coming from the experiments done varying some process parameters in micro-EDM milling of slots. The analysis done putting in straight relation MRR, TWR, surface roughness and discharge gap with the process parameters suggests that great attention must be devoted to voltage and micro-EDM generator capacitance.

Different sets of experiments have been also proposed by Pellicer et al. [9]. The study has been carried out using artificial neural network and regression models to evaluate micro-dimensional and geometrical accuracies. In this work pulsed current, open voltage, ton and toff have been varied. The workpiece is H13 steel and different shaped copper electrodes have been used.

6.3.1 *Micro-EDM Milling Optimisation via Design of Experiments (DoE)*

An example of micro-EDM milling process optimisation in terms of MRR and TWR, Ra and depth error has been carried out by Modica et al. [10] considering: a SARIX SX 200 HP micro-EDM machine, a workpiece made of hardened steel where micro-channels, 5.5 mm long, 0.42 mm wide and 0.05 mm deep have been manufactured; a cylindrical rod tool electrode made of Tungsten Carbide (WC) having a nominal diameter of 0.4 mm and negative polarity. The tool and the workpiece are constantly bathed by a dielectric hydro-carbon oil, which guarantees the flushing during machining.

The parameter settings chosen for the experimentations are:

- Energy level E100 corresponding to finishing regime selected to ensure low surface roughness; this parameter has been kept constant for all trials. The experimental plan has been then implemented by means of Design of Experiments (DoE) [11, 12]. For the experiments, the process parameters have been varied considering two values, minimum and maximum per each:
- Pulse width W , $W = 1\text{--}4 \mu\text{s}$;
- Open voltage V , $V = 100\text{--}140 \text{ V}$;
- Frequency F , $F = 120\text{--}200 \text{ kHz}$;
- Current I , $I = 100\text{--}140$ (index).

The DoE provides a number of trials to be performed according to the number of process parameters and their variation: in this case, a full factorial plan has been selected considering 4 process parameters, each ranging between two values. Each trial is also replicated 3 times, thus ending up in 48 experiments executed in random order. At the end of the experiments, the machining performance have been evaluated: Table 6.1 reports the minimum and the maximum average values estimated at the end of the trials.

Table 6.1 MRR, TWR, Ra minimum and maximum average values resulting from the three replica

Quality index	Min-max values
MRR (mm^3/min)	0.0161–0.0165
TWR	0.1954–0.1981
Ra (μm)	0.12–0.15
Depth error (μm)	0.1–1.6

At the end of the experiments, all quality index values resulting from each trial can be put in relation to the process parameters using statistical approaches (in the present case the ANOVA, Analysis of Variance), in order to investigate the effects induced by the process parameters variation on the quality indices and also to determine which parameter has more influence on machining performance with respect to another. The statistical optimisation is completed when the best process parameter combination giving back the highest value of MRR and the lowest of TWR, Ra and depth error is identified by means of statistical indicators [11].

6.3.2 Monitoring for Evaluating Micro-EDM Performance

Recent works offer novel approaches to evaluate micro-EDM performance: in particular the monitoring of the discharge voltage and current waveforms during experiments can be usefully exploited to provide detailed measurements and new insight about the material removal process.

During process monitoring of discharge voltage and current waveforms, it is important to discriminate among their type: it is mandatory to identify which of them can be labelled as “good or detrimental” for a micro-EDM process. To this aim, a pulse discrimination strategy is frequently implemented in order to gather voltage and current waveforms into different categories. An exhaustive study concerning micro-EDM monitoring and implementation of a pulse-type discriminating system has been proposed by Liao et al. [13]. The presented pulse classification is capable of discriminating discharge voltage and current waveforms as normal, effective arc, transient short circuit and complex. Normal pulses are considered good, since they are controlled by micro-EDM generator and are characterised by the maximum achievable energy available for a spark. The other categories do not depend on the micro-EDM generator, but rather on the random nature of the process and on local conditions eventually promoting sparking. These latest pulses can occur randomly and occasionally, and, for this reason, they may affect the machining performance. The selection of pulse type in [13] is accomplished by setting voltage thresholds and considering the pulse duration. Some experiments conducted during micro-wire-EDM and micro-EDM milling considering a steel workpiece have shown that normal pulses are the most frequent. However, the pulse-type distribution tends to vary when, for instance, the feature depth is increased, and complex pulse types appear and start to influence the process.

Another pulse discrimination strategy has been presented by Yeo et al. [14]. In this work, the experiments focus on the micro-EDM of holes in steel alloy considering a rotating electrode. The pulse types are classified in a slightly different manner with respect to the previous case (normal, delayed, arc and short) and their identification has been done by using current thresholds set after the direct

observation of the acquired gap voltage and current waveforms. The study and the results coming from the pulse type analysis allowed the authors to determine the proper electrode movement direction and to develop an adapting electrode feed rate accordingly.

The pulse type distribution of micro-EDM milling during the manufacturing of micro-channels in hardened steel has been analysed by Modica et al. [15]. Compared to the previous works, the pulse discrimination strategy reported in this work is based on different thresholds, set on both voltage and current. The pulse type are gathered as normal, arc, delayed and short pulses, as suggested in [14]. One of the main result of this study shows that the process instability is underlined by a higher number of arcs occurring during a machining and that the arcing is strictly dependent on sparking gap, erosion speed and feed rate variation. Moreover, a higher number of arcs seems to induce an increase of TW; on the contrary, MRR does not seem to be affected by any means by the frequent occurrence of arcs.

A similar analysis involving $\text{Si}_3\text{N}_4\text{-TiN}$ ceramic alloy workpiece is reported in Marrocco et al. [16], where parameters as frequency F , pulse width W and gap G are varied. An experimental plan is implemented by means of Design of Experiments (DoE) in order to analyse statistically the relation existing among process parameters, machining performance (MRR, TW and surface roughness R_a) and pulse type distribution. In this study, the workpiece material plays a crucial role since unexpected results have been found: indeed, pulse types which are generally considered potentially harmful and undesirable during a micro-EDM milling process seem to have no detrimental effects and, on the contrary, seem to aid MRR.

6.3.3 Tool Wear and Tool Path: How to Obtain Surface and Profile Accuracy in Micro-EDM Features

The key to achieving good surface and dimensional accuracy of the machined features is the control and reduction of some sources of errors. The most common sources of errors in micro-EDM are:

- The positioning of the tool and the workpiece, which also affects repeatability of the process and measurements
- Tool dressing, which also comprises temperature stability error, variation due to sparking gaps, fix and fixtures
- Tool run-out, induced by the rotation of the tool; this error influences the effective tool diameter value and hence the accuracy of final features
- Tool wear: the melting and evaporation mechanisms induce a modification of the tool shape, thus varying the tool section and the working length during machining.

Tool wear has attracted particular attention by the research community and it is acknowledged as one of the most important issues to manage in the micro-EDM process. During machining, the electrode tool wears modifying its length and

section and, consequently, the actual depth and dimension of the features are far from being similar to the design.

Tool wear compensation strategies are required to overcome this problem. Among others, the uniform wear method (UWM) [17, 18], is the most popular one used for wear compensation. UWM is based on some assumptions: the tool section wears in a constant fashion, preserving its original shape, and side erosion of the tool electrode is negligible. Hence, the tool undergoes only a shortening during the process. To this aim, a tool feeding along Z axis (vertical direction) is provided and determined after the estimation of the worn length. This tool feeding for compensation is done in relation to the specific tool path, which is conceived to keep a constant tool section during the wearing process. However, since UWM operates according to a layer-by-layer machining strategy, this compensation can be applied only to micro-EDM milling. Moreover, to guarantee the erosion stability and have good effect on flushing condition, the use of thin layers is usually recommended.

In order to compensate the worn tool length, a measurement of this quantity is required. Typically, the tool length wear estimate is performed by an electrical control touch procedure [19, 20]. This procedure foresees that the tool and the workpiece may be short-circuited, after the machining of a set number of layers, in a specific point located onto the workpiece far from the working zone (control touch point). During the short circuit, the current measurement of the tool length is compared to the previous measurement; the difference between previous and current lengths provides the tool length consumption. The compensation is done according to this value. This “control touch” is frequently used, since the measurements can be directly done during machining. However, different experimental analyses show that despite the use of such compensation-based strategy, the final machined micro-features still suffer from remarkable geometrical inaccuracy. This means that UWM is not always effective. Hence, alternative solutions are proposed in literature considering, for instance, the role of a proper tool path implementation. Narasimhan et al. [21] reported a theoretical model where UWM is combined to specific tool paths generating a desired workpiece surface profile. The aim is to make the tool wear compensation suitable for the micro-EDM of 3D micro-cavities. Dimov et al. [22] modified the CAM system by including the variation of the layer thickness during tool wear compensation and Zhao et al. [23] developed a novel CAD/CAM system based on a slicing strategy aimed to reduce the residual vestige and accomplish smooth surface profile accuracy. Popov and Pektov [24] implemented and verified experimentally a method comprising a layer-based tool-path generator which considers slicing and changes in angle for every layer, in order to optimise the surface quality and edge definition. Nguyen et al. [25] proposed geometric models able to simulate and compensate the effects induced by corner radius variation caused by tool wear.

All the results and efforts made to cope with the tool wear issue stress that an effective compensation strategy requires a reliable estimation of the worn tool. The material volumes involved in this mechanism are very small and therefore difficult to measure. Hence, alternative approaches and methodologies have been proposed in literature. For instance, an optical measurement of the tool wear is reported by

Yan et al. [26]. The tool wear compensation method suggested by the authors is based on the direct measurement of the front tool wear using the image-processing technique. Aligiri et al. [27] proposed a real time estimator of the material removal volume for micro-EDM drilling of micro-holes having different depths and machined in different materials (stainless steel, titanium, and nickel alloy).

The monitoring of the discharge pulses and their analysis and discrimination have been also exploited by several authors to estimate tool wear and compensate it in a more accurate way [28]. In particular, the detection and counting of pulse discharges may be used to estimate TW, as underlined by Bissacco et al. [29] which investigated in this point of view several energy levels in micro-EDM milling, or by Mahardika and Mitsui [30], who focused on tool wear estimate when the spindle rotation and tool electrode vibration are considered.

6.3.4 High Aspect Ratio Cavities: Role of Tool Wear and Dielectric Flushing

The fabrication of micro-features with high aspect ratio (AR) still represents a challenge in micro-manufacturing. Micro-EDM drilling and milling approaches are suitable to overcome the technological limits of conventional top down approaches.

The most simple high aspect ratio features are micro-holes. Micro-holes are frequently affected by tapering, which is due to tool wear and also caused by random discharges induced by the presence of debris which are not well removed by dielectric flushing. An extensive experimental analysis proposed by Wang et al. [28] explored the relation between dimensional accuracy of micro-holes as a function of micro-holes depth: the attention of the authors fell on the hard-to-manage removal of the debris which caused the occurrence of multiple discharges at higher depths. As already said, the local concentration of debris promotes the arcing, so that several unpredictable and undesired discharges can happen due to favourable conditions to spark ignition. Since arcing cannot be controlled, instability of the erosion process, increase of tool wear and dimensional inaccuracy are the predictable outcome of such event. As the dielectric flushing seems to fail when the tool is operating at significant depths, the debris removal can be then aided applying other methods, such as ultra-sonic vibration machine (USM) [31, 32]).

Micro-EDM milling of high aspect ratio micro-slots have been reported by Karthikeyan et al. [33] and Puranik and Joshi [34]. The experimental investigations show a remarkable dependence of MRR and tool wear on some electrical parameters (energy, feed rate, tool speed) and AR values: in particular, less optimised performance are obtained when AR is high (>1.5).

In a recent paper by Modica et al. [35], another geometrical parameter has been put in evidence along with AR: the fill factor (FF-ratio between electrode section and cavity section). The study is about the micro-EDM milling of high aspect ratio

cavities characterized by different FF and AR. The evaluation of MRR and TWR, along with the effect of the tool wear compensation factor and erosion time, show that the machining performance deteriorates according to the combined effect of AR and FF, which both influence the dielectric flushing and the debris removal. Therefore, the machining of very large cavities can result in good process stability and performance. The machining of small cavities report permanent critical machining condition: small cavity with high depth implies generally difficult flushing and multiple discharges affecting the process. However, despite this instability, the manufacturing of the smaller cavities exhibit good MRR and TWR. On the contrary, the intermediate case (cavities with medium FF) shows a different scenario as the machining depth is increased, reasonably due to the changes of the flushing condition and appearance of multiple discharges in the last part of the machining.

6.4 Materials and Effects on Micro-EDM Process

The micro-EDM process requires that the materials acting as electrodes must have good electro-conductivity, and as such, metals are typically used. However, for certain applications such as those in hostile environments, medical fields, aeronautics, other materials are deployed, such as ceramics. These materials exhibit excellent mechanical properties such as high hardness, high compressive strength, chemical and abrasive resistance. However, ceramics are semiconductors, so that EDM cannot be easily applied to machine them, due to their low electrical conductivity. This limit has been overcome by using an additional electro-conductive phase [36].

In order to express the concept, we consider for instance two common ceramic materials: sintered SiC and B₄C. Their electrical resistivity are 0.05 and 0.01 Ωm, respectively. In theory, these values are feasible for EDM machining, the practice is otherwise, though. Luis et al. [37] show that sinking EDM of such materials is very difficult due to the troublesome flushing conditions and cooling issues. Silicon carbide (SiC) is an extremely hard and difficult-to-shape engineering ceramic material. However, since this material is extensively used in industry because of its superior mechanical properties, wear and corrosion resistance even at elevated temperature, free Si is usually infiltrated in SiC in order to improve the conductivity of the matrix and make EDM process easier. Clijsters et al. [38] developed a die-sinking EDM technology for manufacturing components in a commercial available silicon infiltrated silicon carbide (SiSiC). In the work, the influences of the major operating EDM electrical parameters on the MRR, TWR and Ra are examined, and the results show that process parameters providing lower energy may improve the surface quality.

In principle, the second electro-conductive phase allows all types of micro-EDM machining. Among the additional phases, TiN is the most frequently used to obtain the following composites: ZrO₂-TiN, Si₃N₄-TiN, B₄C-TiB₂ [39].

Lauwers et al. [40] report experiments of EDM sinking and milling on SiC, B₄C and Si₃N₄-TiN. The results show that especially for ceramic materials with low electrically conductivity, such as SiC and B₄C, the performance of milling in terms of MRR and surface quality is much better. On the contrary, sinking EDM seems to be a faster technique than milling EDM when larger cavities are realised using Si₃N₄-TiN, which has a relatively high conductivity, though the surface quality is much poorer.

Other experiments presented by Liu et al. [41] demonstrate that higher content of TiN in Si₃N₄-TiN composites leads to higher MRR when processed using EDM. When micro-EDM is used to machine Si₃N₄-TiN composites, the correct selection of process parameters is crucial in order to have a stable process. Liu et al. [42] used the monitoring of discharge pulses to identify the process parameters which accomplish optimised machining performance considering different machining conditions (roughing, semi-finishing and finishing). In another work, Liu et al. [43] pointed out that the machining condition of Si₃N₄-TiN resembles that of hardened steel. Moreover, they noticed that the increase of some parameters such as voltage and current positively affects MRR and TWR and that the flushing using a hydrocarbon oil seems to be preferred to obtain a better performance in terms of surface roughness, since it reduces the intrinsic decomposition of the material.

6.5 Applications

6.5.1 *Straight Bevel Micro-gear*

An example of a product manufactured via micro-EDM milling is the Straight Bevel micro-gear. The component design and dimensions are illustrated in Fig. 6.5.

This micro-gear has been designed for a kinematic component of a robotic arm used in endoscopic surgery. Due to specific application in the medical field, the material proposed for the realisation of the component is titanium, which is characterised by high resistance, lightness and bio-compatibility. Commonly, bevel micro-gears are fabricated by adopting a wire-EDM approach, which provides dimensional accuracy and fine surface quality in a relative short machining time. However, for this component, wire-EDM approach is not suitable due to the angle of the primitive cone ($\delta = 100.94^\circ$) that prevents the use of wire as tool electrode. In this case the micro-EDM milling is the most appropriate approach for producing the gear teeth, since it is possible to realise the micro-features adopting a cylindrical micro-tool with reduced diameter. The diameter reduction is performed by wire-EDM.

Starting from a cylindrical workpiece and adequate stock allowance, each tooth of the gear is obtained by eroding the cavities following two operations (see Fig. 6.6). In the first operation (Op1 in Fig. 6.6) a cylindrical tool made of WC having a diameter equal to 0.4 mm is adopted without any section reduction. The energy level used in this operation is suitable for semi-roughing regime. Since

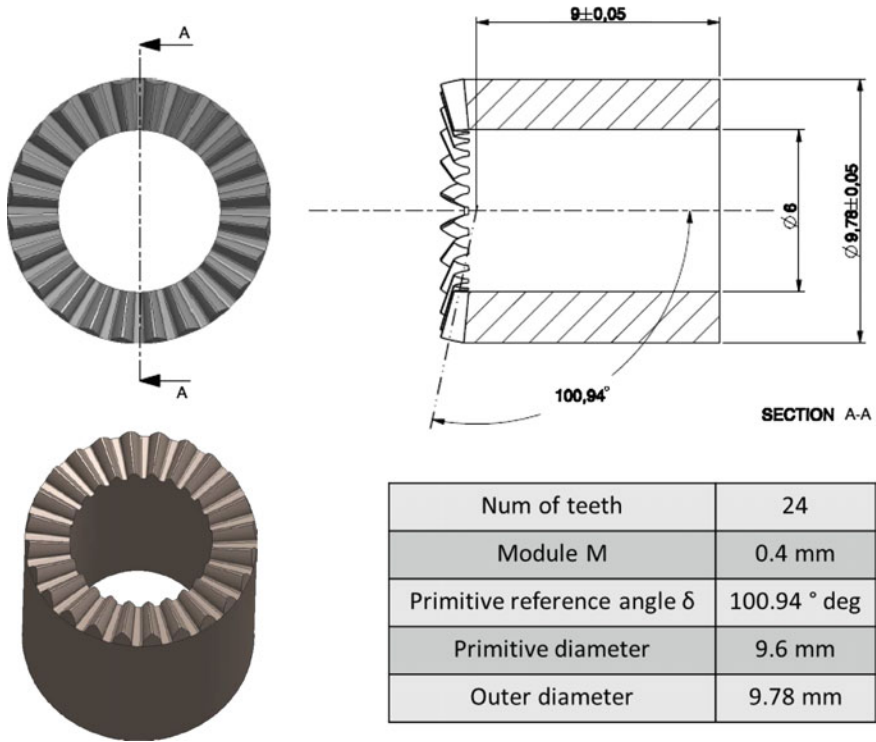


Fig. 6.5 Straight Bevel micro-gear: design and dimensions

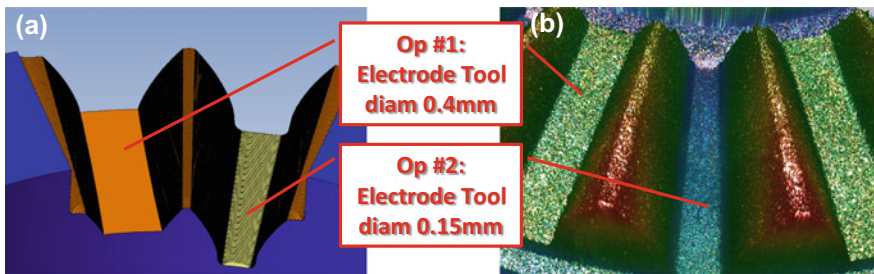


Fig. 6.6 Two operations with two machining parameters and electrode tool size have been adopted for machining the teeth: **a** simulation, **b** confocal acquisition of the machined cavities Straight Bevel micro-gear

micro-EDM milling is implemented via a layer-by-layer strategy, a layer thickness of 0.002 mm is chosen to ensure a smooth surface and avoid step-like effects. Taking into account the tool diameter, the erosion process is performed until a cavity depth of 0.71 mm is reached, where the distance tooth-to-tooth becomes too narrow for the selected tool.

Table 6.2 Main parameters adopted for the two micro-EDM operations and related MRR and machining time

Op.	Tool diameter	Machining regime	Layer thickness	MRR	Machining time
#	(mm)	–	(mm)	(mm ³ /min)	(min)
1.	0.4	Semi-roughing	0.0020	0.043	48
2.	0.15	Finishing	0.0012	0.006	66

The second operation (Op2 in Fig. 6.6) requires the use of a smaller tool diameter: in order to machine the narrower cavity floor and fillet radius at the tooth root, a tool of WC having a diameter of 0.15 mm is employed. The energy level set for this machining step guarantees a finishing regime. The layer thickness is equal to 0.0012 mm. The erosion of the cavities starts from a depth of 0.71 mm (reached by the previous operation Op1) and continues until the final tooth profile is completed at a depth of 1.032 mm.

Table 6.2 summarises the main parameters adopted for the two operations and their performance in terms of MRR and machining times.

A higher MRR is recorded after the first operation. The second operation performed with the smaller tool produces a smaller MRR value, taking into account that the machining time spent for this last step is higher than that recorded for operation 1. However, it must be underlined that since the two operations have been performed using two different machining regimes, different surface qualities are expected: in particular, $R_a = 0.9 \mu\text{m}$ for semi-roughing regime and $R_a = 0.6 \mu\text{m}$ for finishing regime, respectively. The difference in surface quality is minimal and it has been evaluated as acceptable by the end-user. The machining time for producing one single cavity is equal to 114 min, thus, by considering 24 cavities for obtaining 24 teeth, the total machining time spent to machine the whole gear is equal to 2436 min (46 h).

6.5.2 Customised Internal Fixation Devices for Orthopaedic Surgery

Micro-EDM can be successfully employed in the production of customised orthopaedic implants, such as internal mini-fixation devices. These devices are routinely used worldwide for fixation of bone fractures and non-unions, since they allow the force transmission from one end of the bone to the other, by-passing and thus protecting the area of the fractures. Mini-fixations hold the fracture ends together while maintaining proper alignment between the fragments throughout the healing process.

Since each person's anatomy is unique, a customised fixation plate can be more effective than a standard one. Their advantages include the reduction of invasive

surgery, choice of the most suitable bio-mechanical principle for each specific case, and increased comfort for the patient. Common characteristics and functionality of these components are:

- Two-and-half-dimensional shape: although some components present one or more curvatures, the contour can be obtained starting from a suitably bent plate as if the plate was flat. Additional curves can also be obtained after manufacturing, plastically deforming the plate by specific tools as described in some surgical applications.
- Holes for temporary and permanent device fixture: since bones and fractures are all unique, surgery requires flexibility for choosing and adjusting the device position. Thus, some holes are used for temporary device fixture, allowing the correct bone drilling for the permanent screws. Moreover, for better adaptation of the implant, some holes present a spherical housing at their top to allow the adjustment of the screw orientation ($\pm 10^\circ$) (Fig. 6.7).
- Bores for helping the assembling phase during the surgery and for lightening the device weight.
- Device thickness and overall dimensions can vary depending on bone and fracture sizes. Generally, the thickness can range between 1 and 3 mm, and, consequently, the screw diameter and hole sizes can be different.
- Bone plates are made of a variety of materials, but mainly stainless steel (ASTM F-55 and -56), cobalt chromium tungsten nickel alloy (ASTM F-90), pure titanium and one of its alloys (ASTM F-136). Recently, new materials, such as ceramics composite or techno-polymers, have been developed.

With suitable micro-EDM equipment, this technology can also accommodate the limitations imposed by the hospital environment. Considering the specific micro-feature to be machined, it is possible to choose a micro-EDM approach or a combination of different approaches to best fit the requirement of the final device and having reasonable machining times.

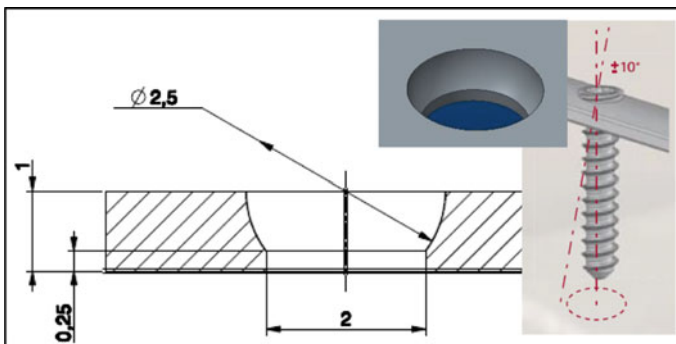


Fig. 6.7 Spherical housing for the orientation adjustment of the screw (dimensions are in mm)

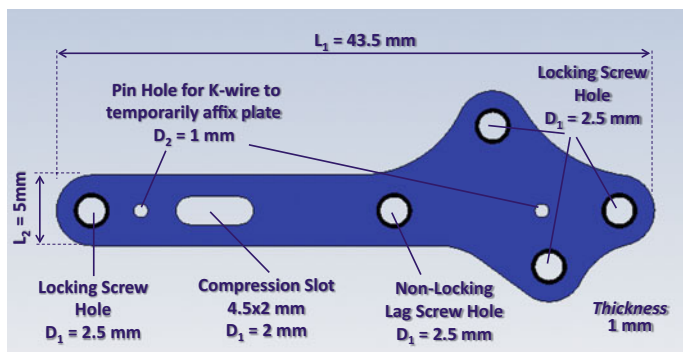


Fig. 6.8 Test case, fixation plate for fracture repair, osteotomy and arthrodesis in the foot

An example about how different micro-EDM approaches can be successfully employed to produce a customised fixation plate is presented by Modica et al. [44]. The test case component is shown in Fig. 6.8: it is a fixation plate inspired by a real component from Vilex (www.vilex.com), employed for fracture repair, osteotomy and arthrodesis of the foot. The component is made of surgical titanium. The design presents different features: four holes with a diameter of 2.5 mm for the permanent clamping, a non-locking lag screw hole having a diameter of 2.5 mm, two straight holes characterised by a diameter of 1 mm for temporary clamping and a compression slot (4.5 mm long and 2 mm wide).

Once the geometry is defined, it is necessary to develop a strategy for manufacturing. To this aim, some simple rules can be followed in order to reduce machining errors and times:

- Starting from a rectangular plate having the right thickness, a straight side of the plate can be used as reference for the drilling of holes. This reference allows an easier re-positioning between table and Z-axis.
- Where possible, wire-EDM and drilling-EDM are preferable to the slower milling-EDM approach.
- When an internal bore is machined via wire-EDM, it needs to drill true pre-holes; therefore, it is preferable to start with the drilling operation. This allows the geometric reference to be set for the workpiece repositioning.

The micro-EDM machine used is the Sarix SX200 HP, equipped with electrode tools having different materials and diameters in dependence on the micro-EDM approach. For milling operations, a WC cylindrical rod having a nominal diameter of 0.4 mm is used. The drilling operation have been performed using Cu cylindrical tube having a nominal diameter of 0.4 mm.

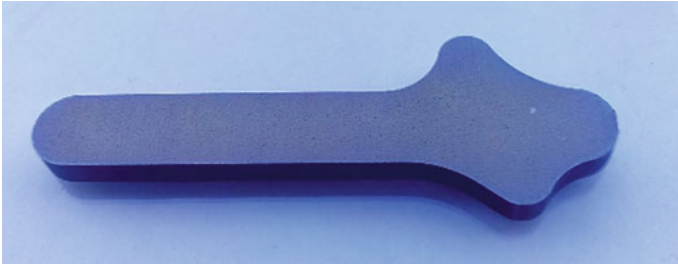


Fig. 6.9 Profile machined by wire-EDM

The test case can be machined according to the following steps:

1. The workpiece is clamped to the Z-axis and referenced to the machine coordinate system. The external profile having a perimeter of 54.53 mm is machined by wire-EDM (Fig. 6.9). Considering a process speed of 1.8 mm/min, the total operation time requires about 30 min.
2. The titanium plate is clamped to the machine table and referenced to the machine coordinate system. The drilling operation has been performed to machine 8 through holes, one for each cavity, with a diameter of 1 mm. The drilling operation of single hole requires one minute of machining, resulting in a total operation time of 8 min.
3. Milling-EDM is used for machining the spherical housing for the screw heads in five holes having diameter equal to 2.5 mm. Each machining operation requires 66 min per housing, resulting in a total operation time of 330 min (Fig. 6.10).
4. The workpiece is clamped on the Z-axis and referred to the machine coordinate system. The wire-EDM is adopted to machine the compression slot (with a perimeter of 13.28 mm). Considering a process speed of 1.8 mm/min, the operation time requires about 7 min.

The total machining time for manufacturing the test case is 375 min.

An evaluation of machining time for the same component made on $\text{Si}_3\text{N}_4\text{-TiN}$ ceramic composite has been also performed. Tests using wire-EDM approach have

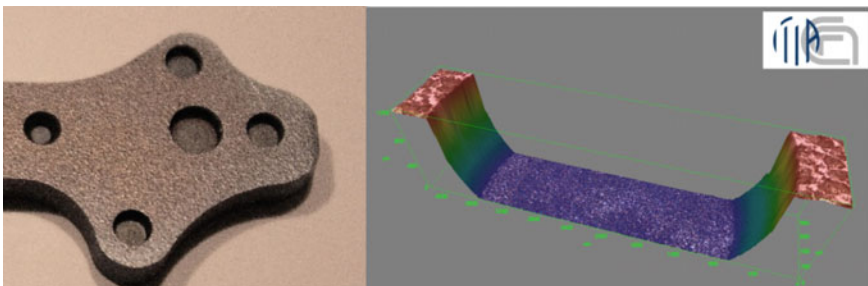


Fig. 6.10 Machined spherical housing scanned by axio-csm 700 confocal microscope

shown that the maximum process speed reached in these experiments is equal to 1.8 mm/min, the same obtained by titanium tests. Despite this, preliminary tests using $\text{Si}_3\text{N}_4\text{-TiN}$ ceramic plate for micro-EDM milling has resulted in higher MRR. The production of a single spherical housing requires 39 min, resulting in a total time of 195 min for machining the five housings. In this case, the total machining time is 245 min.

For bigger sizes and thicker devices, featuring many holes and bores, the machining time can drastically increase, so that the technology proposed here can be less suitable for the production of more complex fixation plates.

6.5.3 *Micro-EDM Milling/Sinking Combined Approaches: Micro-filter Mould*

Micro-EDM sinking and milling approaches can be usefully combined to accomplish good surface quality in reasonable machining times [45].

An example of the benefits provided by both approaches is well represented by the manufacturing of a micro-mould employed for the production of a polymeric micro-filter described by Surace et al. [46]. The micro-filter mould has a diameter of 2.3 mm and it is composed by 76 pins having square section, with a side of 80 μm and height equal to 0.15 mm. The pin-to-pin distance is equal to 70 μm . In order to facilitate the extraction phase of the moulded filter, the pin walls have a nominal inclination of 2°.

The micro-EDM machine used to machine the micro-mould is the SARIX SX 200 HP, which is also equipped with a wire-EDM unit (Ariane). The machining regime chosen for both micro-EDM milling and drilling approaches is the finishing. The micro-pins are produced by machining a grid of micro-channels, eight of which have length of 0.4 mm, sixteen channels have a length of 0.6 mm and twenty-four channels are 0.8 mm long.

The micro-EDM sinking has been implemented in the following fashion.

First, a cylindrical tool of WC having a diameter of 0.4 mm is shaped by using wire-EDM: the final tool shape is reported in Fig. 6.11. Since the tool diameter is kept constant after tool dressing, the micro-channel, which has a length of 0.4 mm, can be machined by operating a vertical movement, so that the tool can imprint its section shape into the workpiece. It is worth stressing that the working tool length of the shaped part is longer than the nominal channel depth: this simple precaution is mandatory since tool length wears during the erosion process. The longer channels (0.6 and 0.8 mm long) are produced by undertaking both a vertical and horizontal movements (on the left of Fig. 6.11). Once the tool is imprinted into the workpiece, it follows a horizontal path. During this movement, the tool is subjected to the erosion of the front side, which undergoes shortening and rounding. This effect can reduce the final channel depth and dimensional accuracy. To solve this problem, an additional horizontal stroke is added, as if the micro-channel is longer

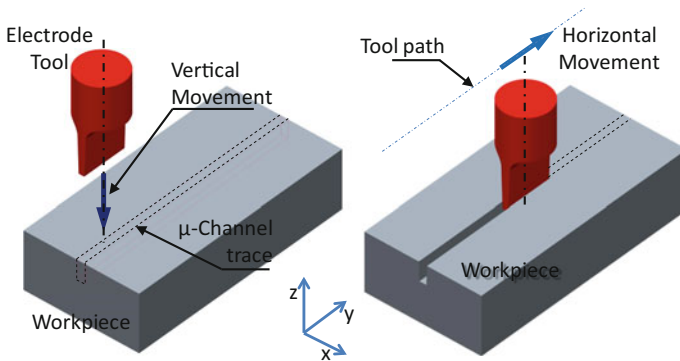


Fig. 6.11 The two movements (on the left—Vertical, on the right—Horizontal), required by the sinking approach

than the nominal values (0.6 or 0.8 mm). Doing so, although the front side wears along the path, the rest of the tool section, which is not yet subjected to wear process, can guarantee to obtain the required channel depth and width. As already stressed, no tool wear compensation strategy is available during micro-EDM sinking, so that it is essential to foresee wear phenomena in advance by properly shaping the tool.

Micro-EDM milling is employed to produce the remaining features of the filter, using a micro-tool having a diameter of 0.15 mm and adopting the layer-by-layer strategy.

It is worth stressing that both approaches have different dimensional accuracy. This is quite reasonable since micro-EDM sinking does not have a tool wear compensation strategy as milling does. In fact, comparing the two approaches on machining the same micro-channel, micro-EDM milling ensures a flatter shape of the channels and more defined walls, on the contrary, micro-EDM sinking can provide less accurate features, as shown in Fig. 6.12. The main differences in the dimensional accuracy related to both approaches concern mainly the rounding of the bottom surfaces. The depth indicated by L_0 is equal to 0.15 mm. The bottom surface is more rounded in sinking than milling ($R_{\text{sink}} = 0.031$ mm and $R_{\text{mill}} = 0.009$ mm). The draft angle is very similar, 2.1° . The distance between upper and ideal flat bottom surface (L_1) is different: 0.130 mm for sinking and 0.140 mm for milling.

The realized mould is shown in Fig. 6.13.

Table 6.3 shows the contributions of each operation to the total machining time, which is equal to 18038 s corresponding to about 5 h. Considering the fabrication of the micro pins only, if the micro-EDM milling is adopted the resulting machining time for this operation will result in 114472 s (31 h 47 min 52 s). By the comparison of the machining times, it is evident that adopting sinking approach is more

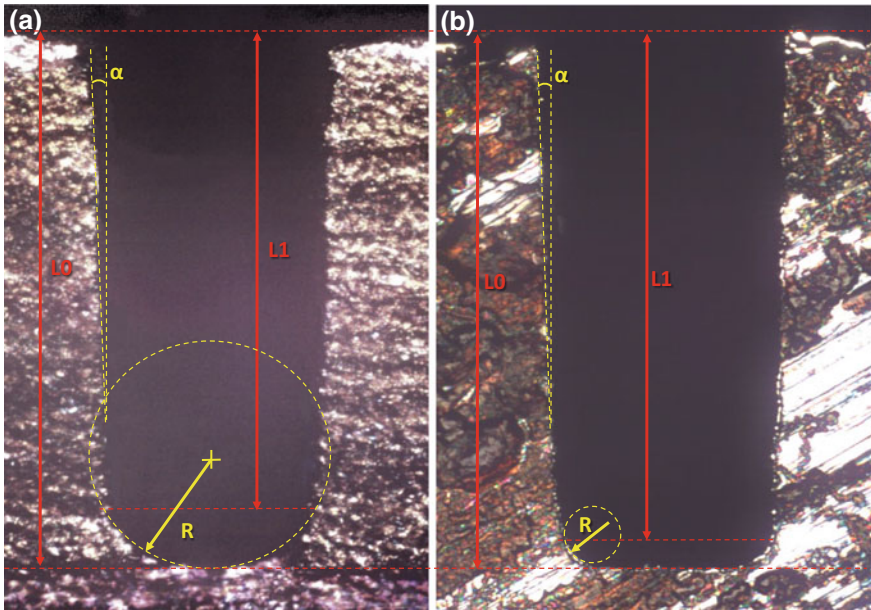


Fig. 6.12 Micro-channel section realised using: **a** sinking and **b** milling

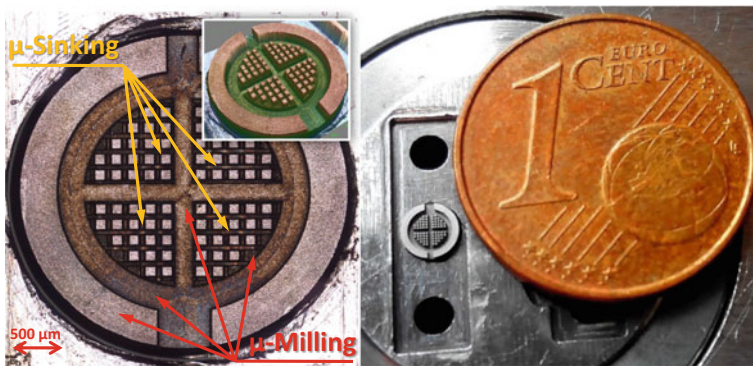


Fig. 6.13 Confocal reconstruction of the micro-filter mould and insert

advantageous, since it allows to save approximately 26 h of machining. However, as already discussed, micro-EDM sinking introduces shape defects at the bottom of some micro channels. To manage and minimise this drawback, it is possible to add further operations for a fine-finishing of micro-channels. Technically, in this approach all operations made for fabricating the micro-channels can be repeated

Table 6.3 Machining times for all operations done in micro-EDM of micro-filter mould

Micro pins			Other features		
Total sinking time (time for tool electrode shaping included) (s)	Erosion time by sinking (only channels) (s)	Tool electrode length used during sinking approach (mm)	Total milling time (time for tool electrode shaping included) (s)	Erosion time by milling (only features) (s)	Tool electrode length used during milling approach (m)
18,038	4613	79	17,017	8627	9
5 h 38 s	1 h 16 min 53 s		4 h 43 min 37 s	2 h 23 min 47 s	

using new electrode tools having precise micro-channel shape which follows the same machining sequence. In this case the machining time is almost doubled (about 10 h), but it is still acceptable if compared to the milling approach.

References

1. Tsai HC, Yan BH, Huang FY (2003) EDM performance of Cr/Cu based composite electrodes. *Int J Mach Tools Manuf* 43(3):245–252
2. Shobert EI (1983) What happens in EDM. In: Jameson EC (ed) *Electrical discharge machining: tooling: methods and applications*. Society of Manufacturing Engineers, Dearborn, pp 3–4
3. Boothroyd G, Winston AK (1989) *Non-conventional machining processes. Fundamentals of Machining and machine tools*. Marcel Dekker Inc., New York, p 491
4. McGeough JA (1988) *Electrodischarge machining*. Adv Methods Mach. Chapman & Hall, London, p 130
5. Krar SF, Check AF (1997) *Electrical discharge machining. Technology of machine tools*. Glencoe/McGraw-Hill, New York, p 800
6. Konig W, Dauw DF, Levy G, Panten U (1988) EDM—future steps towards the machining of ceramics. *Annu-Manuf Technol CIRP* 37(2):623–631
7. Pham DT, Dimov SS, Bigot S, Ivanov A, Popov K (2004) Micro-EDM-recent developments and research issues. *J Mater Process Technol* 149(1–3):50–57 [14th International Symposium on Electromachining (ISEM XIV)]
8. Yu Z, Rajurkar KKP, Narasimhan J (2003) Effect of machining parameters on machining performance of micro EDM and surface integrity. In: *Proceedings of ASPE, 26–31 Oct 2003, Portland Oregon, Precision Machining, Annual*
9. Pellicer N, Ciurana J, Ozel T (2009) Influence of process parameters and electrode geometry on feature micro-accuracy in EDM of tool steel. *Mater Manuf Process* 24:1282–1289
10. Modica F, Marrocco V, Bellantone V, Fassi I (2012) Study on depth error in fabrication of micro channels via μ EDM milling. In: *Proceedings of ICOMM 2012, 12th–14th March, Northwestern University, Evanston, CHICAGO, IL (USA), Paper MOB3*
11. Montgomery DC (2001) *Design and analysis of experiments*, 5th edn. Wiley, New York
12. Minitab Inc. Available at: www.minitab.com. Accessed on 2011
13. Liao YS, Chang TW, Chuang TJ (2008) An on-line monitoring system for a micro electrical discharge machining (micro-EDM) process. *J Micromech Microeng* 18:035009

14. Yeo SH, Aligiri E, Tan PC, Zarepour H (2009) A new pulse discriminating system for micro-EDM. *Mater Manuf Proc* 24:1297–1305
15. Modica F, Guadagno G, Marrocco V, Fassi I (2014) Evaluation of micro-EDM milling performance using pulse discrimination. In: *Proceedings of ASME 2014, IDETC/CIE 2014*, 17–20 Aug 2014, Buffalo
16. Marrocco V, Modica F, Bellantone V, Fassi I (2015) Pulse monitoring and discrimination in micro-EDM milling of Si₃N₄-TiN micro-channels. In: *Proceedings of ICOMM 2015*, March 28–April 2nd 2015, Milan
17. Yu Z, Masazawa T, Fujino M (1998) Micro-EDM for three-dimensional cavities-development of uniform wear method. *CIRP Annu-Manuf Technol* 47(1):169–172
18. Yu Z, Masazawa T, Fujino M (1998) 3D micro-EDM with simple shape electrode. *Int J Electron* 7–12 & 71–79
19. Bissacco G, Tristo G, Valentinčić J (2010) Assessment of electrode wear measurement in micro-EDM milling. In: *Proceedings of the 7th international conference on multi-material micro manufacture*, pp 155–158
20. Modica F, Marrocco V, Trotta G, Fassi I (2011) Micro electro discharge milling of freeform micro-features with high aspect ratio. In: *Proceedings of ASME 2011 the International Design of Engineering Technical Conferences and Computers and Information in Engineering Conference (IDETC Washington, DC, USA) DETC2011-4833*
21. Narasimhan J, Yu Z, Rajurkar KP (2005) Tool Wear compensation and path generation in micro and macro EDM. *J Manuf Proc* 7(1):75–82
22. Dimov S, Pham DT, Ivanov A, Popov K (2003) CAM system for layer based EDM. *Int J Manuf Sci Prod* 5(1–2):27–31
23. Zhao W, Yang Y, Wang Z, Zhang Y (2004) A CAD/CAM system for micro-ED-milling of small 3D freeform cavity. *J Mater Proc Technol* 149:573–578
24. Popov K, Petkov P (2011) Layer based micro-machining-New approach for tool-path generation. *CIRP J Manuf Sci Technol* 4:370–375
25. Nguyen MD, Wong YS, Rahman M (2013) Profile error compensation in high precision 3D micro-EDM milling. *Precision Eng* 37(2):399–407
26. Yan MT, Huang KY, Lo CY (2009) A study on electrode wear sensing and compensation in micro-EDM using machine vision system. *Int J Adv Manuf Technol* 42:1065–1073
27. Aligiri E, Yeo SH, Tan PC (2010) A new tool wear compensation method based on real-time estimation of material removal volume in micro-EDM. *J Mater Process Technol* 210 (2010):2292–2303
28. Wang J, Ferraris E, Galbiati M, Qian J, Reynaerts D (2014) Simultaneously counting of positive and negative pulse parts to predict tool wear in micro-EDM milling. In: *Proceedings of ICOMM 2014*, Singapore, 25–28 March 2014
29. Bissacco G, Valentincic JM, Hansen HN, Wiwe BD (2010) Towards the effective tool wear control in micro-EDM milling. *Int J Adv Manuf Technol* 47(1–4):3–9
30. Mahardika M, Mitsui K (2008) A new method for monitoring micro-electric discharge machining processes. *Int J Mach Tools Manuf* 48(3–4):446–458
31. Yi SM, Lee YS, Chu CN (2006) Straight hole micro EDM with a cylindrical tool using a variable capacitance method accompanied by ultrasonic vibration. *J Micromech Microeng* 16:1092
32. Kuriyagawa T, Zhou L, YAN J, YOSHIHARA N (2008) Fabrication of high-aspect ratio micro holes on hard brittle materials -study on electrorheological fluid-assisted micro ultrasonic machining. *Key Eng Mater* 389–390:264
33. Karthikeyan G, Ramkumar J, Dhamodaran S (2010) Micro electric discharge milling process performance: an experimental investigation. *Int J Machine Tools and Manuf* 50:718–727
34. Puranik MS, Joshi SS (2008) Analysis of accuracy of high-aspect-ratio holes generated using micro-electric discharge machining drilling. *Proceed Inst Mech Eng, Part B: J Eng Manuf* 222 (11):1453–1464
35. Modica F, Marrocco V, Trotta G, Fassi I (2011) Micro electro discharge machine milling of freeform micro-features with high aspect ratio. In: *ASME 2011-International Design*

- Engineering Technical Conferences (IDETC) and Computers and Information in Engineering Conference (CIE) August 28–31, 2011 in Washington, DC
36. König W, Dauw DF, Levy G, Panten U (1988) EDM-future steps towards the machining of ceramics. *CIRP Annu-Manuf Technol* 37(2):623–631
 37. Luis CJ, Puertas I, Villa G (2005) Material removal rate and electrode wear study on the EDM of silicon carbide. *J Mater Process Technol* 164–165:889–896
 38. Clijsters S, Liu K, Reynaerts D, Lauwers B (2010) EDM technology and strategy development for the manufacturing of complex parts in SiSiC. *J Mater Process Technol* 210:631–641
 39. Lauwers B, Kruth JP, Liu W, Eraerts W, Schacht B, Bleys P (2004) Investigation of the material removal mechanisms in EDM of composite ceramic materials. *J Mater Process Technol* 49/1-3/347-352
 40. Lauwers B, Kruth J-P, Brans K (2007) Development of technology and strategies for the machining of ceramic components by sinking and milling EDM. *CIRP Annu-Manuf Technol* 56(1/2007):225–228
 41. Liu C-C, Huang J-L (2003) Effect of the electrical discharge machining on strength and reliability of TiN/Si₃N₄ composites. *Ceram Int* 29:679–687
 42. Liu K, Lauwers B, REYNAERTS D (2010) Process capabilities of Micro-EDM and its applications. *Int J Adv Manuf Technol* 47(1–4):11
 43. Liu K, Paris J, Ferraris E, Lauwers B, Reynaerts D, (2007) Process investigation of precision Micro-Machining of Si₃N₄-TiN ceramic composites by electrical discharge machining (EDM). In: *Proceedings of the 15th International Symposium on Electromachining (ISEM)*, 23–27 Apr 2007, Pittsburgh, PA, USA, pp 221–226
 44. Modica F, Pagano C, Marrocco V, Fassi I (2015) Micro-EDM studies of the fabrication of customised internal fixation devices for orthopedic surgery. In: *Proceedings of the ASME 2015 International Design Engineering Technical Conferences & Computers and Information in Engineering Conference IDETC/CIE 2015*, 2–5 Aug 2015, Boston, Massachusetts
 45. Modica F, Marrocco V, Basile V, Fassi I (2015) Micro-EDM-milling and-sinking combined approach for the fabrication of micro-components. In: *Proceedings of ICOMM 2015*, March 28–April 2nd 2015, Milan, Italy
 46. Surace R, Bellantone V, Trotta G, Basile V, Modica F, Fassi I (2015) Design and fabrication of a polymeric microfilter. In: *Proceedings of ICOMM 2015*, March 28–April 2nd 2015, Milan, Italy

Chapter 7

Moulded Interconnect Devices

Adrien Brunet, Ulrich Gengenbach, Tobias Müller, Steffen Scholz
and Markus Dickerhof

7.1 Overview—Moulded Interconnect Devices

Moulded Interconnect Devices (MID) refer to components made of polymer with added electrical (conductors, isolators, etc.) and mechanical functions (carrier module, housing, etc.). Usually the parts are generated out of micro-injected thermoplastics with structured circuit traces. Nevertheless, more and more substrate materials are being made available and injection moulding is not the only method to fabricate them.

One of the main advantages of MID is the geometry freedom during the fabrication process. While classic Printed Circuit Board (PCB) technology only allows planar circuits, MID makes it possible to generate diverse surfaces at varying angles, i.e. regular surfaces (cylinder) and free form surfaces. Among other things, a circuit pattern with multiple planes allows better spacing of circuitry, as well as the connected switches and buttons. Figure 7.1 gives an overview of the available different geometry classifications.

Keeping in mind that the geometry freedom is a huge advantage in terms of integration it is not surprising that moulded interconnect devices are being used in various industry sectors like telecommunication (antenna), automotive (motorcycle handlebars), medical (hearing aid) and many others.

Innovation potential of 3D-MID

3D-MID shows great perspectives due to the doubled innovation potential for both products and processes.

Product innovations using the geometry freedom, present the advantage of:

A. Brunet (✉) · U. Gengenbach · T. Müller · S. Scholz · M. Dickerhof
Karlsruher Institut für Technologie, IAI, Karlsruhe, Germany
e-mail: adrien.brunet@kit.edu

M. Dickerhof
e-mail: markus.dickerhof@kit.edu

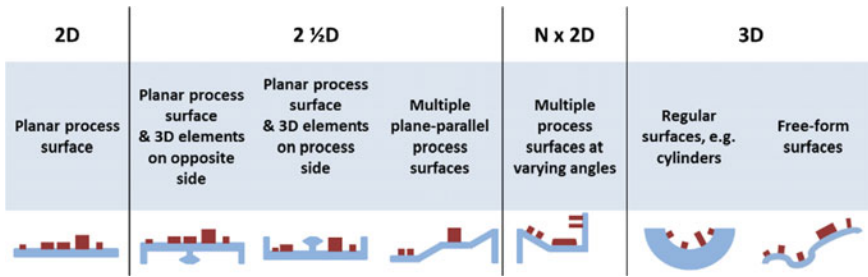


Fig. 7.1 Geometry classification of 3D moulded interconnect devices (MID) [1]

- Design freedom (different angles, surfaces, cavities)
- Function integration (switches, sensors, antenna)
- Miniaturisation (integration of components on different surfaces)
- Weight saving (material saving included).

While Process innovations by means of selective structuring and metallisation result in:

- Fewer parts (many parts combined in one)
- Shortening of process chain (reduction of assembly steps)
- Reduction of manufacturing costs (processes faster and less material consuming)
- Improved reliability (resulting from the previous).

In order to fully benefit from MID innovation potentials and successfully lead an MID project, it is necessary to master certain key points. The first point is to ensure a broad and interdisciplinary understanding of the technology that exists within the project team, followed by the definition of the interfaces between the competences. Design experience is important in order to fully take advantage of the opportunities offered by the MID technology. Other essential factors in achieving the MID innovation potential include establishing accurate costs estimates for the entire process chain and the system as a whole as well as the willingness to take risks in general.

The current research on MID covers different topics

- Substrate materials are, as explained previously, mainly thermoplastics; however, current research focuses on thermally conductive plastics; high-temperature plastics; bio-compatible, transparent or colourised materials; thermosets and ceramics.
- Interconnect manufacture such as printing technology or plasma structuring; multilayer constructions.
- Rapid prototyping.
- 3D assembly and mounting techniques as well as test and inspection criteria for MID; standardisation and specification; forecasts on long-term reliability; simulation models.

- Quality and reliability, e.g. multiple work piece carriers for standard Surface Mounted Technology (SMT), chip-on-MID placement technologies; embedded components and MID housing.
- Planning and development for design tools; development technologies; heat removal concepts and recycling.
- Ceramic material.

7.2 Materials

7.2.1 Introduction

The main material type for the production of moulded interconnect devices MID substrates is plastics. Compared to other materials, e.g. ceramics, plastics are mechanically strong, yet still able to dissipate stress induced by mechanical loading. A key factor for the success of three-dimensional parts using polymers as substrate material is the variability of manufacturing methods. This facilitates the production of either very small or very high quantities in a cost-effective way.

The word plastic is derived from the Greek *plastikos* meaning “capable of being shaped or moulded”, which already implies the aptitude of these materials to be formed into a desired shape by casting, pressing or extrusion. Plastics are made up of large, chain-like molecules consisting of non-metallic elements (carbon, hydrogen, oxygen, nitrogen, fluoride, sulphur) [2]. The internal structure, the degree of cross-linked molecular chains and the chemical composition are often used to classify different plastic materials. An overview of the different plastic classes is given in Fig. 7.2.

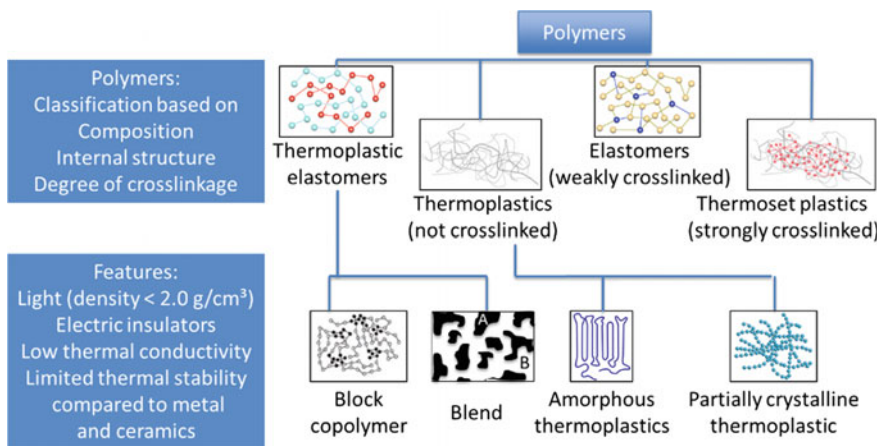


Fig. 7.2 Classification of plastics based on the internal structure and amount of cross-linking [3]

The structure also influences the properties of the plastic such as melting point, softening behaviour or crystallisation. The correct choice of polymer material is crucial for the success both in manufacturing and in sales. When marketing an MID, numerous factors such as cost of the base material, processability, sustainability and ecological impact have to be taken into account.

In the following sections, some of the major requirements for substrate material properties and materials that are currently used in the production of MIDs will be described.

7.2.2 Requirement for Substrate Material

In order to serve as a suitable material for MID substrates, the polymer has to fulfil a variety of required parameters:

- Temperature range for assembly and usage
- Mechanical properties (creep, tensile, flexural)
- Flammability
- Metallisation capability
- Environmental impact
- Electrical properties
- Moulding characteristics
- Cost effectiveness.

These properties can have a major impact on the suitability of the material for the manufacturing of moulded interconnect devices. Furthermore, in order to make a decision between the different available plastics, the available property values have to be comparable and measurable with reasonable accuracy. In the case of polymer materials, the material properties often depend on the actual processing environment, which makes it necessary to evaluate wide range of characteristics. The most important properties in this respect are [3]:

- Rheology
- Hardening
- Degradation
- Shrinkage and tolerances
- Anisotropy
- Crystallisation and melting.

For thermoplastics and thermoset plastics one or more standardised measuring techniques exist, which can be referred to when determining the characteristic values. Most of these standards also contain a description of the specific test specimen; for example, DIN ISO 10350 [4] describes the determination of rheological values. Similar standards are applicable for other material properties.

7.2.3 Typical MID Materials

As mentioned above, a wide variety of polymer materials may be suitable for the production of MIDs. In the past, thermoplastics have proven to be the most commonly used substrate materials, but the development of new materials with improved properties is still progressing. This chapter provides an overview of current widely applied plastics.

Figure 7.3 summarises the typical substrate materials for MIDs, together with some material properties and relative material costs.

The choice for the best material is also highly dependent on the production process chosen for the moulded interconnect device. On the other hand, the requirements given by the finished product are directly linked to the material properties and the chosen manufacturing process. Typically, fairly low-cost and engineering-grade thermoplastics are favoured to high-performance polymers. This is because they suffice for the existing production and they can be further modified

Material	Abbreviation	Peel Strength		Solderability			Relative cost
		Chemical	Hot Embossing	Reflow		Selective	
				normal	Low melting point solders		
A	Polypropylene	PP	+	+	-	0	+
	Acrylonitrile Butadien Styrene	ABS	+	+	-	-	+
	Polycarbonate	PC	+	+	-	+	+
B	Polyethylene Terephthalate	PET	-	+	-	0	+
	Polybutylene Terephthalate	PBT	+	+	0	+	+
	Polyamide	PA	+	+	0	+	+
	Polyphenyle Sulfide	PPS	+	-	+	+	+
C	Polysulfone	PSU	+		0	+	+
	Polyethersulfone	PES	+	+	+	+	+
	Polyetheremide	PEI	+	+	+	+	+
	Liquid Crystal Polymer	LCP	+	0	+	+	+

Material	Peel Strength	Solderability
A: Commodity Thermoplastics	+ > 0.8 N/mm	+ Standard process
B: Technical Thermoplastics	0 0.5-0.8 N/mm	0 Parameter adjustment
C: HT-Thermoplastics	- Usually not plateable	- Special processes

Fig. 7.3 Typical substrate materials for moulded interconnect devices (MID) [5]

by combining them with other materials, blending them with thermoplastics, or adding additives/fillers or post-treatment techniques.

A more detailed description of different materials including their properties relevant to the MID manufacturing process can be found in [3].

7.3 Processes

7.3.1 Overview

Most of the MID processes start with a first shot moulding, in order to create the substrate. This first piece is made out of thermoplastics via (micro) injection moulding; different technologies can be applied to realise the subsequent conductive tracks.

The first option to generate the conductive tracks is to apply the laser direct structuring (LDS) technology, where the substrate surface is partially structured initially according to the electrical circuit pattern and then metallised. The second technology option uses conductive inks for printing of the surfaces, with aerosol jet printing being an example for this printing technology. The third option makes use of hot embossing in which the conductive tracks are created by means of metallic foil.

Two-shot moulding differs from the other technologies as the substrate is moulded twice with different thermoplastics. The first shot consists of a metallisable thermoplastic. The second shot consists of a non-metallisable thermoplastic or of the contrary (first shot made of non-metallisable thermoplastic and second shot made of metallisable thermoplastic). The second shot over-moulds the first shot only partially, so that the uncovered areas are creating the electrical circuit pattern. The complete piece is then dipped into metallisation baths forming successive metal layers on the free surface of the metallisable material.

Film Insert Moulding technology makes use of the integration of a printed or structured film prior to the moulding process. After insertion of the film into the mould, the thermoplastics are added and the film forms the desired electrical circuit.

The following Sects. 7.3.2–7.3.5 will focus on the different technologies; two-shot moulding, LDS, aerosol-jet printing and hot embossing including individual drawbacks and advantages. Comparisons of each technology are addressed in 7.3.6.

7.3.2 Two-Shot Injection Moulding

Two-shot injection moulding is an efficient and cost effective technique that is widely used in the manufacturing of polymer parts. However, the process used in

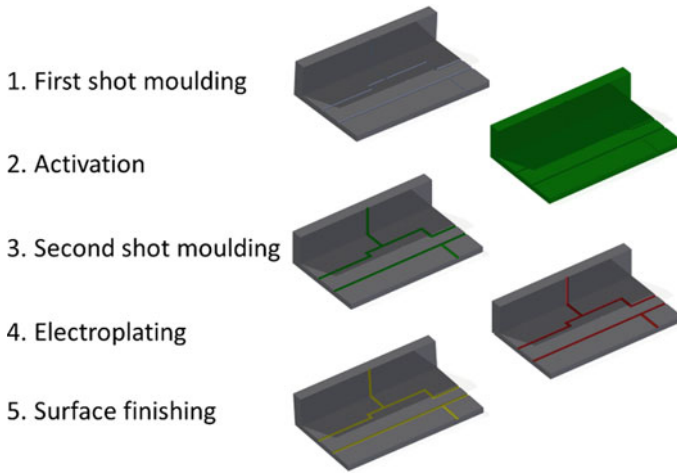


Fig. 7.4 Main steps of the two-shot injection moulding technique for MID

MID technology differs in terms of process flow. While in a typical plastic injection moulding the materials form the different parts of the final product (e.g. inserts, seals, hinges or movable components), in MID technology the material injected during the second moulding step covers partially the first component. This layer determines the conductor paths generated in the following process steps (Fig. 7.4).

Over time, different versions of the basic moulding process were developed and the two main techniques, PCK (Printed Circuit Board Kollmorgen) and SKW (Sankyo Kasei Wiring board), emerged [5], which are being described in detail in the following sections.

Figure 7.5 shows the process sequence for the PCK technology.

The PCK process has two different versions. In version one—the PA process—(left image) first, a non-plateable material is moulded followed by over-mould with a plateable polymer which fills the recesses created in the first step.

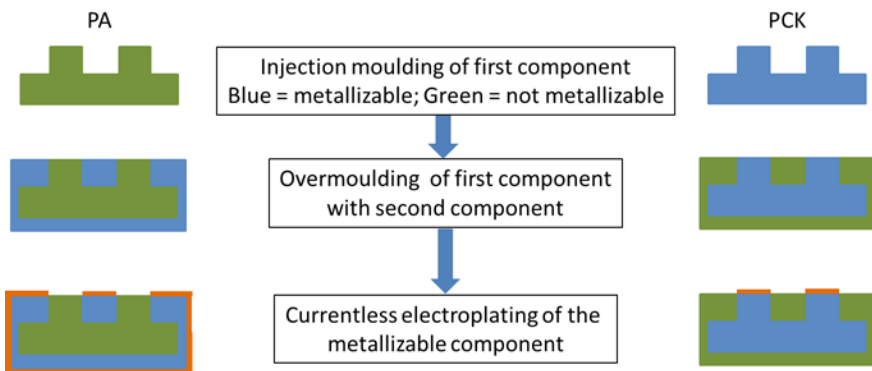


Fig. 7.5 Two variants of the printed board circuit Kollmorgen (PCK) process

The second version, the standard PCK process as shown on the right in Fig. 7.5, starts off with a metallisable material that is over-moulded with a non-metallisable polymer in the second step, leaving exposed plateable areas that represent the later conductor paths. This final plastic part is then transferred to the electroplating stage, where the desired thickness of metal is deposited on the activated surface of the MID substrate.

The SKW process introduces an additional process step between the two moulding steps. The first shot is activated in a Palladium catalyst solution, dried and then over-moulded with the second component [6]. The final moulded specimen is then plated onto the catalysed surface to create the conducting areas (Fig. 7.6).

Advantages and drawbacks of two shot injection moulding technology

Since the basics of two-shot injection moulding process is more or less identical to typical injection moulding techniques, the same can be said in case of advantages and drawbacks.

Two-shot injection moulding allows for a high geometric freedom with the possibility of creating very small details with high accuracy and repeatability. The short cycle times ensure a cost-effective production, even for very high quantities, including also the initial production costs of the moulding tool. Since the first and second shots produce different geometries, two cavities have to be produced and a moulding machine suitable for the two-shot process has to be used. This means that higher investment costs have to be taken into account.

Materials to be used in two-shot injection moulding need to fulfil a certain number of requirements. First, both thermoplastics have to exhibit a sufficient adhesion to avoid separation after the moulding. The second crucial property

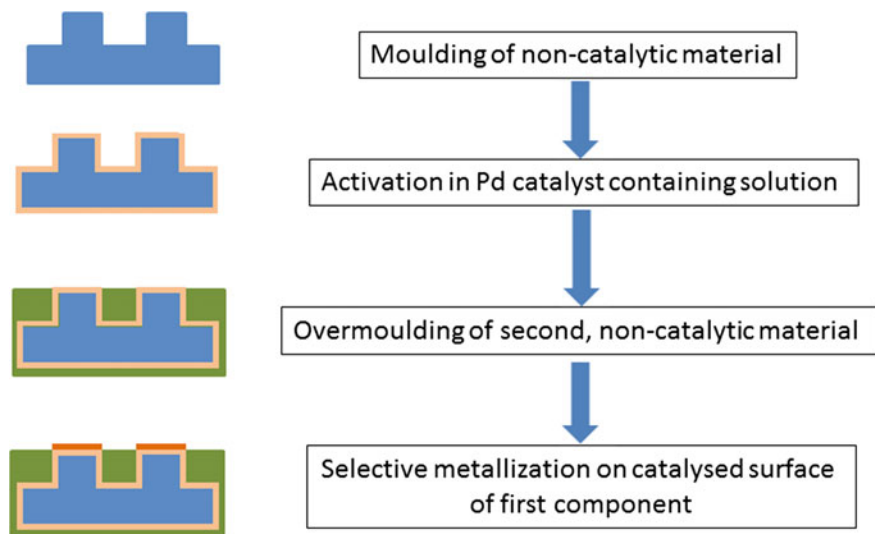


Fig. 7.6 The sankyo kasei wiring board (SKW) process

Table 7.1 Typical geometrical boundaries in two shot injection moulding

Design limit	LCP/SPS	PEI	PPA	PES	PA
Conductor track width	0.25	0.6	0.4	0.6	0.5
Conductor track spacing	0.6	0.6	0.4	0.6	0.5
Min. hole diameter	0.6	0.6	0.6	0.6	0.6
Aspect ratio, length/diameter	<6:1	<6:1	<6:1	<6:1	<6:1
Min. pin diameter	0.8	0.8	0.8	0.8	0.8
Pin length for diameter	2	2	2	2	2
Section thickness (1st shot)	0.25	0.8	0.8	0.8	0.8
Section thickness (2nd shot)		1	1	1	1

All given numbers are expressed in mm [3]

concerns the flow properties of the polymer melt. In order to fully take advantage of the small details possible with the injection moulding technique, the material's viscosity has to be low enough to generate very fine details without solidifying before filling the whole cavity. This requires a sophisticated coordination of material properties, flow length and tool design with respect to the application of heating and cooling elements. Table 7.1 shows an overview of the most common thermoplastic materials used for the two-shot injection moulding in the production of MIDs and the possible geometric limits [7].

7.3.3 Laser Direct Structuring (LDS)

The Laser Direct Structuring (LDS) technology is an additive method for generating 3D conductor structures. LPKF Laser & Electronics AG, a manufacturer of industrial laser technology headquartered in Garbsen, Germany, has developed this technology in the recent years [8]. It can produce high-resolution circuit layouts on complex three dimensional interconnect parts in a multistep process sequence, and the LPKF-LDS technology will be the focus of the following sections. Notably, other laser process technologies exist, such as ADDIMID [9] or MIPTEC [10] technology, although they are less popular.

Process chain

The LDS method is a four-step process starting with the injection moulding, followed by laser structuring, metallisation and surface finishing.

The polymer substrate part is manufactured by single shot injection moulding. Once the part is finished, the pattern of the circuit diagram is drawn on the surface via a laser (Nd:YAG; $\gamma = 1064$ nm). The laser simultaneously activates the additives and destroys the polymer matrix resulting in an ablation of 1–2 μm . This cracks open the complex compounds in the doped plastic and break off the metal

Table 7.2 Typical procedure for creation of conductive tracks by electroless plating [8]

Step	Bath-type	T (min)	T (°C)	Layer thickness (µm)
Ultrasound-cleaning	H ₂ O	5	50	–
Chemical Cu	Enplate Cu872	40	43	4
Activation	Degussa Aktivator 878	5	40	–
Chemical Ni	Enplate MIS select 9065	20	60	2
Flash Au	Immersion gold I	20	70	0.1
Drying	Drying furnace	60	100	–

atoms from the organic ligands.¹ These metal atoms act as nuclei for reductive metal coating. As a result of the surface structuring, microscopic pits and undercuts are created in which the metal is firmly anchored during metallisation, which in turn helps achieve superior peel strength.

The metallisation part of the LPKF-LDS process starts with a cleaning step to remove laser debris followed by an additive build-up of the circuit tracks by means of current-free Copper (Cu) baths (so-called electroplating). Metal is deposited on the structured area forming the conductive tracks. The exposed particles from the additive, which were activated by the laser, subsequently act as nuclei for the reductive plating in the electroless metallisation bath [11, 12]. Application-specific coatings such as Ni, Au, Sn, Sn/Pb, Ag, Ag/Pd, etc. on the initial Copper base are possible [8] and the last step includes the surface finishing.

An example of how conductor paths are currently being produced is shown in Table 7.2. The process starts with a thick layer of copper as described above, followed by subsequent layers of nickel and gold. Usually conductive tracks are made of copper covered with gold to avoid corrosion and places an additional layer of nickel between the two layers to avoid the diffusion of gold into the copper layer.

Substrate material

Different grade materials are suitable for LDS technology, depending on the application area, thermal restrictions, cost or mechanical requirements. For example, PC/ABS (blend of PolyCarbonate and Acrylonitrile Butadiene Styrene) is a low cost amorphous material with low thermal stability that is commonly used for antenna production in smartphones [8]. Consequently, PC/ABS is one of the most used materials [3]. On the other hand, LCP is a high cost semi-crystalline material with high-thermal stability commonly used for micro-packaging. A selection of materials is depicted in Fig. 7.7 according to their thermal stability and their crystallinity.

¹A ligand is an ion or molecule attached to a metal atom by coordinate bonding.

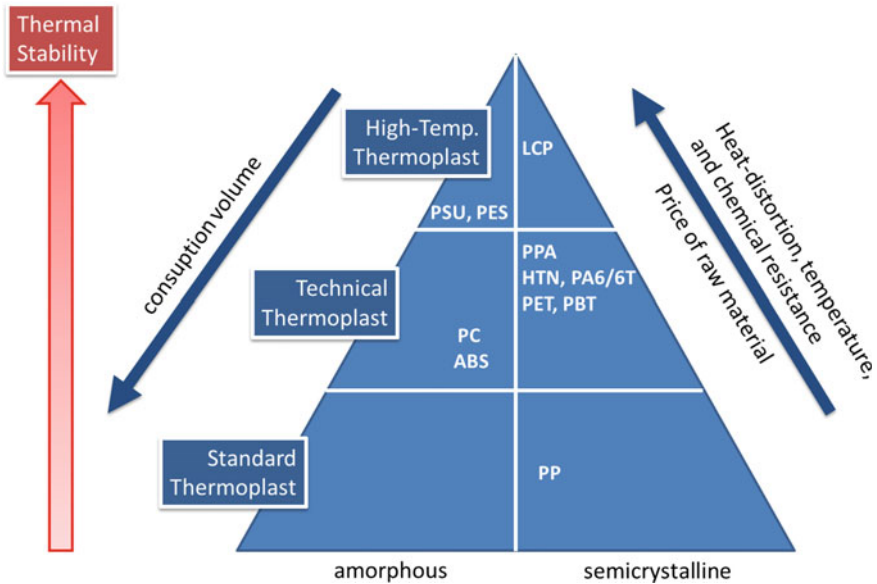


Fig. 7.7 Grade material for laser direct structuring technology [8]. *PP* polypropylene, *PC* polycarbonate, *ABS* acrylonitrile butadiene styrene, *PA* polyamides, *PPA* polyphthalamide, *HTN* high temperature nylon, *PET* polyethylene terephthalate, *PBT* polybutylene terephthalate, *PES* polyethersulfone, *PSU* polysulfone, *LCP* liquid crystal polymers

Requirements for the metallisation nuclei

In the majority of cases, plastics used for LDS technology require specific additives (e.g. a Chelate complex), which are added to the blend during compounding by the material supplier. Although the properties of the plastic might change slightly due to the additive, its extreme heat resistance still facilitates the compounding process and prevents nucleation during the injection moulding process. Therefore, the metallisation nuclei have to fulfil certain requirements:

- Separation of metal nuclei under the influence of laser radiation
- Non-conducting materials
- Finely spreadable in technical polymers with common processing techniques
- No negative influences on the properties of the polymer
- Thermally stable in the injection moulding process
- ROHS (2002/95/EG) conformity.

LDS fabrication equipment

Depending on the specific application (prototyping, series production, low costs, micro-fine structure...) there are various different LDS equipment systems (Fusion 3D 1100, 1200, 1500 and 6000) with a range of costs. Some of the systems allow for use with multiple laser heads, up to four laser heads help minimising process

times and boosting the throughput by simultaneously structuring several sides of the components. Automatic component manipulation ensures precision alignment and high throughput [8].

7.3.4 Hot Embossing

Hot embossing constitutes a simple, cheap and fast process for the production of MIDs. One of its main features is the possible dispensing with a galvanisation step since the metallisation is part of the embossing process itself. It is especially suitable for parts with predominantly planar surfaces and conductor path widths above 300 μm .

The process itself is shown in Fig. 7.8. An injection moulded substrate is loaded into the embossing apparatus and a copper film with a special coating is applied by pressing a heated stamp (20–40 °C above the glass transition or melting temperature of the moulded part), which carries the negative (opposite) of the desired conductor path layout, onto the substrate with defined mechanical pressure. The die cuts the copper film and simultaneously bonds the molten plastic of the substrate in the designated areas. After embossing, the package is cooled and the die retracts allowing for a removal of excess film and withdrawing of the finished metallised product.

The process can be carried out by using a stamp vertically pressing on film/substrate assembly or by using a structured wheel or roller, which allows the production of large, uninterrupted areas [7].

The films are fixed to the surface of the polymer substrate material either by mechanical adhesion or by gluing. The adhesive is activated by temperature, which is applied during the embossing process, and secures a tight bond between the

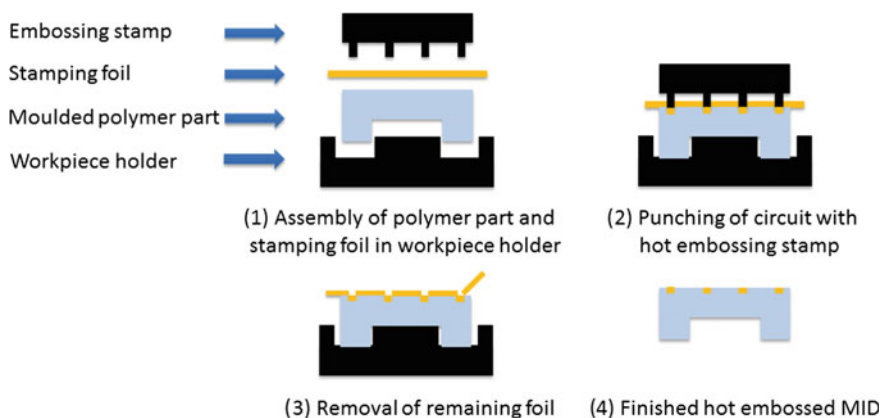


Fig. 7.8 Hot embossing process scheme according to [3]

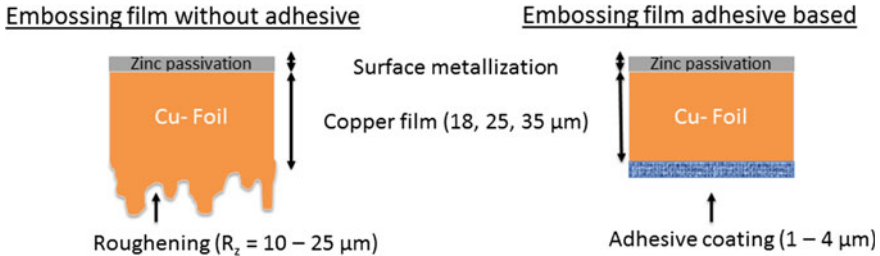


Fig. 7.9 Different films for hot embossing of MID; mechanical adhesion (*left*) or adhesion via gluing (*right*)

Table 7.3 Conductor dimensions versus copper film thickness [7]

Film thickness (μm)	Min. conductor width (μm)	Min conductor spacing (μm)	Distance from edge (μm)
12	300	400	200
18	500	500	300
35	800	800	300
70	1000	1000	500
100	1200	1200	500

coated film and the plastic base. In case of the mechanical bonding, the bottom side of the film is structured and the surface interlocks with the polymer during embossing, creating a strong mechanical connection. Therefore, the copper films mainly consist of three layers, a top layer to prevent oxidation of the copper, the conducting copper layer and the adhesive or interlock layer (Fig. 7.9).

The fine dimensions of the stamps and the dimensions of the copper films also limit the structures that can be realised. The dimensions currently possible are given in Table 7.3.

However, when considering hot embossing, different design limitations have to be taken into account. As mentioned before, the process is mainly suited for planar structures. Slight slopes can be processed but cavities, patterns larger than 100 cm^2 and a length-to-width ratio of 4:1 are currently not feasible [3].

7.3.5 Aerosol-Jet Printing

Like most of the printing technologies, aerosol-jet printing has a straightforward process chain. After the injection moulding of a substrate, the ink is directly applied on the surface and cured in a drying and sintering process.

The types of ink suitable for this technology are quite diverse and range from conductive to semi-conductive ink, or from dielectric to insulating materials. Once

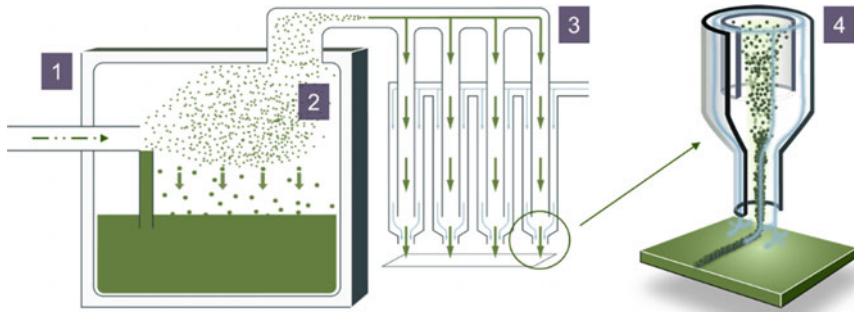


Fig. 7.10 Diagrammatic view of the aerosol-jet process (pneumatic atomisation). *Source* Optomec. 1 Ink atomisation. 2 Drop by gravity of droplet bigger than 5 μm. 3 Transportation of the aerosol to the deposition head. 4 Focusing of the aerosol inside the nozzle by sheath gas

this technology is fully optimised, very fine conductor structures can be produced achieving tracks with less than 10 μm to more than 1 mm in width [13].

Figure 7.10 shows the principle of the pneumatic aerosol jet printing process (atomisation of inks by ultrasonic effect is an alternative process to pneumatic). In the first step, the functional ink (a suspension with a solids content of approximately 60–70%) is placed in the atomiser, generating an aerosol by means of the gas flow. Due to the gravity effect, all aerosol droplets larger than 5 μm return to the ink while the rest of the aerosol droplets with a size between 1 and 5 μm remain suspended in step 2. For the next step, the aerosol is transported to the deposition head where excess gas is removed. During the final step 4, the aerosol is focused inside the nozzle by a secondary gas flow, also called sheath gas. The surface of moulded part is then printed using a non-contacting, maskless and vector-based technique. The standard height of such a deposited layer is 2 μm [13].

The printing process can be performed by moving the nozzle relative to the surface or by moving the component while the nozzle remains stationary. Since aerosol creation is a continuous process (atomisation), the ink jet cannot be simply turn off. Therefore, the ink flow at the end of the nozzle has to be mechanically interrupted in order to temporarily stop the ink deposition.

Curing is the last step of the printing process, normally performed in a drying oven. Here the liquid is separated from the solid phase (generally metal), while the energy load sinters the metallic nanoparticles that then form a cohesive layer. When setting the curing temperature, the thermal resistance of the substrate has to be taken into account as well as the fact that the curing temperature influences the electrical conductivity of the conductive structures. A lower curing temperature will lead to a longer process time.

Other options for the final curing step are laser sintering or light sintering, which are more selective than the drying oven method. The challenge in both cases lays in optimising the power of the system. Wavelength and intensity are two additional factors that have to be taken into account for a successful light sintering [3].

This paragraph compares aerosol-jet technology with inkjet printing. There are three main differences between both: resolution, ink viscosity and distance between print-head and substrate. Initially, the minimum resolution for aerosol-jet printing is reported to be around 10 μm while it is about 20–25 μm for inkjet. Secondly, because of the atomisation process, ink with high viscosity can be used in the aerosol-jet process, 1–1000 mPas versus 1–20 mPas for the inkjet. The last consideration is the distance between the printhead and substrate surfaces.

The aerosol-jet process can support a 2 mm variation of this distance (in the direction of the jetflow) without altering the printing quality, while with ink jet technology the printhead has to stay at a constant distance from the surface. Consequently, a rough surface with a surface variation of less than 2 mm can be easily printed with aerosol-jet technology, without vertically moving the printhead.

On the other hand, inkjet technologies are more mature, easily available on the market and cost less. Moreover, the aerosol-jet is continuous, which means that it has to be shuttered to stop the printing process; shuttering the jet results in material losses. Considering the high cost of such ink, material losses can be expensive.

7.3.6 Advantages and Challenges of Each Technology

Two-shot injection moulding is well adapted for high production volumes compared to the three previous technologies. It requires a high initial investment, but with time and volume, the price per unit becomes advantageous. Nevertheless, two shot technology suffers some dimension limitations compared to aerosol-jet and LDS technologies.

It is difficult to realise a fine structure, although this can be moderated by the design of the part and the gates. Moreover, any layout amendment is very costly. The mould needs to be prefabricated and the gates may have to be reviewed as well, which limits the flexibility of the technology.

Aerosol-jet printing can produce the finest structures and have the highest material diversity among the four technologies, but its cost per unit is relatively high. Although the technology is promising, it is not yet fully mature.

Laser Direct Structuring can be seen as a good compromise since it can achieve fine structure at medium scale for a reasonable price. It also benefits from a reasonable diversity of usable materials; however, most of the materials have a high cost.

Hot embossing technology can be implemented for a low price and great number of parts, as well the range of materials available for this technology. The adhesion of the foil to the substrate and the removal of the residual foil are challenging in this technology. Nevertheless, the design freedom is poor and any layout change requires moderate effort. Table 7.4 summarises the advantages and challenges of each technology.

Table 7.4 Comparison of the important MID structuring processes based on specific properties [3]

Technology	Min. conductor width (μm)	3D design freedom	Layout change	Material diversity	No. of units	Material costs	Tool costs	Investment
LPKF-LDS	100	High	Simple	Medium	High	High	Very low	Medium-high
Aerosol-Jet	10	High	Simple	Very high	Low	Medium	Medium	Medium-high
Two-Shot	150	Very high	Very high	Low	Very high	Low-medium	Very high	Very high
Hot embossing	300	Low	Moderate	Very high	High	Low	Medium	Low

7.4 MID Assembly

As for printed circuit board (PCB), electrical components can be placed on top of a MID component, although its 3D geometry gives rise to some new challenges.

7.4.1 Mounting Techniques

Solder paste, as for PCB mounting, is an established medium to bind the component to the substrate. Nevertheless, robots usually used to apply solder paste and component placement in PCB assembly lines, are either unsuitable or only conditionally suitable for MID production [3].

An MID product can generally be described as having different planar surfaces, the so-called process surfaces. Normally, solder paste or conductive-adhesive (an alternative solution to solder paste) are deposited onto these process surfaces, prior the components (chip, switch...) being placed. In one case, the MID product is heated until the solder paste reaches the melting point, then it cools down and solidifies, achieving an electrical connection between the pad of the electrical circuit and the component. In the second case, the conductive-adhesive medium is cured (e.g. by Ultra Violet radiation or in an oven).

Solder paste is composed of metal powder and a medium called flux. When heated up, the metal powder melts and the flux liquefies. Once the system has cooled down, only the soldered metal joint remains, and the flux has been removed. Conductive adhesives on the other hand, are composed of metallic fillers and a polymer matrix (resin), which require a lower temperature for the curing process. When dealing with a thermally sensitive system, this kind of connection medium is preferable.

Besides solder paste or conductive adhesive bonding, there are other techniques, such as wire bonding, to obtain the electrical connection. Wire bonding is a cost effective and flexible method, which does not require the heating of the whole substrate. Wire diameters range from 20 to 500 μm , and are employed for high power applications. Wire materials are either aluminium, silver, or gold. Thermo-compressing coupled with ultrasound is preferred to bond the wires. In this case, the metal is heated up to 100–500 $^{\circ}\text{C}$, bonded on the chip and then moved to the connection pad where it is bonded again and finally cut from the rest of the wire bobbin.

7.4.2 Positioning

In the automated placement of electronic components during surface mount technology (SMT), a gripping tool—usually a vacuum pipette—picks up the

component from a feeder. The joining direction and the surface must be perpendicular, in order to guarantee the component does not tilt and be poorly positioned. When placing a surface mount device (SMD), traditionally four axes are needed (3 linear $[x, y, z]$ + 1 rotational degree of freedom); however, parts with multiple-process surfaces such as MID often require five to six axes equipment.

Two different cases are known: the circuit carrier is being immobilised and the components are rotated, positioned and placed; or the interconnect device is rotated and positioned as the components are being placed.

7.4.3 Challenges

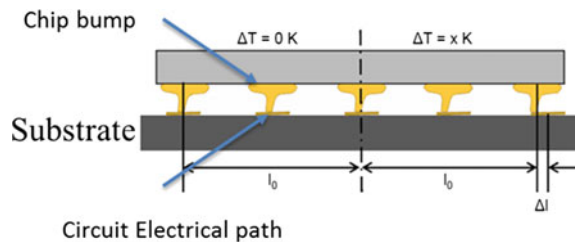
The specifics of connecting an electronic component with a conductor have to be taken into consideration in terms of connection processes, mediums applied and parameters for 3D-MID production. Multiple challenges are specific to MID manufacturing [14]:

- Wide-ranging of the solder joint, creating short circuit
- Roughness of the conductor structure
- De-lamination of the conductive tracks
- Conductor cracks if the thermal loading is high.

De-lamination of the conductive tracks and conductor cracks can be due to anisotropic effects and high coefficient of thermal expansion (CTE). A high thermal load can in some cases produces thermos-mechanical stresses at the boundary surfaces creating cracks or de-lamination.

Another problem linked to CTE is mismatches between chip and MID-substrate. Electronic components in general and ceramic components in particular, have low coefficients of thermal expansion compared to polymers. Consequently, the polymer substrate may expand more under heat load than the chip, which leads to the shearing of the bump from its pad. This results in a permanent mismatch as illustrated in Fig. 7.11.

Fig. 7.11 Shearing between substrate and chip pad due to differences of thermal expansion [9]



7.5 Sectors and Applications

When considering different MID applications, the diversity of the products available, the sectors and the industry using MID technologies is apparent (Fig. 7.12). Two industries in particular demonstrate significant potential for high-end MID application. These two sectors are the automotive industry and the medical technology. On the other hand, IT and telecommunication sectors are characterised by mass production de-localised in Asia [15].

The automotive industry is a very competitive sector, where MID have to be highly reliable and cost effective. Nevertheless, these requirements are reachable. An ever-stronger demand for more security and more functions push designers to integrate MID products into their vehicles. Pressure sensors developed by Bosch for ABS/ESP and 2D switching modules integrated to the steering wheel are significant example applications for this sector.

The telecommunication sector requires slimmer and lighter devices. Integrated antennas to smartphone cases became the biggest market for MID devices. The benefit lies in the combination of the 3D design freedom with electromagnetic transceiver properties for different wireless standards, including for example Wifi, Bluetooth, UMTS and LTE Antenna which can be fabricated with different technology as previously explained. Moreover, more antenna are also being integrated in laptop cases.

The medical industry sees the interest of tiny package applications, integrating electronics, especially in a society where the ageing population and healthy lifestyles increase healthcare expenditure. Hearing aids are probably the star product but others are emerging such as insulin pumps.




Sectors	Application	Example
Automotive	Air conditioning Position sensors Pressure sensors 2D Switching modules	Pressure Sensors (harting) 
Telecommunication	Multi band antennas Passive UHF RFID Transponders	Multi band antennas (TE connectivity) 
Medical	Multi LED Insulin pumps Hearing aid	Hearing aid (phonak) 

Fig. 7.12 Most common MID applications and sectors

7.6 Application Case

The device chosen to illustrate this chapter and to underpin the theory discussed earlier, is a lab-on-chip for immunoassay. MicroWebFab (an SME micro-fabrication network) has developed this device. The purpose of the MrBead device is the detection of antibodies using paramagnetic beads and the Giant Magneto Resistance (GMR) effect. Paramagnetic beads are bound to the GMR sensor surface by the target antibodies (ELISA-assay). Under the influence of a magnetic field generated in the instrument, the GMR sensor detects the field distortion caused by the bound beads.

The device ($27 \times 50 \times 3 \text{ mm}^3$) is composed of two parts. The top part carries the conductive paths and the fluidic network. The fluidic network consists of the inlet, a reagent chamber, the measurement area above the sensor, a waste chamber, and the fluidic port to the instrument, all connected by a micro-channel.

The top part is fabricated by two-shot injection moulding technology. The first component is made of metallisable polymer (LCP 820 i PD) and the second component of non-metallisable polymer (LCP E 471). The resulting conductive paths have a minimum width of $120 \mu\text{m}$ and a distance between the paths of $340 \mu\text{m}$. A schematic of the device can be seen in Fig. 7.13.

The bottom part provides the base surface of the channel and contains a cavity in which the GMR-sensor chip is attached in such a way that the sensor surface is level with the base surface of the channel, see Fig. 7.14. Gold stud bumps on the contact pads of the GMR sensor chip are the interface to the conductive paths in the top part. Once the top and the bottom part are thermally bonded together, the fluid channel is sealed and the gold bumps fuse with the gold coating of the conductive paths. This solution was selected because the dispensing of adhesive was critical

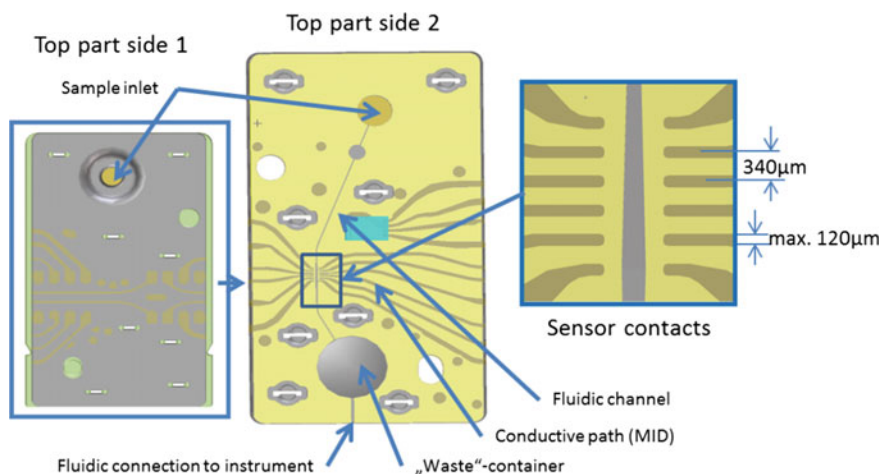


Fig. 7.13 Lab on chip for immunoassay developed by MicroWebFab

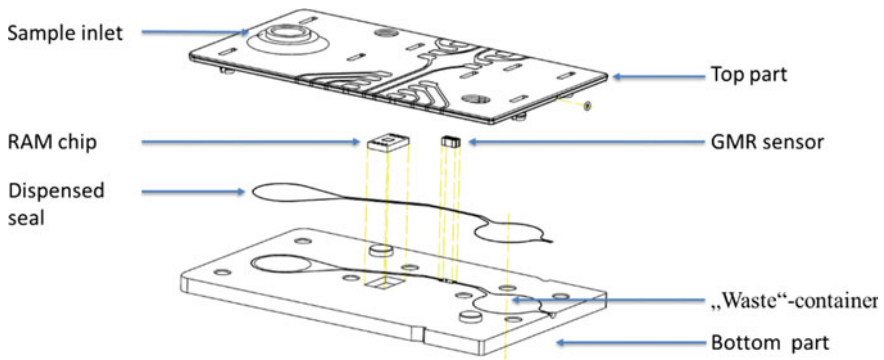


Fig. 7.14 Lab on chip for immunoassay developed by MicroWebFab. Assembly

given the close vicinity of the fluid channel, and the resulting danger of clogging due to over spill of adhesive.

The mould fabrication has been one of the main challenges for the product development due to the fine structured conductive tracks and the resulting long and narrow flow paths.

Once the part has been moulded, the conductive tracks have to be realised. The process is called ‘currentless metallisation’. The first step, pickling, is the immersion of the part into a potash solution, to clean the surface and activate the metallisation nuclei embedded in the material. During the second step the part is placed in a bath of copper until $5\ \mu\text{m}$ grow on the metallisable polymer. The process is repeated with nickel and gold baths to obtain a $2\ \mu\text{m}$ layer of nickel and then a $0.2\ \mu\text{m}$ layer of gold is put on top of the nickel layer.

References

1. Franke J, Gausemeier J, Goth C, Dumitrescu R (2011) MID-Studies 2011—Markt- und Technologieanalyse. Eine Studie im Auftrag von Forschungsvereinigung Räumliche Elektronische Baugruppen 3-D MID e.v. (Ed), Erlangen
2. Franke J (1995) Integrierte Entwicklung neuer Produkt- und Produktionstechnologien für räumliche spritzgegossene Schaltungsträger (3D MID). Hanser, Munich
3. Osswald TA, Baur E, Brinkmann S (2006) International plastics handbook, 4th edn. Hanser, München
4. Franke J (2014) Three-dimensional molded interconnect devices (3D-MID). Materials, manufacturing, assembly, and applications for injection molded circuit carriers. Hanser, München
5. ISO, 1133-1 (2011) Plastics—determination of the melt mass-flow rate (MFR) and melt volume-flow rate (MVR) of thermoplastics. International organization for standardization
6. 3-D MID e.V. Forschungsvereinigung Räumliche Elektronische Baugruppen [Online]. Available <http://www.3d-mid.de/2/technology/manufacturing/two-shot-molding/molding-tool.html>. 21 Sept 2016

7. De Zwart RM, Tacken RA, Bolt PJ (2006) Development of a MID LED housing. In: Proceeding of the global conference on micro manufacture, Grenoble
8. Franke J (2013) Räumliche elektronische Baugruppen (3D-MID), Werkstoffe, Herstellung, Montage und Anwendungen für spritzgegossene Schaltungsträger. Hanser, München
9. LPKF laser and electronics [Online]. Available <http://www.lpkfusa.com/mid/materials.htm> 21 Sept 2016
10. FAPS—Lehrstuhl für Fertigungsautomatisierung und Produktionssystematik [Online]. Available <http://www.faps.de> 21 Sept 2016
11. Panasonic [Online]. Available <https://www.panasonic.com> 21 Sept 2016
12. Barali L, Ernst C, Elspass S (2006) Lasergestützte MID-Technologien. In: Geiger M et al (eds) Laser in der Elektronikproduktion & Feinwerktechnik—Tagungsband, ninth Erlanger Seminars LEF. Meisenbach, Bamberg
13. Heininger N, John W, Boßler H-J (2004) Fertigung von MID-Bauteilen vom Rapid Prototyping bis zur Seriemit innovativer LDS-Technologie. Firmenschrift LPKF Laser & Electronics AG, Garbsen
14. Hoerber J, Goth C, Franke J (2012) Potential of aerosoljet printing For manufacturing 3-D MID. Innov'Days, PEP, Bellignat
15. Goth C (2013) Analyse und optimierung der entwicklung und zuverlässigkeit räumlicher schaltungsträger (3D-MID). Meisenbach, Bamberg

Chapter 8

Micro-scale Geometry Measurement

Samanta Piano, Rong Su and Richard Leach

8.1 Introduction

The ability to produce complex, high-precision, miniature components is key to the transition to high-value manufacturing. The advanced manufacturing industries, using precision machining techniques, such as diamond turning, injection moulding, micro-milling and micro-electro-discharge machining, currently have a number of capabilities for measuring small-scale structures with micro-scale tolerances, either with tactile or non-tactile systems [1].

Metrology is essential for the reduction of dimensional tolerances, which allows the production of more efficient machines and the improvement of their longevity by reducing play or wear. An example is smaller and more efficient injection nozzles in combustion machines, which critically depend on improved dimensional measurement capabilities. Further examples are radio frequency or fibre optic connector components, where feature sizes and tolerances require measurement uncertainties at the 0.1 μm level, or small aspherical/freeform lenses in digital cameras or mobile phones [2]. An emerging sector is high-tech medical products, which very often critically depend on small components, for example, in insulin pumps, cardiac pacemakers, in vivo diagnostic sensors or medical endoscopic imaging systems.

In this chapter, contact and non-contact techniques that can be used to measure 3D features on the micro-metre scale are reviewed.

S. Piano (✉) · R. Su · R. Leach
Manufacturing Metrology Team, Faculty of Engineering, University of Nottingham,
University Park, Nottingham NG7 2RD, UK
e-mail: Samanta.Piano@nottingham.ac.uk

R. Su
e-mail: Rong.Su@nottingham.ac.uk

R. Leach
e-mail: Richard.Leach@nottingham.ac.uk

8.2 Contact Techniques

Stylus instruments and coordinate measuring machines are widely used in modern manufacturing processes as accurate and precise dimensional measuring tools. This section describes the main characteristics of contact techniques, focusing on their capability to measure micro-scale manufactured parts.

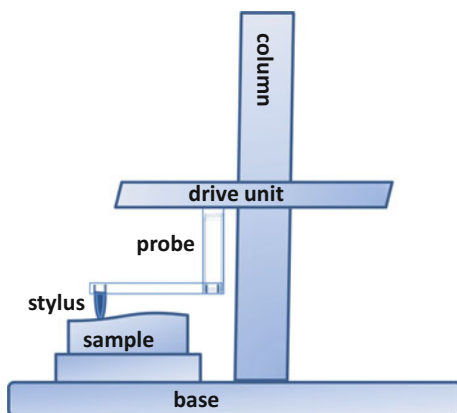
8.2.1 Stylus Instruments

A stylus instrument consists of a sharp tip placed in contact with the surface being measured. By scanning the tip across the surface and monitoring its response to surface heights, it is possible to measure surface topography. A schema of a stylus instrument is shown in Fig. 8.1.

As the stylus tip is scanned across the surface, its vertical displacement is recorded in order to produce a height map and converted into an electrical signal using an electro-mechanical transducer [3–6]. The tip plays a critical role in the performance of a stylus instrument as it is in physical contact with the surface. The stylus tip is usually made of diamond but other materials, such as aluminium oxide, are often employed depending of the material of the surface being measured. Other parameters that should be taken into account are the shape and size of the stylus tip, which directly affect the spatial frequency response of the instrument. Depending on the application, the stylus tip can have different geometries; the most frequently used has a conical shape with a rounded contacting edge and radius of curvature ranging from 2 to 10 μm , and a 90° slope angle [7].

One effect that should be taken into account is the systematic error associated with the shape of the stylus tip that will distort the measured topography [8, 9]. This issue has been intensively studied, and mathematical models have been proposed to include

Fig. 8.1 Schema of a stylus instrument



the distortion effect and improve the accuracy of measurements [10–12]. The ability of a contact stylus to detect samples with steep surfaces has also been a subject of investigation; for this a new slope-adapted sample-tilting method has recently been proposed, showing a significant reduction of the measurement error [13].

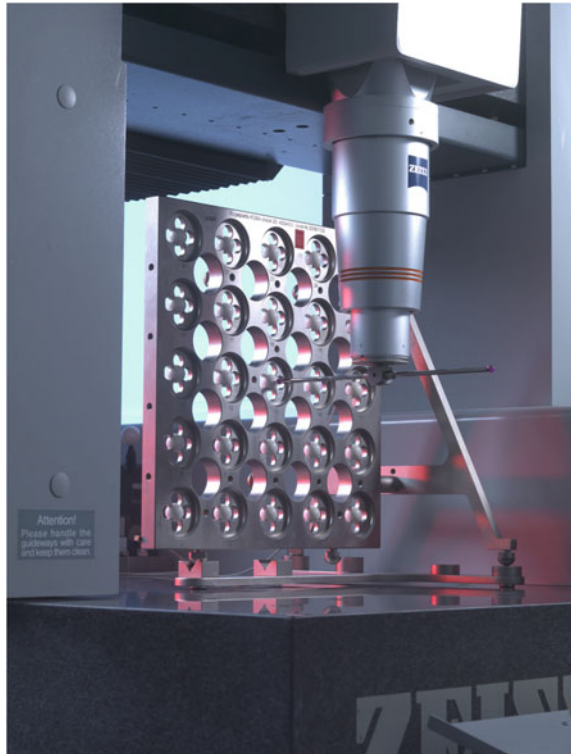
Although stylus instruments are widely used for surface profile measurement, if used with a large radius spherical tip, such an instrument can also be used to measure surface form. However, use of a stylus instrument for 3D measurements in a production or in-line process is limited due to the operating time, which can be up to several hours for a high-density grid of points.

8.2.2 *Micro Coordinate Measuring Machines*

8.2.2.1 Introduction to Coordinate Measuring Machines

A coordinate measuring machine (CMM) measures the physical dimensions of an object [14]. As shown in Fig. 8.2, a CMM generally consists of three orthogonal linear axes for accurate movement of a probe in a Cartesian coordinate system.

Fig. 8.2 Moving bridge type CMM with spherical styli. Image courtesy of Mr. David Flack at the National Physical Laboratory



The probe on a CMM usually has a spherical stylus tip that is used to contact the object being measured. The coordinates of the stylus tip are registered when in contact with the surface of the object being measured. After compensation for the stylus radius, the coordinates of the surface can be determined.

There are many different geometrical configurations of CMM that use different moving bridges and rotary tables [4]. Some configurations may have additional rotational axes [15]. A modern CMM is usually operated using computer numerical control (CNC) software. This allows for automated 3D measurement if the CMM is programmed with input from a computer-aided design (CAD) model of the part being measured.

8.2.2.2 Capability of Commercial Micro-CMMs

The increased demand on the manufacture of micro-scale products requires CMMs to be able to measure micro-scale parts accurately. So-called “micro-CMMs” have been developed to meet this demand. Generally, a micro-CMM can be designed by miniaturisation of the traditional CMM or using a probe that employs optical technology. State-of-the-art micro-CMMs typically have working ranges of tens of millimetres with hundreds of nano-metre volumetric accuracy, and can be used to measure features with milli-scale to micro-scale dimensions. Typical examples of commercial systems are the Zeiss F25 micro-CMM [16] the IBS Isara 400 Ultra precision CMM [17] and the SIOS Nano-measuring Machine (NMM) [18]. The Zeiss F25 CMM has a measurement volume of 100 mm × 100 mm × 100 mm, and a maximum permissible error (MPE) statement of $0.25 + L/666 \mu\text{m}$, where L is the measurement length in millimetres. The Isara 400 minimises the Abbe error [19] by aligning three linear interferometers to the centre of the stylus tip. The measurement volume is 400 mm × 400 mm × 100 mm, and the stated 3D measurement uncertainty is 109 nm (at $k = 2$). The NMM is a laser interferometer-based micro-CMM developed by the Ilmenau University of Technology. The measurement range is 25 mm × 25 mm × 5 mm with a sub nano-metre resolution of motion. In addition, several other micro-CMMs exist and several reviews of existing micro-CMMs can be found elsewhere [4, 20, 21].

8.2.2.3 Micro-probing Systems

One of the most important components of a micro-CMM is the probing system. The probing system is defined in ISO 10360 part 1 [22] for conventional tactile CMMs and Fig. 8.3 shows the main components. In general, probe technologies for micro-CMMs include mechanical probes, silicon-based probes, opto-mechanical probes and vibrating probes. An in-depth review of micro-CMM probes can be found elsewhere [23].

Mechanical micro-CMM probes are based on the same concepts as classical CMM probes, but they are highly-refined and optimised for sensitive detection and low-force probing. As styli with 100 μm or smaller diameters become available, the measurement is highly sensitive to the probing force. Reducing the probing force may reduce the possible damage caused by plastic deformation and increase the accuracy of the measurement significantly.

Examples of mechanical micro-CMM probes include the probe developed at METAS, which relies on precision flexure hinges and inductive sensors [24], the IBS Triskelion (three-legged) design and highly sensitive capacitors [17], and the 3D mechanical probe design that uses DVD pickup heads as the sensing element [25]. The IBS Triskelion and METAS probes are shown in Fig. 8.4.

The advantage of silicon-based probes is the reduced probing force by using silicon flexures, membranes or meshes to suspend the stylus [26]. Production techniques from the integrated circuit industry are used to design and manufacture silicon-based micro-probes. Highly complex designs are enabled by etching and deposition techniques.

The displacement of the stylus can be detected by using optical detection based on deflection of a laser beam, interferometric measurements, a capacitive sensor, or a piezo-resistive strain sensor on silicon flexure or membrane. For example, Physikalisch-Technische Bundesanstalt (PTB) developed the “Boss-probe” where piezo-resistive strain sensors are etched onto silicon membrane (as shown in Fig. 8.5). The deformation that results from probe contact with the surface being measured is detected [27].

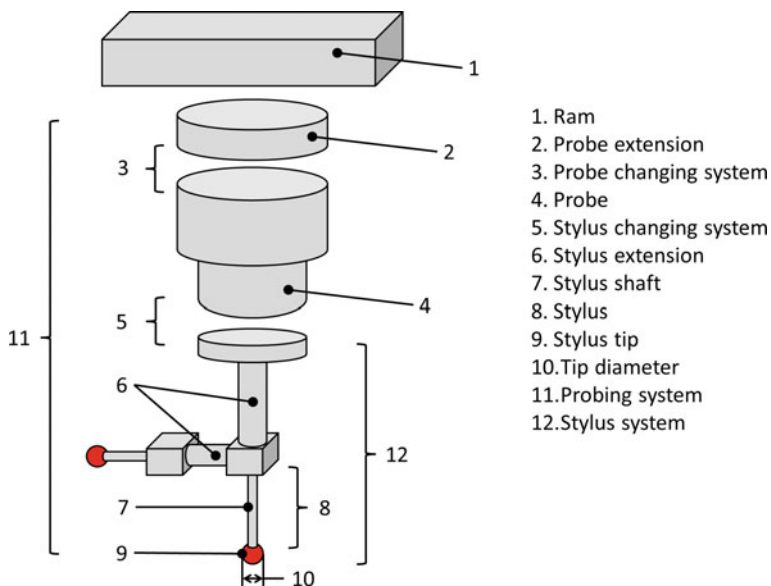
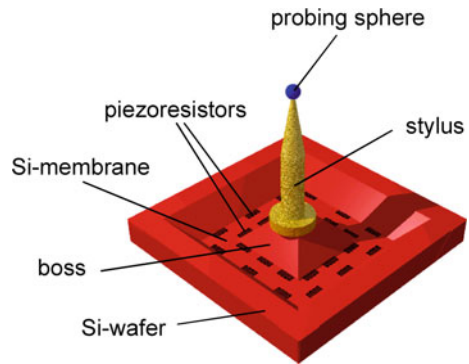


Fig. 8.3 Typical tactile probe and stylus system



Fig. 8.4 The IBS Triskelion [17] and METAS micro-CMM probes [24]

Fig. 8.5 Schema of the Boss-probe developed at PTB [27]



Details of other silicon-based micro-probes can be found elsewhere [28, 29]. A problem with silicon-based micro-CMM probes is anisotropy of probe stiffness. Opto-mechanical probes are designed to address this problem and the need for low force probing. Opto-mechanical probes rely on optical measurement of the stylus tip that is in contact with the surface being measured, so that flexure elements are not needed.

A probing system designed by PTB [27] uses an optical fibre with a spherical tip as the stylus. As shown in Fig. 8.6, two microscope objectives are used to measure the movement of the probe tip in the x , y and z axes. The measuring force of this fibre probe is on the order of $10\ \mu\text{N}$. However, the probe tip is likely to stick to the surface being measured, and probing forces are not isotropic. Another example of an optical fibre probe has been developed at the National Institute for Standards and Technology [30].

Vibrating micro-CMM probes have been designed and developed to address the problem of surface interaction forces, which become significant when a stylus tip diameter is of the order of $100\ \mu\text{m}$ and lower. The influences of surface interaction forces can be reduced by using a vibrating probe tip, and the problem of sticking is

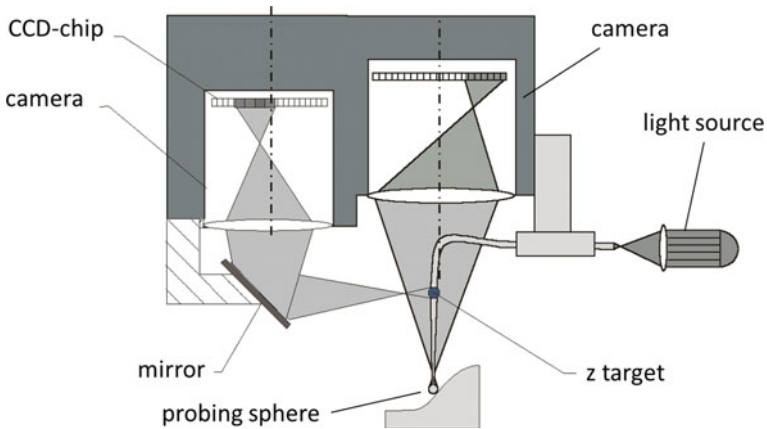


Fig. 8.6 Schema of the 3D PTB fibre probe [27]

minimised. With vibrating probes, the surface is measured by analysing the detected vibration characteristics.

An example of a commercial vibrating micro-CMM probe is the UMAP system from Mitutoyo [23]. The UMAP probe vibrates the stylus vertically at several kilohertz. The estimated repeatability of the system is about 100 nm, which is often not suitable for high-accuracy measurement. Other vibrating probes with nano-metre repeatability and/or nano-newton contact force exist [31, 32]. There are various methods to vibrate the probe tip, for example, oscillation at a frequency of several tens of kilohertz by a quartz oscillator, or by laser trapping an 8–10 μm diameter silica sphere and vibrating the probe in the z axis at frequencies up to 50 MHz [31].

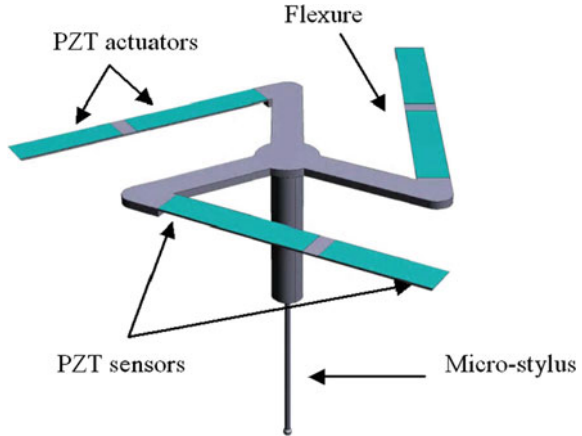
These vibrating probes can only oscillate in one dimension. A 3D vibrating micro-CMM probe has been developed at the National Physical Laboratory (NPL) [33], see Fig. 8.7. The NPL probe consists of a triskelion flexure and a micro-stylus, and vibrates by using six piezoelectric (PZT) actuators.

8.2.2.4 Sources of Error on CMMs

A typical CMM has twenty-one sources of geometric error [4]. Each axis has a linear error, three rotation errors and two straightness errors (six per axis gives eighteen). The final three errors are the orthogonality errors between any two pairs of axes. The CMM geometric errors are measured in one of the four following manners:

- using instruments such as straight edges, autocollimators and levels;
- using a laser interferometer system and associated optics;
- using a calibrated-hole plate [34]; and
- using a tracking laser interferometer [35].

Fig. 8.7 NPL vibrating micro-probe [33]



With modern computers, CMMs can be error-mapped (volumetric error compensation) with corrections to geometric errors made in software [36, 37]. Temperature dependent measurement error can be compensated using a parametric approach [38]. The measurement uncertainty of a CMM can be assessed by using a simulation method [39]; CMM software also needs to be tested based on ISO 10360 part 6 [40].

8.3 Non-contact Techniques

There are different types of commercial non-contact techniques. This section focuses on optical instruments that are suitable to measure 3D micro-systems: focus variation microscopy, coherence scanning interferometry, confocal microscopy, laser triangulation and micro-fringe projection. In contrast to traditional contact techniques, optical instruments are able to perform 3D measurements without touching the surface, they can be much faster when imaging over an area and can determine colour information.

8.3.1 Focus Variation Microscopy

Focus variation (FV) microscopy provides information about the topography and colour of a measured surface [41, 42]. FV is able to perform high-resolution form and texture measurements [43]. A schema of a FV microscope is given in Fig. 8.8.

In a typical FV microscope, the light generated by a broadband source, is focused onto the sample through a system of objective lenses and a beam-splitting mirror. The light is scattered from the sample into different directions depending on

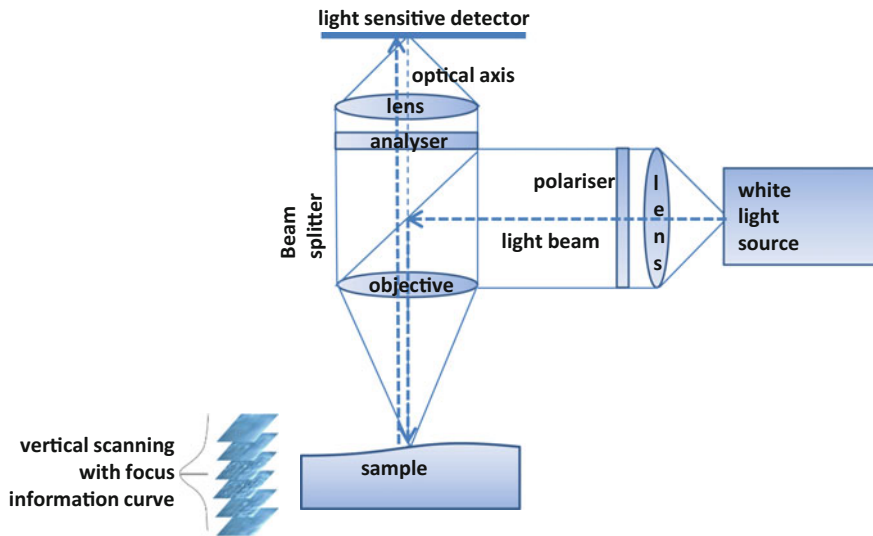


Fig. 8.8 Schema of a focus variation microscope, adapted from [42]

the topography. The scattered light reaching the objective lenses is then transmitted through the beam-splitting mirror and received by a light sensitive detector. In order to have a 3D complete map of the surface of the sample, the objective lenses are moved vertically along the optical axis. Due to the surface topography, only a single plane will be in focus, resulting in a changing of contrast on the light sensitive detector. Algorithms are used to analyse the variation of the focus in the vertical axis in order to convert the acquired data into 3D information and a colour image of the sample [44, 45]. The vertical scan range, depending on the working distance of the objective, can vary from 3.2 to 22 mm, with a resolution as high as 10 nm. The xy range typically varies from around $0.1 \text{ mm} \times 0.1 \text{ mm}$ to $5 \text{ mm} \times 5 \text{ mm}$ for a single measurement (depending on the objective), but can be increased up to $100 \text{ mm} \times 100 \text{ mm}$ by using stitching algorithms and a motion stage. The FV technique can be used to measure samples with high slope angles, exceeding 80° [46].

Relying on the contrast and sharpness in the images taken from the measurements to determine the point of focus, the FV technique is limited to surfaces with a certain degree of roughness (or needs another contrast-generating mechanism).

8.3.2 Coherence Scanning Interferometry

Coherence scanning interferometry (CSI) refers to low coherence interferometry techniques, also known as scanning white light interferometry, coherence cor

synchrotron, XCT relation interferometry and vertical scanning interferometry [47–49]. Many other terms are used to refer to CSI, but they all refer to the same fundamental principle that uses the coherence property of light to measure surface topography and object geometry.

As shown in Fig. 8.9, a typical CSI system contains a broadband source for generation of low temporal coherence illumination, a CCD camera for capturing the image, and an interferometer with a high-precision motion system (often PZT) for axial scanning of the reference mirror [48]. Usually a Mirau interferometer configuration is used when employing a high-magnification objective lens and a Michelson interferometer is used with a low magnification lens.

The operating principle of CSI is based on low coherence interferometry; where the interference signal is generated when the reference and sample beam have equal optical path length. The peak position of the interference signal corresponds to the position of the sample surface. By scanning the reference mirror, the sample surface is scanned axially and a height map is established. The details of the operating principle can be found elsewhere [48]. Usually the interference signal received by a pixel of the camera is similar to that shown in Fig. 8.9b. The signal is a sinusoidal carrier that is modulated by a slowly varying modulation envelope. The surface location can be extracted as the peak position of the envelope of the interference

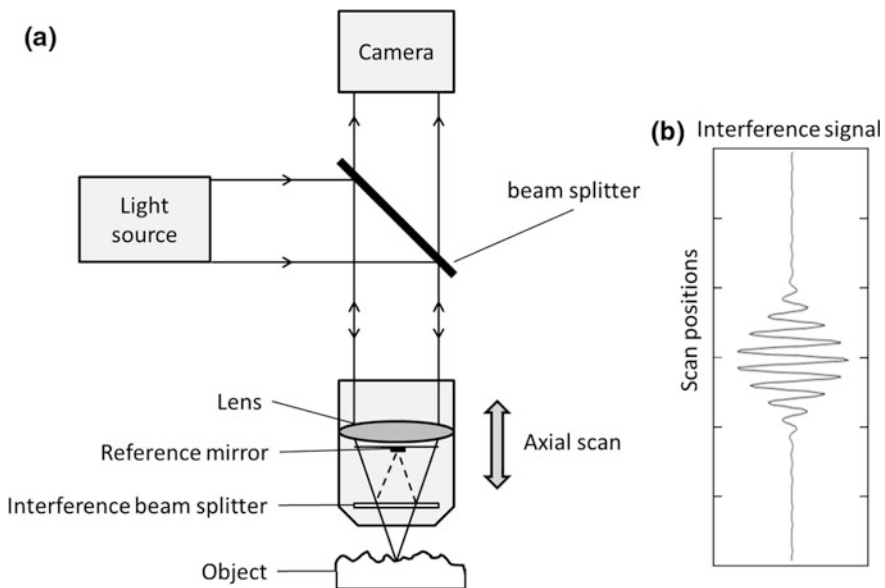


Fig. 8.9 Schema of a CSI system with Mirau objective (a) and simulation of the CSI signal recorded by a pixel (b)

signal or by the centroiding method that is more robust against noise in some cases [47]. Most modern CSI instruments combine envelope detection with interference phase information to improve the precision [50]. After signal processing, the extracted height at each pixel forms the measured height map of the surface. Typically, the field of view (FOV) is from around $0.1 \text{ mm} \times 0.1 \text{ mm}$ to $4 \text{ mm} \times 4 \text{ mm}$ (depending on the objective), and the scanning depth is around a few hundred micro-metres. Larger FOVs can be achieved at the cost of sacrificing lateral resolution [51]. Stitching techniques may increase the measurement range in the lateral and axial directions [52], but the accuracy will degrade and be dependent on the accuracy of the motion system and data processing.

Sub-nano-metre axial resolution and repeatability can be achieved in modern CSI systems, but the absolute accuracy is difficult to determine [53]. The accuracy is influenced by the interaction between the light and different materials with different optical properties. For example, for a flat surface containing multiple materials, a pseudo height effect can be observed which is caused by the phase change on reflection [48].

CSI techniques can also operate without mechanical axial scanning, which is carried out by means of spectroscopic analysis or wavelength scanning [54, 55]. Wavelength scanning interferometry may increase the measurement speed and be used for in-line applications requiring high immunity to external vibration [56].

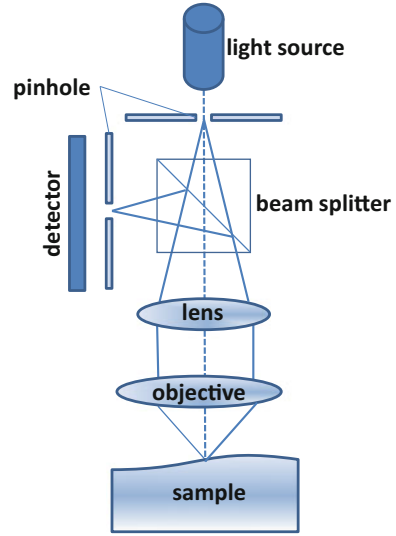
A recent development is model-based CSI. This development allows for measurement of semi-transparent thin film thickness and features with lateral critical dimensions on nano-metre scales, which is smaller than the diffraction limit [57]. Model-based CSI has found application in the semiconductor and flat panel display industries [58].

8.3.3 *Confocal Microscopy*

The principle of confocal microscopy (CM) was originally developed by Minsky in the mid-1950s [59, 60], and the first commercial instrument appeared in 1987. The development of CM has been possible thanks to progress in optics and electronics, and today it is a 3D optical imaging technique used in many applications, from semiconductor materials to life science systems [61–63]. Depending on the application, different CM configurations have been proposed and realised, varying in the way to illuminate the sample and/or to detect the returning beam. It is possible to distinguish three categories of CM: laser scanning, disc scanning and array scanning [64]. The principle of CM is illustrated in Fig. 8.10.

In a typical laser scanning CM, the light emitted by a laser illuminates the sample after passing through a pinhole aperture, a beam-splitter and an objective lens. The light reflected back from the sample is incident on the detector after passing through a second pinhole, which minimises the effect of the out-of-focus light. In this way, only the in-focus light is recorded and contributes to the

Fig. 8.10 Confocal microscopy set-up with the sample in focus



reconstruction of the sample topography. The image created by CM is a planar section of the sample and the 3D topography of the sample is obtained by scanning the sample along the optical axis and reconstructing the 2D images.

The resolution of a CM depends on the diffraction limit and can be further enhanced by reducing the size of the pinholes, via the so-called “pinhole effect” [64]. For larger pinhole size, the confocality degrades and the signal is broadened, on the other hand the pinhole size cannot be reduced arbitrarily because this also reduces the incident light intensity and consequently the signal-to-noise ratio [65]. In particular, for pinhole sizes larger than 0.25 AU (AU = Airy unit, defined as the diameter of a diffraction-limited spot on the plane of the objective), the instrument is in the regime of geometric-optical confocality and the lateral resolution is given by the radius of the Airy disk, defined as the distance from the centre of the bright spot to the centre of the first dark ring [64, 66, 67]

$$R_{Airy} = 0.61 \frac{\lambda}{A_N}, \quad (8.1)$$

where λ is the wavelength of the light and A_N is the numerical aperture. For pinhole sizes smaller than 0.25 AU, the instrument is in the wave-optical confocality regime, where the effects of diffraction have to be taken into account, which results in an enhanced lateral resolution given by [64]

$$R_{Airy} = 0.37 \frac{\lambda}{A_N}, \quad (8.2)$$

where λ is the wavelength of the incident light and A_N is the numerical aperture.

The lateral resolution thus varies typically between 0.25 μm (blue light source) and 1.5 μm (red light source) [4]. The axial resolution, instead, is defined by the full width at half maximum of the point spread function of the Airy disk, and is given by [64]

$$R_{axial} = \sqrt{\left(\frac{0.88\lambda}{1 - \sqrt{1 - A_N^2}}\right)^2 + \left(\frac{\sqrt{2}d_{hole}}{A_N}\right)^2}, \quad (8.3)$$

in the geometric-optical confocality regime (where d_{hole} is the size of the detection pinhole), and

$$R_{axial} = \frac{0.64\lambda}{1 - \sqrt{1 - A_N^2}}, \quad (8.4)$$

in the wave-optical confocality regime.

The measurement speed of CM depends on the time it takes to scan in the xy direction; a laser scanning microscope needs to scan point by point and usually can generate 5–10 images per second (512×512 pixels per image) [64]. Disc scanning and micro-display scanning CMs are often much faster than a scanning system using galvo-mirrors [4].

Unlike the other optical techniques in this chapter, CM has a high numerical aperture, which leads to a high lateral resolution. Moreover, due to the pinhole effect, the resolution can be increased over the limits defined by the Abbe criterion [4]. The CM is also able to measure high local slope angles, that for rough surfaces can be close to 90° [64]. Furthermore, CM instruments are able to measure surfaces containing dissimilar materials without the need for any correction of the measurements.

8.3.4 Laser Triangulation

In laser triangulation (LT) a light pattern, generated from a laser, is projected on to an object and the reflection is captured by a digital camera [68]. A typical configuration of a LT system is shown in Fig. 8.11.

With reference to Fig. 8.11, if (x, y, z) is a 3D point on the object illuminated by the laser light, and f is the focal length of the lens, its projection (x', y') on the image plane will be $x' = xf/z$, $y' = yf/z$. By knowing the baseline distance d and the angle θ between the laser and the lens, which obey the condition

$$d = \frac{z}{\tan \theta}, \quad (8.5)$$

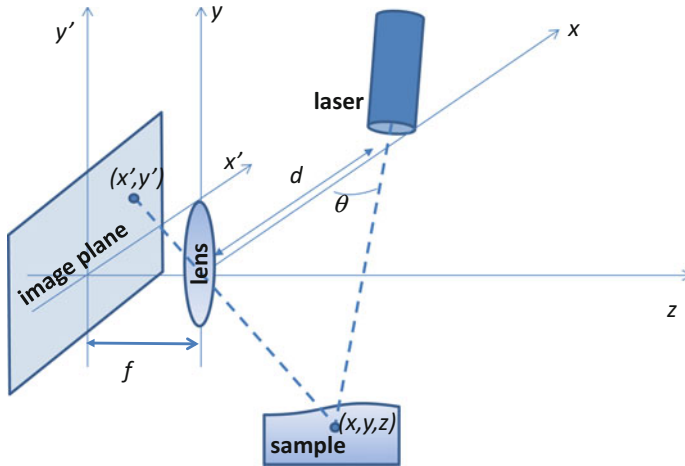


Fig. 8.11 Principle of laser triangulation

it is possible to define the real coordinates (x, y, z) in terms of the focal length f and the angle θ ,

$$x = \frac{dx'}{f \cot \theta - x'}, y = \frac{dy'}{f \cot \theta - x'}, z = \frac{df}{f \cot \theta - x'}. \quad (8.6)$$

To have a complete map of the object, images are captured for different values of θ and for each image the values of x' and y' are determined on the CCD camera. The real coordinates are calculated using Eq. (8.6).

Due to its simplicity, the LT method is used in many sensors with applications ranging from measuring surfaces with large structures [4], to fuel cells [69] and plant phenotypes [70]. Different configurations of LT have been proposed in order to improve the resolution and the accuracy of the measurements. For example, some authors proposed to use two colour lasers to minimise the occlusion problem in the direction of movement of the camera [71]. The main advantages of LT are: the measuring speed, i.e. data rates up to 10,000 measurements per second, and the accuracy, as some sensors report a resolution of 2000:1–20,000:1 [72], in other words for a few millimetres range is it possible to achieve a sub micro-metre vertical resolution [4].

Despite its advantages, the LT technique has some inherent limitations that should be taken into account in order to obtain reliable information from the measured data. In principle, the laser spot should be infinitely small, but in practice it has a finite size. Also, due to the focus of the laser beam, its diameter can vary along the vertical scan. Moreover, as a consequence of some imperfections of the laser system, blur [73] and shadow [74] effects can appear in the image. Further sources of error are associated with the tilt angle of the surface, edge effects and

linearity errors [27]. A complete knowledge and understanding of the error sources should help to overcome some of the limitations of these sensors, making them suitable for many applications in micro-manufacturing.

8.3.5 *Micro-fringe Projection*

In a fringe projection (FP) instrument, a structured pattern, for example, a sinusoidal fringe pattern, is generated by a computer and projected onto the object to be measured [75]. The fringes, deformed by the object surface topography, are recorded by a camera and sent to a computer. The fringe data is analysed to obtain 3D shape information about the object. In Fig. 8.12, a typical schema of a FP instrument is shown.

The FP technique is typically used to measure objects from the metre to the millimetre scale and its first application to the micro-scale was proposed by Leonhardt et al. [76]. Even though the use of FP on the micro-scale is increasing, there have been only a small number of applications reported to date (see for example [77–82]). Micro-FP is generally based on a modification to a stereo microscope [81], or by employing a long working distance objective lens [83]. Because different types of lens can be used, the latter technique is more flexible and can be used in many different applications [82].

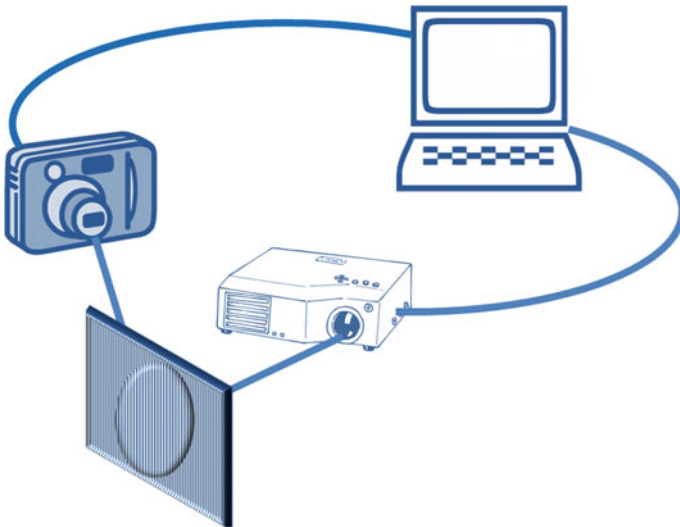


Fig. 8.12 Schema of a fringe projection instrument

The FP techniques differ in the way they generate the fringe pattern and in the methods used to analyse the fringe pattern [75]. Another important aspect of the FP technique is the calibration of the system in order to allow a measurement of the 3D height distribution, and different approaches have been proposed [75, 82].

Some authors have shown that, by using a FP technique, it is possible to measure a micro-V-groove with a size of $150\ \mu\text{m} \times 250\ \mu\text{m}$ and an angle larger than 45° with an error below 1% of the full-scale measurement range [78]. Others report that with a phase-shifting detection scheme it is possible to achieve accuracy better than one part in ten thousand of the FOV [78]. The resolution of the optics and the camera determine the lateral and vertical resolution in FP. The vertical resolution is also determined by the frequency of the projection pattern. A typical vertical resolution for FP systems is of the order of $1\ \mu\text{m}$ [82].

8.4 Tomographic Methods

The word tomography is derived from the Ancient Greek word “tomos”; meaning to slice and section. Usually tomographic imaging is referred to a 3D imaging method that is able to obtain dimensional and material information of the internal and external features of an object. Two tomographic methods suitable for micro-manufactured parts are introduced in this section, namely optical coherence tomography and X-ray computed tomography.

8.4.1 *Optical Coherence Tomography*

Optical coherence tomography (OCT) has been growing in popularity since 1991 [84]. OCT uses non-invasive detection and produces depth-resolved high-resolution 2D or 3D images of the back-scattering from internal micro-structures in an object. In general, OCT is based on the principle of low-coherence reflectometry and measures the “echoes” of backscattered light. As a tomographic imaging modality, a series of 1D depth z-scans, similar to ultrasound A-scans, are performed pointwise along a line in the lateral x-direction. By combining these scans for a given y-position, a 2D cross-sectional image (B-scan) is obtained in the xz plane. By further combining these cross-sectional images recorded at adjacent y-positions, a full 3D tomographic image can be obtained. OCT is a complementary method to other high-resolution 3D imaging techniques, such as ultrasound imaging, X-ray computed tomography (XCT) and magnetic resonance imaging (MRI).

Biomedical and clinical applications are the conventional driving force of OCT development, for example, real-time in vivo visualisation of tissue microstructures in eyes, arteries and nervous tissues [84]. However, new applications have spread broadly outside the biomedical field into materials investigation. Detailed overviews of OCT-based methods and applications in the fields of dimensional

metrology, materials research, non-destructive testing, art diagnostics, botany, micro-fluidics, data storage and security applications can be found elsewhere [85]. Specifically, OCT is suitable for detection of sub-surface and embedded features inside dielectric materials, such as glasses, plastics, polymers, ceramics and additive manufacturing materials [86]. The signal acquisition rate of OCT is high and has grown from two A-scans per second in the original version in 1991 to today's megahertz technology [87]. This advantage of high speed imaging shows potential for roll-to-roll manufacturing of ceramic micro-devices, printable electronics [88] and polymer solar cells [89]. The typical resolution of OCT is of the order of $10\ \mu\text{m}$ for both the axial and lateral directions.

OCT is usually divided into two groups: time-domain OCT (TD-OCT) and Fourier-domain OCT (FD-OCT). The principle of TD-OCT is very similar to CSI (see Sect. 1.3.2) but operates in the infra-red part of the spectrum. In the past decade, FD-OCT has attracted more attention and been developed rapidly. The most important advantage over traditional TD-OCT is that FD-OCT offers the possibility of much faster imaging speeds and higher detection sensitivities. Mechanical scanning of a reference mirror is no longer needed in FD-OCT. An A-scan is obtained by a Fourier transform of the spectrally-resolved interference fringes detected by using a spectrometer, for example, a line array camera. Such a system is called spectral-domain OCT (SD-OCT). Another option is swept-source OCT (SS-OCT), which uses a swept laser source (wavelength-tuning) with a single photodetector to record the spectrally-resolved interference fringes sequentially, while tuning the wavelength. More details of the principle of OCT can be found elsewhere [84]. A schema of SS-OCT is shown in Fig. 8.13 and a typical volumetric OCT image is shown in Fig. 8.14.

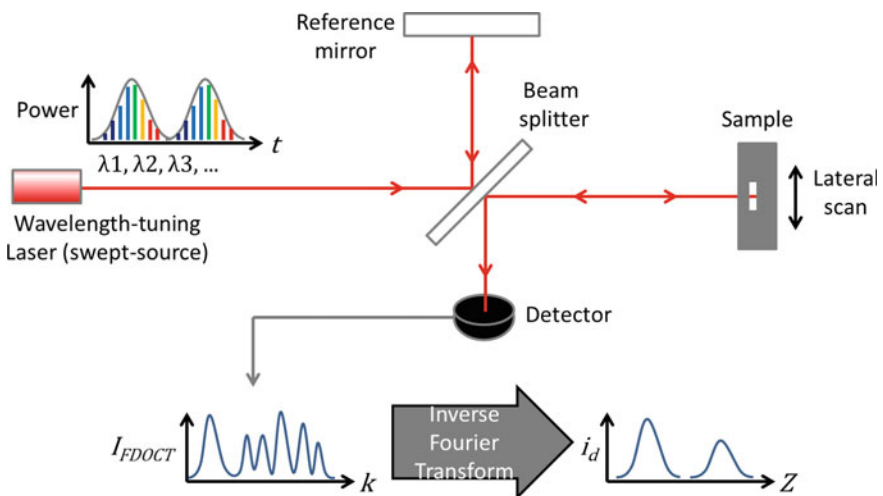


Fig. 8.13 Schematic setup of a swept-source OCT

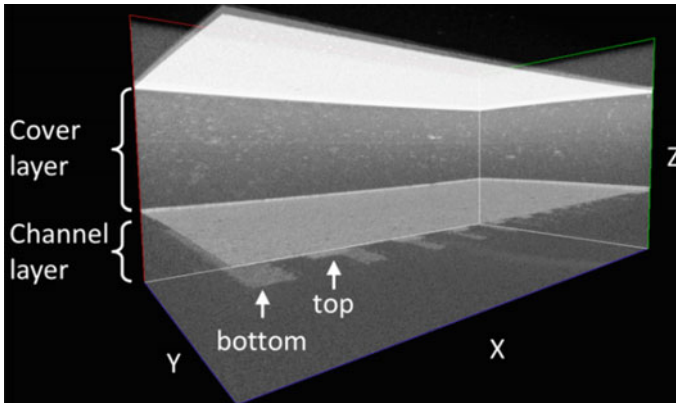


Fig. 8.14 Volumetric OCT image of a two-layer ceramic stack (image rendered for visualisation). A micro-machined channel layer is embedded beneath a zirconia layer. The z axis represents optical distance [90]

Various functional OCTs have been developed, including Doppler OCT [91], which measures the displacement of an object or flow, polarisation-sensitive OCT [92], which measures the birefringence properties of materials, ultrahigh-resolution full-field OCT, which produces tomographic images in the en-face orientation with micro-metre resolution for both axial and lateral directions [93], endoscopic OCT, which performs radial scanning [94], and a second harmonic generation (SHG) microscope combined with OCT for the investigation of subsurface regions of corrosion sites formed on metals below organic coatings [95].

The major problem regarding dimensional metrology and defect detection using OCT is the limited penetration of light due to high scatter. The central operating wavelengths of modern commercial OCT setups are usually around 800, 1300 nm or 1550 nm, which are optimised for the optical transparency window in biomedical tissues and take advantage of well-established optical communication technologies. However, for industrial applications, different wavelengths may be more suitable, for example the mid-infrared region for ceramic materials [96].

The uncertainty of dimensional measurement by OCT is difficult to determine. Speckle degrades image quality significantly [97]. The group velocity dispersion may degrade the axial resolution and the detection sensitivity [98]. Wavefront distortion from the scanning optics, image ambiguity due to inhomogeneity of the refractive index of the material being measured and multiple reflection effects have been observed [90]. Image analysis is also essential for ensuring the accuracy of surface segmentation [99].

8.4.2 X-ray Computed Tomography

X-ray computed tomography (XCT) is a powerful 3D imaging tool that has been used for clinical and industrial applications for decades. Industrial XCT has attracted much attention in recent years as it is promising for non-destructive dimensional metrology of micro-manufacturing parts with complex internal cavities and lattice structures, for quality inspection of complex assembled products and for checking interfaces of multi-material components [100, 101]. XCT is widely used for various applications due to the good penetration of X-rays in many engineering materials.

An XCT system usually contains an X-ray tube, a manipulation system, a detector and a computer [102]. Electrons are accelerated in the X-ray tube and hit an anode target (usually tungsten) to generate X-rays [103]. The highest energy of the X-rays is determined by the peak tube voltage, which usually ranges from 20 to 450 keV in commercial XCT systems [101]. Synchrotron sources that generate monochromatic X-rays can also be used for tomographic imaging [104], but at a much higher cost.

XCT detectors usually consist of a 1D or 2D array of pixels, corresponding to line detectors and flat panel detectors, respectively. A typical flat panel detector contains 2048×2048 pixels for an area of $400 \text{ mm} \times 400 \text{ mm}$. Most detectors use a scintillator to convert X-rays to visible light that can be captured by a camera [105]. Alternatively, ionization detectors that respond to energy deposition per unit mass can be used [105].

The manipulation system is used for translating and rotating the object being measured. A few thousand 2D X-ray radiographs, taken from different angles of an object, are recorded for further 3D reconstruction of the tomographic image using the Fourier slice theorem. The reconstruction is usually carried out by filtered back-projection, which is based on the linear integral transformation model developed by Radon [102, 106]. Different amounts of X-rays are absorbed when passing through different materials corresponding to the linear attenuation coefficients of the materials at a certain X-ray energy level. The linear attenuation coefficient is the desired value after reconstruction and relates to the material mass density.

Among the family of XCT systems, poly-energetic cone-beam XCT (CBCT) is used widely in both medical and industrial applications (as shown in Fig. 8.15). The magnification of the object relies on a simple principle of geometrical optics, i.e. a point source is assumed and the magnified projection of the object is dependent on the distance between the source and the object. A survey of different reconstruction methods for CBCT can be found elsewhere [106]. The scanning time of CBCT usually ranges from 30 min to a few hours. It is very difficult to achieve traceability in XCT due to the high number of influence factors and the stability of many set-ups. The most common systematic errors include geometrical errors [107], beam drift due to thermal expansion of the X-ray tube [108], beam hardening effects caused by errors in the estimation of the attenuation coefficient of the material

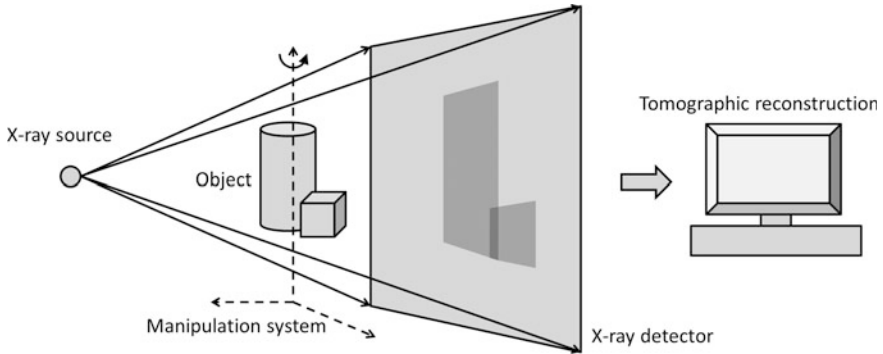


Fig. 8.15 Schema of a CBCT system

[109], partial volume artefacts caused by the limited field of view of the XCT system [110], and errors due to effects of scattering [111] and image lag [112]. Recently several studies and international comparisons have been conducted on uncertainty evaluation of XCT for dimensional measurements [113–115].

Industrial XCT is a fast growing technique. The scanning time is reduced significantly due to advances in XCT components and computing power. Several methods are available for extending the scanning field of view [116]. Multi-energy XCT may differentiate materials by using different X-ray spectra or energy-resolved detectors [117]. Phase-sensitive XCT can be used to enhance image contrast and edges of structures [118].

For micro-manufacturing, the spatial resolution of XCT is important. The resolution is influenced by many factors, for example focal spot size of the X-ray source, quality and pixel size of the detector, magnification of the image, and reconstruction algorithms [119]. Micro or nano-metre-scale imaging resolutions are achieved in state-of-art XCT systems [120]. By applying Kirkpatrick–Baez optics a synchrotron, XCT can reach 40 nm resolution [104].

References

1. Tosello G, Hansen HN, Marinello F, Gasparin S (2010) Replication and dimensional quality control of industrial nanoscale surfaces using calibrated AFM measurements and SEM image processing. *Ann CIRP* 59:563–568
2. Fang FZ, Zhang XD, Weckenmann A, Zhang GX, Evans C (2013) Manufacturing and measurement of freeform optics. *Ann CIRP* 62:823–846
3. ISO 25178 part 601 (2010) Geometrical product specifications (GPS)—surface texture: Areal—Part 601: Nominal characteristics of contact (stylus) instruments. International Organization for Standardization
4. Leach RK (ed) (2014) *Fundamental principles of engineering nanometrology*, 2nd edn. Elsevier, Amsterdam

5. Whitehouse DJ (2010) Handbook of surface and nanometrology, 2nd edn. CRC Press, Florida
6. Thomas TR (1999) Rough surfaces, 2nd edn. Imperial College Press, London
7. Leach RK (2001) The measurement of surface texture using stylus instruments. NPL Good Practice Guide. National Physical Laboratory, UK
8. Radhakrishnan V (1970) Effect of stylus radius on the roughness value measured with tracing stylus instruments. *Wear* 16:325
9. McCool JI (1984) Assessing the effect of stylus tip radius and flight on surface topography measurements. *ASME J Tribol* 106:202–209
10. Mendeleyev V (1997) Dependence of measuring errors of rms roughness on stylus tip size for mechanical profilers. *Appl Opt* 36:9005–9009
11. Lee C-O, Park K, Park BC, Lee YW (2005) An algorithm for stylus instruments to measure aspheric surfaces. *Meas Sci Technol* 16:1215
12. Lee DH (2013) 3-dimensional profile distortion measured by stylus type. *Measurement* 46:803–814
13. Fang H, Xu B, Chen W, Tang H, Zhao S (2015) A slope-adapted sample-tilting method for profile measurement of microstructures with steep surfaces. *J Nanomater* ID 253062 (in press)
14. Hocken RJ, Pereira PH (eds) (2011) Coordinate measuring machines and systems, 2nd edn. CRC Press, New York
15. ISO 10360 part 3 (2000) Geometrical product specifications (GPS)—acceptance and reverification tests for coordinate measuring machines (CMM)—Part 3: CMMs with the axis of a rotary table as the fourth axis. International Organization for Standardization
16. Vermeulen MMPA, Rosielle PCJN, Schellekens PHJ (1998) Design of a high-precision 3D-coordinate measuring machine. *Ann CIRP* 47:447–450
17. Widdershoven I, Donker RL, Spaan HAM (2011) Realization and calibration of the “Isara 400” ultra-precision CMM. *J Phys: Conf Ser* 311:012002
18. Jäger G, Manske E, Hausotte T, Büchner H-J, Grünwald R, Schott W (2001) Nanomeasuring technology—nanomeasuring machine. In: Proceedings of the ASPE, Crystal City, VA, Nov. 2001, pp 23–27
19. Leach RK (2015) Abbe error/offset. In: Laperrière L, Reinhart G (eds) CIRP encyclopaedia of production engineering. Springer, Berlin
20. Fan K-C, Fei Y-T, Wang W, Chen Y, Chen Y-C (2008) Micro-CMM. In: Smart devices and machines for advanced manufacturing, pp 319–335
21. Claverley JD, Leach RK (2015) A review of the existing performance verification infrastructure for micro-CMMs. *Precis Eng* 39:1–15
22. ISO 10360 part 1 (2001) Geometrical product specifications (GPS)—acceptance and reverification tests for coordinate measuring machines (CMM). International Organization for Standardization
23. Weckenmann A, Estler T, Peggs G, McMurtry D (2004) Probing systems in dimensional metrology. *Ann CIRP* 53:657–684
24. Küng A, Meli F, Thalmann R (2007) Ultraprecision micro-CMM using a low force 3D touch probe. *Measur Sci Technol* 18:319–327
25. Chu C-L, Chiu C-Y (2007) Development of a low-cost nanoscale touch trigger probe based on two commercial DVD pick-up heads. *Measur Sci Technol* 18:1831–1842
26. Haitjema H, Pril WO, Schellekens PHJ (2001) Development of a silicon-based nanoprobe system for 3-D measurements. *Ann CIRP* 50:365–368
27. Brand U, Kleine-Besten T, Schwenke H (2000) Development of a special CMM for dimensional metrology on microsystem components. In: Proceedings of the ASPE, Scottsdale, AZ, Oct. 2000, pp 542–546
28. Ruther P, Bartholomeyczik J, Trautmann A, Wandt M, Pau O, Dominicus W, Roth R, Seitz K, Strauss W (2005) Novel 3D piezoresistive silicon force sensor for dimensional metrology of micro components. In: Proceedings of the IEEE sensor, pp 1006–1009

29. Dai G, Bütefisch S, Pohlenz F, Danzebrink H-U (2009) A high precision micro/nano CMM using piezoresistive tactile probes. *Measur Sci Technol* 20:084001
30. Muralikrishnan B, Stone J, Stoup J (2007) Roundness measurements using the NIST fibre probe. In: *Proceedings of the ASPE*, Dallas, TX, Oct. 2007, pp 89–92
31. Takaya Y, Takahashi S, Miyoshi T, Saito K (1999) Development of the nano-CMM probe based on laser trapping technology. *Ann CIRP* 48:421–424
32. Seugling R, Darnell I (2008) Investigating scaling limits of a fibre based resonant probe for metrology applications. In: *Proceedings of the ASPE*, Livermore, CA, Oct. 2008
33. Claverley JD, Leach RK (2013) Development of a three-dimensional vibrating tactile probe for miniature CMMs. *Precis Eng* 37:491–499
34. Lee ES, Burdekin M (2001) A hole plate artifact design for volumetric error calibration of a CMM. *Int J Adv Manuf Technol* 17:508–515
35. Schwenke H, Franke M, Hannaford J, Kunzmann H (2005) Error mapping of CMMs and machine tools by a single tracking interferometer. *Ann CIRP* 54:475–478
36. Schwenke H, Knapp W, Haitjema H, Weckenmann A, Schmitt R, Delbressine F (2008) Geometric error measurement and compensation for machines—an update. *Ann CIRP* 57:660–675
37. Zhang G, Veale R, Charlton T, Borchardt B, Hocken R (1985) Error compensation of coordinate measuring machines. *Ann CIRP* 34:445–448
38. Krutha J-P, Vanhercka P, Van den Bergha C (2001) Compensation of static and transient thermal errors on CMMs. *Ann CIRP* 50:377–380
39. Aggogeri F, Barbato G, Barini EM, Genta G, Levi R (2011) Measurement uncertainty assessment of coordinate measuring machines by simulation and planned experimentation. *CIRP-JMST* 4:51–56
40. ISO 10360 part 6 (2001) Geometrical product specifications (GPS)—acceptance and reverification tests for coordinate measuring machines (CMM)—Part 6: estimation of errors in computing Gaussian associated features. International Organization for Standardization
41. Danzl R, Helml F, Rubert P, Prantl M (2008) Optical roughness measurements on specially designed roughness standards. *Proc SPIE* 7102:71020M
42. Hemli F (2011) Focus-variation instruments. In: Leach RK (ed) *Optical measurement of surface topography*. Springer, Berlin
43. Scherer S (2007) Focus-variation for optical 3D measurement in the micro- and nano-range. In: Bauer N (ed) *Handbuch zur Industriellen Bildverarbeitung*. Fraunhofer IRB Verlag, Stuttgart
44. Zhang Y, Zhang Y, Wen CY (2000) A new focus measure method using moments. *Image Vision Comput* 18:959–965
45. Helml FS, Scherer S (2001) Adaptive shape from focus with an error estimation in light microscopy. In: *ISPA 2001*, Pula, Croatia, June 2001, pp 188–193
46. Danzl R, Helml F, Scherer S (2011) Focus variation—a robust technology for high resolution optical 3D surface metrology. *J Mech Eng* 57:245–256
47. ISO 25178 part 604 (2001) Geometrical product specification (GPS)—surface texture: Areal—Part 604: Nominal characteristics of non-contact (coherence scanning interferometry) instruments. International Organization for Standardization
48. de Groot P (2011) Coherence scanning interferometry. In: Leach RK (ed) *Optical measurement of surface topography*, vol 9. Springer, Berlin
49. de Groot P (2015) Principles of interference microscopy for the measurement of surface topography. *Adv Opt Photon* 7:1–65
50. de Groot P, Colonna de Lega X, Kramer J, Turzhitsky M (2002) Determination of fringe order in white-light interference microscopy. *Appl Opt* 41:4571–4578
51. Colonna de Lega X, Biegen J, de Groot P, Häusler G, Andretzky P (2003) Large field-of-view scanning white-light interferometers. In: *Proceedings of the ASPE*, Portland, OR, Oct. 2003, p 1275
52. Wyant JC, Schmit J (1998) Large field of view, high spatial resolution, surface measurements. *Int J Mach Tools Manuf* 38:691–698

53. Gao F, Leach RK, Petzing J, Coupland JM (2008) Surface measurement errors using commercial scanning white light interferometers. *Measur Sci Technol* 19:015303
54. Schwider J, Zhou L (1994) Dispersive interferometric profilometer. *Opt Lett* 19:995–997
55. Marron JC, Gleichman KW (2000) Three-dimensional imaging using a tunable laser source. *Opt Eng* 39:47–51
56. Jiang X (2012) Precision surface measurement. *Phil Trans R Soc A* 370:4089–4114
57. Paz VF, Peterhansel S, Frenner K, Osten W (2012) Solving the inverse grating problem by white light interference Fourier scatterometry. *Light: Sci Appl* 1:e36
58. Colonna de Lega X, de Groot P (2005) Optical topography measurement of patterned wafers. *AIP Conf Proc* 788:432–436
59. Minsky M (1961) Microscopy apparatus. US patent, vol US3013467A
60. Minsky M (1988) Memoir on inventing the confocal microscope. *Scanning* 10:128–138
61. Wilson T (ed) (1990) *Confocal microscopy*. Academic Press, London
62. Diaspro A (ed) (2002) *Confocal and two-photon microscopy: foundations, applications, and advances*. Wiley-Liss, New York
63. Hibbs AR (2004) *Confocal microscopy for biologists*. Kluwer Press, New York
64. Artigas R (2001) *Imaging confocal microscopy*. In: Leach RK (ed) *Optical measurement of surface topography*. Springer, Berlin
65. Semwogere D, Weeks ER (2005) *Confocal microscopy*. In: *Encyclopedia of biomaterials and biomedical engineering*. Taylor&Francis, London
66. Brakenhoff GJ, Blom P, Barends P (1976) Confocal scanning light microscopy with high aperture immersion lenses. *J Microsc* 117:21932
67. Wilson T (2011) Resolution and optical sectioning in the confocal microscope. *J Microsc* 244:113–121
68. Leach RK (ed) (2011) *Optical measurement of surface topography*. Springer, Berlin, Germany
69. Muralikrishnan B, Ren W, Everett D, Stanfield E, Doiron T (2011) Dimensional metrology of bipolar fuel cell plates using laser spot triangulation probes. *Meas Sci Technol* 22:075102
70. Kjaer KH, Ottose C-O (2015) 3D laser triangulation for plant phenotyping in challenging environments. *Sensors* 15:13533–13547
71. Peiravi A, Taabbodi B (2010) A reliable 3D laser triangulation-based scanner with a new simple but accurate procedure for finding scanner parameters. *J Am Sci* 6:80
72. Clarke TA, Grattan KTV, Lindsey NE (1991) Laser-based triangulation techniques in optical inspection of industrial structures. *Proc SPIE* 1332:474–486
73. MacKinnon D, Beraldin J-A, Cournoyer L, Picard M, Blais F (2012) Lateral resolution challenges for triangulation-based three-dimensional imaging systems. *Opt Eng* 51:021111
74. Zeng L, Matsumoto H, Kawachi K (1997) Two-directional scanning method for reducing the shadow effects in laser triangulation. *Measur Sci Technol* 8:262–266
75. Gorthi SS, Rastogi P (2010) Fringe projection techniques: whither we are? *Opt Lasers Eng* 48(2):133–140
76. Leonhardt K, Droste U, Tiziani HJ (1994) Micro shape and rough-surface analysis by fringe projection. *Appl Opt* 33:7477–7488
77. Quan C, Tay CJ, He XY, Kang X, Shang HM (2002) Microscopic surface contouring by fringe projection method. *Opt Laser Technol* 34(7):547–552
78. Chen L-C, Liao C-C, Lai M-J (2005) Full-field micro surface profilometry using digital fringe projection with spatial encoding principle. *J Phys: Conf Series* 13:147–150
79. He X, Sun W, Zheng X, Nie M (2006) Static and dynamic deformation measurements of micro beams by the technique of digital image correlation. *Key Eng Mater* 326–328:211–214
80. Chen L, Chang Y (2008) High accuracy confocal full-field 3-D surface profilometry for micro lenses using a digital fringe projection strategy. *Key Eng Mater* 364–366:113–116
81. Li A, Peng X, Yina Y, Liua X, Zhao Q, Korner K, Osten W (2013) Fringe projection based quantitative 3D microscopy. *Optik* 124:5052–5056

82. Yin Y, Wang M, Gao BZ, Liu X, Peng X (2015) Fringe projection 3D microscopy with the general imaging model. *Opt Express* 23:6846
83. Chen J, Guo T, Wang L, Wu Z, Fu X, Hu X (2013) Microscopic fringe projection system and measuring method. *Proc SPIE* 8759:87594U
84. Drexler W, Fujimoto JG (eds) (2008) *Optical coherence tomography: technology and applications*. Springer, Berlin
85. Stifter D (2007) Beyond biomedicine: a review of alternative applications and developments for optical coherence tomography. *Appl Phys B* 88:337–357
86. Guan G, Hirsch M, Lu ZH, Childs DT, Matcher SJ, Goodridge R, Groom KM, Clare AT (2015) Evaluation of selective laser sintering processes by optical coherence tomography. *J Mater Design* (accepted)
87. Wieser W, Biedermann BR, Klein T, Eigenwillig CM, Huber R (2010) Multi-megahertz OCT: high quality 3D imaging at 20 million A-scans and 4.5 GVoxels per second. *Opt Express* 18:14685–14704
88. Czajkowski J, Vilmi P, Lauri J, Sliz R, Fabritius T, Myllylä R (2012) Characterization of ink-jet printed RGB color filters with spectral domain optical coherence tomography. *Proc SPIE* 8496:849308
89. Thrane L, Jørgensen TM, Jørgensen M, Krebs FC (2012) Application of optical coherence tomography (OCT) as a 3-dimensional imaging technique for roll-to-roll coated polymer solar cells. *Solar Energy Mater Solar Cells* 97:181–185
90. Su R, Kirillin M, Ekberg P, Mattsson L (2015) Three-dimensional metrology of embedded microfeatures in ceramics by infra-red optical coherence tomography—advantages and limitations. In: *Proceedings of the 11th LAMDAMAP*, March 2015. Swindon, UK, pp 74–83
91. Ahn Y, Jung W, Chen Z (2008) Optical sectioning for microfluidics: secondary flow and mixing in a meandering microchannel. *Lab Chip* 8:125–133
92. Stifter D, Leiss-Holzinger E, Major Z, Baumann B, Pircher M, Götzinger E, Hitzenberger CK, Heise B (2010) Dynamic optical studies in materials testing with spectral-domain polarization-sensitive optical coherence tomography. *Opt Express* 18:25712–25725
93. Dubois A, Grieve K, Moneron G, Lecaque R, Vabre L, Boccara C (2004) Ultrahigh-resolution full-field optical coherence tomography. *Appl Opt* 43:2874–2883
94. Chen T, Zhang N, Huo T, Wang C, Zheng J, Zhou T, Xue P (2013) Tiny endoscopic optical coherence tomography probe driven by a miniaturized hollow ultrasonic motor. *J Biomed Opt* 18:086011
95. Prylepa A, Duchoslav J, Keppert T, Luckeneder G, Stellnberger K-H, Stifter D (2013) Nonlinear imaging with interferometric SHG microscopy using a broadband 1550 nm fs-fiber laser. In: *CLEO EUROPE/IQEC*, Munich, Germany, May 2013, p 1
96. Su R, Kirillin M, Chang EW, Sergeeva E, Yun SH, Mattsson L (2014) Perspectives of mid-infrared optical coherence tomography for inspection and micrometrology of industrial ceramics. *Opt Express* 22:15804–15819
97. Schmitt JM, Xiang SH, Yung KM (1999) Speckle in optical coherence tomography. *J Biomed Opt* 4:95–105
98. Hitzenberger CK, Baumgartner A, Fercher AF (1998) Dispersion induced multiple signal peak splitting in partial coherence interferometry. *Opt Commun* 154:179–185
99. Su R, Ekberg P, Leitner M, Mattsson L (2014) Accurate and automated image segmentation of 3D optical coherence tomography data suffering from low signal-to-noise levels. *J Opt Soc Am A* 31:2551–2560
100. Chiffre LD, Carmignato S, Kruth J-P, Schmitt R, Weckenmann A (2014) Industrial applications of computed tomography. *Ann CIRP* 63:655–677
101. Kruth JP, Bartscher M, Carmignato S, Schmitt R, Chiffre LD, Weckenmann A (2011) Computed tomography for dimensional metrology. *Ann CIRP* 60:821–842
102. Hsieh J (2009) *Computed tomography: principles, design, artifacts, and recent advances*, 2nd edn. SPIE Press, Bellingham

103. Boone JM (2000) X-ray production, interaction, and detection in diagnostic imaging. In: Beutel J, Kundel HL, Van Metter RL (eds) Handbook of medical imaging, physics and psychophysics. SPIE Press, Bellingham, pp 1–78
104. Requena G, Cloetens P, Altendorfer W, Poletti C, Tolnai D, Warchomickaa F, Degischer HP (2009) Sub-micrometer synchrotron tomography of multiphase metals using Kirkpatrick-Baez optics. *Scripta Mater* 61:760–763
105. Yaffe MJ, Rowlands JA (1997) X-ray detectors for digital radiography. *Phys Med Biol* 42:1–39
106. Smith BD (1990) Cone-beam tomography: recent advances and a tutorial review. *Opt Eng* 29:524–534
107. Ferrucci M, Leach RK, Giusca C, Carmignato S, Dewulf W (2015) Towards geometrical calibration of x-ray computed tomography systems—a review. *Meas Sci Technol* 26:092003
108. Flay N, Sun W, Brown S, Leach RK, Blumensat T (2015) Investigation of the focal spot drift in industrial cone-beam x-ray computed tomography. In: Proceedings of the DIR 2015, Ghent, Belgium, June 2015
109. Brooks RA, Di Chiro G (1976) Beam hardening in x-ray reconstructive tomography. *Phys Med Biol* 21:390–398
110. Santiago P, Gage HD (1995) Statistical-models of partial volume effect. *IEEE Trans Image Processing* 4:1531–1540
111. Schorner K, Goldammer M, Stephan J (2011) Comparison between beam-stop and beam-hole array scatter correction techniques for industrial X-ray cone-beam CT. *Nucl Instrum Meth B* 269:292–299
112. Mail N, Moseley DJ, Siewerdsen JH, Jaffray DA (2008) An empirical method for lag correction in cone-beam CT. *Med Phys* 35:5187–5196
113. Carmignato S, Pierobon A, Savio E (2011) First international intercomparison of computed tomography systems for dimensional metrology. In: Proceedings of the 11th Euspen international conference, Como, Italy, May 2011, pp 84–87
114. Dewulf W, Kiekens K, Tan Y, Welkenhuyzen F, Kruth J-P (2013) Uncertainty determination and quantification for dimensional measurements with industrial computed tomography. *Ann CIRP* 62:535–538
115. Hiller J, Maisl M, Reindl LM (2012) Physical characterization and performance evaluation of an X-ray micro-computed tomography system for dimensional metrology applications. *Measur Sci Technol* 23:085404
116. Hsieh J, Chao E, Thibault J, Grekowicz B, Horst A, McOlash S, Myers TJ (2004) A novel reconstruction algorithm to extend the CT scan field-of-view. *Med Phys* 31:2385–2391
117. Krämer P, Weckenmann A (2010) Multi-energy image stack fusion in computed tomography. *Measur Sci Technol* 21:045105
118. Fitzgerald R (2007) Phase-sensitive x-ray imaging. *Phys Today* 53:23–26
119. Flay N, Leach RK (2012) Application of the optical transfer function in x-ray computed tomography—a review. NPL Report ENG 41
120. Landis EN, Keane DT (2010) X-ray microtomography. *Mater Charact* 61:1305–1316

Chapter 9

Micro-assembly

Serena Ruggeri, Gianmauro Fontana and Irene Fassi

9.1 Introduction

The trend toward miniaturisation of the last decade has caused a real revolution in the manufacturing of many products and systems in several fields, trying to reduce volume and weight, and integrate more functions in a smaller space. Besides the various manufacturing techniques presented in the previous chapters, growing interest has been gained by the manipulation and the assembly of different micro-components for the production of such complex systems. In this context, this chapter aims to get an overview on different micro-assembly aspects. Firstly, in Sect. 9.2 hybrid micro-products are introduced and the need for micro-assembly is highlighted. Then, in Sects. 9.3 and 9.4, micro-assembly methods are classified and described. Robots for micro-assembly with related actual examples are presented in Sect. 9.5. In Sect. 9.6, after an introduction to the issues in manipulating micro-components, micro-manipulation strategies and tools are discussed, and a review on possible release methods provided. The importance of vision and force sensing for micro-assembly is addressed in Sect. 9.7, including consideration of environmental conditioning. Finally, in Sect. 9.8, an example of a robotized micro-assembly work-cell developed at the authors' laboratory is presented.

S. Ruggeri (✉) · G. Fontana · I. Fassi
Consiglio Nazionale delle Ricerche, Institute of Industrial Technologies
and Automation, Milan, Italy
e-mail: serena.ruggeri@itia.cnr.it

I. Fassi
e-mail: irene.fassi@itia.cnr.it

9.2 Hybrid Micro-systems Production

A variety of micro-products, called *hybrid micro-systems*, has recently emerged. They are characterised by increased performance and functionality and they are made of assembled non-semiconductor components. These components can be metallic, polymeric or ceramic, each of them fabricated with the most appropriate method [1]. Fabrication processes include micro-manufacturing techniques as those described in the previous chapters. Some examples of these products are micro-pumps, micro-motors, and micro-cameras (Fig. 9.1).

However, these so-called *hybrid three-dimensional micro-products* have not consolidated their market yet, mainly due to the limits of the overall micro-manufacturing processes that require both high precision fabrication techniques and accurate assembly of the micro-components. Micro-assembly strongly affects the product cost: assembly costs can account for 60–90% of the total cost of the final product.

Current manufacturing technology, indeed, is not yet consolidated to allow the mass production of hybrid micro-products. On the other hand, automated assembly is difficult and expensive because standard automatic devices are not suitable to handle sub-milli-metric parts [2, 3].

In many cases, manual assembly of the components is chosen. This requires highly skilled human operators who have to manipulate the micro-parts by means of very delicate micro-tweezers and high-magnification microscopes, resulting in a time consuming, difficult and very expensive phase of the process. Moreover, the small scale introduces new issues and challenges related to the predominance of surface forces, making the handling significantly different from that at macro-scale (please refer to Sect. 9.6.1).

For this reason, the development of innovative computer-based automated micro-assembly methods should “increase efficiency, reliability and reduce costs” [4]. Indeed, flexible stations allowing components to be automatically assembled will benefit and further develop MST¹ [5]. The strategies and their classification for the current micro-assembly of hybrid micro-products will be addressed in Sect. 9.4.

9.3 Micro-assembly Definition

As per [6], micro-assembly is the “discipline of positioning, orienting, and assembling of micron-scale components into complex microsystems”. The goal of micro-assembly is to provide a means to achieve hybrid micro-scale devices of high complexity while maintaining high yield and low cost [6].

¹Micro-System Technologies.



Fig. 9.1 Examples of micro-products

Micro-assembly is an enabling technology for constructing complex hybrid three-dimensional micro-systems [2, 7, 8], going beyond the constraints of silicon technologies.

As discussed later, different approaches to micro-assembly can be pursued. However, firstly considering the most intuitive strategy of taking a component and assembling it with another, a slight distinction can be made between micro-manipulation and micro-assembly, even if both terms refer to the handling of parts with sub-milli-metric features. It is interesting how, in making this distinction, in [8] the author develops the concept for the design of all micro-parts and micro-gripping devices.

“Micromanipulation is generally the act of translating and rotating micro-parts from one location and orientation to another” [8]. Therefore, micro-manipulation does not imply the assembly of these micro-parts, which could be manipulated for

examination purposes only. Since micro-parts may have different shapes and variable properties, the tools are designed to handle many types of micro-parts. On the other side, “microassembly is the act of building, constructing, or collecting two or more microparts into a microstructure, in a permanent manner” [8]. It allows the production of hybrid micro-scale devices which cannot be fabricated by means of standard monolithic techniques. The geometry of the desired final micro-structure is specified by design, thus the micro-parts have totally known features. Thus, it is proposed that “the end-effectors for microassembly can be more specialized than those for general manipulation” [8].

“The general domain dealing with both manual and automated assembly of micro-devices can be referred to as *Micro Device Assembly (MDA)*” [4]. The new emerging field involving the development of computer-based methods to perform the assembly of micro-parts, can instead be called *Automated Micro Device Assembly (AMDA)* [4].

9.4 Micro-assembly Methods

When dealing with extremely small components, the assembly process becomes particularly challenging due to many factors including [9]:

- sub-micron precision often required;
- predominance of surface forces over gravitational force;
- difficult manual handling.

For these reasons, the research of better and better solutions is still on-going, although in many contributions, focused for example on manipulation strategies and tools, innovative automatic platforms and related control methods can be found.

9.4.1 Classification

More than a system of classification of assembly methods can be found in literature [6–8, 10–12].

A structured approach to micro-assembly methods considers that the classification can be applied to for example [7]:

- throughput: serial or parallel assembly;
- level of human intervention: manual, tele-operated or automated;
- deliberate intervention: deterministic or stochastic.

With regard to the first classification method, two different types of micro-assembly strategies can be distinguished:

- serial micro-assembly;
- parallel micro-assembly.

The serial micro-assembly consists in “putting together parts one by one according to the traditional pick and place paradigm” [6] (indeed also called *micro pick and place* [10]). It is a sequential operation consisting of a series of tasks, such as: identification of part 1 of the complex micro-device, pick of part 1, place of part 1 in the assembly area, identification of part 2, pick of part 2, assembly of part 2 and part 1, and so on, until the last part has been assembled. Robotic assembly, which will be addressed in detail later in the chapter, usually falls into this category, even if some applications can also be found in a parallel approach. It is considered a key approach to obtain complex assembly with high flexibility.

When “multiple micro-parts of identical or different design are assembled simultaneously” [6, 10], the implemented approach is called parallel micro-assembly. In this way, the throughput of a system can be significantly increased [13].

Based on the level of automation, micro-assembly approaches can be divided into:

- manual assembly with special tools (e.g. tweezers) and microscopes;
- tele-operated assembly using a joystick/haptic interface;
- automated assembly, based on the use of high-performance robots, precision stages and micro-gripping tools which constitute an assembly work-cell. The system could exploit vision feedback, force feedback, or their combination.

In manual assembly, it is necessary to execute high-precision tasks and the availability of microscopes or magnifying glasses is essential to allow the operator to have a clear view of the parts and the scene. The parts are usually very delicate therefore small forces have to be applied that are not perceived during operation. Insufficient force can lead to inadequate part holding, whilst excessive force can lead to damage or deformation of the parts or the gripping tools.

With tele-operated systems a man-machine interface is used to transfer the operator actions to the actuators of a machine that actually interacts with the components. This interface allows a scaling of both movements and forces. In this way, and with the support of visual and force feedback (e.g. haptic interface), the operator can perform the assembly task at the micro-scale in a way which is similar to operating at the macro-scale.

Automated assembly could be further divided into semi-automated and fully automated assembly respectively if there is a partial intervention of the operator for the execution of certain operations or the operator is completely excluded. In this latter case, once the system has been designed and the tasks defined, the system operates autonomously under open-loop or, more often, closed-loop automatic control.

According to the third classification method, the assembly can be:

- deterministic;
- stochastic.

With deterministic assembly, “the relationship between the micro-part and its destination is known in advance” [6].

Deterministic assembly can be both serial or parallel. Apart from the serial approach, parallel deterministic assembly can be achieved in different ways. One possible approach is the wafer-to-wafer transfer. For the sake of clarity, consider the case of the assembly of two types of micro-components: the first type lies neatly on a wafer, while another wafer keeps the second set of micro-components. This latter wafer is pressed on the former to allow the transfer and assembly of its components with the first group, and then removed. Another way of performing parallel deterministic assembly is to use micro-gripper arrays, able to execute pick and place operations in parallel [14, 15].

In case of stochastic assembly, “the relationship between the micro-part and its destination is unknown or random” [6]. Here the parts assemble themselves spontaneously. This type of assembly is called *Self-Assembly* (SA).

SA is generally defined as “the structural self-organization of physical entities without external guidance” [16], but simply subjecting them to the influence of an external motive force. “It is a reversible process in which disordered pre-existing components form stable and well-defined patterns or structures of higher order” [16]. Some practical examples of self-assembly are the formation of molecular crystals and many proteins.

Two main classes of micro-assembly techniques can be highlighted [11] and will be considered throughout this chapter: self-assembly and robotic assembly.

Finally, several joining methods are adopted in micro-assembly, including soldering, welding, ceramics, polymer adhesives, wafer bonding, electroplating and mechanical fasteners (including micro-Velcro and snap fasteners) [10]. The first five were commonly recognised as suitable within a clean room environment, while the last two were emerging techniques [17]. More recently, the snap-together component is common [7].

The concept of micro-mechanical assembly, well described in [18], is the assembly method “where the relative position of components is retained by exchange of contact forces provided by mechanical constraints”. Micro-mechanical assembly methods are then classified according to the mechanical constraint and the process through which the material passes to reach assembly (material constraint). In more detail, for the former group the possibility or not for dis-assembly is considered, while for the latter the characteristics range from no deformation, elastic deformation, plastic deformation, up to flow and solidification. The micro-mechanical assembly methods that are considered most relevant are: snap fits, screw, Velcro, micro-joinery (e.g. dovetail micro-joint), micro-injection moulding and micro-riveting, folding and clinching. Not limited to

micro-mechanical assembly, however, the most widely adopted method, in particular when assembling optical components, is gluing [19].

9.4.2 *Robotic Micro-assembly*

Robotic micro-assembly is performed in robotic systems consisting of a gripping device, sensing systems, a robot and a controller, and it consists of three phases: picking, handling and release.

Robotic micro-assembly has some characteristics typical of standard or meso-scale robotic assembly [13]. Common aspects include control of robot motion quantities, force control and feedback, and cooperative manipulation. On the contrary, working at the micro-scale introduces further challenges such as more complex and expensive equipment to cope with high precision specifications, difficulties in using a single mechanical gripper, and frequent inadequacy of solutions deriving from a down-scaling of macro-concepts. Indeed, a first approach to micro-assembly could be to miniaturise solutions working properly at the macro-scale by simply reducing the dimensions of the system. However, this usually does not work at the micro-scale due to the unfeasible manufacturing tolerances and handling solutions [18].

For the production of small batches, tele-operated micro-assembly is often preferred over fully automated systems [20], due to the current high cost required by automatic stations, or the lack of flexibility and re-configurability necessary to cope with frequent product changes. However, improved concepts would allow enhanced automatic systems to be the first choice by engineers.

In [13] an interesting table comparing assembly considerations (e.g. motion, force-related factors, throughput, manipulation type) at meso-scale, micro-scale and nano-scale is reported. It is worth noting that micro-assembly represents a real border among the adjacent domains because most of the choices are not definite and clear, but highly dependent on the specific applications.

Robotic micro-assembly can be often seen as a serial automated approach, carried out in a micro-assembly work-cell or a specific space of a micro-factory, whose main devices are miniaturised robots (fixed or mobile), other micro-positioning devices (e.g. micro-stages), micro-grippers, micro-feeders, sensing and control equipment.

An example of serial micro-assembly is reported in [21], where two tasks for the micro-assembly of three-dimensional structures have been demonstrated. The former assembling two identical puzzle parts, the latter two different parts. All parts had a squared shape with side of 40 μm and thickness of 5 μm . The station consisted of a robotic structure, an optical microscope and a two-finger piezoelectric gripper.

9.4.3 *Self-assembly*

Self-assembly is a parallel stochastic method to assemble micro-parts based on the principle of minimum potential energy, stating that a micro-part will move to the state where the total potential energy of the system is the smallest. Self-assembly exploits the surface energy typical at the micro-scale and an external force to agitate the micro-parts. The key point for a successful assembly is that part and receptor have to be designed to represent a state of minimum potential energy when mated.

The application of self-assembly for micro-assembly started about 30 years ago, and it is a well-known phenomenon in chemistry and biology.

Different self-assembly techniques can be used, such as: geometric shape matching, capillary self-assembly in fluid or in air, magnetic or electrostatic self-assembly [22] (see Fig. 9.2).

In geometric shape matching, as suggested by the name, the assembly is obtained when the part and the site where the part has to fit have matching shapes, as in a peg-in-a-hole assembly. Matching parts have particular shapes that ease the final assembly like for example sloped walls. The process occurs under an external force such as the gravity, random vibrations or centrifugal force [23].

Exploiting the surface interaction, the capillary self-assembly can be achieved. In this case, one can exploit the interactions between metals or use adhesive fluids in a liquid environment such as water or ethylene glycol [24]. Capillary forces can be used even in air, and an example is the self-alignment of components through liquid solder [25]. The combination of capillarity and geometric shape-matching allows for effective assembly.

Also magnetic forces can be adopted. Indeed, opposite poles attract each other allowing the part to reach the designed site. Finally, electrostatic self-assembly has been demonstrated, mainly based on dielectrophoresis and contact electrification.

9.4.4 *Robotic Micro-assembly and Self-assembly Compared*

The properties of self-assembly are very different from those of the robotic assembly, which is a deterministic process. Self-assembly exploits micro-forces and is based on the principle of the minimum potential energy, while robotic handling predominantly has to cope with undesirable forces that cause undesired effects in grasping and releasing a micro-part.

The robotic micro-handling exploits the positive capabilities and flexibility of robotics: indeed, a well-designed system can handle three-dimensional parts and, by re-programming, many different operations can be performed. On the other hand, self-assembly is less flexible, since most processes are two-dimensional and since parts and receptor sites need to be re-designed when the process changes [22].

A significant summary of different components of robotic micro-assembly and self-assembly is presented in [26]. The comparison is depicted from the analysis of

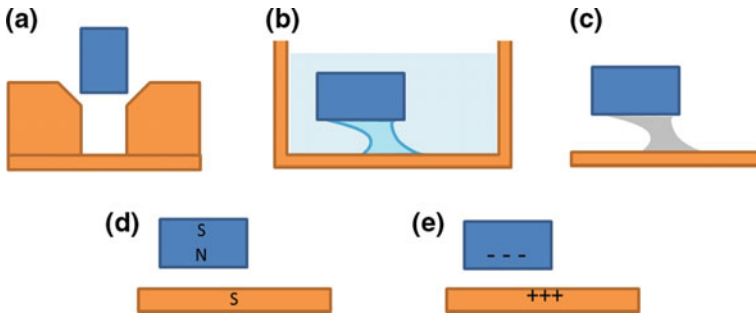


Fig. 9.2 Examples of self-assembly techniques: **a** geometric shape matching; **b** capillary self-assembly in fluid; **c** capillary self-assembly in air; **d** magnetic; **e** electrostatic

the phases of the micro-assembly process (feeding, positioning, releasing, alignment and fixing) also addressing different aspects related to the ambient environment, surface properties, external disturbance and excitation, showing that the two technologies have similarities in process phases, related aspects and physical principles.

These two methods, although both aim at the assembly of micro-parts, are used mostly in different contexts: self-assembly is historically used for biology and chemistry for the assembly of extremely small parts and cells (often in liquid medium), while robotic assembly is more frequently adopted for the assembly of micro-devices in the mechanics, electronics, optics or biomedical fields.

9.4.5 Hybrid Micro-assembly

As described in previous sections, both robotic micro-assembly and self-assembly present advantages and limitations. At this point, great benefit could derive from combining the two strategies and exploiting the respective advantages. This approach is called *hybrid micro-assembly*. Self-assembly can offer solutions to the adhesion issues in robotic applications, while the flexibility of the robotics can widen assembly possibilities. As highlighted in [26], robotic micro-assembly can help improve the yield of self-assembly, compensating for stochastic errors. On the other hand, the introduction of well-designed interactions among parts and receptors proper of self-assembly can enhance the reliability and the performance of the assembly process.

An example of hybrid assembly is presented in [27], where droplet self-alignment and robotic micro-handling are combined to assemble parts of 300 μm . In this case, the feeding and positioning are performed by the robotic system mounting micro-tweezers. Once the micro-tweezers gripping a part have approached the releasing site (another part), a droplet of water is released between part and site. The gripped part contacts the droplet that wets it. At this point the

tweezers open and the part is attracted by capillary force aligning to the other part. This method has been proved also in aligning parts of different size and stacking multiple parts (where the top squared part has side of 100 μm).

9.5 Robots for Micro-assembly

In a micro-factory (please refer to Chap. 1), and in particular in a robotized micro-assembly work-cell, micro-robots perform an important role.

A micro-robot integrates micro-actuators and sensors, has some intelligence and is able to move, apply forces, manipulate objects, etc. [5]. Micro-robots have to meet specific requirements depending on the application. Complexity, accuracy, speed, range of motion, robustness, mobility, capability to manipulate different parts, the environment in which they have to operate, the available space, being some of them. Reliability and cost are also significant considerations.

Many works in literature highlight the need for micro-assembly to position the end effector precisely and over long distances [19].

Researchers have been working on the development of systems suitable for the effective and reliable execution of the different tasks of the micro-assembly process, based on the idea of miniaturising macro-scale robots, and of innovative approaches specifically developed for the micro-scale. This led to a number of micro-robots tested for different applications, whose classification and examples are reported in the following.

9.5.1 Definition

A micro-robot can be defined as a small robot which operates at the microscopic scale. This definition includes two families of micro-robots: miniature robots, with characteristic dimensions less than 1 mm, and robots capable of handling micro-metre size components (also referred to as micro-manipulators).

The main features of the micro-robot technology are a size ranging from micro-metres to centimetres, a mechanical, chemical and electro-magnetic interaction with the environment, and micro-assembly as main application [28].

In [5] “a microrobot is characterised by its programming feature, task-specific sensors and actuators, and, in general, by unrestricted mobility”. The manipulation capability of the micro-robot is determined by the actuators for manipulating objects (robot arms and hands) while its mobility is determined by the actuators for moving the robot platform (robot drive).

For [29] the micro-robot is not only a miniaturised machine but also an integrated system consisting of sensors, actuators, and a logic circuit. Even if the term “micro” refers to a machine under a millimetre size, it does not necessarily have to be that small. The main consideration is whether the size is extremely small when compared with that of standard machines. The main characteristics of a micro-robot are: simplicity, pre-assembly, functional integration, multitude, and autonomous decentralisation.

A micro-manipulator has to be suitable for working in the environment required by the application (e.g. dry or liquid media, presence of electric fields). Moreover, the required accuracy, generally very tight, has to be guaranteed. Therefore the structure has to be stiff enough and little sensitive to changing environmental conditions (e.g. temperature), otherwise compensations have to be made [30]. The systems should also be compact to fit in the available space of a small station. Finally, the kinematics of the structure and the number of degrees of freedom are important to define the capabilities of the micro-manipulator.

9.5.2 *Classification*

Micro-robots can be classified based on size, functionality, and task specificity [5].

Considering functionality, a micro-robot has sensors and actuators for positioning and operation (AP and AO), a control unit (CU) and a power source (PS), and a different combination of these components defines a category of micro-robots. In this case, three criteria must be considered: presence or not of mobility, power source on board or not, control with or without cables.

Task specificity is defined as the ratio between the robot dimensions and its operating range. When the ratio is much smaller than 1, it is defined as a mobile microscopic robot. When the ratio is much higher than 1, the robot is stationary but very precise. Again, the need for manipulating micro-parts very precisely and move over long distances is emphasised.

Based on the various solutions provided in the literature, one can distinguish between mobile or fixed micro-robots, and serial or parallel robotic structures [30].

Mobile micro-robots are attractive because they can move over long distances, they are compact, autonomous and can be used and set up for micro-manipulation tasks. Many examples of this type of micro-robots are available (see Sect. 9.5.4), however they suffer of basically two limitations: energy autonomy and limited accuracy.

On the other hand, the development of fixed micro-robots is a topic of interest. They have a relatively wide working space, can achieve significant displacement velocities and their model is known and exploitable by the control. However, major issues are related to the presence of backlash and sensitivity to the environmental conditions that cause a degradation of the accuracy of the system, therefore limiting their use to applications where the required accuracy is greater than a few micro-metres.

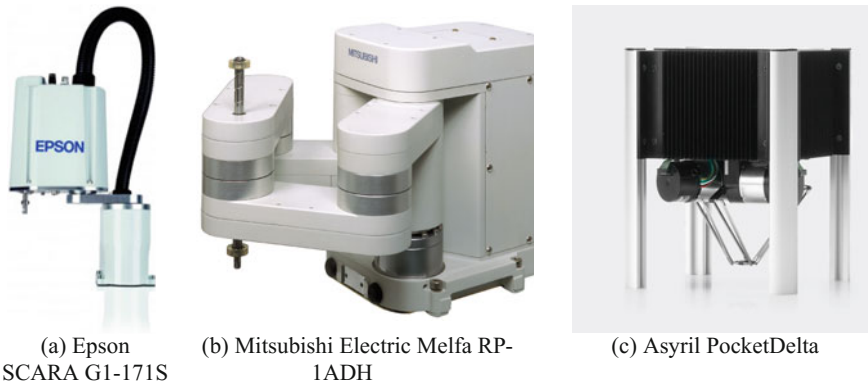


Fig. 9.3 Examples of robotic structures: **a** SCARA robot (by EPSON, [31]); **b** two-arm SCARA robot (by Mitsubishi, [32]); **c** Delta robot (by Asyri SA [33])

Micro-robots can have serial or parallel kinematic structure. In the former case, the micro-robot presents open kinematics, where elements are connected in series, by rotational or linear joints. They could be for example SCARA² robots. These robots have a good working volume, are simple and modular; however, they have poor rigidity and unavoidably presence of cumulative errors throughout the chain of elements, which results in limited accuracy at the end effector.

Parallel kinematic micro-robots have a closed kinematic chain. The rigidity of the structure is higher than serial structures and they can be more precise, although the working volume is generally small. For these reasons, parallel structures are often preferred for micro-assembly applications. Examples of this kind of robot are two-arm SCARA robots (also called parallel SCARA) or Delta robots (see Fig. 9.3).

An interesting summary of industrial micro-manipulators is presented in [34], where a table compares 15 robots in terms of workspace, accuracy, velocity, and pay-load, since considered the most important parameters. The table highlights that the most common structures are SCARA and Cartesian robots, where the former are faster although less accurate than the latter.

9.5.3 Design Considerations

When designing and using a miniaturised robot, a number of challenges arise due to predominant forces, scalability of the parts, moving masses, non-linearity effects, and cabling. A very interesting framework describing the different factors that affect

²Selective Compliance Assembly Robot Arm.

the design and the use of robots in a micro-factory is reported in [35]. The main factors include:

- **Size.** The obtainment of small sizes, although often desirable, limits some solutions. Indeed, it could be difficult to find commercial components and often their cost is rather high. Moreover, as dimensions become smaller, the integration of actuators and sensors become more difficult. Finally, too tight manufacturing tolerances imposed by the design could be unfeasible or too expensive to achieve using current manufacturing techniques.
- **Performance.** It refers to accuracy, speed, payload, degrees of freedom, working space. Performance is closely related to the type of robot structure.
- **Structure.** Structures can be parallel or serial, based on rotary joints or linear axes. As stated in Sect. 9.5.2, parallel structures are more commonly used for miniaturised robots, because of their higher rigidity and speed, but their main disadvantage is the limited workspace. Note that the presence of non-linearities such as friction or backlash in the structure can affect the performance of the robot.
- **Integration.** This factor can be considered at multiple levels. Firstly, as cited above, the integration of sensors and actuators in the robot can be difficult requiring good design, but also the integration of the robot in the work-cell has to be taken into account. Indeed, the requirement related to small dimensions has to be met by the controller and any auxiliary equipment, keeping in mind modularity, as well as the other principles for a flexible robotic assembly micro-factory.
- **Cost.** Last but not least, the cost of the robot and the devices has to be reasonable and present an attractive proposition in order to be considered by industry and to such enable micro-assembly stations to penetrate the market.

Furthermore, the approach to micro-assembly includes the development of micro-robots that could be fabricated on the same wafer with the parts, avoiding the need for an external assembly system. Due to the difficulties in fabrication and sensors and actuators integrations, the micro-robot design has to be simple [13].

9.5.4 Example of Robots for Micro-assembly

Examples of commercial serial robots for micro-assembly are the Yamaha YK120X SCARA robot with repeatability of 5 μm , or the EPSON G1-171S SCARA robot (Fig. 9.3a) with the same repeatability, reach of 175 mm and four axes [31].

An example of a Cartesian serial robot is the Sysmelec Autoplace 411 [36], built with linear axes with very good resolution and that can achieve a repeatability lower than 3 μm .

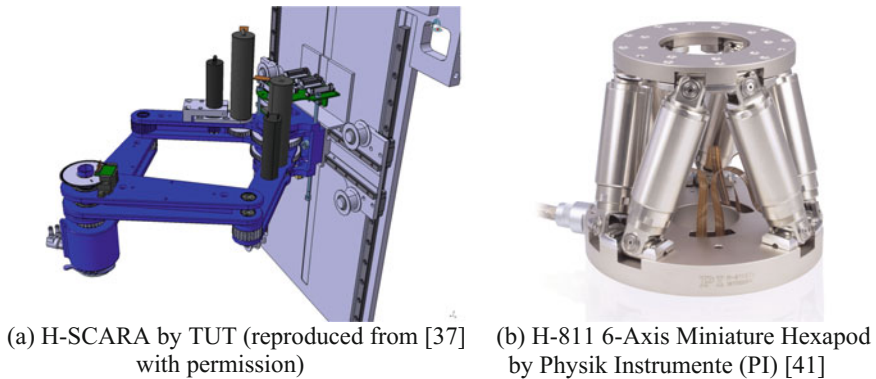


Fig. 9.4 Examples of micro-robots

Many examples can be found in literature for parallel structure robots. In this direction, the Tampere University of Technology (TUT) has been prototyping different robots. They developed the TUT H-Portal robot, a belt-driven parallel Cartesian manipulator where the belt forms an H-pattern allowing the x and y movement while the z movement is provided by a ball screw.

TUT also developed the H-SCARA (Fig. 9.4a) with 4 degrees of freedom, consisting of two parallel structures mounted in series; the first is an H-belt driven structure for the movement in xz plane, the second is a parallel SCARA for the movement in xy plane. The fourth degree of freedom is a rotation available at the end effector of the parallel SCARA. Moreover, the TUT Parallel SCARA was developed, having three degrees of freedom and an improved stiffness. They also developed a Low Cost Cartesian whose structure is essentially combining a cartesian with a ball screw. A comparison of the characteristics of the H-Portal, H-SCARA, Low Cost Cartesian, TUT parallel SCARA and Pocket Delta is reported in [37].

The University of Braunschweig—Institute of Machine Tools and Production Technology (IWF) [38] in collaboration with Micromotion GmbH, developed the PARVUS robot, with 4 degrees of freedom, an accuracy of $10\ \mu\text{m}$, and a footprint of $170 \times 130\ \text{mm}^2$.

A commercial example of a parallel SCARA robot is the Mitsubishi RP-1AH (Fig. 9.3b), with 4 degrees of freedom and a repeatability of $\pm 5\ \mu\text{m}$ in the xy plane (see also Sect. 9.8).

Another example of a parallel structure for micro-assembly is the IWF Micabo, developed in two structural versions: planar and volumetric. IWF also developed the Triglide robot [39] with repeatability better than $1\ \mu\text{m}$.

Another significant example of type of parallel micro-robot is the PocketDelta [40] that is a sort of miniaturisation of the macro Delta structure. It was developed

by the CSEM³ and currently commercialised by Asyril SA (Fig. 9.3c). It has reduced masses in motion and direct drive motors that allow increased speed. It has three degrees of freedom, a repeatability of $\pm 3 \mu\text{m}$ and a cylindrical workspace with diameter of 150 mm and height of 27 mm [33].

Physik Instrumente commercialises 6-axis miniature hexapods (Fig. 9.4b) with a repeatability less than $0.5 \mu\text{m}$ in all axes, that can be used as micro-positioning system in micro-assembly applications [41].

Many mobile micro-robots have been developed so far. Within the MiCRoN project, mobile micro-robots with dimensions $12 \times 12 \times 17.5 \text{ mm}$ have been developed [42, 43]. The working principle is based on stick-slip piezoelectric actuators producing planar movement (two translations and one rotation) with a precision for absolute positioning of about $5 \mu\text{m}$. The micro-robot can be used for the manipulation of rigid or flexible components with minimum size of some tens of microns for the assembly of endoscopes.

A mobile micro-robot, called MINIMAN, has been developed at the University of Karlsruhe within the ESPRIT Project “MINIMAN”. MINIMAN can operate automatically or in tele-operation. It consists of a mobile platform driven by three tube-shaped piezoceramic legs [44] and the walking is based on inertia forces. It can be equipped with different tools, e.g. with gripper driven by piezoelectric actuation. Another prototype is the RobotMan equipped with a gripper having two fingers actuated by three micro-motors and mounting a CCD camera [44].

In [45], an electrostatic MEMS micro-robot with dimensions of $60 \times 250 \times 10 \mu\text{m}$ is presented. This device has 2 degrees of freedom and consists of a curved cantilevered steering arm with an electrostatically driven scratch-drive actuator (SDA).

Another example is the Programmable Micro Autonomous Robotic System (PMARS), developed by Nagoya University [46]. It is less than $20 \times 20 \times 20 \text{ mm}$ in size and has communication capabilities with the host computer and other micro-robots.

In [47], a precise positioner for a micro-mirror in high-density optical disk drives tracking is driven by four thermal bimorph actuators.

An example of mobile micro-robot using rotary axis is given by the Kleindiek Nanotechnik Micromanipulator for Electron Microscopy (MM3A) [48]. The robot is very compact and precise and can be used inside SEMs,⁴ FIBs⁵ and other microscopes. It has dimensions of about $60 \times 20 \times 25 \text{ mm}$. The payload is of a few grams and gripping tools of different types can be mounted on the ending part.

Recently, the Physical Intelligence Department in Germany has started working on mobile milli-robots and mobile micro-robots made of smart and soft materials [49]. In particular one of the research topics is related to untethered magnetic

³Centre Suisse d'Électronique et Microtechnique (Swiss Center for Electronics and Microtechnology).

⁴Scanning Electron Microscope.

⁵Focused Ion Beam.

micro-scale mobile robotics and locomotion based on rotational stick-slip and rolling dynamics. Also UTARI (the University of Texas at Arlington Research Institute) is currently working on untethered micro-robots actuated with focused permanent magnetic field [50].

9.6 Micro-manipulation Systems

The design and development of suitable tools is essential for the effective manipulation and assembly of components with micro-metric dimensions or with micro-metric features. According to the difference between general manipulation and assembly discussed in Sect. 9.3, these tools can be more or less specialised and can present optimal features for a specific component and the desired application. In the context of micro-assembly, these tools manipulate the objects so that they “will go to the destination in a desired manner” [26]. They can be mounted on manual, tele-operated or automatic systems. When the components to be assembled have different properties such as shape, material, surface roughness etc., a micro-tool alone may not be sufficient. In such cases (for example the need of two different contact-based tools, see Sect. 9.6.2.1) a common interface and an easy tool changing system would be desirable.

In the following sections, after introducing the issues related to micro-manipulation, a classification of the possible methods will be described and solutions for the release when hindered by surface forces will be reported.

9.6.1 *Issues in Micro-manipulation*

Many issues have to be taken into account during the design of the micro-gripping systems. In micro-manipulation, due to charging effects, the components move into their energetically most advantageous state, thus affecting the precise control of the grasping or release phases [51]. Moreover, when the micro-tool makes contact with the micro-parts, they adhere to it as a result of the surface forces. Since the weight of the parts is much smaller than the resultant of these forces, the release becomes unfeasible if not properly assisted. It is important to note that electrostatic, capillary and Van der Waals forces have significant effects at the micro-scale (please refer to Chap. 1).

It is also important to note that not all the micro-grippers will be suitable for a micro-part, and similarly, not all parts can be manipulated by a single type of micro-gripper.

Therefore, many aspects have to be considered while choosing a strategy and designing a micro-tool, in order to avoid incompatibilities and to find the best combination of part, tool, and release method (if needed) [2].

This includes the evaluation of component characteristics such as:

- material (e.g. soft/hard, hydrophobic/hydrophilic);
- surface properties;
- sensitivity to electric fields, magnetic fields, or thermal gradients;
- fragility;
- geometry and available contact areas.

For example, a component made of a porous material is difficult to manipulate using a vacuum pipette or very fragile components by tweezers applying a significant force.

9.6.2 *Micro-manipulation Strategies*

The conception, development and test of effective, efficient, and reliable micro-tools have been a topic of interest to many researchers for decades. The need to manipulate micro-parts, each of a different nature, for various applications has led to a rapid enrichment of the literature with a number of manipulation strategies, tools, and their actuation and sensing methods, aiming at reaching high performance, ease of fabrication, low cost and high productivity.

Two approaches for micro-handling followed:

- methods exploiting the surface forces or
- methods trying to minimise the effects of these forces.

In both cases, the manipulation can be either with or without contact between tool and micro-part, thus one can identify the following methods [52]:

- contact methods;
- contact-free methods.

According to this classification, the following paragraphs aim at offering an overview on some possible solutions that can be found in the literature.

9.6.2.1 **Contact Manipulation**

In this case, the micro-gripper is in contact with the micro-part during the manipulation (see Fig. 9.5). In general, contact micro-grippers can manipulate micro-parts with a wide range of shapes and materials and can exert forces useful, for example, during micro-assembly operations.

Friction grippers

Many types of friction micro-grippers consisting of two opening and closing fingers (micro-tweezers), have been manufactured to manipulate micro-parts, similar to the way common at the macro-scale. They are widely used for micro-handling, micro-assembly and bio-manipulation, both in micro and nano applications.

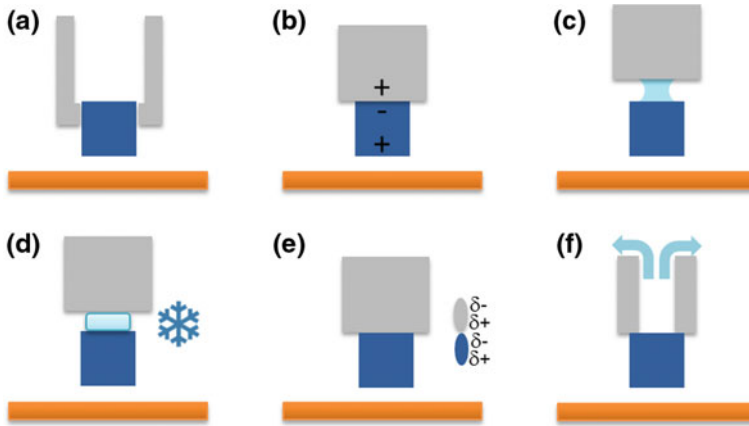


Fig. 9.5 Contact manipulation strategies: **a** friction grippers; **b** electrostatic; **c** capillary; **d** phase changing; **e** adhesive; **f** vacuum

Several types of actuations can be adopted for micro-grippers, which can be grouped into two main classes: miniaturised conventional actuators and specifically dedicated micro-actuators. The former class includes pneumatic or hydraulic actuators, and electric motors, although their implementation can be critical, due to low precision and difficult downscaling [53].

For these reasons, it is often more efficient to adopt different types of actuators exploiting physical effects that are not relevant at the macro-scale. These include:

- piezoelectric actuation; e.g. in [54] a modular gripper based on piezoelectric actuation is presented. It is equipped with interchangeable tips having different shapes and made of different materials;
- electrostatic actuation; a commercial example is the FT-G micro-gripper by Femtotools, consisting of two parts; an electrostatic lateral comb-drive actuator which generates a displacement of an actuated arm, and a capacitive force sensor attached to the sensing arm with a resolution of 50 nN [55];
- thermal actuation; e.g. in [56] a thermal gradient, generated by a resistor, is used to bend the fingers causing their opening and closure. A commercial example is the Bent Beam Gripper by Zyvex company [57], based on a thermal gradient micro-actuator;
- Shape Memory Alloys (SMA); based on the two-way shape memory effect. An example is provided in [58], where the gripper consists of two small fingers, an active part changing its shape when heated and a parallel elastic structure used as a bias spring.

It has to be noted that SMA and thermal grippers usually have a long response time.

From the examples above, the use of active materials for micro-actuators (please refer to Chap. 1) is notable. When the physical effect is reversible (i.e. the mechanical work produces, for example, an electrical or magnetic field/signal), the material can be used for sensing. In this case the term *self-sensing* is used. This property can be exploited in the case of micro-tweezers and, when a closed-loop position control is implemented, excellent resolution can be achieved.

Almost all mechanical grippers are very fragile and should be used, stored and transported with care. These grippers are not suitable for very fragile parts and have showed undesired sticking effects, preventing the release or the accurate placement of the part.

Electrostatic grippers

Electric fields can also be used to manipulate parts, controlling the electrostatic force. In [59] the development of a centring electrostatic micro-gripper is described.

Capillary grippers

The capillary force can be suitably exploited too. In fact, a small drop can be used at the surface of the gripper in order to create a liquid bridge and the meniscus to increase this force between gripper and part. Capillary gripping has been investigated by many researchers [60, 61] with interesting results.

Phase-changing

The use of the so-called phase-changing methods is also quite common. In this case, the liquid meniscus between gripper and micro-part is solidified, making the part picking possible. The liquid is typically water, which is iced to pick the part [62, 63].

Adhesive grippers

Among the manipulation tools based on a mechanical contact with the component, one simple solution is the manipulation using basic adhesive contact. An example of micro-assembly planning with the use of a Van der Waals gripper is presented in [64].

Vacuum grippers

A strategy downsized from the macro-world is the use of the force generated by the pressure difference between the gripper and the atmosphere. Indeed, vacuum grippers are commonly used in the assembly of fragile macro-components [65]. They can be easily and cheaply miniaturised, as they consist mainly of a micro-nozzle connected to a vacuum ejector. However, they can be easily occluded and both the gripper and the part need to have smooth surfaces to prevent air leakage.

A review of the most used contact-based techniques can be found in [51], which also underlines their advantages and limitations, focusing in particular on capillary micro-grippers.

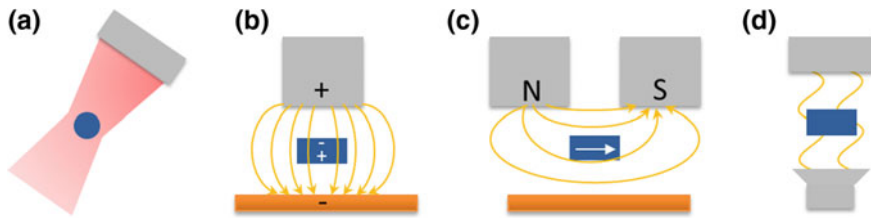


Fig. 9.6 Contact-free manipulation strategies: **a** optical pressure, **b** electrostatic, **c** magnetic, **d** acoustic pressure

9.6.2.2 Contact-Free Handling

As previously stated, contact handling solutions generally suffer from adhesive effects, so that the micro-part adheres to the gripper preventing the release or an accurate positioning. The contact force between the gripper and the part may also damage the part itself, scratching or deforming it. In order to overcome these limitations, other types of grippers based on contact-free solutions have been investigated (Fig. 9.6). The resultant forces are relatively weak but their use is limited to parts having specific characteristics in terms of shape and material.

Optical pressure

One possible contact-free strategy is based on the use of optical tweezers. They use the optical pressure that occurs when the light is reflected, absorbed or refracted by the component. If a transparent part has a refractive index higher than the refractive index of the medium within the manipulation is performed, the part is attracted to the region of highest light intensity [52]. A laser beam directed to the part can thus be used as an optical trap, allowing the part to move [66]. This method can be used to manipulate parts with size ranging from hundreds of nano-metres to tenths or hundreds of micro-metres and it is usually used for manipulation of biological samples, such as cells, DNA strands. By moving several optical traps, it is possible to simultaneously move several parts [67].

Electrostatic force

Electrostatic forces can also be used to manipulate micro-parts without touching them by using an electric field. In fact, a dielectric micro-part can be manipulated exploiting the dielectrophoresis force and torque applied on it.

Dielectrophoresis is largely used in cell micro-manipulation to perform cell sorting or catch individual cells. In [68], dielectrophoretic assembly principles of MEMS/NEMS devices are proposed and experimentally verified with micro-tweezers and nano-electrodes for carbon nanotube assembly. Feeders for micro-parts based on electrostatic fields have also been developed [69].

Magnetic force

Manipulation of ferromagnetic micro-parts is possible by controlling the magnetic fields. A system of magnetic tweezers is presented in [70]. In [71], magnetically driven micro-tools on a chip to achieve non-contact cell manipulation in a closed space are presented.

Acoustic pressure

Acoustic levitation also enables the handling of micro-components. In [72], “handling technology based on the ultrasound-air-film-technology and its applications for non-contact handling in PV-Thin-Film and micro-assembly” are presented. In [73] the various advantages of this contactless handling method are reviewed and the most common models of acoustical levitation are inspected.

9.6.3 Release Strategies

In micro-assembly, the release phase is often the most critical, due to the predominance of adhesive effects over gravitational force. Therefore, many solutions have been proposed to improve the performance of the releasing phase.

These release techniques can be classified into *passive* and *active* release. In [74], “passive release techniques depend on the adhesion forces between the micro-part and the substrate to detach the micro-part from the end effector”; alternatively, “active release methods intend to detach the micro-part from the end effector without touching the substrate”. A more general definition is provided in [75] and considered here: in the case of passive releasing strategies, “suitable gripper features or environment conditions make possible the reduction of adhesive forces between gripper and microparts”. Active releasing strategies can be adopted when “parts can be released by means of additional actions”.

9.6.3.1 Active Techniques

In this case, additional forces for detaching the micro-component from the gripper or means for reducing the area where the gripper acts can be used [20].

An active release technique makes use of mechanical vibration, taking advantage of inertial effects of both the end effector and the micro-part to overbalance adhesion forces [76].

Moreover, a short pressure pulse can be applied to assist the release of the micro-component, even if it affects the accuracy of positioning [65]. The authors also proposed alternative releasing strategies: “adhering parts can be stripped off at a sharp edge”, or an auxiliary tool can be used “to push the part away from the main tool”.

The removal of the gripping medium represents another release strategy, as for example in the case of ice grippers [63], where the ice is destroyed by heating it.

In [77], an electric field was created to detach the part from the probe by applying a voltage between the probe and the substrate.

The release can be achieved by rolling, that is the positioning of a micro-part by rolling it to its required position. In [78] a theoretical analysis of micro-part rolling and experiments of release by rolling are presented.

Gluing the part to the substrate on the right place is a common method [79].

The design of a proper mechanical engagement can also aid the release, such as the snap fasteners, that is “deformable devices consisting of a pair of mating surfaces that snap together during assembly” [17].

9.6.3.2 Passive Techniques

In this case the release can be favoured by specific micro-gripper features or environmental conditions [20]. For example, the adhesion due to the electrostatic force can be reduced coating the glass pipette for the suction with a conductive layer of gold connected to the ground [80]. The gripper can be coated with hydrophobic coating to prevent moisture adsorption or it can also be made of the same material as the micro-part to reduce the contact interaction forces [20].

A schematic representation of the basic principles of the cited release strategies is presented in Fig. 9.7.

A review of releasing strategies in micro-parts handling has been provided in [75], where a scheme to classify various releasing strategies for micro-assembly is proposed. In particular, the authors focused on possible releasing strategies for capillary micro-grippers and drew a useful map for the selection of the suitable grasping and releasing couple depending on the micro-component. A more general framework has been recently published [20].

In [2], the problem of choosing the most suitable techniques according to the micro-part features has been investigated. A Decision Support System (DSS) was developed and tested to support and suggest to the designer the best techniques for executing the assembly of micro-mechanical components.

9.7 Sensors and Control Methods for Micro-assembly

9.7.1 Vision

The integration of vision systems in robotic work-cells is particularly useful because of the various issues it can address, e.g. inspection, quality control, supervision or vision-based robot control, performing the so-called *machine vision*. In this last case, the visual information, called *features*, extracted from images, is

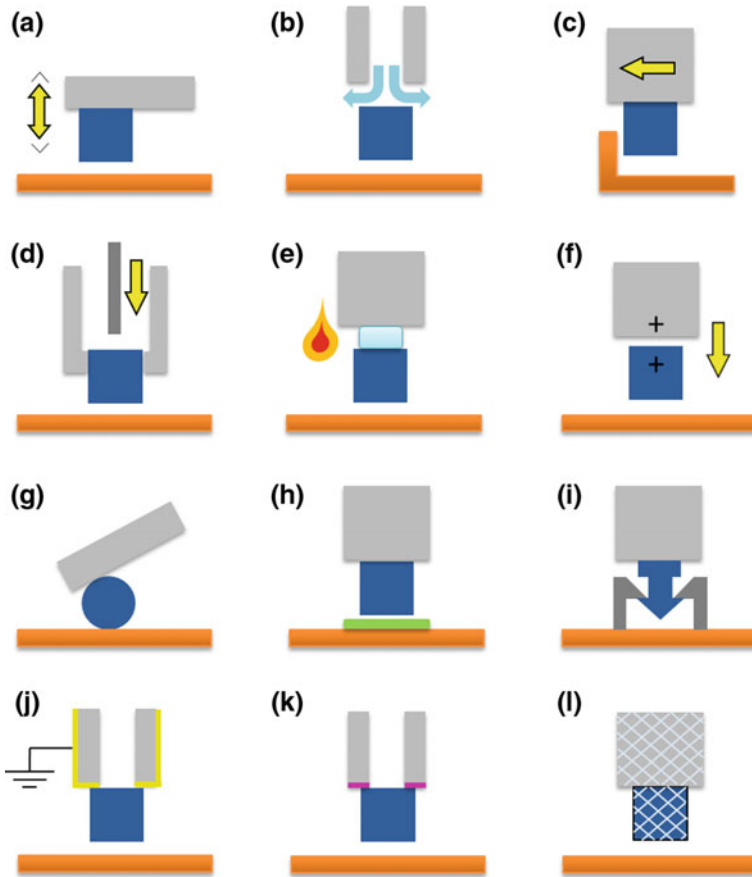


Fig. 9.7 Release strategies: **a** vibration; **b** pressure pulse; **c** edge; **d** additional tool; **e** vanishing of the medium; **f** electric repulsion; **g** rolling; **h** gluing; **i** mechanical engagement; **j** coating and grounding; **k** hydrophobic coating; **l** same material

used to control and guide the robot, increasing its flexibility and autonomy in a non-structured or poorly-structured environment. This is particularly true in micro-manipulation, either tele-operated or fully automated, where the physical dimensions of the parts require the use of magnification tools.

The nature of micro-manipulation limits the range of available vision techniques to standard-objective video, conventional optical microscopy video and SEM.

SEMs are only used for specific applications, due to the confined atmosphere in the vacuum chamber and high cost. In contrast, the standard-objective video imaging and the conventional optical microscopy video imaging can be found in a widely range of micro-manipulation and micro-assembly applications. These techniques offer a compromise between resolution and ease of use, and they can operate in the ambient environment, in a humid environment, in liquids or even in

vacuum [30]. This section deals only with these types of vision source and the general term “vision system” is used in relation to camera-lens technology.

A vision system is a sensor consisting of one lens or a series of lenses, associated with a camera providing a source of numerical images. To improve the contrast of the images, suitable illumination systems have to be used. The camera outputs two-dimensional images, thus only two-dimensional information can be extracted. In order to obtain information on the third dimension, depth or relief, it is required to use some sort of stereovision strategy using one or more image sources.

Several parameters can be used to characterise the behaviour of a vision system: resolution, optical aperture, magnification, focal, contrast, depth of field, field of view, and working distance (Fig. 9.8). The vision system resolution must be compatible with the size of the manipulated micro-objects. To achieve a high level of resolution in order to distinguish the maximum level of detail from images, the

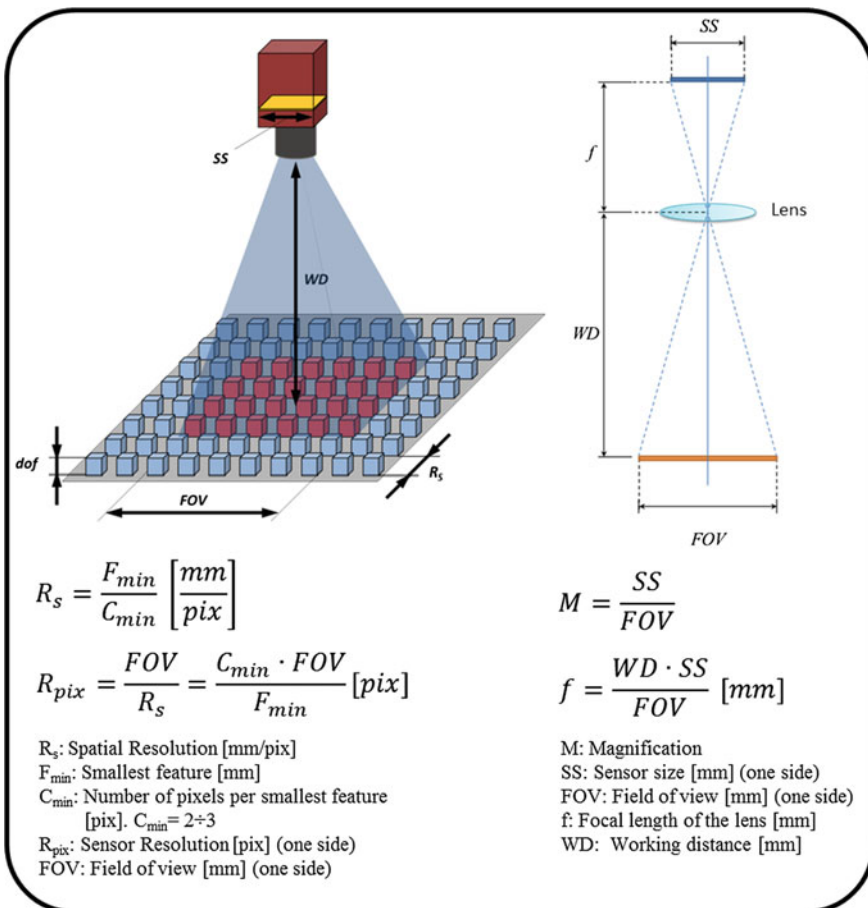


Fig. 9.8 Vision system parameters

optics of the vision system must provide a high magnification. This requirement causes a small field of view of the system that limits the viewable micro-assembly area. This introduces a trade-off between the resolution and the field of view. Moreover, the high magnification requires a small working distance, but this distance must be large enough that the components can be accessed and manipulated with tools and robots. Furthermore, under normal conditions of use of a vision system in a micro-assembly task (air, visible light, large numerical aperture, high magnification), the depth of field is fairly small. Another trade-off is needed between resolution and depth of field, because these two parameters follow opposing trends.

To overcome the issues arising from the limited field of view, different solutions can be considered. The first solution is the multi-source solution. This involves combining vision systems with different resolutions and fields of view. There will be at least two sources: a high-resolution source with a small field of view (localised images within the scene), and another low-resolution source with a wide field of view (global images of the scene) [81]. An alternative is a single-source solution using an optical system with several zoom settings: low zooms give low resolution images over wide fields of view, while high zooms provide high-resolution images over small fields of view [82]. Moreover rather than directly increasing the field of view, new views of the scene can be produced using multiple views of the same scene taken from different viewpoints in order to extract more information. For example, given two frontal images of a scene, it is possible to compute a side-on view, hence be able to measure the depth of that scene, in addition to the measurements in the focal plane. There are many available 3D techniques ideal for this task, such as interpolation, triangulation, epipolar transfer, trifocal transfer, etc. [30, 83]. These 3D techniques are difficult to apply at the microscopic scale, because of the small depth of field of the vision systems for micro-manipulation. To increase the depth of field of the vision systems, automated focusing (autofocus) techniques can be used [84].

A calibration of the vision system has to be performed to compute image pixel to real-world unit transformation and to compensate for perspective, distortion and spatial referencing errors [85]. Typically, camera lenses introduce radial distortion, which means that the image information is misplaced relatively to the optical centre of the lens [86]. Since the vision system is a source of optical images, it can be modelled through a traditional pin-hole camera model and a lens distortion model. The camera calibration is usually performed by taking a picture of an object of known shape and size (calibration test pattern) and comparing the position of some image features measured in image pixels with the known actual position expressed in microns or other suitable units. This calibration procedure, commonly used at the macro-scale, is very onerous at the micro-scale. Therefore, in the micro-domain, a widely used method involves the construction of a virtual calibration test pattern using the high position resolution of the displacement tools (e.g. the robots). A target is tracked across the field of view. The obtained points are used directly in the calibration algorithms.

Since a vision system is absolutely indispensable in micro-assembly systems, the use of vision-based control is the obvious choice. The key to visual control is the use of image information in the motion control loop of the devices (e.g. robot), called *visual servoing*. In the micro-manipulation literature, visual servoing in the image, and look-and-move techniques, are often used [30]. These are sometimes combined with alternative control methods based on the use of, for example, force sensors [82, 87] or optical position sensors [88]. The look-and-move technique is a pseudo servoing technique in open loop; rather than performing the full process of extracting information from the image, calculating the commands and carrying them out for every sampling step, each of these actions is carried out at a different time step (e.g. when a part must be picked or released). This is an empirical approach that does not require any modelling [82, 89]. The main advantage is its ease of implementation. Instead, the visual servoing in the image is a closed-loop control technique and, during the visual servoing in an image, the commands are expressed in image space, in the form of attributes of visual indicators such as points, lines and regions. For this reason, visual servoing requires a kinematic relationship to be established between the scene and the image [90].

9.7.2 Force Sensing

At the micro-scale, either the robots must overcome the unwanted force scale effects, technologically or through their control logic, or alternatively it may be possible to turn these effects to their advantage [91]. Measurement and control of the forces acting on manipulated micro-components is very important also to avoid damages.

Force sensing can be divided into two main categories based on whether they use a *direct* or *indirect* measurement strategy. The term “direct” refers to measurement methods where the sensors are integrated as close as possible to the object being measured, while the term “indirect” refers to contact-free measurement methods, remote methods and those which make use of static and dynamic models.

There is a range of indirect force measurement methods described in the literature, and according to the classification of [30] they can be divided based on their position in the micro-manipulation device:

- Contact-free remote measurement. Vision systems or contact-free sensors are currently used. The quantity to be measured is the deformation or flexion of the tool. A detailed knowledge of the stiffness of the tool is needed in order to determine the force acting on it.
- The manipulation table (area) is instrumented. Sensors are installed on the table supporting the parts to be manipulated, with the aim of measuring the interactions between these parts and the micro-gripper. Indeed, this method is adopted to avoid undesirable collisions between the tool and the table, or alternatively to measure insertion forces. It does not measure the gripping force acting on the parts.

- The base or the end effector flange of the micro-manipulator is instrumented. This method is common in conventional robotics. It requires a high rigidity in order to transmit information on the forces acting on the gripper along to the measurement points in the base or in the end effector flange of the micro-manipulator. Unfortunately, the micro-assembly systems (robot, gripper, manipulated parts, etc.) have low rigidity, thus the implementation of this measurement technique is difficult.
- The micro-gripper is instrumented. Such micro-grippers often use active materials (SMAs, piezoelectric materials); it is possible to exploit their behavioural model or their physical properties, such as variation in resistivity or charge measurement, in order to determine the applied forces.

Different from the indirect methods, the direct measurement methods use sensors which are directly integrated into the device. This configuration is one of the most efficient available, since it brings the sensors closer to the forces to be measured. Continuing advances in micro-fabrication techniques are making it possible to integrate sensors even into the micro-gripper. These devices, which come in many different designs, can be categorised in terms of the physical process used in the measurement. The most common are resistive strain gauges and capacitive sensors. Other techniques also exist such as sensors measuring changes in charge through the piezoelectric effect, or alternatively, variations in frequency using a mechanical oscillator. In [56], a thermal micro-gripper, that uses a resistive strain gauge in order to measure and control the gripping force, is presented. The strains resulting from the flexion of the cantilevers produce a variation in resistances of the strain gauge, that is proportional to the force. For this example, the measurable range is 10 μN .

9.7.3 *Environmental Conditioning in Micro-assembly*

Changes in ambient temperature, humidity, number of suspended particles and mechanical vibrations are all environmental effects that tend to degrade the overall performance of the micro-assembly system. In particular, these effects can affect the accuracy of relative positioning of two components, as well as the dexterity with which a micro-manipulation operation can be performed. Indeed, many superficial forces, such as capillary, electrostatic and Van der Waals depend on the temperature and humidity (see Chap. 1), and these forces can influence the manipulation of micro-parts then the process significantly. Moreover, temperature variations produce for example the expansion of various system elements, and changes in the characteristic coefficients of some actuators and detectors.

The air around a micro-manipulation station has many suspended particles and micro-organisms of size often comparable to the dimensions of the components to be assembled: dust particles can range from less than a micro-metre to a few hundreds of micro-metres. The presence of these particles can hinder or prevent the process. Therefore, it is advisable to execute it under filtered air in a clean room

with at least a clean class performance ISO 5 according to the ISO14644-1 standard. However, due to the reduced size of the parts and equipment in micro-assembly, the actual space that has to be clean is much smaller than a conventional clean room. Such solution is therefore not efficient, also considering the high cost of clean rooms, and not consistent with the micro-factory paradigm. In this context, the concept of “minienvironment” combined with that of micro-factory has been introduced, based on the idea of conditioning the environment only where needed, keeping the user outside [92]. This has obvious advantages e.g. less air volume to be treated, smaller dimensions, no dust introduced by the user (no human contamination), and setting of the optimal conditions for the application that have not to be compatible with the human needs anymore. Moreover, the integration of a system for a clean and conditioned environment avoids, when required by the application, the need for installing the micro work-cells in big and expensive clean rooms.

Therefore, during the design of the work-cell, in order to increase the efficiency and reliability of the process, it is important to consider the integration of:

- a protective box to limit pollution from external particles;
- suitable filters to reduce the suspended particles;
- ionising systems to reduce and eliminate electrostatic charges;
- conditioning systems for temperature and humidity to control these environmental parameters in a suitable range for the micro-assembly;
- mechanical isolation systems to eliminate vibrations, for example by mounting the work-cell on a base plate or on a vibration isolating table (passive or active).

Few systems enabling the control of the local environment of a micro-manipulation station are available [93]. An example is reported in [92], where miniaturised clean room production units for micro-systems are presented. The size of such miniaturised clean rooms is 1 dm³ for each module, operating in standard external environment. Each module is equipped with an air filtration system consisting of a compact laminar flow generator (ISO 5), and entry ports adapted to the parts trays (e.g. palettes), which permit a clean transfer between micro-boxes and the external environment.

Another example is given at the University of Aalto, Finland: the Micro and Nano robotics Lab developed a micro-assembly system with controlled environment [94], consisting of a micro-assembly platform and an environmental control system. It controls the temperature in the range of $-10/+40$ °C and the relative humidity in the range 5–80% RH. The assembly is also supported by a vibration isolated environment.

9.8 A Case Study: The ITIA Micro-assembly Work-Cell

In previous sections, the main aspects and the devices related to micro-assembly of hybrid micro-products have been presented. In this section, a case study developed by the authors is presented with the aim to provide a practical insight of the main issues and challenges arising when approaching micro-manipulation and micro-assembly.

In recent years, the Micro-Enabled Devices and Systems (MEDIS) group at the Institute of Industrial Technologies and Automation (ITIA) of the Italian CNR has designed and developed a flexible and reconfigurable work-cell for the automatic manipulation and serial assembly of micro-components [95], including a 4 degree-of-freedom robot with Schönflies motion (Mitsubishi Melfa RP-1AH), interchangeable micro-grippers, and a three-camera vision system, enclosed by an isolating box (Fig. 9.9).

The work-cell was designed focusing on the possibility to reproduce various layouts of micro-manipulation work-cells, thus creating a test bench to support the development of suitable automatic micro-manipulation techniques in different environments and conditions. Each module in the work-cell was developed taking

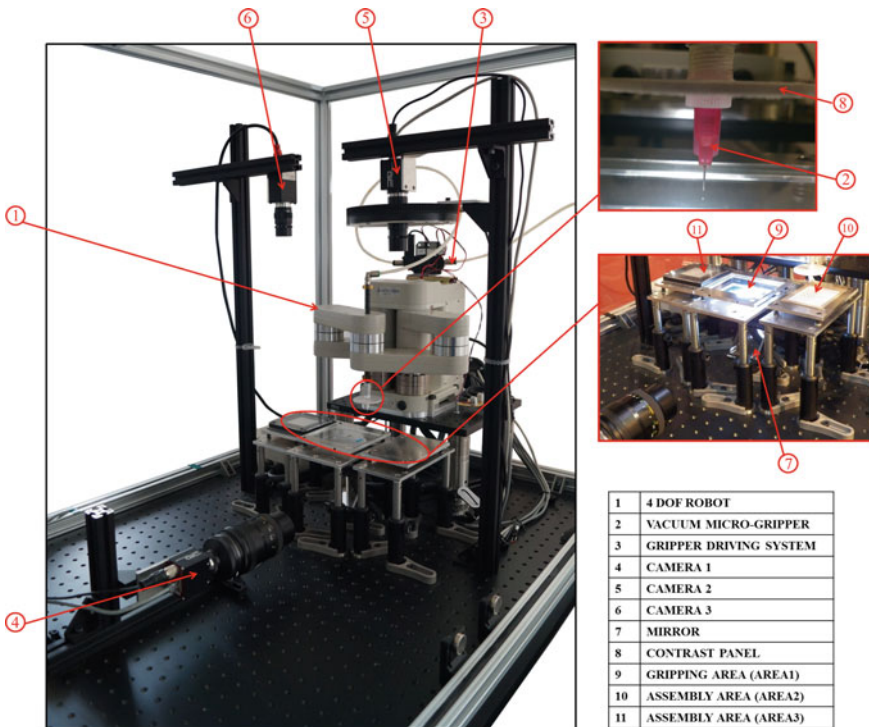


Fig. 9.9 ITIA micro-assembly work-cell

into account the issues related to the micro-scale, the different physical scenario and the high accuracy requirements, in order to obtain a complete, flexible and high-performance system.

The work-cell setup is intrinsically adaptable, redundant and reconfigurable to many tasks and applications: for example, with simple modifications on the hardware, functionalities can be added and removed.

In the work-cell, the robot end effector has been equipped with two types of micro-grippers. The former consists of vacuum micro-grippers and the latter of miniaturised two-finger grippers. In particular, an innovative vacuum micro-gripping tool has been conceived, designed and prototyped at ITIA facilities to overcome the limitation of commercially available vacuum micro-grippers in the release of the micro-components. A patent application has been filed in March 2013 and recently released [96]. Similarly to a standard vacuum micro-gripper, this device is based on the pressure difference between the gripper and the atmosphere and basically consists of a cannula connected to a vacuum generation system to grasp a component. An innovative mechanical system has been integrated in the device to assist the release phase of micro-components precisely, reliably and safely. A main feature of this micro-gripper consists in using the actuation principle for the component picking to move the release system, without additional actuators, that would make the system more complex, heavier, bigger and more expensive [97]. Figure 9.10 shows a longitudinal section of the gripper in which it is possible to see the detail of the release system inserted into the gripper cannula.

As stated above, the integration of suitable vision systems is very beneficial.

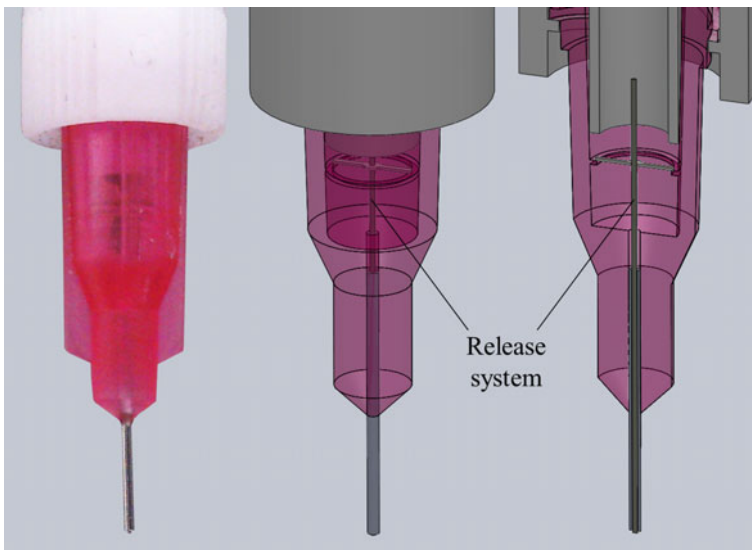


Fig. 9.10 Micro-gripper with integrated release system: section view on the right

In this work-cell, the look-and-move strategy is used. The developed machine vision module of the work-cell includes three different searching and matching algorithms, that is pattern matching, geometric matching, and particle analysis for identification, gauging, and alignment [98].

The various devices in the work-cell must be able to interact automatically to perform micro-manipulation and micro-assembly tasks. It is indispensable to equip the micro-manipulation work-cells with a control and supervision system. Therefore, a modular and reconfigurable control system was created, according to the *plug-and-produce* philosophy, able to interface with different devices and to control different micro-manipulation tasks [99]. Furthermore, the work-cell is completely reconfigurable in terms of the scheduling of operations. The idea was to develop a programming environment which was, as much as possible, device-independent in such a way that the micro-manipulation tasks can be programmed independently of the used hardware (robot, gripper, vision system, etc.). In particular, it is possible to substitute, add, and eliminate devices without modifying the control system software and to plan the operations via the HMI (Human Machine Interface).

Due to the limits of the standard calibration methods, in this work-cell, two non-conventional calibration strategies have been developed.

The former represents an adjustment of the standard method, thus called *hybrid strategy*, while the latter is a fully non-conventional method, named *virtual grid strategy*. These calibration procedures have been tested within the ITIA work-cell, but they are exploitable for any robotised micro-manipulation and assembly

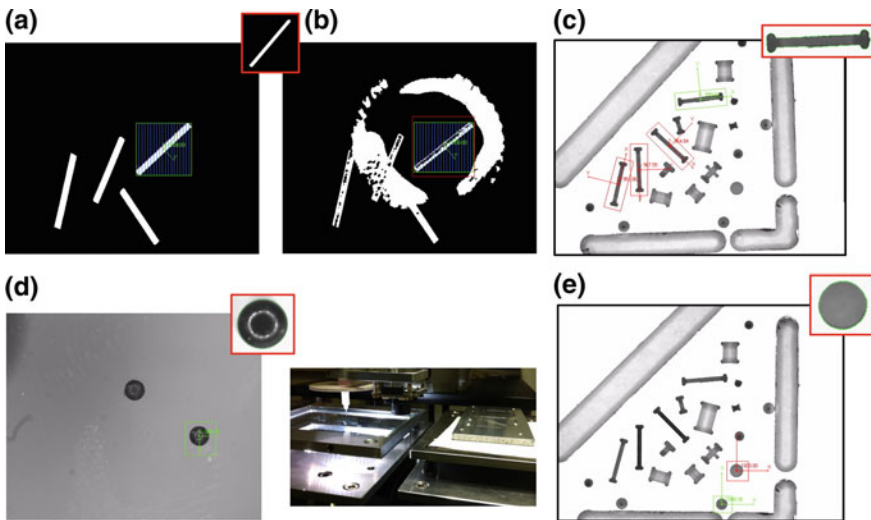


Fig. 9.11 Examples of pick and place of micro-components: **a** optical fibre segment gripping; **b** fibre segment inspection; **c** fibre segment release; **d** sphere gripping; **e** sphere release

work-cell with vision systems. The results, obtained with the different approaches, have been discussed, analysing performance and limitations in [100].

Several tasks were performed with the work-cell. Firstly, the work-cell functionality has been used to investigate the performance of the available vacuum micro-grippers. In particular, the investigation considered the grasping and releasing phases in the execution of pick and place tasks of micro-spheres of various diameters and SMD resistors. The performance of the tested micro-grippers was critically analysed and the limitations, mainly in the releasing phase, were highlighted. The results showed the better performance of the patented vacuum micro-gripper with the integrated release system compared to those of the others [97, 101, 102]. Finally, the ITIA work-cell was used for the executions of actual pick and place tasks, such as palletisation of micro-components (see Fig. 9.11).

References

1. Ruggeri S (2013) *Advanced robotic applications: performance improvement techniques for industrial robots acting at the macro- and micro-scale*. Scholar's Press, Germany. ISBN 978-3-639-51557-2
2. Antonelli D, Fantoni G, Porta M, Santochi M (2010) A methodology for the selection of micro-assembly techniques. *Am J Eng Appl Sci* 3:718–722
3. Santochi M, Fantoni G, Fassi I (2005) Assembly of micro-products: state of the art and new solutions. In *AMST'05 advanced manufacturing systems and technology*, pp 99–115
4. Cecil J, Powell D, Vasquez D (2007) Assembly and manipulation of micro devices-A state of the art survey. *Robot Comput Integr Manuf* 23(5):580–588
5. Fatikow S, Rembold U (2010) *Microrobotics*. In: *Microsystem technology and micro-robotics*. Springer, Berlin
6. Böhringer KF, Fearing RS, Goldberg KY (1999) *Microassembly*. In: Nof SY (ed) *Handbook of industrial robotics*, 2nd edn. Wiley, New York
7. Popa DO, Lee WH, Murthy R, Das AN, Stephanou HE (2007) High-yield automated MEMS assembly. In: *Proceedings of the 3rd annual IEEE conference on automation science and engineering*, Scottsdale, AZ, USA, 22–25 Sept
8. Dechev N (2010) *Robotic microassembly of 3D MEMS structures*. In: Gauthier M, Régnier S (eds) *Robotic micro-assembly*. Wiley, Great Britain
9. Van Brussel H, Peirs J, Reynaerts D, Delchambre A, Reinhart G, Roth N, Weck M, Zussman E (2000) *Assembly of microsystems*. *CIRP Ann* 49(2):451–472
10. Cohn MB, Boehringer KF, Noworolski JM, Singh A, Keller CG, et al. (1998) *Microassembly technologies for MEMS*. In *Proceedings of SPIE 3514, Micromachined Devices and Components IV*, 8 September 1998
11. Gauthier M, Régnier S (2010) Preface. In: Gauthier M, Régnier S (eds) *Robotic micro-assembly*. Wiley, Great Britain
12. Mayyas MA (2007) *Methodologies for automated microassembly*. Ph.D. thesis, The University of Texas at Arlington
13. Popa DO, Stephanou HE (2004) Micro and mesoscale robotic assembly. *J Manuf Processes* 6(1):52–71
14. Keller C, Howe RT (1997) Hexsil tweezers for teleoperated micro-assembly. In: *Proceedings of IEEE workshop on micro electro mechanical systems (MEMS)*, Nagoya, Japan, January 1997, pp 72–77

15. Randall J, Hughes G, Geisberger A, Tsui K, Saini R, Ellis M, Skidmore G (2004) Realizing complex microsystems: a deterministic parallel assembly approach. In: Technical proceedings of the 2004 NSTI nanotechnology conference and trade show, 3(11):499–502. ISBN 0-9728422-9-2
16. Nelson B (2010) Self-assembly. Lecture slides, Summer school in microrobotics and self-assembly for hybrid MEMS, Besançon, France, 29 June–2 July 2010
17. Prasad R, Böhringer KF, MacDonald NC (1995) Design, fabrication, and characterization of SCS latching snap fasteners for micro assembly. In: Proceedings of ASME international mechanical engineering congress and exposition (IMECE'95), San Francisco, California, November 1995
18. Hansen HN, Arentoft M, Tosello G, Gegeckaitė A (2010) Micro-mechanical-assembly. In: Qin Yi (ed) Micro-manufacturing engineering and technology. William Andrew Publishing, Boston
19. Lutz P, Régnier S (2010) Future Prospects. In: Chaillet N, Régnier S (eds) Microrobotics for micromanipulation. Wiley-ISTE, Great Britain
20. Fantoni G, Santochi M, Dini G, Tracht K, Scholz-Reiter B, Fleischer J, Lien TK, Seliger G, Reinhart G, Franke J, Hansen HN, Verl A (2014) Grasping devices and methods in automated production processes. *CIRP Ann 2014—Manuf Technol* 63(2):679–701
21. Gauthier M (2010) Microhandling strategies and microassembly in submerged medium. In: Gauthier M, Régnier S (eds) Robotic micro-assembly. Wiley, Great Britain
22. Sariola V (2010) Hybrid microassembly. Lecture slides, Summer school in microrobotics and self-assembly for hybrid MEMS, Besançon, France, 29 June–2 July 2010
23. Fang J, Böhringer KF (2005) High yield batch packaging of micro devices with uniquely orienting self-assembly. In: Proceedings of IEEE international conference on micro electro mechanical systems (MEMS), Miami, USA, 30 January–3 February 2005
24. Stauth SA, Parviz BA (2006) Self-assembled single-crystal silicon circuits on plastic. In: Proceedings of national academy of sciences of United States of America, 103(38):13922–13927
25. Harsh KF, Bright VM, Lee YC (1999) Solder self-assembly for three-dimensional microelectromechanical systems. *Sens Actuators A* 77:237–244
26. Zhou Q, Sariola V (2010) Unified view of robotic microhandling and self-assembly. In: Gauthier M, Régnier S (eds) Robotic micro-assembly. Wiley, Great Britain
27. Zhou Q, Chang B (2006) Microhandling using robotic manipulation and capillary self-alignment. In: Proceedings of IEEE/RSJ international conference on intelligent robots and systems, IROS 2006, Oct 2006, pp 5883–5888
28. López Tarazón R (2010) Chapter 19—robotics in micro-manufacturing and micro-robotics. In: Qin Y (ed) Micro and nano technologies. William Andrew Publishing, Boston, pp 315–323, *Micro-Manufacturing Engineering and Technology*, ISBN 9780815515456
29. Fukuda T, Arai F (1999) Microrobotics. In: Nof SY (ed) Handbook of industrial robotics, 2nd edn. Wiley, New York
30. Agnus J, Boukallel M, Clévy C, Dembélé S, Régnier S (2010) Architecture of a micromanipulation station. In: Chaillet N, Régnier S (eds) Microrobotics for micromanipulation. Wiley-ISTE, Great Britain
31. G1-171S SCARA robot by EPSON ROBOTICS. Available <http://robots.epson.com/product-detail/1>. 11 Oct 2016
32. RP-1ADH robot by Mitsubishi Electric. Available <https://www.mitsubishielectric.it/en/>. 11 Oct 2016
33. PocketDelta robot by ASYRIL SA. Available <http://www.asyрил.com/en/products/delta-robots.html>. 11 Oct 2016
34. Sánchez AJ (2010) Chapter 18—handling for micro-manufacturing. In: Qin Y (ed) Micro and nano technologies. William Andrew Publishing, Boston, pp 298–314, *Micro-Manufacturing Engineering and Technology*, ISBN 9780815515456
35. Prusi T, Vuola A, Siltala N, Heikkilä R, Tuokko R (2010) Robots for micro and desktop factories: examples and experiences. In: Proceedings of 41st international symposium on

- robotics (ISR 2010) and 6th German conference on robotics (ROBOTIK 2010), 7–9 June 2010, pp 1–7
36. Hesselbach J, Wrege J, Raatz A, Heuer K, Soetebier S (2005) Microassembly—approaches to meet the requirements of accuracy. In: Löhle D, Haußelt J (eds) Proceedings of microengineering of metals and ceramics: part ii: special replication techniques, automation and properties. Wiley-VCH Verlag GmbH, Weinheim
 37. Siltala N, Vuola A, Prusi T, Heikkilä R, Tuokko R (2012) Comparison of five low cost manipulators for microfactories. In: Proceedings of 8th international workshop on microfactories (IWMF 2012), Tampere, Finland, 8–20 June 2012, pp 1–8
 38. Burisch A, Wrege J, Raatz A, Hesselbach J, Degen R (2007) PARVUS—miniaturised robot for improved flexibility in micro production. *Assembly Autom* 27(1):65–73
 39. Hesselbach J, Raatz A, Wrege J, Soetebier S (2004) Design and analysis of a macro parallel robot with flexure hinges for micro assembly tasks. In: Proceedings of 35th international symposium on robotics (ISR), Paris, France, 23–26 Mar 2004
 40. Codourey A, Perroud S, Mussard Y (2006) Miniature reconfigurable assembly line for small products, precision assembly technologies for mini and micro products. In: Ratchev S (ed) Proceedings of international precision assembly seminar (IPAS'06), precision assembly technologies for mini and micro products, Springer, Bad Hofgastein, Austria, 19–21 Feb 2006, pp 193–200
 41. Hexapods by Physik instrumente. Available <http://www.physikinstrumente.com/products/parallel-kinematic-hexapods.html>. 11 Oct 2016
 42. Driesen W, Varidel T, Régnier S, Breguet JM (2005) Micro manipulating by adhesion with two collaborating mobile micro robots. *J Micromech Microeng* 15(10):S259–S267
 43. Driesen W, Varidel T, Mazerolle S, Bergander A, Breguet JM (2005) Flexible micro manipulation platform based on tethered cm3-sized mobile micro robots. In: Proceedings of IEEE international conference on robotics and biomimetics (ROBIO), Shatin, N.T., China, 5–9 July 2005
 44. Woern H, Seyfried J, Fahlbusch S, Buerkle A, Schmoedel F (2000) Flexible microrobots for micro assembly tasks. In: Proceedings of IEEE symposium on micromechanics and human science, Nagoya, Japan, 22–25 Oct 2000, pp 135–143
 45. Donald B, Levey C, Mcgray C, Paprotny I, Rus D (2006) An untethered, electrostatic, globally controllable MEMS micro-robot. *J Microelectromech Syst* 15(1):1–15
 46. Mitsumoto N, Fukuda T, Arai F, Tadashi H, Idogaki T (1996) Self-organizing multiple robotic system (a population control through biologically inspired immune network architecture). In: Proceedings of 1996 IEEE international conference on robotics and automation vol 2, Minneapolis, MN, 1996, pp 1614–1619
 47. Yang JP, Deng XC, Chong TC (2005) An electro-thermal bimorph-based microactuator for precise track-positioning of optical disk drives. *J Micromech Microeng* 15(5):958–965
 48. Micromanipulator for Electron Microscopy by Kleindiek Nanotechnik. Available <http://www.nanotechnik.com/mm3a-em.html>. 11 Oct 2016
 49. Physical Intelligence Department, Germany. Available <http://pi.is.mpg.de/index.html>. 11 Oct 2016
 50. Torres NA, Ruggeri S, Popa DO (2014) Untethered microrobots actuated with focused permanent magnet field. In: Proceedings of the ASME 2014 international design engineering technical conferences and computers and information in engineering conference IDETC/CIE 14, Buffalo, New York, USA, 17–20 Aug 2014
 51. Pagano C, Fassi I (2013) Devices and techniques for contact microgripping. In: Zhang D (ed) Advanced mechatronics and MEMS devices, microsystems vol 23. Springer, New York, pp 165–178
 52. Gauthier M, Lambert P, Régnier S (2010) Microhandling and micromanipulation strategies. In: Chaillet N, Régnier S (eds) Microrobotics for micromanipulation. Wiley-ISTE, Great Britain

53. Hubert A (2010) Actuators and micro-actuators for robotics applications. Lecture slides, Summer school in microrobotics and self-assembly for Hybrid MEMS, Besançon, France, 29 June–2 July 2010
54. Agnus J (2003) Contribution à la micromanipulation. Étude, réalisation, caractérisation et commande d'une micropince piézoélectrique. Ph.D. thesis, University of Franche-Comté
55. Boudaoud M, Haddab Y, Le Gorrec Y (2010) Modelling of a MEMS-based microgripper: application to dexterous micromanipulation. In: Proceedings of international conference on intelligent robots and systems (IROS'10), Taipei, Taiwan, 18–22 Oct 2010
56. Mølhave K, Hansen O (2005) Electro-thermally actuated microgrippers with integrated force-feedback. *J Micromech Microeng* 15:1265–1270
57. Micro-gripper by Zyvex. Available <http://www.zyvex.com/Documents/9703.PDF>. 11 Oct 2016
58. Zhang H, Burdet E, Huttmacher DW, Poo AN, Bellouard Y, Clavel R, Sidler T (2002) Robotic micro-assembly of scaffold/cell constructs with a shape memory alloy gripper. In: Proceedings of IEEE international conference on robotics and automation (ICRA'02), pp 1483–1488, Washington, DC, USA, 11–15 May 2002
59. Hesselbach J, Buettgenbach S, Wrege J, Bueteftisch S, Graf C (2001) Centering electrostatic microgripper and magazines for microassembly tasks. In: Proceeding of SPIE 4568, microrobotics and microassembly III, pp 270–277, Boston, MA, USA, 28 Oct 2001
60. Biganzoli F, Fassi I, Pagano C (2005) Development of a gripping system based on capillary force. In: Proceedings of the 6th IEEE international symposium on assembly and task planning: from nano to macro assembly and manufacturing (ISATP 2005), pp 36–40. Canada, 19–21 July 2005
61. Lambert P, Seigneur F, Koelmeijer S, Jacot J (2006) Design of a capillary gripper for a submillimetric application. In: Ratchev S (ed) Proceedings of international precision assembly seminar (IPAS'06), Springer, Bad Hofgastein, Austria, 2006, pp 3–10
62. Kochan A (1997) European project develops “ice” gripper for micro-sized components. *Assembly Autom* 17(2):114–115
63. Lang D, Tichem M, Blom S (2006) The investigation of intermediates for phase changing microgripping. In: Proceedings of international workshop on microfactories (IWMF), Besançon, France, Oct 2006
64. Feddema JT, Xavier P, Brown R (1999) Micro-assembly planning with Van der Waals force. In: Proceedings of international symposium on assembly and task planning, Porto, Portugal
65. Zesch W, Brunner M, Weber A (1997) Vacuum tool for handling microobjects with a NanoRobot. In: Proceedings of the IEEE international conference on robotics and automation (ICRA), vol 2, Albuquerque, New Mexico, USA, 20–25 Apr 1997, pp 1761–1776
66. Arai F, Endo T, Yamuchi R, Fukuda T (2006) 3D 6DOF manipulation of micro-object using laser trapped microtool. In: Proceedings of the IEEE international conference on robotics and automation (ICRA), Orlando, Florida, USA, 15–19 May 2006
67. Chapin SC, Germain V, Dufresne ER (2006) Automated trapping, assembly, and sorting, with holographic optical tweezers. *Opt Express* 14(26):13095–13100
68. Subramanian A, Vikramaditya B, Nelson BJ, Bell D, Dong L (2005) Dielectrophoretic micro/nanoassembly with microtweezers and nanoelectrodes. In: Proceedings of the IEEE international conference on advanced robotics (ICAR), Seattle, USA, 18–20 July 2005
69. Fantoni G, Santochi M (2005) A modular contactless feeder for microparts. *CIRP Ann* 54(1):23–26
70. Gosse C, Croquette V (2002) Magnetic tweezers: micromanipulation and force measurement at the molecular level. *Biophys J* 82(6):3314–3329
71. Sakuma S, Yamanishi Y, Arai F (2009) Magnetically driven microtools actuated by a focused magnetic field for separating of micro-particles. *J Robot Mechatron* 21(2):209–215
72. Reinhart G, Heinz M, Stock J, Zimmermann J, Schilp M, Zitzmann A, Hellwig J (2011) Non-contact handling and transportation for substrates and microassembly using ultrasound

- air-film-technology. In: Proceedings of advanced semiconductor manufacturing conference (ASMC), 22nd annual IEEE/SEMI, Saratoga Springs, NY, USA, 16–18 May 2011, pp 1–6
73. Vandaele V, Lambert P, Delchambre A (2005) Non-contact handling in microassembly: acoustical levitation. *Precis Eng* 29(4):491–505
 74. Chen BK, Zhang Y, Sun Y (2009) Active release of microobjects using a MEMS microgripper to overcome adhesion forces. *J Microelectromech Syst* 18(3):652–659
 75. Fantoni G, Porta M (2008) A critical review of releasing strategies in microparts handling. In: Ratchev S, Koelemeijer S (eds) Proceedings of international precision assembly seminar (IPAS'08), micro-assembly technologies and applications, Springer, Chamonix, France 10–13 Feb 2008, pp 223–234
 76. Haliyo DS, Régnier S, Guinot JC (2003) μ mad, the adhesion based dynamic micro-manipulator. *Eur J Mech A Solids* 22:903–916
 77. Saito S, Himeno H, Takahashi K (2003) Electrostatic detachment of an adhering particle from a micromanipulated probe. *J Appl Phys* 93(4):2219–2224
 78. Haliyo DS, Dionnet F, Regnier S (2006) Controlled rolling of microobjects for autonomous manipulation. *J Micromechatronics* 3(2):75–101
 79. Bark C, Binnenboese T (1998) Gripping with low viscosity fluids. In: Proceedings of the IEEE eleventh annual international workshop on micro electro mechanical systems (MEMS'98), Heidelberg, Germany, 25–29 Jan 1998, pp 301–305
 80. Petrovic D, Popovic G, Chatzitheodoridis E, Del Medico O, Almansa A, Sümezc F, Brenner W, Detter H (2002) Gripping tools for handling and assembly of microcomponents. In: Proceedings of 23rd international conference on microelectronics (MIEL 2002) vol 1, Niš, Yugoslavi, 12–15 May 2002, pp 247–250
 81. Schacklock A, Sun W (2005) Integrating microscope and perspective views. In: Proceedings of the IEEE international conference on robotics and automation (ICRA'05), Barcelona, Spain, 18–22 Apr 2005, pp 454–459
 82. Chen H, Xi N, Li G, Saeed A (2004) CAD-guided manufacturing of nanostructures using nanoparticles. In: Proceedings of the IEEE/RSJ international conference on intelligent robots and systems (IROS'04), Sendai, Japan, 28 Sept–2 Oct 2004, pp 595–600
 83. Bert J, Dembélé S, Lefort-Piat N (2006) Trifocal transfer based novel view synthesis for micromanipulation, advances in visual computing. *Lecture notes in computer science*, vol 4291. Springer, Berlin, pp 411–420
 84. Yang G, Nelson BJ (2003) Wavelet-based autofocusing and unsupervised segmentation of microscopic images. In: Proceedings of the IEEE/RSJ international conference on intelligent robots and systems, Las Vegas, NV, USA, 27–31 Oct 2003
 85. Zhang Z (2000) A flexible new technique for camera calibration. *IEEE Trans Pattern Anal Mach Intell* 22(11):1330–1334
 86. Fryer JG, Brown DC (1986) Lens distortion for close-range photogrammetry. *Photogram Eng Remote Sens* 52:51–58
 87. Nelson BJ, Ralis S, Zhou Y, Vikramaditya B (1999) Force and vision feedback for robotic manipulation of the microworld. In: *Experimental robotics VI*, vol 250. *Lectures notes in control and information sciences*, Springer, Berlin, pp 433–442
 88. Enikov E, Nelson BJ (2000) Three-dimensional microfabrication for a multi-degree-of-freedom capacitive force sensor using fibre-chip coupling. *J Micromechatronics Microeng* 10(4):492–497
 89. Rougeot P, Dauge M, Dembélé S, Chaillet N (2003) Vision-based control of AFM-based micromanipulation. In: Proceedings of international advanced robotics program, Moscow, Russia
 90. Ralis S, Vikramaditya B, Nelson BJ (2000) Micropositioning of a weakly calibrated microassembly system using coarse-to-fine visual servoing strategies. *IEEE Trans Electron Packag Manuf* 23(2):123–131
 91. Haliyo D, Rollot Y, Regnier S (2001) Dynamical strategies for the micro-manipulation by adhesion. In: Proceedings of SPIE 4568, microrobotics and microassembly III, pp 261–269, Boston, MA, USA, 28 Oct 2001

92. Verettas I, Clavel, R Codourey A (2005) Pocket factory: concept of miniaturized modular cleanrooms. In: 1st Topical meeting on microfactories “Desktop MEMS and nano factories” TMMF2005, Tsukuba, Japan, 17–19 Oct 2005
93. Verettas I (2006) Microfabrique: méthodologie de conception de systèmes de production miniaturisés et modulaires, disposant d’un environnement salles blanches. Ph.D. thesis, EPFL, Lausanne
94. Zhou Q, Aurelian A, Chang B, del Corral C, Koivo HN (2002) Microassembly system with controlled environment. *J Micromechatronics* 2(3):227–248
95. Fontana G, Ruggeri S, Fassi I, Legnani G (2014) A mini work-cell for handling and assembling microcomponents. *Assembly Autom J Emerald* 34(1):27–33. ISSN: 0144-5154
96. Ruggeri S, Fontana G, Fassi I, Legnani G, Pagano C (2015) Dispositivo di manipolazione e metodo per manipolare a vuoto un componente (A vacuum manipulation device and a method for manipulating a component by means of a vacuum). Italian Patent No. MI2013A000451, filed on 26 Mar 2013, Milan. Publication date: 27 Sept 2014. Released on 20 July 2015. EP (European Patent) pending No. EP2978570. Publication date 3 Feb 2016
97. Fontana G, Ruggeri S, Fassi I, Legnani G (2014) Precision handling of electronic components for PCB rework. In: Ratchev S (ed) Precision assembly technologies and systems—7th IFIP WG 5.5 international precision assembly seminar, IPAS 2014, Chamonix, France, 16–18 Feb 2014, Revised Selected Papers, Proceedings Series: IFIP advances in information and communication technology, vol 435, pp 52–60. Springer, Berlin. ISBN: 978-3-662-45585-2
98. Fontana G, Ruggeri S, Fassi I, Legnani G (2013) Flexible vision based control for micro-factories. In: Proceeding of the ASME international design engineering technical conferences and computers and information in engineering conference (IDETC/MNS 2013), Portland, OR, USA, 4–7 Aug 2013. ISBN: 978-0-7918-5584-3
99. Fontana G (2014) Assembly at the microscale: design and implementation of a robotised work-cell. Ph.D. thesis, University of Brescia
100. Fontana G, Ruggeri S, Fassi I, Legnani G (2012) Calibration strategies for a manipulation work-cell. In: Proceeding of 8th international workshop on microfactories (IWMMF 2012), Tampere, Finland, 18–20 June 2012
101. Ruggeri S, Fontana G, Pagano C, Fassi I, Legnani G (2012) Handling and manipulation of microcomponents: work-cell design and preliminary experiments. In: Ratchev S (ed) Precision assembly technologies and systems—6th IFIP WG 5.5 international precision assembly seminar, IPAS 2012, Chamonix, France, 12–15 Feb 2012, Proceedings Series: IFIP advances in information and communication technology, vol 371, pp 65–72, Springer, Berlin. ISBN: 978-3-642-28162-4
102. Ruggeri S, Fontana G, Fassi I, Legnani G (2014) Performance evaluation methods for microgrippers. In: Proceeding of the ASME international design engineering technical conferences and computers and information in engineering conference (IDETC/CIE 2014), Buffalo, New York, USA, 17–20 Aug 2014. ISBN: 978-0-7918-4635-3

Chapter 10

Market Analysis, Technological Foresight, and Business Models for Micro-manufacturing

Golboo Pourabdollahian and Giacomo Copani

10.1 Introduction

Micro-parts and micro-systems based products are considered as a crucial value-adding factor for many industrial sectors in Europe and thus an increasingly important contributor to Europe's industrial and economic future. In this regard, it is quite relevant and important to understand the existing and future trends of micro-manufacturing not only from technological perspective but also from non-technological and managerial perspective. This chapter aims to provide a required body of knowledge for the readers in terms of market analysis, technological foresights and business models for micro-manufacturing. It will specifically discuss about current existing business drivers, sectors of application, market trends, future technologies and sectors of application, as well as existing and potential future business models for micro-manufacturing. The trend became more focused on the adoption of micro and nano-manufacturing technologies (MNT) through applying a variety of materials, parts, components and knowledge-based technologies that contribute to the intelligence and functionality of micro-systems [1].

In this regard, it is quite relevant and important to understand the existing and future trends of micro-manufacturing not only from technological perspective but also from non-technological and managerial perspective. To this end, this chapter aims to provide a required body of knowledge for the readers in terms of market analysis, technological foresights and business models for micro-manufacturing. In the first section we will study the current market of micro-manufacturing and present a market analysis by focusing on the market demand and business drivers, main sectors of application, key stakeholders and players in the market, and a

G. Pourabdollahian (✉) · G. Copani
National Research Council of Italy, Institute of Industrial Technologies
and Automation (CNR-ITIA), Milan, Italy
e-mail: golboo.pourabdollahian@itia.cnr.it

concluding SWOT (Strengths, Weakness, Opportunities, and Threat) analysis. Then, we will have a look at future market trends and propose some technological foresight to identify future trends, future markets, future application sectors and the future of technologies. We will close the chapter by introducing business models for micro-manufacturing where examples of both existing and future innovative business models will be presented.

10.2 Micro-manufacturing Market Analysis

The economic relevance of micro-parts and components has previously been investigated and confirmed by several market reports [2, 3]. According to these reports, many areas and sectors that are related to micro-manufacturing will experience an increasing market share on a continuous basis. Innovative and more affordable products, ranging from health safety and communication to those for ambient living and mobility, have been already developed thanks to the micro-manufacturing technologies. Based on the official reports it is estimated that in 2019 the market for micro-electronic and mechanical systems (MEMS) will reach nearly 25 billion Dollars [4]. Such an economic relevance has been a trigger for many industries to pursue, apply, and develop new technologies for micro-manufacturing.

It is now widely accepted that developments in micro and nano-manufacturing technologies are essential for sustaining the industrial base of the European Community and allowing European business to maintain its key role in the drastically increasing global market of micro and nano-parts and manufacturing processes.

In the following sections we have a closer look at the micro-manufacturing market by analysing the market demand and drivers, main sectors for micro-manufacturing applications, the key stakeholders in the market, and eventually the main characteristics of the micro-manufacturing market in terms of strengths, weaknesses, opportunities and threats.

10.2.1 *Business Drivers and Market Demands*

Since the first developments of micro-manufacturing technologies and the emergence of the micro-manufacturing market, there have been several business drivers not only to create such a market but also to foster its rapid growth. A company operating in this market needs to understand these drivers in order to be able to create a competitive advantage. The main business drivers for micro-manufacturing include:

- **Market demand for micro-parts:** There is an increasing market demand for micro-parts such as micro-actuators, micro-optics, etc.
- **Need for product competitiveness:** Customers request for products that boost performance, customisability, reliability and functionality.

- **Manufacturing capabilities:** Emerging technologies have increased the production capabilities in terms of reliability, agility, flexibility, timeliness and performance.
- **Legislation and environmental issues:** The increasing number of regulations set by governments to meet the environmental sustainability thresholds and targets.
- **Cost:** Manufacturers need to be cost-efficient in order to be economically sustainable.
- **New opportunities and potential markets:** There are several potential markets which can be targeted by players in the micro-manufacturing sector.

In addition to the business drivers for micro-manufacturing, there are several demand factors in this market. Below we list the main demands in the micro-manufacturing market [5]:

- **Demand for more precise manufacturing systems at higher production rates and more precise parts:** Miniaturisation is a trigger for development of new technologies aiming at efficient manufacturing of micro-components. There is an increasing demand for micro-manufacturing systems that not only facilitate precise manufacturing of micro-parts but also enhance efficiency and thus increase production rates. Some of the main examples include reel-to-reel hot embossing and micro-injection moulding of multi-materials, which facilitate high-throughput and precise manufacturing systems.
- **Demand for multi-material manufacturing processes:** Currently there is a notable demand in the micro-manufacturing market for the development of processes that enable utilisation of a wide range of materials, such as alloys and composites. In specific cases, where certain physical properties for a product should be covered, development of these multi-material manufacturing processes is relevant and crucial.
- **Demand for micro-parts:** Micro-manufacturing technology enables the manufacturing and development of smaller and better sensors such as micro-accelerometers and pressure sensors that are widely used in the automotive market. In recent years a notable increasing demand has emerged for MEMS sensors from the consumer electronics market. There is a wide application of these sensor and micro-parts in cell phones, cameras, laptops, etc. resulting in rapidly increasing demand from the producers of these electronic devices for micro-parts.

10.2.2 Main Sectors of Application

Micro-components currently impact on numerous aspects of our day-to-day life. We can find them in most of the products that surround us. A clear example of this is the automotive industry. According to car makers and suppliers, there are more than 200 micro-actuators and sensors, which are integrated in modern vehicles and automobiles [6]. However, the broad range of application of micro-manufacturing

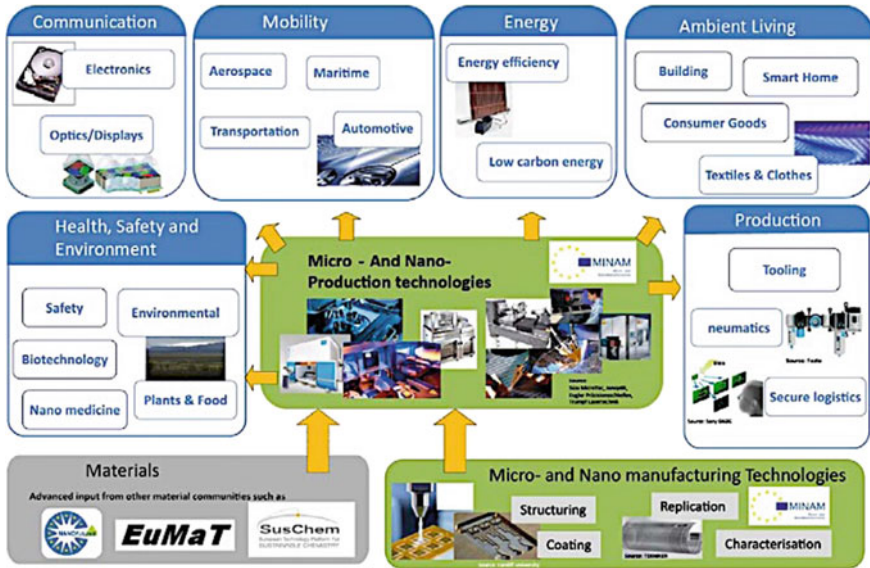


Fig. 10.1 Application areas of micro and nano-manufacturing technologies (Adapted from [6])

technology is not only limited to the automotive industry. Considering that micro-manufacturing technologies enable and facilitate the integration of functionalised micro-surfaces and micro-parts in macro-products, the end market for these technologies is quite broad. Accordingly, the number of benefiting sectors is continuously increasing and includes sectors such as: Healthcare, ICT, energy, aerospace, consumer goods and etc. The significant impacts of micro-components can be observed in many tangible application areas. It can help us to save energy, to assist elderly people and overall, to make our lives more comfortable. Figure 10.1 illustrates the domains in which the micro and nano-technologies are expected to influence and contribute significantly.

As indicated in Fig. 10.1, the target market for micro-manufacturing is quite broad and covers several sectors. According to an EU funded road-mapping report on micro and nano-manufacturing (μ -Sapient), the main opportunities are in the following sectors: automotive/transportation, communications, computer/business, consumer/entertainment, energy/water/chemicals, food and drink, medical/pharmaceutical, military/aerospace, and security.

Among these sectors, healthcare (medical/pharmaceutical) and military/aerospace are the leading sectors having an expected opportunity value more than 4 billion Euro, followed by energy, consumer electronics and food having the opportunity value around 3.5 billion Euro each.

In the following sections a brief description of three main sectors for micro-manufacturing is presented.

Table 10.1 Applications of MNT in healthcare sector

Application	Example
Advanced surfaces	Encoded self-assembly, repair, bio-inspired materials
Drug delivery	Targeted delivery and release, structured materials, bio-drugs, cancer therapy
Medical devices	Implantable devices, motion devices, personalised devices
Diagnostics	Microfluidics system, remote and intelligent sensing, bio-sensing
Drug discovery	Cell-based analysis, toxicology, biochips
Hybrid bio devices	Tissue engineering, organ development

10.2.2.1 Healthcare

Healthcare is considered as one of the main markets for micro-manufacturing technology. The size of the market itself and its potential for micro-manufacturing applications make it an extremely attractive target for micro-manufacturing. As recently as 2010, the market value of medical devices was around 300 billion dollars [7]. Having an annual expected growth rate of 8%, the market value in 2015 will reach 420 billion dollars. The EU is the second main player (following the US) in the market holding 26% of the market share. Considering the size of the healthcare market, even securing a small part of the market, micro-manufacturing can generate substantial revenues. This converts healthcare to an extremely critical and attractive sector for micro-manufacturing. Currently healthcare applications account for approximately 25% of the total value of the MEMS market. Table 10.1 shows the application of MNT in healthcare [7].

10.2.2.2 Energy

Energy is considered as one of the main sectors for micro-manufacturing technologies. The potential influence of micro-manufacturing technologies on the energy sector is impressive. It is acknowledged by experts that micro-manufacturing technologies will play a critical and decisive role in the mass production of energy and energy systems. A clear example in this regard is photovoltaic energy. Photovoltaic energy is one of the most promising technologies in the energy sector and it is expected to have significant market growth. Manufacturing photovoltaic systems depends on a broad usage of both surface micro-texturing and thin film deposition. Meanwhile emerging trends in the energy sector can be realised through the application of MNT [6]. It is widely acknowledged by technology experts that new micro and nano-technologies can enable (with new developed processes and components) a profitable value chain from the development of primary energy sources over the conversion, storage, transport, and utilisation of energy. For instance, with respect to energy transport, there are long-term options such as wireless energy transport by laser, microwaves or electromagnetic resonance. Micro and nano-technologies can be used to contribute to this vision through the use of micro/nano-sensors and electronic power components in order to handle the

Table 10.2 Applications of MNT in energy sector [6]

Application	Example
Electricity production and conversion	Surface micro-structuring for light management in 3G photovoltaic, smart micro-designs for CPV optics, new materials and processes for organic electronics and OPV
Electrochemical storage	Higher power and energy dense batteries, more durable and safe batteries
Hydrogen production and storage	Micro-fractionated materials and compounds for fast and reversible H ₂ storage in solid phases, catalysts for gas reforming
Heat exchange, harvesting and insulation	Surface micro-structuring for improved heat transfer. Surface micro-structuring for improved heat harvesting. Bulk micro-structuring for low heat conductive materials
Lighting	Micro-integrated electro-photonic features, energy efficiency through MM-enabled LEDs sources and optics
Fossil fuel efficiency	Surface micro-structuring for hydrophobic functionality, Micro-materials to improve heat resistance

complicated steering and monitoring of the huge electricity networks. Table 10.2 highlights the potential applications of MNT in the energy sector.

10.2.2.3 Aerospace

The aerospace sector is one of the leading sectors in applying new micro-manufacturing technologies. The suppliers and part manufacturers are constantly trying to minimise costs, while improving cycle times and production efficiency. In order to achieve this goal an increasing number of players are turning to MNT. Technologies such as micro-additive manufacturing have been the centre of attention of manufacturers in the aerospace sector. The application of MNT in this sector can be divided into two categories of MNT materials and MEMS.

Regarding the MNT materials the main applications are [8]:

- Lighter and stronger materials
- Surface treatments resulting in a better performance of the aircraft
- Fuel additives resulting in improving fuel efficiency and lower emission.

Potential applications for MEMS include [8]:

- Oil control for full authority digital engine control
- Pressure sensors for energy generation
- Flow, temperature and humidity sensors inside the cabin
- Accelerometer for avionic and flight control
- Pressure sensors for air data measurements
- Airbag sensors.

Moreover, it is expected that MNT will have a wider range of applications in aerospace and military sectors in future. Some of these future applications have been listed in Table 10.3.

Table 10.3 Future applications of MNT in aerospace sector [8]

Application	Example
Navigation and altitude	Radar, air data, instruments, GPS receivers and antennas, inertial measurements units
Man-machine interfaces	Displays, sighting, integrated helmet, head-up displays
Navigation optronics	Radar, reconnaissance sensors
Mission optronics and electronics	Target detection, Electro-Optical missile guidance, IFF systems
Engine and reactors	Hydraulics, intake flow control
Energy management	Generation, monitoring, pressure, humidity
Structure monitoring	Stabilisation, vibration, corrosion monitoring, structural fatigue
Landing systems	Hydraulic pressure, tyre pressure

10.2.3 Key Stakeholders

Like any other market, the micro-manufacturing market has a set of key stakeholders. These are the stakeholders who affect the market in one way or another, and their role is considered critical for the future of micro-manufacturing markets. Figure 10.2 depicts the main stakeholders of micro-manufacturing market.

- **Manufacturing technology suppliers:** The companies who provide the key micro-manufacturing techniques such as laser micro-manufacturing, reel-to-reel technology, micro-injection moulding, micro-additive technologies, etc.
- **Material providers:** The suppliers of materials that are used in micro-manufacturing machines such as polymeric materials, powder metal, paper, glass, etc.



Fig. 10.2 Key stakeholders of micro-manufacturing market

- **End-user companies:** The producer of micro-manufacturing products such as companies producing micro-fluidics, micro-actuators, micro-optics, micro-fuel cells, and MEMS etc.
- **Government:** is considered an important stakeholder taking into account the increasing number of initiatives by governments to improve the micro-manufacturing domain.
- **Knowledge providers:** The organisations that pursue innovation and research in terms of micro-manufacturing and create the innovation initiatives such as academic institutions and research organisations.

10.2.4 Strengths, Weaknesses, Opportunities, Threats

In previous sections we presented an overview of the current micro-manufacturing market focusing on market demands, business drivers, and the sectors that benefit from the application of micro-manufacturing technologies. In order to obtain a more detailed understanding of the situation of micro-manufacturing market in Europe, below we present a SWOT analysis. SWOT analysis is a widely used framework to identify and analyse the business environment from both internal and external perspectives. It is considered as one of the most effective tools to carry out a market analysis. SWOT analysis generates information that is helpful in matching an organisation's objectives. Moreover it is an instrument for strategic planning. From an internal point of view the SWOT analysis highlights strengths and weaknesses. It depicts the positive tangible and intangible attributes internal to the organisation as well as factors that detract the organisation from its ability to attain the core goal. Both strengths and weaknesses are in control of the organisation. From an external perspective, the analysis highlights external attractive factors that represent a reason for an organisation to exist and develop a specific strategy, as well as external factors that could place the organisation's mission or operation at risk. Both opportunities and threats are out of control of the organisation.

The results of SWOT analysis for micro-manufacturing market in Europe are described below [1].

The main strengths include:

- Trained personnel and technical expertise
- Technology diversity and many new ideas
- Deep expertise in fundamental technologies
- Technology maturity
- Mature machine tool industry
- Strong leadership in precision engineering
- Capability to adapt existing technology to new products
- Political and economic stability.

The main weaknesses include:

- Lack of awareness
- High costs associated with micro-manufacturing equipment
- Infrastructural cost
- Existing process complexity for the development of 3D structures
- Lack of shared knowledge with industry
- Labour cost
- Need critical mass of research in design for manufacture
- Bureaucracy in funding R&D.

The main opportunities include:

- Current industry demand for more precise manufacturing systems at higher production rates
- Novel markets requiring micro-parts
- Design knowledge
- Infrastructure
- Integration of process chains
- Established machine tool industry
- Standardisation and unification of metrology standards
- Increasing interest of funding agencies
- Key governmental initiatives to support the generation of micro-manufacturing technologies.

The main threats include:

- Conservative market industry resistance to the adoption of disruptive technologies
- Materials (more highly regulated in EU)
- Packaging
- Material development is occurring outside of EU
- Lack of shared knowledge leading to increased development time
- Unification and standardisation of micro-manufacturing approaches
- USA sets metrology standards
- Dominance of the far-east on key consumer markets
- Reliance on adapted solutions.

In summary, the analysis of European micro-manufacturing markets reveals that:

- The main strength of Europe is in the availability of skilled and trained personnel, strong machine tool industry and multidisciplinary product development and know-how.
- The main weaknesses that might slow down the growth of European micro-manufacturing market are the required cost to implement and pursue these technologies, the conservatism and reluctance of some industrial sectors, the lack of knowledge sharing between R&D actors and industry, and the lack of standards and metrology support.

- The possible opportunities for Europe in micro-manufacturing market compared to the other players in the rest of the world are in integration of process chains, establishment of capabilities for 3D processing, creation of prototyping capabilities, effective use of design for manufacture, and high research efficiency and focus.
- The main threats for Europe come from standards and packaging solutions developed outside Europe, and the dominance of the far-east in key consumer markets.

10.3 Future of Micro-manufacturing Market and Technological Foresighting

Any business needs a long-term vision to survive. Therefore having a clear understanding of the future, and planning for it, is essential. One critical analysis is related to the forecasting of the future market. In this section we will have a closer look into the future of the micro-manufacturing market by analysing market trends, identifying the most prominent and significant future sectors for micro-manufacturing technologies, and presenting some of the future applications and technologies.

10.3.1 Market Trends

The analysis presented in the previous sections highlights that the future of micro-manufacturing market is positive. The main current and future trends in micro-manufacturing are [5, 9].

- The disruptive development of micro-manufacturing technologies (i.e. surface micro-machining, bulk micro-machining) has resulted in the development of new products. It is expected that in the near future the development of novel products in different sectors will be facilitated (i.e. micro-engines, batteries, organic photovoltaic, etc.) thanks to the further improvement of both disruptive and continuous micro-manufacturing technologies.
- These new micro-manufacturing technologies will not only facilitate the development of new products but also will accelerate the development of process and thus reduce the design to manufacture time for the new products.
- The increasing awareness of environmental and social sustainability along with the regulations set by governments will push many sectors (i.e. energy, manufacturing, transport, consumer electronics, etc.) toward the broader implementation of micro-manufacturing technologies in order to increase environmental and social impact.

- There is a key demand for micro-manufacturing technologies that enable the fabrication of multi-material components. This is quite important and relevant due to the positive impact it could have in terms of enabling flexible and cost-efficient manufacturing of multi-functional products made of different materials in all manufacturing sectors.
- Replication methods are likely to be the most promising among the technologies. Despite this, they are not widely implemented within industry. They are good candidates for replacement of existing lithography methods. One such important development would relate to the production of the master-stamp, which is currently very expensive.
- There is a critical need for further development of existing processes and tools for micro/nano-assembly—for integration of nano-scale to the micro-scale. In addition, there is an increasing demand for cost-efficient and reliable micro/nano-assembly and 3D packaging.

Knowledge-based development is a major trend in the development of micro-devices and manufacturing technologies. The adoption of numerical simulation tools allows efficient integration of nano-metre sized devices with micro-metre sized devices. In addition, the generation and adoption of novel microscopic technologies enable manipulation and enhancement of micro-metre sized structures.

- Development of novel smart and miniaturised sensors and actuators provide more intelligence to the manufacturing chain. Development of MEMS-based smart and miniaturised sensors can impact positively in production supply-chains, facilitating a more sophisticated method to control the entire production process. Apart from this, novel methods to integrate them are required. In this respect, on-line control and supervision of the manufacturing process chain, machines, equipment, etc. is a vital for industry. The prominent drivers for the adoption of miniaturisation across many vertical markets are low energy consumption, reduced noise, and minimal associated costs.

Despite the promising future market for micro-manufacturing, it should be noticed that the manufacturing cost will be always a competitive factor. This might result in a notable challenge where those engaging should focus on developing new technologies to facilitate the low-cost and high-quality production.

10.3.2 Future Sectors

In Sect. 10.2.2 of this chapter an overview of the current micro-manufacturing market and the significant sectors of application were presented. Although currently there are several sectors of application, some markets are more attractive than others. Nevertheless, the attractiveness and importance of these markets will change

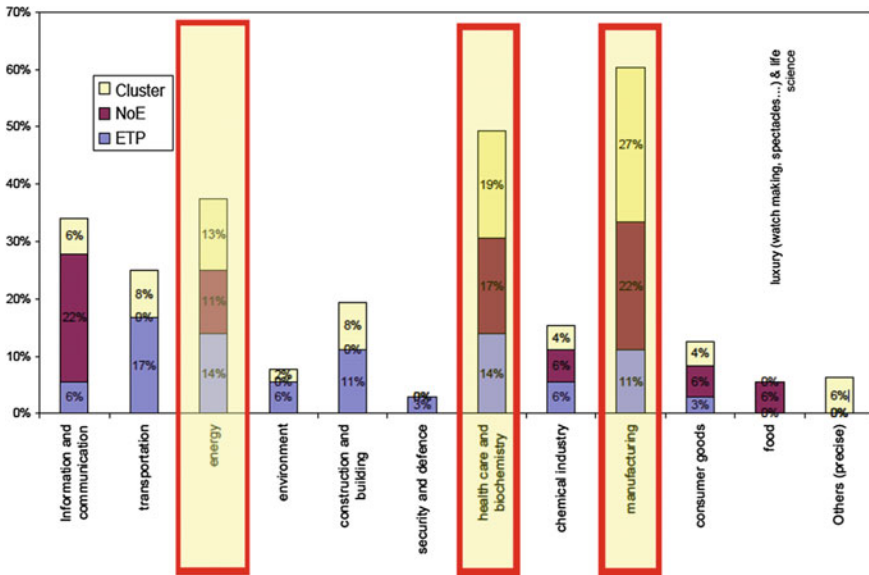


Fig. 10.3 Main markets between 2012–2015 [6]

and thus it is relevant to assess not only their current importance but also their potential future attraction. According to the results of a survey published in the MINAM roadmap, the main current and future markets for micro-manufacturing are identified. Figures 10.3 and 10.4 illustrate the results.

As shown in Fig. 10.3, for the timeframe 2012–2015, the most significant market for micro-manufacturing is “manufacturing”. The other leading sectors are healthcare and energy. Meanwhile, ICT, transportation and construction were also identified as important sectors but not the main ones.

On the other hand, for 2015 onwards (Fig. 10.4), healthcare is identified as the leading sector for application of micro-manufacturing. Energy has been identified as the second most important sector, followed by transportation and ICT.

10.3.3 Future Applications and Technologies

Having identified the main future markets for micro-manufacturing, it is also important to identify the applications of micro-manufacturing in the future market. In this part we introduce the main future applications, and have a deeper look into the future of micro-parts and micro-manufacturing technologies. Figure 10.5 presents the major applications of micro-manufacturing within a timeline.

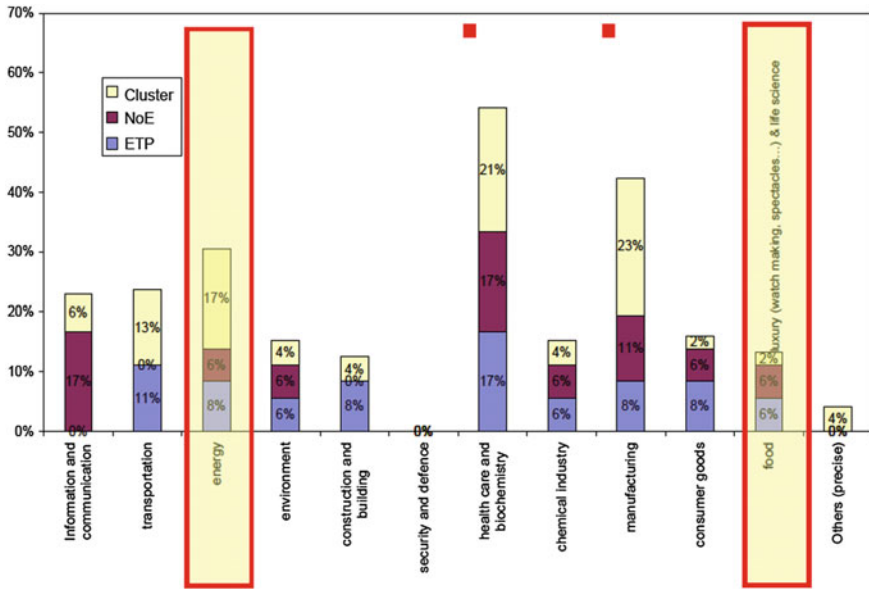


Fig. 10.4 Main markets beyond 2015 [6]

	Time period (year)		
	2011-2013	2013-2015	2015 on
Major Application of MicroManufacturing	<ul style="list-style-type: none"> • Micro fuel cells • Microfluidics • Development of point-of-care devices • Further development of MicroManufacturing sensors 	<ul style="list-style-type: none"> • Integration of nano/micro technologies • Replication methods • Multi-material microinjection molding • Further development of microactuators • Knowledge-based manufacturing systems 	<ul style="list-style-type: none"> • Micro-cell power • Energy harvesting systems • Further development in solar cells manufacturing • Further development in thin-film technology • Energy storage devices based on flexible substrates • Polymeric-based point-of-care facilities. Wearable medical devices • Knowledge-based manufacturing systems

Fig. 10.5 Major future applications of micro-manufacturing [5]

10.3.3.1 Future of Micro-parts

Micro-components represent the connection between applications and technologies. From the application point of view they represent some of the enabling

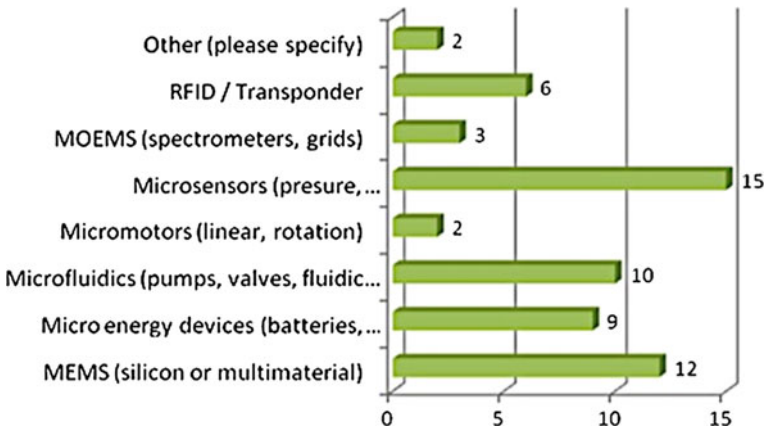


Fig. 10.6 Current criticality of micro-components [6]

components, providing essential or additional functionality. From the technological point of view, micro-components represent the result of a single technology or a set of replication, structuring, coating and assembly technologies (process chain). Based on the results of a MINAM survey, micro-components are considered as a “critical issue” in the future of micro-manufacturing. Figures 10.6 and 10.7 illustrate the current and future criticality of the micro-parts.

Figures 10.6 and 10.7 show that micro-sensors are identified as the most critical micro-part in the future. Moreover, while the silicon or multilayer MEMS will not be considered as significant, they still remain as the second most critical. Micro-fluidic and micro-energy devices will emerge as new critical micro-parts and potential bottlenecks. The other components do not show the same level of criticality.

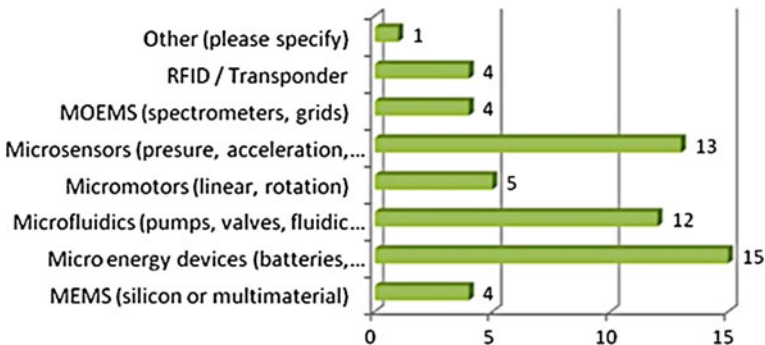


Fig. 10.7 Future criticality of micro-components [6]

10.3.3.2 Future of Micro-manufacturing Technologies

Micro-manufacturing applies techniques to produce the micro-sized components and structures. Accordingly the micro-manufacturing technologies involve scaling down of the common and widely used machining processes (i.e. milling and drilling). At the micro-scale level, these technologies are known as micro-technologies (i.e. micro-drilling, micro-machining, micro-embossing).

We now take a closer look at two micro-manufacturing technologies and their future perspectives, namely replication technologies and micro-structuring technologies.

Replication technologies

Micro-injection moulding is one of the major replication technologies. In recent years micro-injection moulding has been recognised and applied as a technology for high volume production of polymer based components with micro or nano-features or structured surface topography. Micro-injection moulding is also recognised as an efficient, reliable and cost-effective technology in order to replicate polymer micro-parts. The trends in micro-injection moulding suggest it will be one of the major technologies for use in micro-manufacturing.

Below we present the future trends in micro-injection moulding and replication technologies [6].

- There is a clear trend towards micro-rapid prototyping. The production of injection moulding tools has been facilitated by techniques such as micro-rapid prototyping processes and technologies such as micro-stereo lithography. This is used for very small production quantities.
- The replication of nano and micro-size components represents another major trend. This is more significant for components with high aspect ratio (i.e. components with optical properties).
- There is a trend towards the development of smaller sensors that allow a more precise monitoring and control of processes.
- A significant trend is related to the development and use of new materials (i.e. bulk metallic glasses) to overcome the challenges in replication process.
- Another major trend relates to function integration. This results in opportunities for technologies such as 3D MID (Moulded Interconnected Devices), printing technologies, multi-component injection moulding, laser direct structuring, and polymer film-based technology.

Micro-structuring technologies

Micro-structuring technologies such as micro-milling technologies enable the required 3D structuring on a wider range of materials. Generally, the materials, which are applied for these micro-machining processes, are the same as to the ones used in macro-manufacturing processes. Therefore the range of the materials is quite broad and includes metals, polymers, ceramics and glass.

Below we present the future trends in micro-structuring technologies [6].

- The most important areas for micro-structuring technology in future will be laser cutting, stereo lithography, wire EDM and deep reactive-ion etching.
- For micro-cutting, there are several major technological trends including generation of advanced models and strategies aiming at overcoming the challenge of heat extension of micro-milling tools, analysis of the wear behaviour of ultra-small micro-cutting tools and development of models and techniques for precise prediction of micro-tool breakage.
- For laser material processing, there is a significant trend in terms of green energy technologies. Moreover some technologies such as micro-drilling laser micro-scribing, and thin-film patterning and structuring will be more prevalent.
- Another significant trend in the field of laser processing is the use of ultrafast laser systems instead of nano-second laser pulses.

10.4 Business Models for Micro-manufacturing

Recently, the term “business model” has become prevalent in many management publications. Although the term has become fashionable and has received much attention, there is still confusion about what exactly a business model is and how it can be used by companies. In fact, how a company can differentiate the terms “business model” and “strategy” and consequently constructing a business model to pursue a specific strategy is still considered challenging.

10.4.1 *What Is a Business Model?*

From the early emergence of the term “business model” by Jones [10], different definitions have been suggested to explain the term and its role. These definitions reflect various perspectives that can be covered by a business model; such as value creation, simplification of a complex system, money generation, company behaviour representation, etc. In the late 90s Timmers presented one of the first structured, but still simple, definitions of business model. He described business model as a general architecture for the product, service and information flow [11]. Later, Petrovic et al. [12] followed the same logic of Linder and Cantrell [13] to introduce value creation as the main role of a business model. Magretta and Stähler took a further step by differentiating “business model” from “strategy” [14]. They described a business model as a system that illustrates how different pieces of a business can fit together to pursue a specific strategy. In 2004, Osterwalder presented his broad definition when he stated, “business model is a conceptual tool that contains a set of elements and their relationships and allows expressing a company’s logic of earning money. It is a description of the value a company offers to one or several segments of customers and the architecture of the firm and its

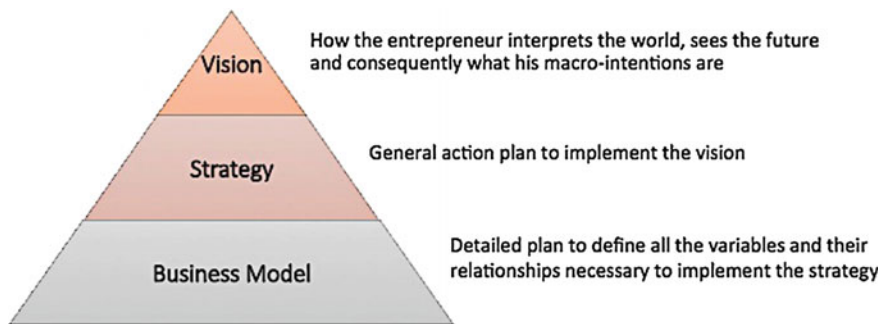


Fig. 10.8 The concept of business model

network of partners for creating, marketing and delivering this value and relationship capital, in order to generate profitable and sustainable revenue streams [15]. Later Osterwalder and Pigneur proposed a business model canvas as a tool to realise the previous definition of business model [16].

In this study, we see business model as a tool containing a set of strategic choices and alternatives to support a company to create, deliver and capture different forms of value within a value chain [17]. Figure 10.8 illustrates the concept of business model and its relation with strategy and vision in a business.

The Business Model is an intermediate layer between strategy and operations that allows designing a holistic view of the business. It makes explicit all the design variables that must be taken into account for success overcoming the local optimisation approaches (of the technology, supply chain, etc.). It also verifies that all variables are aligned and mutually consistent (i.e. it makes no sense to offer a “pay per machine availability” concept if machines do not have embedded a remote monitoring system, and if an IT system and a system for collecting data is missing). Moreover it enables progression to detailed process and technology design after having agreed on the pillars of the business and having solved inconsistencies at a systemic level. A business model also communicates more precisely to investors and stakeholders, what the business goals are, and in which way entrepreneurs intended to structure the company to reach the goals.

10.4.1.1 Business Model Elements

A business model can be seen as a system consisting of several components. Based on the objective and structure of business model, the components vary from one model to another. Elements of a business model enable fulfilment of its objectives. Consequently they are also dependent, in a large extent, on the definition of the term. In the last decade and during the evolution of the concept, several proposals have been presented in literature identifying main building blocks of a business model. While some of these models are built upon a few general building blocks

Table 10.4 Business model elements

Reference	Business model components
Chesbrough and Rosenbloom [21]	Value proposition, market segment, structure of value chain, cost structure, position of the firm within value network, formulation of competitive strategy
Afuah [18]	Activities, resources, positions, industry factors, costs
Shafer et al. [20]	Strategic choices, value creation, value network, value capture
Doganova and Renault [19]	Value proposition, architectural value, revenue model
Osterwalder and Pigneur [16]	Key resources, key partners, key activities, value proposition, channels, customer segment, customer relationship, cost structures, revenue streams

[18–20]; others entail more specific and detailed building blocks taking into account different parts of a value chain [16, 21]. Table 10.4 illustrates a summary of proposals for business model components in the last decade.

Chesbrough and Rosenbloom defined 6 blocks in their business model. They intended to cover different parts of the value chain in the defined building blocks; however the blocks are not exactly at the same level (e.g. formulation of competitive strategy vs. structure of value chain). For instance, the block related to structure of the value chain is mainly related to create and deliver of the value proposition, while formulation of competitive strategy aims at definition and achievement of competitive advantage for the company [21]. Afuah developed a strategic management approach to define building blocks of business model. His model is made of four dimensions dividing to internal (firm-specific factors) and external factors (industry factors) [18]. Combination of these factors helps a company to design a successful business model. Later Shafer et al. proposed four main elements of a business model: strategic choices, value network, create value and capture value [20]. While strategic choices are related to internal business practices such as strategy, branding, value proposition etc.; the value network has a focus on company's interaction with external partners including suppliers and customer relationships. The financial structure of the business model is covered with the two other categories of "create value" and "capture value". The first category is concerned with the resources and processes of the company, and the latter focuses on the cost and profit structure. In 2009, Doganova and Renault defined structure of their business model based on three main building blocks: Value proposition to focus on the offered product or service to the customers, Architectural value to manage interaction with partners and define proper channels to deliver the product/service to end customers, and Revenue model to cover the financial aspects of a business [19].

Recently Osterwalder and Pigneur proposed a business model canvas consisting of 9 different elements [16]. Each element is designed to cover a specific part of value chain so that the whole value chain can be addressed using business model canvas. The canvas can be logically grouped into 3 areas: The left-hand blocks

relate to efficiency (key partners, key activities, key resources, and cost structure), the right-hand blocks relate to value delivery (customer segment, customer relationship, channels, and revenue streams) and finally the value proposition which is located in the middle and acts as a link connecting the two sides of the canvas. Figure 10.9 illustrates the business model canvas.

Considering the proposed elements of the business model described above and the other existing models outlined, our consideration of business models and its constitutive elements is depicted in Fig. 10.10.

As it can be seen in Fig. 10.10, the business model consists of four main building blocks namely value proposition, market, infrastructure and financials. The value proposition block identifies what a company offers in terms of products and services (i.e. machine tools, software solutions, maintenance services, etc.). The market block describes the customers to whom the value proposition is addressed, and the distribution channels used to bring the value proposition to the customers. The infrastructure block identifies how the company is able to supply the market with the value proposition. This includes; the supply chain architecture and description of what the company produces internally, and what it buys or outsources to other companies, the type of relationships with other supply chain companies; the production technologies and the manufacturing processes; and the business process or the internal organisation and the capabilities for manufacturing, sourcing, marketing and delivering the value proposition. Eventually the financials block describes the financial mechanisms through which the company realises

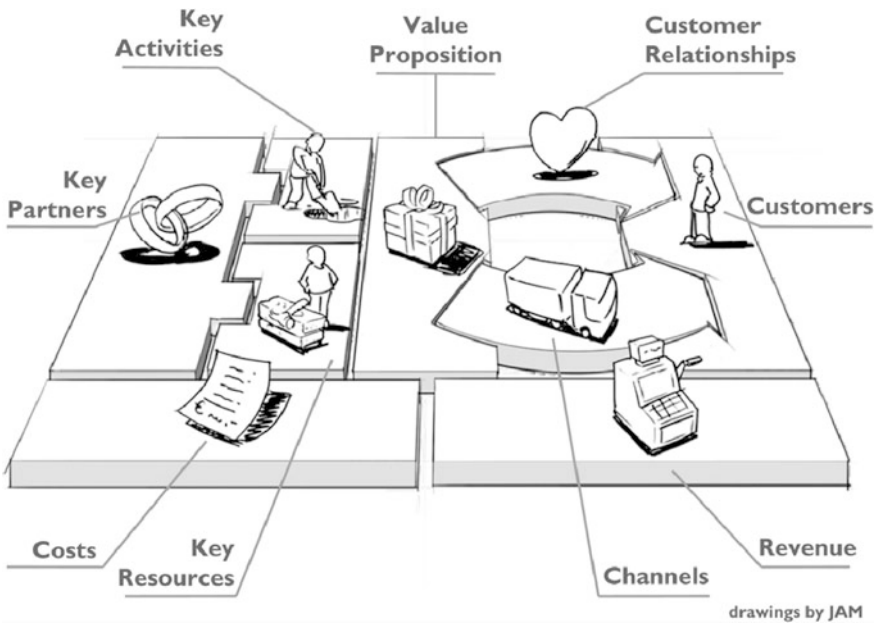


Fig. 10.9 Business model canvas [22]

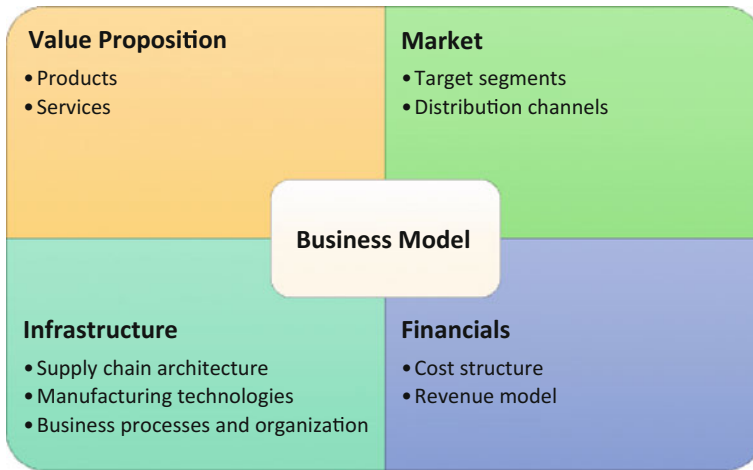


Fig. 10.10 Constitutive elements of business model

profits from the supply of the value proposition to the market. This includes the cost structure for all activities necessary to bring products to the market and the revenue model through which the company recovers costs and realises profits.

10.4.2 Innovative Business Models

In recent years, the emergence of innovative business models in different industries and sectors is quite observable. Indeed, it is believed that an innovative business model is a powerful tool for the future success of an enterprise. The drivers for business model innovation are different, such as:

- **Market:** Customers request (i.e. in the automotive sector, OEMs (original equipment manufacturers) ask more and more to have a “total cost of ownership” guarantee)
- **Technology:** A new technology is available to support new processes or to support existing processes better or more efficiently (i.e. the internet and progress in IT have enabled the e-commerce business model)
- **Competitors:** The new business model becomes the new standard in the market (i.e. copy machines sector, “pay per click” web advertising).

The innovation with respect to a business model can be either incremental or radical. A business model is incrementally innovative when some of its components are innovative. For instance, offering innovative products or services, targeting new market segments not being served yet, generating new revenue mechanisms, developing new supply chain configurations, etc. On the other hand, a radical business model innovation is achieved when all the business model variables

evolve together with coherence (innovative products/services offered with new payment mechanisms which require innovative infrastructure). Empirical evidence shows that incremental business model innovation can sometimes lead to serious failure given certain aspects of the business evolve radically—in isolation, but are then inadequately supported by existing model components or systems.

Some examples of business model innovation are:

- Service and servitisation: A business model can be innovative if the value proposition includes services, and the offered services are high added-value services, which means that they are oriented to support (guarantee) a business result for customers rather than to assist customers in using physical products.
- A business model can be innovative from an infrastructure perspective if:
 - (1) There is a wide recourse to networking and supply chain partnerships compared to vertical integration;
 - (2) A process-oriented organisation is adopted;
 - (3) Modern manufacturing technologies are used for manufacturing;
 - (4) It comprehends an integrated manufacturing/de-manufacturing supply chain.
- From the financial perspective, a business model can be innovative if supplier's revenues are linked to results rather than to the exchange of physical products (pay per results rather than selling products). In this case the supplier undertakes (part of) customer's operational risks and is compensated for that.

10.4.3 Current Business Models for Micro-manufacturing

Currently the business models applied by the players in micro-manufacturing market can be divided into two categories:

1. A traditional machinery selling business model; in which a company buys the micro-manufacturing equipment from the machinery suppliers and operates them in-house.
2. A production service business model; in which a company has multiple micro-manufacturing machinery and competencies in the process, offers production as a service to manufacturers.

Below we describe each business model and its characteristics.

10.4.3.1 Traditional Machinery Selling

Traditional machinery selling is a traditional type of business model where the producer of the micro-manufacturing equipment (supplier) sells the physical tangible product (micro-manufacturing equipment) to the user of micro-manufacturing technology (customer). Moreover, the after-sales services are generally regarded as

Innovation dimensions		Options				
Operating personnel		Equipment producer	Operating Joint Venture	Third party	Customer	
Maintenance personnel		Equipment producer	Operating Joint Venture	Third party	Customer	
Location		Equipment producer	Third party	"Fence to Fence" to the customer	Customer	
Payment modus		Pay per Part	Pay per Use (Rent)	Pay for availability	Fixed rate	
Ownership	During phase of use	Equipment producer	Equipment producer	Equipment producer	Equipment Producer	Leasing bank
	After phase of use	Equipment producer	Equipment producer	Equipment producer	Equip. Producer	Leasing bank
					Customer	Pay for equipment
Procurement of raw materials		Equipment producer	Operating Joint Venture	Third party	Customer	
Transport of final products		Equipment producer	Operating Joint Venture	Third party	Customer	

Fig. 10.11 Configuration for traditional machinery selling

necessary add-ons to physical products. In this business model the operation takes place in-house and the customer (user of technology) is responsible for the operation of machinery.

Figure 10.11 depicts the configuration of traditional machinery selling business model, highlighting the features of the business model for each innovation dimension. It should be mentioned that the current configuration is developed based on the methodological box for configuration of new business models proposed by Copani et al. [22].

The green circles in Fig. 10.11 represent the features of the business model in terms of innovation dimensions. As can be seen, all dimensions in this business model are covered by the customer. This includes areas such as operating personnel, maintenance, procurement, transport, etc.

10.4.3.2 Production Service

Micro-manufacturing technologies can act as an enabler for micro-production in many sectors of the market. However, adopting the traditional business model presents challenges for customers such as: high level of investment and lifecycle cost, lack of competency and resources, and changing the traditional production processes. In order to overcome these challenges (and minimise risk) business models are adopted to offer a production service, where a company owning several types of micro-manufacturing machines can act as an external skilled partner. These business models are called production service. A micro-manufacturing production service business model is based on offering the service of production or prototyping of final products to the customer through using various micro-manufacturing

technologies owned by the provider. In addition to the physical production service, the provider usually offers also other services dealing with product/process design, product industrialisation, etc. Figure 10.12 illustrates the configuration of the production service business model.

As shown in Fig. 10.12, the equipment producer plays a critical role in the production service business model. Many activities such as maintenance, procurement, and transport are carried out by the equipment producer while the operation takes place in equipment producer’s plant using its own personnel. Having a production service business model, the company operates as a provider of micro-manufacturing services and solutions. While the core value proposition of the company is usually focused on production service, it can propose additional value propositions such as engineering and software development. In order to run this business model, the company needs a large fleet of micro-manufacturing machines and equipment to ensure the production of custom prototypes and end-use parts for the customers. Usually, the provider is specialised in a range of micro-manufacturing technologies. The target market segments usually include several sectors, but the main final markets are: Medical devices (healthcare), electronics, machinery, biotech, military, aerospace, etc.

Figure 10.13 highlights the elements of the production service business model.

One of the notable examples of companies applying this business model in micro-manufacturing market is Materialise. Materialise is a Belgium-based company that provides an additive manufacturing (AM) service to its customers. The company offers different services to the customers such as: Manufacturing and prototyping of parts and products, software development for owners of AM equipment, engineering and design service, and co-creation through online 3D printing service for end users.

Innovation dimensions		Options				
Operating personnel		Equipment producer	Operating Joint Venture	Third party	Customer	
Maintenance personnel		Equipment producer	Operating Joint Venture	Third party	Customer	
Location		Equipment producer	Third party	"Fence to Fence" to the customer	Customer	
Payment modus		Pay per Part	Pay per Use (Rent)	Pay for availability	Fixed rate	
Ownership	During phase of use	Equipment producer	Equipment producer	Equipment producer	Equipment Producer	Leasing bank
	After phase of use	Equipment producer	Equipment producer	Equipment producer	Equip. Producer	Leasing bank
Procurement of raw materials		Equipment producer	Operating Joint Venture	Third party	Customer	
Transport of final products		Equipment producer	Operating Joint Venture	Third party	Customer	

Fig. 10.12 Configuration of production service business model

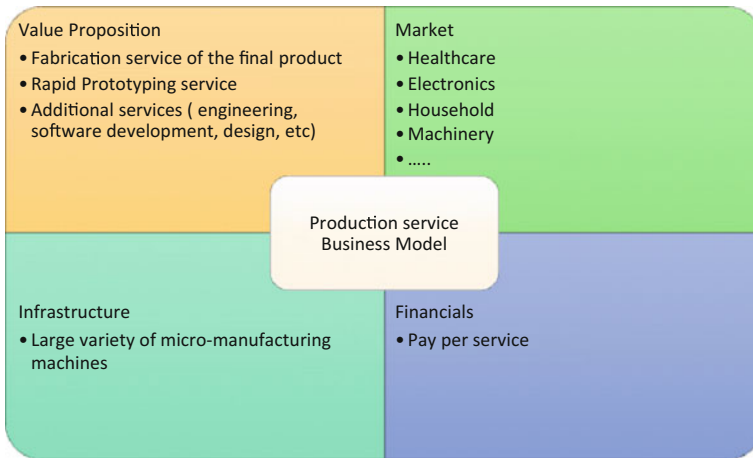


Fig. 10.13 Elements of production service business model

10.4.4 Innovative Business Models for Micro-manufacturing

Emerging trends in the market for micro-manufacturing require the generation and development of innovative business models which can embrace the new technological development in order to satisfy the evolving needs of the users. As discussed, the innovation can take place in different elements of a business model, based on the ultimate objective of the enterprise. The same applies to micro-manufacturing businesses. Innovative business models can reflect the different aspects. In this section we present three examples of innovative business models for micro-manufacturing.

10.4.4.1 Personalised Manufacturing for Healthcare with Closed Integration with Hospitals

Today customers ask for the products that are designed and produced based on their individual needs and desire. For some sectors such as healthcare, the production of personalised medical devices and products is more critical and has had more attention—since it directly affects the quality of patient’s life. In fact, the trends towards an aging population, combined with rapid technological evolution, have been of real interest to the healthcare sector for the production of customised medical devices [23]. In existing business models, the customer of the personalised medical device receives the final product from the supplier. However, there are major barriers and challenges for the existing business model such as:

- Time-consuming process of supplier selection, ordering, designing, producing and delivery of the product (for hospitals)
- No, or very low, levels of interaction between the medical staff (e.g. surgeon in the case of implantable devices) and the producer during the design phase
- High cost of the final product
- No real personalisation and a limited degree of customisation, due to high costs.

Micro-manufacturing technologies can act as true enablers for the production of personalised medical devices. In order to overcome the current barriers, the production of the personalised medical devices can take place in proximity, or inside of the hospital. This can result in an increased level of integration between producers and hospitals and even to change the role of the hospitals from a user to a producer of these devices. Implementation of this triggers the manufacturing of customised medical devices inside the hospitals. However, pursuit of this strategy requires the development and implementation of an innovative business model in order to facilitate such a radical integration of a product service system concept [23]. As such, new business models need to be adopted to integrate hospitals within the overall provision of personalised medical devices. Figure 10.14 shows two examples of a business model configuration for personalised manufacturing in healthcare.

The business model configuration on the top illustrates a scenario in which the micro-manufacturing equipment is owned by hospital. However, production takes place either in-house or fence-to-fence. The internal hospital personnel are responsible for running the manufacturing operation and payment is made per purchased machinery.

The business model configuration on the bottom depicts a scenario which is based on offering the usage of the machines to the hospital instead of out-right purchase. In this case the ownership and the maintenance of the micro-manufacturing equipment remain in the hands of supplier, and the hospital purchases the usage of machines from the suppliers of micro-manufacturing machinery through leasing or renting. The production is still undertaken within or in close proximity to the hospital [23].

Hence, both configurations enable the implementation of a new business model in which the production of personalised medical devices is realised through utilisation of micro-manufacturing technology, and the level of integration with hospital is quite high. Such a business model brings advantages through decreased lead time, improved service for patients increasing their quality of life, more cost-efficient production of such personalised devices, and better utilisation of surgery and of medical processes. The business model does however present some challenges, such as; strict regulations and standards in healthcare for in-house production, certification of the final product, and ensuring the continuing economic sustainability.

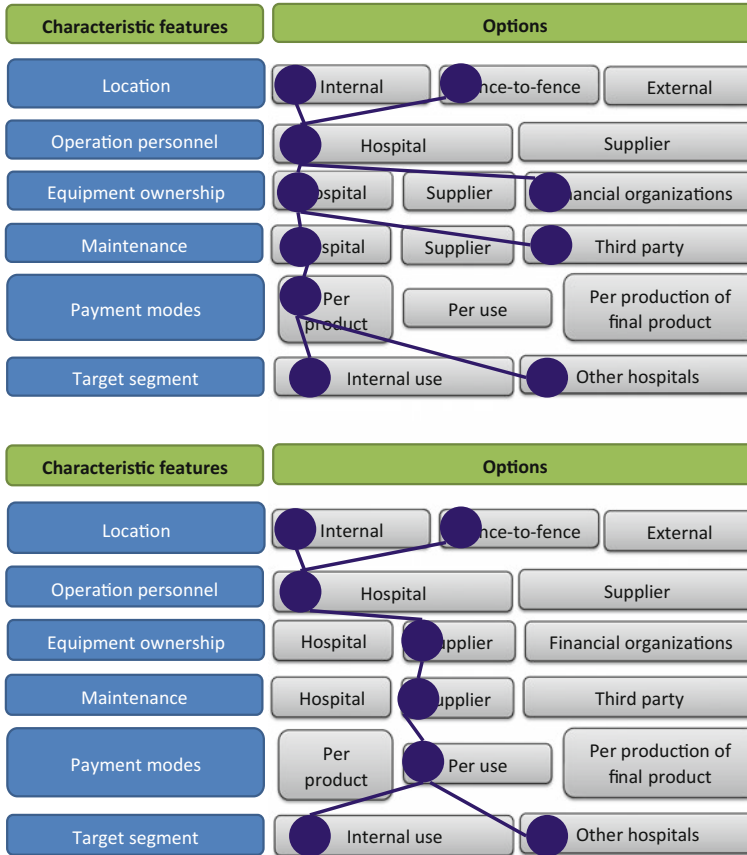


Fig. 10.14 Examples of a business model configuration for personalised manufacturing in healthcare (adapted from [23])

10.4.4.2 Micro-factory

The relatively small micro-manufacturing equipment can also allow innovative “micro-factories”, which can be situated in small physical spaces such as offices or even within houses. Micro-factory or desktop manufacturing refers to miniaturised production equipment such as micro-machining units, robotic cells and micro-rapid prototyping units. A micro-factory (desktop) usually fits on a table, is mobile and fully integrated. It is ideally modular and enables the manufacture of small (micro-sized) parts and products. Thanks to the small dimensions of the micro-factory, it can move the production downstream in the supply chain and even to the point of sale. Considering the advanced micro-manufacturing technologies used in a mini-scale factory, micro-factories enable efficient and effective manufacturing of micro-parts. Moreover, the micro-factory business model enables the efficient production of personalised goods. In some cases, even the user of a specific

product can become a manufacturer by the establishment of a micro-factory for in-house production. This small scale manufacturing and business model can be applied in many sectors. Figure 10.15 shows examples of micro-factory units.

Applying micro-factory as a novel business model brings advantages to the company. A good example of this is a famous Japanese watch producer's use of a micro-factory for machining of precision watch parts. The introduction of such a business model resulted in 99% of work-piece material savings, and 90% space saving for the company. Apart from these remarkable savings in investment, energy, space and resources, this new business model can also facilitate other benefits including: a shorter ramp-up time; the production layout can easily be changed; the proximity of production to the customer is more easily achieved; and ubiquitous manufacturing becomes much more feasible (mobile, onsite, etc.). However it should be noted that the limited availability of small-scale equipment is still a challenge facing this type of business model.

10.4.4.3 Micro-machinery Producers

The extensive application and capability potential of micro-manufacturing technologies have caused a rapid diffusion of the technology across different sectors where more and more companies are having to apply micro-manufacturing technologies. However, these companies face several barriers in this regard such as:

- High initial investment and high lifecycle cost of machines
- Lack of knowledge and competency in the application of micro-manufacturing technology and materials
- Complexity of process design and set up
- Unpredictable demand for production capacity.

In order to address some of these barriers, micro-manufacturing machinery manufacturers can apply new and innovative business models. Below we introduce several configurations of new business model for micro-machinery.



Fig. 10.15 Examples of micro-factory units [24]

Build—operate at customer plant

Within this business model, the capital goods (machinery) producer, remains the owner of the equipment, runs this equipment at the customer’s plant exclusively for this customer, employs operating and maintenance personnel and is paid per use or per part. The same model can be applied with final purchase option for the customer. Figure 10.16 illustrates this configuration.

Equipment supplier turns into a part supplier

Within this business model, the capital goods (machinery) producer implements the product in its own premises and manufactures customer orders on site. The manufacturer is the owner of the equipment, operates and maintains the equipment with their own personnel and is paid per part. This concept can be organised for one or several customers. Figure 10.17 illustrates this configuration.

Supply park concept

The supply park configuration is based on the fact that the capital goods producer provides its customer with machinery implemented in establishments newly built in the surrounding of customer facilities. He remains the owner of machines, which are operated and maintained with its own personnel, and produces often “just in sequence” supply parks for this unique customer. This model type is commissioned especially by larger OEMs of the automotive industry. Figure 10.18 illustrates this configuration.

Innovation dimensions		Options					
Operating personnel		Equipment producer	Operating Joint Venture	Third party	Customer		
Maintenance personnel		Equipment producer	Operating Joint Venture	Third party	Customer		
Location		Equipment producer	Third party	"Fence to Fence" to the customer		Customer	
Payment modus		Pay per Part	Pay per Use (Rent)	Pay for availability	Fixed rate		
Ownership	During phase of use	Equipment producer	Equipment producer	Equipment producer	Equipment Producer	Leasing bank	Customer
	After phase of use	Equipment producer	Equipment producer	Equipment producer	Equip. Producer	Leasing bank	
Procurement of raw materials		Equipment producer	Operating Joint Venture	Third party	Customer		
Transport of final products		Equipment producer	Operating Joint Venture	Third party	Customer		

Fig. 10.16 Build-operate at customer plant-own configuration

Innovation dimensions		Options				
Operating personnel		Equipment producer	Operating Joint Venture	Third party	Customer	
Maintenance personnel		Equipment producer	Operating Joint Venture	Third party	Customer	
Location		Equipment producer	Third party	"Fence to Fence" to the customer	Customer	
Payment modus		Equipment producer	Pay per Use (Rent)	Pay for availability	Fixed rate	
Ownership	During phase of use	Equipment producer	Equipment producer	Equipment producer	Equipment Producer	Leasing bank
	After phase of use	Equipment producer	Equipment producer	Equipment producer	Equip. Producer	Leasing bank
Procurement of raw materials		Equipment producer	Operating Joint Venture	Third party	Customer	
Transport of final products		Equipment producer	Operating Joint Venture	Third party	Customer	

Fig. 10.17 Equipment supplier turns into a part supplier configuration

Innovation dimensions		Options				
Operating personnel		Equipment producer	Operating Joint Venture	Third party	Customer	
Maintenance personnel		Equipment producer	Operating Joint Venture	Third party	Customer	
Location		Equipment producer	Third party	"Fence to Fence" to the customer	Customer	
Payment modus		Pay per Part	Pay per Use (Rent)	Pay for availability	Fixed rate	
Ownership	During phase of use	Equipment producer	Equipment producer	Equipment producer	Equipment Producer	Leasing bank
	After phase of use	Equipment producer	Equipment producer	Equipment producer	Equip. Producer	Leasing bank
Procurement of raw materials		Equipment producer	Operating Joint Venture	Third party	Customer	
Transport of final products		Equipment producer	Operating Joint Venture	Third party	Customer	

Fig. 10.18 Supply park concept configuration

Reconfiguration guarantee

In this configuration the machine supplier guarantees the option to reconfigure supplied machines should new products and/or production volumes are required. A set of reconfiguration scenarios are identified and the supplier guarantees a fixed reconfiguration cost if the customer requires this service.

Capacity guarantee

Within this configuration of business model, the machine supplier owns equipment, which is operated by the customer. The machine supplier guarantees to provide the customer with the type of production capacity that is necessary over time to manufacture the products demanded by the market in terms of type and volumes. Should reconfigurations to machines and/or layout be required, the machine supplier will undertake as required. The customer pays a fixed fee to use the capacity. The implementation of each configuration of the micro-machinery business model has several potential benefits to the company such as: solving variable demand and uncertainty; maintaining state-of-the-art capabilities in non-core competence areas; mitigating investment risk for the customer especially with respect to new technological developments, sharing risks between the customer and equipment supplier.

Balancing these benefits, such a model will present a different set of challenges to the company including: a lack of management competencies to design and manage such new business models; a reduced level of understanding to quantitatively assess the parameters of new business models (price, contract durations, life cycle costs, etc.) and to manage risks.

References

1. Dimov SS, Matthews C, Glanfield A, Dorrington P (2006) A roadmapping study in multi-material micro manufacture. In: Proceedings of second international conference on multi-material micro manufacture 4M2006, Grenoble, France, 20–22 Sep 2006
2. Eloy JC (2012) MEMS Packaging Market and Technology Trends, Yole Developments, SEMICON West 2012, San-Francisco. http://www.semiconwest.org/sites/semiconwest.org/files/data14/docs/SW2014_JC%20Eloy_Yole%20Developpement_0.pdf. Accessed 17 July 2015
3. Bouchaud J (2011) High value MEMS market overview, HIS iSupplie, DTIP Conference 2011, Marseilles, France, 12 May 2011
4. Mounier E (2014) Future of MEMS: a market and technologies perspective, Yole Developments, MEMT Tech Seminar 2014, Oct 2014. <http://www.semi.org/eu/sites/semi.org/files/images/Eric%20Mounier%20-%20Future%20of%20MEMS.%20A%20Market%20and%20Technologies%20Perspective.pdf>. Accessed 10 July 2015
5. Frost & Sullivan (2012) Advances in micro-manufacturing technologies (Technical Insights)
6. MINAM 2.0 (2012) Roadmap 2012: Final version; MINAM—Micro- and NanoManufacturing
7. Dennison S. Applications of micro and nanotechnologies in healthcare: medical devices and products, UK MNT Network
8. Johnston C, Advanced F, UK MNT Network. Applications of micro and nanotechnologies In the Aerospace sector, Prepared in partnership between Colin Johnston, Faraday Advanced and the UK MNT Network
9. Qin Y (2010) Micro manufacturing engineering and technology, 1st edn. William Andrew
10. Jones GM (1960) Educators, electrons, and business models: a problem in synthesis. *Acc Rev* 35(4):619–626
11. Timmers P (1998) Business models for electronic markets. *Electron Markets* 8(2):3–8
12. Petrovic O, Kittl C, Teskten RD (2001) Developing business models for e-business. International conference on electronic commerce, Vienna, Austria, 31 Oct 2001

13. Linder J, Cantrell S (2000) Changing business models: surveying the landscape. Accenture Institute for Strategic Change
14. Magretta J (2002) Why business models matter. *Harvard Bus Rev* 80(5):86–92
15. Osterwalder A (2004) The Business Model Ontology—a proposition in a design science approach. Ph.D. Dissertation. University of Lausanne, Switzerland
16. Osterwalder A, Pigneur Y (2010) Business model generation. Hoboken, Wiley
17. Pourabdollahian G, Copani G (2014) Proposal of an innovative business model for customised production in healthcare. *Mod Econ* 5(13):1147–1160
18. Afuah A (2004) Business models: a strategic management approach. McGraw-Hill
19. Doganova L, Eyquem-Renault M (2009) What do business models do? innovation devices in technology entrepreneurship. *Res Policy* 38:1559–1570
20. Shafer SM, Smith HJ, Linder J (2005) The power of the business models. *Bus Horiz* 48: 199–207
21. Chesbrough H, Rosenbloom RS (2002) The role of the business model in capturing value from innovation: evidence from Xerox Corporation’s technology spin-off companies. *Ind Corp Change* 11(3):529–555
22. Copani G, Molinari Tosatti L, Lay G, Schroeter M, Bueno R (2007) New business models diffusion and trends in European machine tool industry. In: Proceedings of 40th CIRP International Manufacturing Systems Seminar, Liverpool, UK, 30 May–1 June 2007
23. Pourabdollahian G, Copani G (2015) Development of a PSS-oriented business model for customised production in healthcare. *Procedia CIRP* 30:492–497
24. Tuokko R, Heikkilä R, Järvenpää E, Nurmi A, Prusi T, Siltala N, Vuola A (2012) Micro and desktop factory roadmap. Tampere University of Technology

Index

A

- Abrasive waterjet cutting, 129
- Acrylonitrile Butadiene Styrene (ABS), 52, 184, 185
- Aerosol-Jet printing, 180, 187, 189
- Aluminium, 79, 135, 191, 198
- Antenna, 175, 176, 184, 193, 267
- Aspect ratio, 1, 37, 49, 106, 125, 151, 160, 275

B

- Bench-top machines. *See* Micro-factory
- Burr, 104, 115, 116
- Business model
 - innovative business model, 262, 280, 284, 285, 287

C

- CAD, 80, 82, 105, 200
- Ceramic sponge, 144, 145
- Chip formation, 104, 106, 107, 110, 114, 115
- Coherence Scanning Interferometry (CSI), 204–207, 213
- Comb-drive, 10, 240
- Computer aided manufacturing (CAM), 120, 137, 138, 151, 159
- Crystalline structure, 99
- Cyclic olefin copolymer (COC), 26

D

- Decoating, 142
- Design of Experiments, 156, 158
- Desktop factory. *See* Micro-factory
- Device
 - dental device, 84
 - gripping device, 229
 - medical device, 65, 67, 84, 88, 265, 283–285
- 3D printing

- 3D printing via binder jetting, 80, 81
- 3D printing via material jetting, 84

E

- Effect
 - Minimum chip thickness effect, 98
 - size effect, 98, 99, 113, 115
- Electro discharge machining
 - electro discharge machining drilling, 151, 166
 - electro discharge machining milling, 65, 151, 155, 158, 160, 162, 166, 167
 - micro-electro discharge machining, 2, 61, 64, 65
 - sinking electro discharge machining, 161, 162
 - wire electro discharge machining, 117
- Engraving, 116
- Environmental Conditioning. *See* Environmental conditions
- Environmental conditions, 223, 233, 244

F

- Factory-in-a-suitcase. *See* Micro-factory
- Filament deposition. *See* Fused deposition modelling, 89–91
- Film insert moulding, 180
- Focused Ion Beam (FIB), 2, 28, 116
- Force
 - adhesion force. *See* superficial force
 - capillary force, 9, 10, 230, 232, 241
 - casimir force, 10
 - electromagnetic force, 9, 12
 - electrostatic force, 8, 10, 56, 70, 241, 242, 244
 - superficial force, 17, 249
 - van der Waals force, 7, 10, 11, 238
- Force measurement

- Force measurement (*cont.*)
 direct force measurement strategy, 248
 indirect force measurement strategy, 248
 Fused deposition modelling, 89–91
- G**
 Garnet, 135, 136, 142
 Gripping system. *See* Gripping device
- H**
 High temperature nylon (HTN), 185
 Hot embossing, 180, 186, 187, 189, 263
 Hybrid micro-products, 223, 224, 251
- I**
 Injection
 injection pressure, 28, 35
 injection screw, 32, 34, 45
 injection speed, 26, 35, 37
 Injection moulding
 micro-injection moulding, 2, 39, 48
 two shot injection moulding, 180–183, 189, 194
 Internal fixation plate, 164, 166
- J**
 Jewellery, 79, 80, 83, 84, 125
- L**
 Lab-on-chip, 125, 194
 Laser direct structuring, 180, 183, 189, 275
 Laser triangulation, 204, 209, 210
 Liquid Crystal Polymer (LCP), 26, 184, 185, 194
- M**
 Machine-tool, 48, 99, 112, 114, 119, 120, 122, 269, 279
 Machining centre, 99, 104, 112, 120–122, 132, 136, 140
 Material
 bio-compatible material, 89, 162, 176
 ceramic composite material, 154, 155, 167
 electrostrictive material, 13, 16
 inhomogeneous material, 137, 144
 magnetostrictive materials, 13
 piezoelectric material, 13, 249
 smart materials, 13
 Material removal rate, 154
 Measurement
 micro-scale geometry measurement, 122
 process parameter measurement, 122
 Measurement technique
 contact measurement technique, 197, 198, 204
 non-contact measurement technique, 197, 204
- MEMS**
 BIOMEMS, 125
 Micro-additive manufacturing, 68, 91, 266
 Micro-assembly
 hybrid micro-assembly, 231
 robotized micro-assembly, 232
 Micro-assembly work-cell, 223, 227, 229, 232, 251, 286
 Micro-AWJ, 129, 131, 132, 135, 140, 141, 143–146
 Micro-CMM, 200, 201–203
 Micro-factory, 17–19, 21, 229, 232, 235, 250, 286, 287
 Micro-filter, 60–62, 65, 168, 170, 171
 Micro-fringe projection, 204, 211
 Micro-gear, 28–30, 50
 Micro-gripper, 228, 229, 238–241, 244, 248, 249, 251, 252, 254
 Micro-handling
 contact-free micro-handling, 242
 contact micro-handling, 239
 Micro-lathe, 17, 18
 Micro-machining
 micro-drilling, 125, 275, 276
 micro-milling, 49, 99, 109, 114, 125, 197
 Micro-mould, 38, 39, 125, 168
 Micro-robot, 5, 52, 67, 232–238
 Microscopy
 confocal microscopy, 204, 207
 focus variation microscopy, 204
 Micro-sensor, 52, 74, 97, 274
 Micro-stereolithography, 69, 71
 Micro-tool, 104, 106, 108, 112, 113, 115–117, 119, 125, 151, 162, 169, 238, 239, 243, 276
 Micro-valve, 75, 97
 Modelling method, 109
 atomic-scale finite element method, 109
 finite element analysis, 109
 mechanistic modelling, 105, 108
 molecular dynamics, 109, 110
 multi-scale modelling, 111
 Moulded Interconnect Devices (MID), 175–183, 186, 187, 190–193, 275
- O**
 Optics, 55, 67, 125, 126, 203, 207, 212, 214–216, 247, 266

P

- Palm-top factory. *See* Micro-factory
- Perfluoroalkoxy (PFA), 26
- Plasticisation, 33, 42, 44, 45
- Ploughing, 100, 104, 107, 108, 113, 114
- Polyamide (PA), 26, 185
- Polyamide-imide (PAI), 26
- Polybutylene terephthalate (PBT), 26, 185
- Polycarbonate (PC), 26, 184
- Polyetheretherketone (PEEK), 26
- Polyetherimide (PEI), 26
- Polyethylene terephthalate (PET), 26, 185
- Polymer
 - amorphous polymer, 31
 - electroactive polymer, 15, 16
 - photopolymer, 69, 71, 73, 74, 87
 - semi crystalline polymer, 31, 32
 - thermally conductive polymer, 176
 - thermoplastic polymer, 26, 38, 87, 176, 178–180, 183
 - thermoset polymer, 176, 178
- Polymethyl methacrylate (PMMA), 26
- Polyoxymethylene (POM), 26, 57, 146
- Polyphenyl ether (PPE), 26
- Polyphenylene sulphide (PPS), xi
- Polyphthalamide (PPA), 185
- Polypropylene (PP), 93, 185
- Polystersulfone (PES), 185
- Polystyrene (PS), 26
- Polysulfone (PSU), 26, 185
- Portable factory. *See* Micro-factory
- Powder bed fusion, 76, 77, 79
- Printed Circuit Board (PCB), 175
- Printed Circuit Board Kollmorgen (PCK), 181
- Probe
 - mechanical probe, 200, 201
 - opto-mechanical probe, 200, 202
 - silicon-based probe, 200, 201
 - vibrating probe, 200, 203
- Probe-card, 124
- Pure waterjet cutter, 129

Q

- Quartz, 13, 144, 203

R

- Release method. *See* Release strategy
- Release strategy
 - active release strategy, 243
 - passive release strategy, 27, 243, 244
- Release technique. *See* Release strategy

- Resonance frequency, 4
- Robotic cell. *See* Micro-assembly work-cell

S

- Sankyo Kasei Wiring board (SKW), 181, 182
- Scaffold, 67, 89, 91–93
- Scaling law, 2, 3, 9, 17
- Sector, 84
 - aerospace, 52, 55, 67, 125, 264, 266, 283
 - automotive, 52, 54, 125, 193, 263, 280, 288
 - biomedical sector, 125, 145, 231
 - communications, 67, 264
 - electronics, 52, 231, 283
 - energy, 265, 266
 - food sector, 264
 - information technology (IT), 52, 193
 - military sector, 67, 264, 266, 283
 - pharmaceutical sector, 53, 264
- Selective laser melting (SLM). *See* Powder bed fusion
- Selective laser sintering. *See* Powder bed fusion
- Shape memory alloy (SMA), 13–16, 84, 240
- Steel
 - carbon steel, 142
 - magnetic steel, 147
 - stainless steel, 78, 79, 83, 131, 146, 160, 165
 - tool steel, 79
- Straight Bevel micro-gear, 162, 163
- Stylus instrument, 198, 199
- Super alloy, 79
- Surface finish, 57
- Surface Mounted Technology (SMT), 177, 191
- Suspended beam, 3, 4
- Syndiotactic Polystyrene (SPS), 183

T

- Terminal velocity, 5
- Titanium, 79, 83, 160, 162, 165–168
- Tomography
 - optical coherence tomography (OCT)
 - Fourier-domain OCT, 213
 - spectral-domain OCT, 213
 - swept-source OCT, 213
 - time-domain OCT, 213
 - X-ray computed tomography (XCT), 212
 - industrial XCT, 215, 216
 - poly-energetic cone-beam XCT, 215
- Tool wear ratio, 154
- Two-photon polymerisation, 69, 70, 72, 74

V

Vision-based control, [248](#)

W

Watch, [52](#), [125](#)

Wear, [65](#), [104](#), [105](#), [110](#), [114](#), [116](#), [119](#),
[159–161](#), [197](#)

Work-cell. *See* Micro-assembly work-cell